



UNIVERSIDAD
NACIONAL
DE COLOMBIA

**Bioprospección de bacterias
aisladas de ambientes marinos con
actividad biocontroladora frente a
Fusarium oxysporum f. sp.
*lycopersici***

Diana Marcela Vinchira Villarraga

Universidad Nacional de Colombia

Facultad de ciencias

Bogotá, Colombia

2020

Bioprospección de bacterias aisladas de ambientes marinos con actividad biocontroladora frente a *Fusarium oxysporum* f. sp. *lycopersici*.

Bioprospection of marine-derived bacteria with biocontrol activity against *Fusarium oxysporum* f. sp. *lycopersici*.

Diana Marcela Vinchira Villarraga

Tesis presentada como requisito parcial para optar al título de:

Doctora en Biotecnología

Director (a):

Ph.D. Freddy Alejandro Ramos Rodríguez

Codirector (a):

Ph.D. Zulma Rocío Suarez Moreno

Línea de Investigación en Microbiología marina

Estudio y aprovechamiento de productos naturales marinos y frutas de Colombia

Universidad Nacional de Colombia

Facultad de ciencias

Bogotá, Colombia

2020

To my family, especially those that, in spirit, still walk by my side: my grandmother Antonia and my grandfather Salvador.

Acknowledgments

I want to express my gratitude to Universidad Nacional de Colombia, COLFUTURO and COLCIENCIAS for funding me and my research through the national PhD. scholarship 647, and the agreement 776-2017 (Conformación de un banco de proyectos elegibles de generación de nuevo conocimiento – 2017) through the project “Desarrollo de estrategias de control biológico en cultivos forestales y transitorios de interés comercial para Colombia empleando bacterias nativas colombianas”.

Also, I want to extend my gratitude to the “Instituto de Biotecnología de la Universidad Nacional de Colombia. IBUN”, the program “Doctorado en biotecnología”, specially Dr. Sonia Ospina and Raquel Noguera, and BIOCULTIVOS S.A. for providing all the facilities and support during the development of this research. I want to express my gratitude to ANLA and the “Ministerio de Ambiente y Desarrollo Sostenible de Colombia” for providing the collection, use and exportation authorizations for the development of this research (Permiso No. 4 de 10/02/2010, Anexo 2, Contrato de Acceso a Recurso Genético No. 108).

I want to extend my deepest gratitude to my Ph.D. advisors Freddy A. Ramos and Zulma R. Suarez, and to my “informal advisors” Nubia Moreno and Leonardo Castellanos. Thank you all for your support, patience, and enthusiasm for my project. Thank you for showing me the amazing world of metabolomics and increasing my love for microorganisms and science. Your faith in me never wavers. I hope that with this thesis, I can give you back at least a piece of all the kindness, support, and knowledge that I receive from you during all these years.

I would like to thank Mauricio Soto, Jaime Simbaqueba, Sandra Lorena Carmona, and the “Bancos de Germoplasma de la Nación” from Agrosavia (Colombia), who kindly provided the FOL59 strain and the infection protocol for the development of the *in vivo* assays presented in this research.

From the “Estudio y aprovechamiento de productos naturales marinos y frutas de Colombia” research group, my “familia de marineros” I would like to thank Luz Adriana, Sandra, Adriana, Paola, Michelle, Vanessa, Mateo, Juan David, and Carlos. We started as lab-mates, and now we are friends, almost family. Thank you for introducing me to the chemical world, for every advice, and for making my lab days full of laughs, music, food, coffee, and work.

I want to thank all the fantastic people who work at the IBUN, particularly in the “Biosprocesos y bioprospeccion” research group. I would like to thank specially to Ibonne

García, Mauricio Bernal, Elssy Bermudez, Claudia Parra, Sebastian Parra, Wilder Sierra, Sandra Gonzalez, Alvaro Rincón, and Raul Villarraga. Everyone help me in so many ways that I would need a whole chapter to finish saying thank you.

From the “Natural products laboratory”, I would like to express my gratitude to Dr. Young Hae Choi, who accepted me for work with him in The Netherlands. Also, I would like to especially thanks to Martine Huberty, Ana Marin, Alisa Willacey, and Thomas Van der Toorn. All of you guys gave me support in a different land, allow me to deal with the biggest challenge of my thesis, and let me know a little part of the European life. Thanks to all of you, I have grown as a scientist and as a person.

At Leiden, I meet an amazing, intelligent, caring, and wonderful person. A person that once was part of the “familia de marineros”. She helped me in every way she could, she never let me alone, she made me laugh and taught me so many things, that I do not have how to thank her. Lina, part of my thesis was done thanks to your support. Thus, this thesis is also your achievement; thank you so much.

I also want to express my gratitude towards my friends Eliza, Jeimy, Viviana, and Vicky. During all these chaotic years, you have stayed by my side. You patiently listened to me whenever I wanted to quit, each time I did not know what to do. You lend me your strength, physically and emotionally, and that is something that I do not know how to pay. Thank you so much, my dear friends.

Finally, I send my endless gratitude to my family. To my parents Dora and Antonio, my sister Liliana, and my grandmother Margarita. In the good moments, you were happy with me, and in the bad moments, you did not let me down. Your love and faith are the reasons why I could finish this project. Thus, this thesis is for you.

Resumen

la marchitez vascular, causada por el hongo fitopatógeno *Fusarium oxysporum* f. sp. *lycopersici* (FOL), es una limitante importante en la productividad de los cultivos de tomate (*Solanum lycopersicum*). Las bacterias derivadas de ambientes marinos producen metabolitos activos estructuralmente diversos. Estos compuestos han sido usados para el control de fitopatógenos, y recientemente, se ha propuesto evaluarlos junto con las bacterias que los producen como potenciales agentes de control biológico. En la presente investigación, se propuso usar bacterias derivadas de ambientes marinos como posibles biocontroladores de FOL.

Para ello, este estudio se dividió en tres fases: (I) La selección y caracterización de bacterias con actividad antifúngica frente a FOL, (II) El análisis de competencia rizosférica y la evaluación de actividad antifúngica *in vivo* de las bacterias activas, y, (III) El análisis metabolómico no dirigido de la interacción tomate-*Paenibacillus* sp.-FOL59 bajo condiciones de invernadero y la interacción *Paenibacillus* sp.-FOL59 en co-cultivo.

En la fase I, se llevó a cabo el tamizaje primario de actividad antifúngica con una colección de bacterias obtenidas de ambientes marinos compuesta por 152 aislamientos. De estas, 28 bacterias fueron seleccionadas con base en su actividad antifúngica *in vitro* contra nueve aislamientos de *F. oxysporum* y el fitopatógeno control FOL59. La caracterización fenotípica y la identificación molecular de estas bacterias se obtuvo con el fin de priorizar las cepas que deberían ser evaluadas en los ensayos de la fase II. Este proceso condujo a la selección de nueve aislamientos de bacterias pertenecientes al orden Bacillales, que presentaron la mayor actividad antifúngica contra FOL.

A partir de los resultados obtenidos en la fase II, la bacteria *Paenibacillus* sp. PNM200 se seleccionó como el candidato más apropiado para el control de FOL. *Paenibacillus* PNM200 colonizó el sistema radicular de dos variedades de tomate (Milano y Santa Cruz Kada) bajo condiciones de invernadero, y generó un efecto positivo sobre el crecimiento

de las plantas tratadas (Santa Cruz Kada) a los 30 días post inoculación. Este efecto fue correlacionado con la capacidad de *Paenibacillus* sp. PNM200 de producir Ácido indolacético y solubilizar fosfatos.

En un esfuerzo por caracterizar la interacción tripartita tomate-*Paenibacillus* PNM200-FOL59, en la fase III se llevó a cabo un perfilado metabólico por LCMS bajo condiciones controladas. En los experimentos de perfilado metabólico de la interacción tomate-FOL59, se observó la acumulación de los glicoalcaloides esteroidales α -tomatina, hidroxitomatina, tomatidina tetrahexósido, y la aglicona tomatidina en las raíces de la planta. Sin embargo, este efecto no se observó en la interacción tripartita tomate-*Paenibacillus* sp. PNM200-FOL59, ni en el perfil metabólico de las raíces de plantas de tomate tratadas solo con *Paenibacillus* sp. PNM200.

En ensayos metabólicos adicionales, que pretendían caracterizar la interacción *Paenibacillus* sp. PNM200, se observó la producción diferencial de metabolitos en ambos microorganismos en mono y co-cultivo. Se evidenció también que la adición de tejido vascular de tomate genera cambios significativos en el perfil metabólico de ambos microorganismos.

Al ser cultivado en un medio suplementado con tejido de tomate, el fitopatógeno FOL59 induce la síntesis de ácido fusárico, beauvericina J, y al menos cinco depsipéptidos estructuralmente relacionados a la beauvericina. Estos metabolitos son bien conocidos por su rol en la patogenicidad de *Fusarium* en plantas de tomate. Sin embargo, en co-cultivo con *Paenibacillus* sp. PNM200, se observó una reducción en la producción de estos metabolitos. Esta respuesta podría estar correlacionada con la disminución en la patogenicidad de FOL59 contra tomate en la interacción tripartita.

Por otra parte, los cambios más relevantes en el perfil metabólico de *Paenibacillus* sp. PNM200 en su interacción con FOL59 se asociaron a la producción de una familia de nueve péptidos, con pesos moleculares entre 1100-1600 Da, que se relacionan estructuralmente con los lipopéptidos Pelgipeptina B y Paneipaptina C. Tres de los péptidos se produjeron exclusivamente en el co-cultivo en medio suplementado con tomate. Los demás péptidos detectados en el co-cultivo presentaron un incremento de

entre 2 y 56 veces en su abundancia relativa en comparación con el monocultivo. Los extractos etanólicos enriquecidos en esta familia de péptidos mostraron actividad antifúngica contra la cepa tipo FOL CBS 164.85, con un valor de IC_{50} de $125 \mu\text{g}\cdot\text{mL}^{-1}$, confirmando su rol como antibióticos frente a FOL. Ninguno de estos péptidos fue identificado por derreplicación usando bases de datos y fuentes bibliográficas, lo que permite sugerir que pueden tratarse de metabolitos nuevos.

En este contexto, se propone que la actividad antifúngica *in vivo* de *Paenibacillus* sp. PNM200 está asociada a la síntesis de esta familia de péptidos, y que su producción es modificada (inducida o sobre-expresada) en respuesta a la presencia de FOL59. Esta hipótesis debe ser confirmada con nuevos experimentos dirigidos a evaluar la producción de los péptidos de interés bajo condiciones *in vivo*.

Palabras clave: Marchitez vascular, control biológico, *Paenibacillus*, bacterias derivadas de ambientes marinos, antibiosis, metabolómica.

Abstract

Vascular wilt (VW), caused by the phytopathogenic fungus *Fusarium oxysporum* f. sp. *lycopersici* (FOL), is a significant disease that limits the yield in tomato crop (*Solanum lycopersicum*). Marine-derived bacteria produce structurally diverse bioactive metabolites. These compounds have been used for phytopathogens control, and recently, alongside marine-derived bacteria proposed as biological control candidates. In the present research, the use of marine-derived bacteria, isolated from the Colombian Caribbean Sea as biocontrol agents for FOL was proposed.

The study was developed in three phases: (I) the selection and characterization of bacteria with antifungal activity against FOL, (II) the analysis of rhizospheric competence and in vivo antifungal activity of the active bacteria, and (III) the untargeted-metabolomic analysis of the interaction between tomato – *Paenibacillus* sp. - FOL under controlled greenhouse conditions and *Paenibacillus* sp. PNM200 - FOL by co-cultivation.

In phase I, primary screening was carried out with a marine -derived bacterial collection composed of 152 isolates. Twenty-eight bacterial strains were selected based on *in vitro* antifungal activity test against nine *F. oxysporum* isolates and one control pathogen FOL59. The phenotypical characterization and molecular identification of these isolates were done aiming to prioritize the better candidates to be tested on phase II. These processes lead to the selection of nine bacteria belonging to the Bacillales order, which presented the higher antifungal activity against FOL.

From phase II, isolate *Paenibacillus* sp. PNM200 was selected as a potential biocontrol strain. *Paenibacillus* sp. PNM200 colonized the root system of the tomato cultivars Milano and Santa Cruz Kada under greenhouse conditions and generated a positive effect on the

growth of the treated plants after 30 days inoculation (Santa Cruz Kada tomato cultivar). This effect was correlated with the ability of *Paenibacillus* sp. PNM200 to produce IAA (Indoleacetic acid) and solubilize phosphates. These results are one of the first evidence of marine-derived bacteria's rhizospheric competence of for its use as biocontrol agents.

As an effort to characterize the tripartite tomato plant-*Paenibacillus* sp. PNM200-FOL59 interaction, a LCMS metabolic profiling approach was developed as part of phase III. A significant accumulation of the steroidal glycoalkaloids (SGA) α -tomatine, hydroxytomatine, tomatidine tetrahexoside, and the aglycone tomatidine on the plant's root of was observed in the metabolic profiling experiments to characterize the tomato-FOL59 interaction. However, this effect was not detected in the tripartite tomato-*Paenibacillus* sp. PNM200-FOL59 interaction, nor in the metabolic profiles of the tomato root system treated with *Paenibacillus* sp. PNM200.

In other metabolomic experiments aimed at characterizing *Paenibacillus* sp. PNM200-FOL59 interaction, differential production of metabolites could be observed in the mono- and co-cultivation metabolic profiles of both microorganisms. Moreover, the addition of tomato vascular tissue also generated significant changes in the metabolic profile of both microorganisms.

The pathogenic strain FOL59, when cultured in a growth medium supplemented with tomato plant tissue, induced the synthesis of fusaric acid, beauvericin J, and at least five additional depsipeptides structurally related to beauvericin. These are well-known metabolites related to the pathogenic effect of *Fusarium* against plants. However, in co-cultivation with *Paenibacillus* sp. PNM200, a reduction in the production of these metabolites was observed. This response could be related to the decrease of FOL59 pathogenicity against the tomato.

On the other hand, the most relevant changes in the metabolic profiles of *Paenibacillus* sp. PNM200 were associated to the production of a family of nine peptides, with molecular weights between 1100-1600 Da, and structurally related to the peptide pelgipeptine B and paenipeptin C. Three of these peptides were produced exclusively in the co-culture when the growth medium was supplemented with tomato plant tissue. The other peptides detected in the co-culture showed a significant increase in their abundance compared to

the monoculture (2 to 56-fold change), suggesting their role in the biocontrol of FOL59. The ethanolic extracts enriched in this family of peptides showed antifungal activity against FOL CBS 164.85, with an IC₅₀ of 125 µg·mL⁻¹, confirming the role mentioned above as antibiotics against FOL. None of these peptides could be identified by dereplication using databases and literature sources, suggesting that they may be new metabolites.

In this context, it is proposed that the *in vivo* antifungal activity of *Paenibacillus* sp. PNM200 is associated with the synthesis of this family of peptides, and its production is modified (triggered and enhanced) in response to the presence of FOL59. This hypothesis must be confirmed by new experiments aimed at evaluating the peptides' production under *in vivo* conditions.

Keywords: Vascular wilt, biological control, *Paenibacillus*, marine-derived bacteria, antibiosis, metabolomics

Content

| | Pag. |
|---|-----------|
| 1. State of the art..... | 5 |
| 1.1 Tomato (<i>Solanum lycopersicum</i> L. var. <i>lycopersicum</i>) | 5 |
| 1.1.1 Taxonomy, origin, and relevance of cultivated tomato | 5 |
| 1.1.2 Tomato botany and general crop conditions..... | 6 |
| 1.1.3 Tomato worldwide production and cropping systems..... | 8 |
| 1.1.4 Tomato crops in Colombia. | 9 |
| 1.2 Phytosanitary problems related to tomato crops | 11 |
| 1.2.1 <i>Fusarium</i> vascular wilt..... | 13 |
| 1.2.2 Biology and pathogenicity of <i>Fusarium oxysporum</i> f. sp. <i>lycopersici</i> | 14 |
| 1.2.3 Management strategies for tomato vascular wilt. | 17 |
| 1.3 Biological control. | 19 |
| 1.3.1 Mechanisms used by biological control agents. | 21 |
| 1.3.2 Biological control of <i>Fusarium</i> vascular wilt. | 27 |
| 1.4 Marine-derived bacteria as a source of biological control agents against fungal phytopathogens..... | 30 |
| 1.5 Study of Colombian marine-derived microorganisms. | 33 |
| 2. Selection and characterization of marine-derived bacteria with antifungal activity against FOL..... | 35 |
| 2.1 Introduction and scope..... | 35 |
| 2.2 Materials and methods..... | 38 |
| 2.2.1 Microorganisms used in this study. | 38 |
| 2.2.2 Primary screening of marine-derived bacterium with antifungal activity against <i>F. oxysporum</i> | 39 |
| 2.2.3 Phenotypic and molecular characterization of active strains..... | 40 |
| 2.2.4 Active strain prioritization. | 41 |
| 2.3 Results and discussion | 42 |
| 2.3.1 Marine-derived bacteria display antifungal activity against <i>F. oxysporum</i> | 42 |
| 2.3.2 Potential biocontrol agents against <i>F. oxysporum</i> belongs to the order Bacillales..... | 44 |
| 2.3.3 Antifungal activity range leads to bacterial strains prioritization. | 48 |
| 2.4 Final remarks..... | 49 |
| 3. Colonization ability and <i>in vivo</i> antifungal activity of antagonist bacteria | 51 |
| 3.1 Introduction and scope..... | 51 |
| 3.2 Materials and methods..... | 54 |
| 3.2.1 Gnotobiotic root colonization assay on tomato plants. | 54 |

| | | |
|-----------|--|------------|
| 3.2.2 | Effect of tomato root exudates on the chemotactic response of <i>Paenibacillus</i> and <i>Bacillus</i> strains (in vitro assays)..... | 55 |
| 3.2.3 | <i>in vivo</i> biocontrol pot experiments..... | 56 |
| 3.3 | Results and discussion | 58 |
| 3.3.1 | Biocontrol <i>Paenibacillus</i> strains adapt to the tomato rhizosphere and promote plant growth under greenhouse conditions..... | 58 |
| 3.3.2 | <i>Paenibacillus</i> sp. PNM200 reduce tomato vascular wilt severity caused by FOL59..... | 64 |
| 3.4 | Final remarks..... | 69 |
| 4. | Metabolic profiling of tomato-<i>Paenibacillus</i> PNM200-FOL59 interaction..... | 71 |
| 4.1 | Introduction and scope..... | 71 |
| 4.2 | Materials and methods..... | 73 |
| 4.2.1 | <i>In vivo</i> interaction assay under controlled conditions..... | 73 |
| 4.2.2 | Metabolites extraction and sample preparation..... | 74 |
| 4.2.3 | Ultrahigh-Performance Liquid Chromatography-MS (UHPLC-MS) analyses..... | 75 |
| 4.2.4 | Data analyses..... | 76 |
| 4.2.5 | Metabolite annotation and semi-quantitative comparison | 77 |
| 4.3 | Results and discussion | 77 |
| 4.3.1 | Inoculation of <i>Paenibacillus</i> sp. PNM200 does not induce significant changes in tomato roots metabolic profile and reduces the effect caused by FOL59..... | 77 |
| 4.3.2 | FOL59 infection generates tomatidine and steroidal glycoalkaloid accumulation on tomato roots..... | 83 |
| 4.4 | Final remarks..... | 90 |
| 5. | Metabolic profiling of <i>Paenibacillus</i> sp. PNM200-FOL59 interaction..... | 93 |
| 5.1 | Introduction and scope..... | 93 |
| 5.2 | Materials and methods..... | 96 |
| 5.2.1 | Binary co-cultures..... | 96 |
| 5.2.2 | Metabolite extraction and sample preparation..... | 96 |
| 5.2.3 | Ultrahigh-Performance Liquid Chromatography-MS/MS (UHPLC-MS7MS) analyses..... | 97 |
| 5.2.4 | Data analyses..... | 99 |
| 5.2.5 | Metabolite annotation | 99 |
| 5.2.6 | Biological activity..... | 99 |
| 5.2.7 | GNPS Feature-based molecular networking workflow | 100 |
| 5.2.8 | Compound isolation..... | 101 |
| 5.3 | Results and discussion | 102 |
| 5.3.1 | FOL59 metabolome changes in presence of tomato tissue and <i>Paenibacillus</i> sp. PNM200..... | 102 |
| 5.3.2 | Metabolites produced by FOL59 on TPDA are related to Beauvericin phytotoxins family..... | 107 |
| 5.3.3 | <i>Paenibacillus</i> sp. PNM200 produces peptides with antifungal activity during co-culture with FOL59 on TPDA medium..... | 110 |
| 5.3.4 | Antifungal peptides produced by <i>Paenibacillus</i> sp. PNM200 are lipopeptides related to Pelgipeptin B and Paenipeptin C..... | 117 |
| 5.4 | Final remarks..... | 121 |
| 6. | Conclusions and recommendations | 122 |
| 6.1 | Conclusions..... | 122 |

| | |
|---|------------|
| 6.2 Future perspectives..... | 125 |
| Appendix A. Phenotypic characteristics of active selected bacteria..... | 127 |
| Appendix B. Fungal phytopathogen used in this study | 129 |
| Appendix C. Isolation of FOL59 on tomato cv. Santa Cruz Kada root system, and symptoms of VW observed at 4, 15 and 30 dpi..... | 130 |
| Appendix D. Concentration of BCA candidates on tomato roots..... | 131 |
| Appendix E. Principal Component Analyses (PCA) score-plot of P (a), PB (b), PF (c) and PBF (d) treatments..... | 132 |
| Appendix F. Metabolic profile of FOL59 ethyl acetate extracts..... | 133 |
| Appendix G. Global molecular network of ethyl acetate extracts of <i>Paenibacillus</i> sp. PNM200-FOL59 interaction..... | 134 |
| Appendix H. Representative ¹H- NMR spectra of paenipeptin C (a) and compound 28 (b)..... | 135 |
| Appendix I. Global molecular network of ethanolic extracts of <i>Paenibacillus</i> sp. PNM200-FOL59 interaction..... | 136 |

Figure list.

| | Pag. |
|--|-------------|
| Figure 1-1: Growth stages of tomato..... | 7 |
| Figure 1-2: Planted area and tomato production in Colombia during the first semester of 2019 according to ENA-DANE reports..... | 10 |
| Figure 1-3: Representative symptoms of tomato vascular wilt, described by Carmona et al. | 13 |
| Figure 1-4: General vascular wilt disease cycle caused by members of the FOC (129). | 16 |
| Figure 1-5: Commonly used BCA for <i>Fusarium</i> VW control between 2000-2016..... | 27 |
| Figure 2-1: Dual-cultured assay of Firmicutes-like bacteria against FOL59..... | 43 |
| Figure 2-2: Antifungal activity of the pre-selected 28 firmicutes-like bacteria on agar well diffusion assay against <i>F. oxysporum</i> | 43 |
| Figure 2-3: Molecular Phylogenetic analysis by Maximum Likelihood method of partial 16S rDNA sequences | 46 |
| Figure 2-4: Bacterial strains prioritization by PCA..... | 49 |
| Figure 3-1: General phases of root colonization by beneficial microorganisms as proposed by Pieterse et al. | 52 |
| Figure 3-2: Examples of colonization profiles of different Firmicutes strains on tomato roots (Milano cv.). | 59 |
| Figure 3-3: Colonization profile of the selected bacteria on Milano and Santa Cruz Kada cultivars. | 60 |
| Figure 3-4: SEM depicts root colonization by <i>Paenibacillus</i> sp. PNM65 (a) and PNM210 (b) in tomato cv. Santa Cruz Kada roots at 4 dpi..... | 61 |
| Figure 3-5: Chemotactic response of <i>Paenibacillus</i> strains towards tomato root exudates (1X) on the modified soft agar chemotactic assay | 62 |
| Figure 3-6: Effect of bacterial inoculation on tomato plant growth (Santa Cruz Kada cultivar). | 63 |
| Figure 3-7: <i>In vivo</i> antifungal activity of <i>Bacillus</i> and <i>Paenibacillus</i> strains against FOL59. | 65 |
| Figure 3-8: <i>In vivo</i> antifungal activity of <i>Paenibacillus</i> PNM200 against FOL59 | 67 |
| Figure 3-9: Growth kinetics and antifungal activity of <i>Paenibacillus</i> PNM200 under liquid fermentation..... | 68 |
| Figure 4-1: Chromatographic profile of tomato roots (blue), soil (red), rhizospheric soil (green) and solvent blank samples. | 78 |

| | |
|---|-----|
| Figure 4-2: Principal components analysis (PCA) score plot indicating the general grouping of the variables in the data sets of root and soil extracts..... | 79 |
| Figure 4-3: PCA score plot indicating the general grouping of the variables in the data sets of root extracts..... | 82 |
| Figure 4-4: Chromatographic profile of P (blue), PB (red) and PBF (black) treatments at 10 dpi. | 82 |
| Figure 4-5: OPLS-DA model of P and PF treatments. The figure presents the score plot (a) and the S-plot (b) of the OPLS-DA model. | 84 |
| Figure 4-6: Chromatographic profile of uninoculated (P, black) and infected (PF, red) plants at 10 dpi. | 84 |
| Figure 4-7: Changes in SGA and related molecules levels in tomato roots on uninoculated (P) and infected plants (PF) 10 dpi..... | 88 |
| Figure 4-8: Chromatographic profile of FOL59 culture on tomato supplemented solid medium. | 89 |
| Figure 5-1: Scheme representation of mono and co-cultures of <i>Paenibacillus</i> sp. PNM200 and FOL59..... | 96 |
| Figure 5-2: Principal components analysis (PCA) score plot indicating the general grouping of the variables in the ethyl acetate extracts datasets..... | 103 |
| Figure 5-3: OPLS-DA model score plot (a,b) and S-plot (c,d) of ethyl acetate extracts of FOL59. | 104 |
| Figure 5-4: Relative amounts of fusaric acid produced by FOL59 in PDA and TPDA mediums. | 105 |
| Figure 5-5: Relative amounts of metabolites 13 to 18 produced by FOL59 in PDA and TPDA mediums..... | 106 |
| Figure 5-4: Ethyl acetate extracts molecular networks 1 (a) and 14 (b) created from FOL59 dataset. | 108 |
| Figure 5-7: Principal components analysis (PCA) score plot indicating the general grouping of the variables in ethanolic extracts from monoculture and co-culture of <i>Paenibacillus</i> sp. PNM200 growth zone..... | 110 |
| Figure 5-8: Chromatographic profile of ethanolic extracts from monoculture and co-culture of <i>Paenibacillus</i> sp. PNM200 on PDA and TPDA medium. | 111 |
| Figure 5-9: Structural elucidation of cyclic lipopeptide Permetin A/PGP-B and compound 26 by tandem MS analysis. | 113 |
| Figure 5-10: Structural elucidation of cyclic lipopeptide Paenipeptin C and compound 28 by tandem MS analysis..... | 115 |
| Figure 5-11: Peptide bio-guided isolation workflow..... | 116 |
| Figure 5-11: Cluster 2 from the molecular network obtained from the ethanolic extracts from <i>Paenibacillus</i> sp. PNM200 dataset. | 120 |
| Figure 6-1: Proposed model of tomato- <i>Paenibacillus</i> sp. PNM 200-FOL59 interaction. | 124 |

Table list

| | Pág. |
|---|------|
| Table 1-1: Common bacterial and fungal disease of tomato crops (97). | 12 |
| Table 1-2: Main modes of action of biological control agents (165)..... | 21 |
| Table 1-3: Examples of BCA used for <i>Fusarium</i> VW control in tomato. | 28 |
| Table 1-4: Marine-derived bacteria with antifungal activity against fungal phytopathogens. | 31 |
| Table 2-1: Active bacterial strains source and CWDE production. | 45 |
| Table 3-1: PGPR related characteristics of the tomato growth-promoting <i>Paenibacillus</i> sp. PNM200 and PNM210. | 63 |
| Table 4-1: Treatments and control groups established for the metabolic profiling of tomato-FOL59- <i>Paenibacillus</i> sp. PNM200 interaction. | 74 |
| Table 4-2: Data processing parameters use in MzMine for data matrix generation of tomato-FOL59-PNM200 interaction. | 76 |
| Table 4-3: OPLS-DA models cross-validation. | 80 |
| Table 4-4: Annotation of the statistically significant secondary metabolites identified within methanolic extracts of roots from uninoculated (P) and infected (PF) plants treatments. | 85 |
| Table 5-1: Data processing parameters use in MZmine for data matrix generation of ethyl acetate and ethanol extracts of co-culture samples..... | 98 |
| Table 5-2: OPLS-DA models cross-validation. | 104 |
| Table 5-3: Statistically significant secondary metabolites identified within FOL59 ethyl acetate extracts..... | 105 |
| Table 5-4: PCA and OPLS-DA models cross-validation of ethanolic extracts from <i>Paenibacillus</i> sp. PNM200 monoculture and co-culture. | 111 |
| Table 5-5: Statistically significant secondary metabolites identified within ethanolic extracts from <i>Paenibacillus</i> sp. PNM200 monoculture and co-culture on TPDA. | 112 |
| Table 5-6: Antifungal activity of ethyl acetate and ethanolic extracts of <i>Paenibacillus</i> sp. PNM200 against FOL CBS 164.85 | 116 |

Symbols and abbreviations list

Symbols with Latin letters

| Symbol | Term |
|--------|--------------------|
| B | Billion dollars |
| d_4 | Deuteration degree |
| Da | Daltons |
| g | Grams |
| Hz | Hertz |
| Kg | Kilogram |
| L | Liters |
| M | Million dollars |
| mg | Milligrams |
| mL | Milliliters |
| mM | Millimolar |

Symbols with Greek letters

| Symbol | Term |
|---------------|------------|
| μL | Microliter |
| μm | Micrometer |
| μM | Micromolar |

Abbreviations

| Abbreviation | Term |
|------------------------|---|
| ACN | Acetonitrile |
| ANLA | Autoridad Nacional de Licencias Ambientales |
| AUDPC | Area under the disease progress curve |
| BNF | Biological Nitrogen Fixation |
| CCP | Co-culture on PDA medium |
| CCT | Co-culture on TPDA medium |
| CD_3OD | Metanol- d_4 |
| CFU | Colony forming units |
| CTAB | Cetyl Trimethyl Ammonium Bromide |
| CWDE | Cell wall degrading enzymes |
| DAD | Diode Arrangement Detector |
| DNA | Desoxyribonucleic Acid |

Abbreviation Term

| | |
|---------|---|
| dpi | Days post-inoculation |
| EDTA | Ethylenediaminetetraacetic acid |
| ELSD | Evaporative light scattering detector |
| EPS | Exopolysaccharide |
| ESI | Electrospray Ionization |
| FOL | <i>Fusarium oxysporum</i> f. sp. <i>lycopersici</i> |
| f. sp. | <i>Formae specialis</i> |
| GNPS | Global Natural Products Social Molecular Networking |
| HPLC | High performance liquid chromatography |
| IAA | Indoleacetic Acid |
| ISR | Induced systemic resistance |
| LB | Luria Bertani |
| MCP | Monoculture on PDA medium |
| MCT | Monoculture on TPDA medium |
| MeOH | Methanol |
| MS | Mass spectrometry |
| MS/MS | Tandem mass spectrometry |
| OPLS-DA | Orthogonal partial least squares discriminant analysis |
| P | Plant control |
| PB | Plant-bacteria interaction |
| PBF | Plant-bacteria-fungi interaction |
| PF | Plant-Fungi interaction |
| PCA | Principal component analysis |
| PCR | Polymerase Chain Reaction |
| PDA | Potato Dextrose Agar |
| PGPR | Plant growth promoting rhizobacteria |
| PGPB | Plant growth promoting bacteria |
| ppm | Parts per million |
| ROC | Receiver Operating Characteristic |
| SEM | Scanning Electron Microscopy |
| SI | Severity index |
| SCL | <i>S. lycopersicum</i> L. var <i>cerasiforme</i> |
| SLL | <i>Solanum lycopersicum</i> L. var. <i>lycopersicum</i> |
| SP | <i>S. pimpinellifolium</i> L |
| SPE | Solid-phase Extraction |
| TPDA | Tomato-supplemented PDA medium |
| VW | Vascular wilt |
| ZIP | Inhibition zone on PDA media |
| ZITP | Inhibition zone on TPDA media |

Introduction

Tomato (*Solanum lycopersicum* L. var. *lycopersicum*) is one of the world's most economically and socially essential crops. This solanaceous plant is cultivated in tropical and subtropical regions under greenhouse or field conditions (1). Tomatoes are commercialized as fresh or processed commodities (2). By 2017 the world area cultivated with tomatoes was close to 4.8 million hectares, from which approximately 182 million tons were produced (3). Given its extension and productivity, the tomato market obtained incomes close to 190.4 billion dollars during 2018, being the second most cultivated solanaceous in the world, only behind potatoes (3, 4).

Given its physiological characteristics and economic importance, tomato is recognized as a model plant for basic and applied research (5-8). Most of such research is focused on studying of the interaction between this plant and fungi from the *Fusarium oxysporum* complex (FOC) (9-11).

Fusarium oxysporum Schlecht. F. sp. *lycopersici* (Sacc.) Snyder & Hansen (FOL), the causal agent of vascular wilt (VW), is of great interest in plant-pathogen interaction studies due to the co-evolution process developed with its host plant (tomato) (12), its hemibiotrophic lifestyle (13, 14), its wide distribution, and the impact that generates on crop productivity (15, 16).

FOL is a soil-borne pathogen with three physiological races described according to pathogenicity towards specific tomato cultivars (12). This microorganism colonizes tomato root system's surface and invades the root system and vascular vessels (10). Once inside the plant, FOL spreads rapidly, causing interference with the water transport systems (17), which leads to the collapse of the vascular vessels, causing wilting and subsequent death of the host (18-20).

FOL can survive for long periods in the form of chlamydospores in soil or within the vascular tissue of infected plants, being a constant constraint in tomato crops (17). The main strategies for FOL control include the implementation of cultural practices, chemical control, resistant varieties, and biological control (14, 15).

Biological control is a sustainable and eco-friendly strategy that reduces the negative impacts of phytopathogens on crop yield. Although commercial biological control agents (BCA) for FOL management are available, reproducibility problems under field conditions have limited their use (21, 22). Overcoming this problem requires a proper assessment of the performance for the new BCAs. The most comprehensive strategy used for this purpose is the bioprospection of potential BCA with several modes of action in rhizospheric environments (23, 24).

Other approaches take into consideration microorganisms isolated from poorly explored environments. This new group of interest includes marine-derived bacteria. These microorganisms are characterized by their ability to survive in environments with fluctuating conditions (25), and produce a wide diversity of bioactive metabolites, including compounds with antifungal activity against phytopathogens such as *Rhizoctonia solani*, *Botrytis cinerea*, *F. oxysporum*, *P. capsici*, *Colletotrichum acutatum*, *C. gloeosporioides*, and *Phytophthora ultimum* (26-33).

Despite their potential, studies on these bacteria focused on *in vitro* evaluation of the bioactive metabolites and, to a lesser extent, have addressed their use as BCA through inoculation tests in leaves, fruits, or soil (31, 34, 35). To date, obtained data reveal the potential of marine-derived bacteria to act as effective BCA. However, it is necessary to carry out rigorous evaluations to provide evidence on marine bacteria's survival and persistence in terrestrial niches. Additionally, it is essential to establish the effects of these bacteria on healthy plant growth, verify their ability to reduce disease symptoms under *in vivo* conditions, and characterize its interaction with the plant host and the pathogen to increase the amount of information regarding the biocontrol phenotype.

Omics approaches have been suggested as the best workflow options to obtain relevant information about the effects of BCA-inoculation in plant development. From them, non-target metabolomics studies have been used for characterizing plant-pathogen and plant-

beneficial microbes interactions (36-40). Obtaining the metabolic profiles of the tritrophic BCA-phytopathogen-plant interaction makes feasible to evaluate the metabolites' quantitative and qualitative changes that may be associated with the phenotype observed in the interaction (41, 42). The information generated from those profiles can be used to construct metabolic signatures that identify biomarkers that can be followed under field conditions to evaluate either the disease progress, or the biocontrol efficiency on early and late stages of the interaction (43, 44).

In this context, the present research describes the characterization and selection process of one marine-derived bacteria with antifungal activity against FOL under *in vitro* and *in vivo* conditions and a metabolic profiling of such bacterial interaction with FOL and tomato under controlled conditions. The selected strain was obtained from a marine-derived collection of 152 isolates obtained from Santa Catalina and Providencia coral reef (Colombia) recovered by the research group "Estudio y aprovechamiento de productos naturales y frutas de Colombia" (27).

Chapter 1 presents the state of the art regarding tomato, *Fusarium* vascular wilt, biological control, and marine-derived bacteria as BCA candidates. Chapter 2 includes the screening for potential BCAs against Colombian isolates of *F. oxysporum* within the bacterial collection. This chapter also presents the phenotypic characterization, taxonomical classification, and prioritization of active strains for *in vivo* assays. Colonization and antifungal *in vivo* assays performed with the selected group of active bacteria are described in chapter 3. Chapter 4 shows the results obtained from the no-targeted metabolomic study of tomato-FOL-BCA interaction under gnotobiotic conditions, followed by chapter 5 that describes the metabolic profiling of FOL-BCA co-culture. A final chapter (chapter 6) shows the conclusion and recommendations derived from these results.

1.State of the art

1.1 Tomato (*Solanum lycopersicum* L. var. *lycopersicum*).

1.1.1 Taxonomy, origin, and relevance of cultivated tomato

Solanaceae is an angiosperm family with over 3000 species described so far. The largest genus of this family, *Solanum*, encompasses nearly half of the species reported in the entire family (1200-1700 spp.). This genus includes some major crop species such as potato (*S. tuberosum*), eggplant (*S. melongena*), and tomato (*S. lycopersicum*) (45).

Tomato (*Solanum lycopersicum* L. var. *lycopersicum*; SLL) is a widely distributed plant with high socio-economic importance. Initially, the tomato plant was classified as *Lycopersicon esculentum* until data from chloroplast DNA restriction and phylogenetic analyses allowed its re-integration into the *Solanum* genus, Lycopersicon section (46, 47). This section consists of SLL and twelve wild relatives: *S. arcanum*, *S. cheesmaniae*, *S. chilense*, *S. chmielewskii*, *S. corneliomulleri*, *S. galapagense*, *S. habrochaites*, *S. huaylasense*, *S. neorickii*, *S. pennellii*, *S. peruvianum*, and *S. pimpinellifolium* (48).

The wild relatives of SLL are native from South America (49). It is inferred that tomato domestication started from *S. pimpinellifolium* L (SP) (50), which gives rise to five populations of semi-domesticated *S. lycopersicum* L. var *cerasiforme* (SCL) through natural divergence. These groups were distributed in Ecuador, Peru, Mexico, Central America, and northern South America. Later, SCL was fully domesticated in Mesoamerica, giving rise to SLL, which was taken to Europe around the sixteenth century (51).

Initially, tomatoes were not used as food in Europe. The first reports indicating consume of tomatoes are from the seventeenth and eighteenth centuries in southern European

countries (52). Nowadays, tomatoes are consumed as fresh, preserved (e.g. dried fruits, tomato pulp) or processed forms (e.g. juice, tomato sauces, and ketchup), (53).

Either in fresh or processed forms, tomatoes are a rich source of nutrients including carbohydrates, proteins, vitamins (A and C), and minerals (calcium, magnesium, phosphorus, potassium, manganese, and zinc) (54). Other constituents, such as lycopene (carotenoid) and some glycoalkaloids, have antioxidant and anticancer activities, increasing tomatoes nutritional value (55-57). Given its commercial demand, tomato is subject to constant research in breeding programs that aim to obtain accessions (cultivars) with higher productivity and tolerance to biotic and abiotic stresses, that produce fruits with better sensory and health value (53).

Beyond agronomical purposes, tomato is a model plant for basic research useful for its short generation time, elementary diploid genetics, and inbreeding tolerance (58). Unlike other plant models, tomato produces fleshy fruits, has sympodial shoots, compound leaves, and a well-known genetic transformation protocol as well as transcriptomic, proteomic, and metabolomics data publicly available (1, 59-61).

Moreover, in 2012, the genome of tomato (cultivar 'Heinz 1706') was sequenced and annotated, alongside its wild relative SP (8). That project increased the already vast genetic information available for this plant (62) and supported the tomato pan-genome creation in 2019 (63). Altogether, these data allow using tomato as a model plant for the study of fruit development, ripening and quality (7, 53, 63-65), disease resistance (66-69), plant-pathogen interactions (9, 20, 70-73), and novel metabolites with beneficial effects on human health (56, 57, 74, 75).

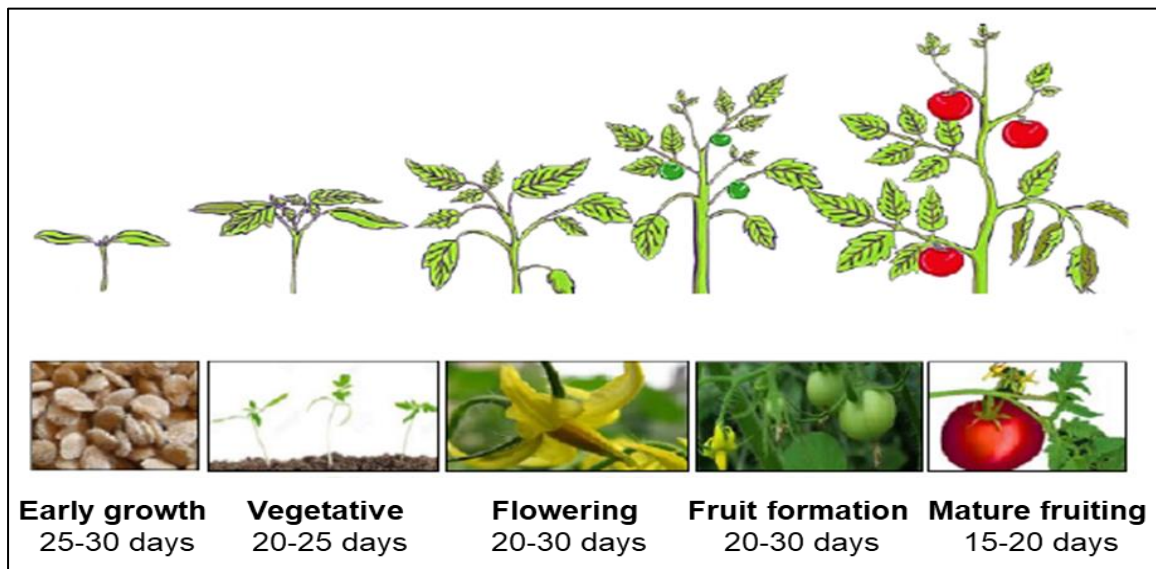
1.1.2 Tomato botany and general crop conditions.

Cultivated tomato (SLL) is a diploid, perennial, and autogamous C3 plant with a high degree of homozygosity (49). Its stems are hairy, and its leaves bipinnate (compound leaves). Its flowers have five to seven petals, and inserted styles. Originally, tomato and its wild relatives were distributed in diverse habitats that cover from the Pacific coast (sea level) to mountainous Andean regions (altitude of 3,300 meters), which contributed to the variability of this species (49).

Tomato plants have five growth stages: (i) germination and early growth, (ii) vegetative period, (iii) flowering, (iv) early fruiting, and (v) mature fruiting (Figure 1-1) (76). Depending on the cultivar and variety, the tomato lifecycle could have an estimated duration between 50 to 160 days (77). Two tomato types are currently grown: determinate tomato (also known as bushy) and indeterminate tomato. Determinate tomato has a one-time flowering and fruit development period, while indeterminate tomato produces inflorescence and flowers continuously throughout their lifecycle.

Germination, leaf and truss appearance, and fruit development depends on temperature. During germination, a minimum temperature of 13°C is needed (optimum temperatures are between 20°C and 25°C), while a range between 18 to 25 °C is optimal for vegetative growth and leaf and fruit development (78). Standard salinity conditions for tomato grown, expressed as the electrical conductivity (EC), can range from 1.6 to 5.0 dS/m. Higher EC conditions can negatively affect nitrogen uptake, increase sodium (Na⁺) and chloride (Cl⁻) uptake, and induce stress by dehydration that conduces to nutritional imbalance and wilting (79).

Figure 1-1: Growth stages of tomato (76).



Tomato can grow on a wide variety of soil types with high organic matter (80). For optimal tomato grown, soil pH and humidity must be between 6-7 and 65-75%, respectively. This plant requires a light intensity ranging from 10.000 to 15.000 lux. Other considerations that directly affect tomato yields, such as plant density, irrigation, and fertilization, vary

according to the cropping system (open-field or greenhouse) and the selected cultivar (81-83).

1.1.3 Tomato worldwide production and cropping systems.

Tomato is cultivated in open-field systems or controlled greenhouse conditions (2, 52). In 2018, the estimated global area dedicated to this crop was 4.76 million hectares with production above 182 million tons, becoming the second most cultivated solanaceous worldwide and accounting 15% of the world vegetable production (3).

In the same year, the tomato market had a revenue amounted to 190.4B dollars, and 7.3 M tons were exported globally with an estimated value of 9.7B dollars (4). Tomato's leading producers include China, the United States of America (USA), India, Turkey, Egypt, Italy, Iran, Spain, Brazil, and Mexico (3). Mexico, Spain, and Turkey, alongside The Netherlands and Morocco, have the highest exportations of this vegetable. Some of these countries do not have the ideal climate conditions for tomato grown neither have a large area dedicated to this crop. Their productivity and quality are related to the use of controlled greenhouse systems (2).

Many factors influence tomato crop yield, including genetics, environmental conditions (biotic and abiotic), and crop management (i.e. production system). It has been estimated that tomato yield is higher in greenhouse systems than on field conditions. Greenhouse crops allow to control cultivation period's length and optimize environmental conditions (e.g. light, humidity, temperature, CO₂ levels) and fertilization practices, irrigation, and pest, and disease control (80, 84). Open-field systems expose the crop to conditions that cannot be controlled, such as climate (85). Also, disease and pest management are more laborious and expensive, to a certain extent, in open-field than in greenhouse conditions.

Even when tomato plants originated in western South America, only Mexico and Brazil appear as significant producers of this Solanaceae (3). From them, Mexico stands as the main exporter, but its fruit economic value is lower than products from other countries such as The Netherlands (2). Reduced fruit value could be related to the lower technification in tomato growing systems in South America, where the agriculture modernization has polarized the agronomic production structure.

Countries like Brazil, Chile, Colombia, Ecuador, Mexico, and Nicaragua implement the family farming system for vegetables and fruit production (86). These farming units can be classified as subsistence, transition, or consolidated, being the first one, subsistence family farming, the most common in Latin America. This kind of farming unit has low technification, limited land, capital, reduced production, and minor participation in markets and productive chains (87).

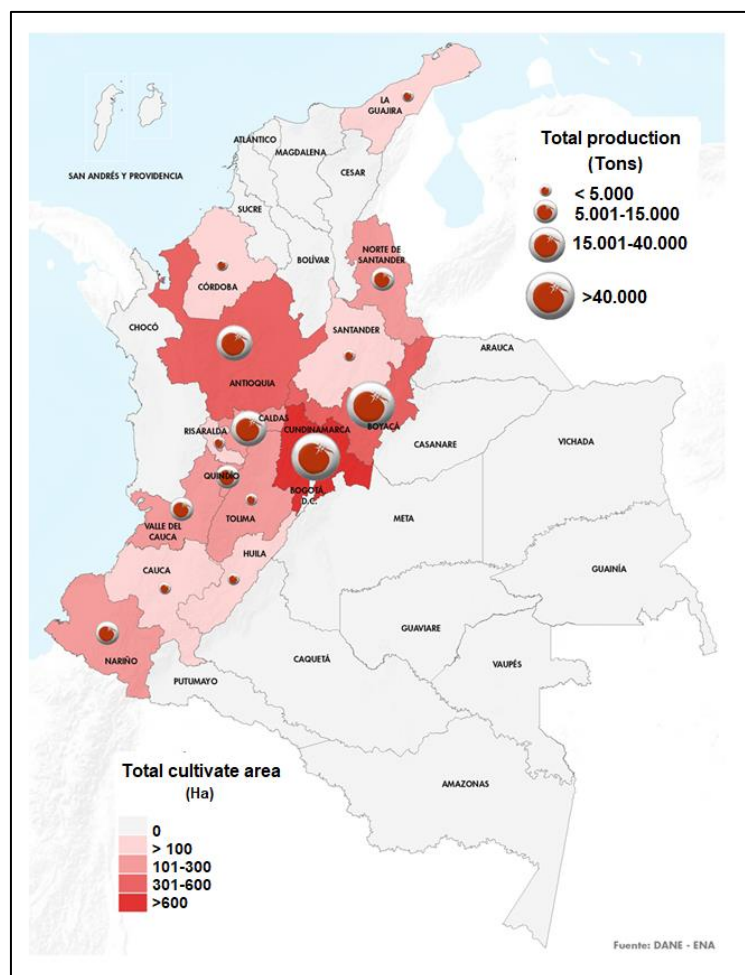
Even so, these systems generate between 57-77% of agricultural employments and support agrarian families in overcoming poverty (87). Thus, it is necessary to implement management programs that improve crop yield in this farming unit making them competitive in the local and international agricultural market.

1.1.4 Tomato crops in Colombia.

In Colombia, tomato represents one of the staple foods with an estimated annual consumption per capita of 9.4 Kg (88). During the first semester of 2019, tomato total planted area and total harvested area in the country were 5.449 and 3.572 Hectares, respectively (89). From them, 248.887 tons were produced, achieving yields of 69.7 Ton per hectare (89) which is higher than the reported yields from open-field systems in Mexico (36.1-45.5 Ton per hectare) but lower than greenhouses and shade cloth greenhouses (122.1 and 176.1 Ton per hectare) (90).

Colombia has several lands with optimal conditions for tomato growth. This crop is present in 19 departments, from which Cundinamarca, Antioquia, Boyacá, and Norte de Santander have the largest cultivated area and higher productivities (Figure 1-2). Either in open-field or greenhouse conditions, tomato production is carried out by employing soil as a substrate, and the obtained fruits are used mainly for Colombian local markets. Open-field is the most common system (14.768 ha in 2014), established for small processing-type “Chonto” tomato (91). Unfortunately, this production system uses sub-optimal practices as a consequence of limitations in the size of cultivated area (carried out by smallholders), lower planting density, level of investment on infrastructure, and incorrect use of inputs (mainly agrochemicals) that reduce tomato yield (92-94).

Figure 1-2: Planted area and tomato production in Colombia during the first semester of 2019 according to ENA-DANE reports (89).



Colombian greenhouse systems account for nearly 30% of the planted area (2.305 ha in 2014) and produce mainly “Chonto” and beefsteak-type tomato (91, 92). Most greenhouse crops are fairly high-intensive systems with low-tech structures that adopt primary climate control, fertigation, pruning, and training systems (93, 94). In Boyacá and Santander, greenhouses are used only for tomato production, while open-field systems have a rotative schedule that includes corn (*Zea mays*), green beans (*Phaseolus vulgaris*), cucumber (*Cucumis sativus*), and squash (*Cucurbita* spp.) (94). Interestingly, tomato plant averages yields are higher in open-field crops (4.88 Kg· planta⁻¹) than in greenhouses (2.48 Kg·planta⁻¹), indicating that under proper management programs, it is possible to improve open-field productivity of this solanaceous plant (94, 95).

In the study conducted by Gil, Bojacá & Schrevens, the authors mentioned that Colombian small farmers have the pre-conceived idea that larger agrochemical applications lead to larger productions (94, 95). As a consequence of this conception, Colombian farmers tend to use inadequate amounts of fertilizers, pesticides, and fungicides, aiming to increase plant productivity and control of pest and fungal phytopathogens (84, 93, 95).

This practice increases production costs and directly reduces fruit value due to residual components of the used agrochemicals in the fresh fruits, making them inadequate for exportation (93). In order to prevent this outcome, it is necessary to implement strategies such as the use of cultural practices, biological inoculants, and organic amendments that reduce the number of agrochemicals applied, increasing the efficiency of nutrient uptake, limiting the effects of pest and diseases on tomato yields and reducing the residual agrochemicals on harvested fruits.

1.2 Phytosanitary problems related to tomato crops

Production and quality of tomato are affected by pests and diseases in the field/greenhouse and during post-harvest processing. To date, more than 200 pests and diseases have been reported in tomato crops, including insects, fungi, oomycetes, nematodes, bacteria, and viruses (96).

Tomato pests include plant-feeding mites, aphids, psyllids, whiteflies, mealybugs, leaf miners, caterpillars, and thrips (97). Currently, the pinworm *Tuta absoluta* (Meyrick), an invasive species native of Peru, is considered the major pest in tomato crops. It has spread from South America to different European and Asiatic countries, generating significant economic losses in tomato crops (98-101).

Similarly, a high diversity of viruses (more than 136) have been identified as tomato pathogens (102). Most of these viruses, such as *Tomato yellow leaf curl virus*, belong to the *Begomovirus* genus and are the most representative viral pathogens of tomato (103). Other viruses like the *Pepino mosaic virus* (PepMV) and the *Tomato torrado virus* (ToTV) cause diseases that have emerged in greenhouse tomato crops as a consequence of the efficiency of their vectors, and the virus itself, to spread and survive in the controlled conditions of greenhouses (102).

Likewise, Oomycetes like *Phytophthora infestans*, are considered one of the most destructive pathogens in tomato and potato crops, causing significant production losses (20–70%) (104-106). Other members of the genus *Phytophthora* that infects tomato are *P. capsici* (107) and, *P. parasitica* (108). Although they are less studied, these pathogens also cause multibillion-dollar losses in crop production (109).

Diseases caused by bacteria and fungi on tomato crops are widespread, infect all tomato tissues (roots, stem, leaves, flowers, and fruits), and affect tomato plants during the five phenological stages. Due to its relevance in the crop system, bacterial and fungal pathogens have driven plant resistance breeding programs to reduce the traditional chemical management on field conditions. Table 1-1 presents some of the most relevant bacterial and fungal phytopathogens of tomato (described in detail in (97)).

Table 1-1: Common bacterial and fungal disease of tomato crops (97).

| Type of microorganism | Disease | Pathogen | Affected tissue |
|-----------------------|------------------------------------|---|-----------------------------|
| Fungi | Anthraxnose | <i>Colletotrichum</i> spp. | Foliar disease |
| Fungi | Grey leafspot | <i>Stemphylium</i> spp. | Foliar disease |
| Fungi | Grey mould | <i>Botrytis cinerea</i> Fr. | Above-ground tomato tissues |
| Fungi | Leaf mould | <i>Passalora fulva</i> (Syn. <i>Cladosporium fulvum</i>) | Foliar disease |
| Fungi | Septoria leaf spot | <i>Septoria lycopersici</i> | Above-ground tomato tissues |
| Fungi | Target spot | <i>Corynespora cassicola</i> | Foliar disease |
| Fungi | <i>Fusarium</i> vascular wilt | <i>F. oxysporum</i> f. sp. <i>lycopersici</i> | Systemic (roots and xylem) |
| Fungi | <i>Fusarium</i> crown and root rot | <i>F. oxysporum</i> f. sp. <i>radicis-lycopersici</i> | Systemic (roots and xylem) |
| Fungi | Early blight | <i>Alternaria solani</i> | Foliar disease |
| Bacteria | Bacterial wilt | <i>Ralstonia solanacearum</i> | Systemic (roots and xylem) |
| Bacteria | Bacterial spot | <i>Xanthomonas vesicatoria</i> , <i>X. euvesicatoria</i> , <i>X. perforans</i> and <i>X. gardneri</i> | Foliar disease |
| Bacteria | Bacterial speck | <i>Pseudomonas syringae</i> pv. <i>tomato</i> | Foliar disease |
| Bacteria | Bacterial canker | <i>Clavibacter michiganensis</i> ssp. <i>michiganensis</i> (Smith) | Foliar disease |

In Colombia, the most prevalent diseases of tomato crops are anthracnosis, early and late blight, bacterial canker, bacterial spot, crown root rot, and *Fusarium* vascular wilt (110). Although there is no clear information about economic losses, the mentioned diseases are considered a factor that limits tomato yield in the country. The present research focused on

Fusarium vascular wilt, a widespread disease in Colombia's principal producer departments, that can spread rapidly, resulting in devastating losses and does not have a unique chemical control method that entirely eliminates the pathogen (111).

1.2.1 *Fusarium* vascular wilt.

Fusarium vascular wilt (VW) is a disease caused by members of the *F. oxysporum* complex. More than 100 plant species are susceptible to FOC infection, including some economically important crops such as Melon, Bean, Banana, Chickpea, Lettuce, Tobacco, grapes (10). Tomato VW, caused by *F. oxysporum* f. sp. *lycopersici* (Sacc.) Snyder & Hansen (FOL), has been reported in more than 32 countries, particularly in countries with a warm climate (112).

VW can generate production losses up 45% to 80% in susceptible tomato cultivars (12, 113-115). In tomato seedlings, FOL can cause damping-off typified by yellowing, stunting, and wilting (15). In mature plants, VW causes foliage yellowing symptoms that are usually seen on one side of the plant during the early stages of infection. As the infection progress, the yellowing advance until it can be seen in the entire plant, followed by the wilting of a part of the plant that develops in the whole plant (Figure 1-3). These symptoms are usually seen at the flowering and fruit set stages (15) and can lead to minimal or absent crop yield.

Figure 1-3: Representative symptoms of tomato vascular wilt, described by Carmona et al. (115). From left to right: initial plant chlorosis symptoms, wilting symptoms on plant and vascular browning of the xylem vessels.



Both yellowing and wilting are consequences of xylem vessel clogging and severe water stress caused by FOL spread in vascular tissue and its ability to inhabit the plant xylem vessel (116, 117). Discoloration and posterior browning of the vascular system also indicate FOL vascular colonization (Figure 1-3) (15). Although vascular browning is a typical FOL infection symptom, it is not confirmatory as other phytopathogenic fungi and bacteria can cause similar phenotypes within the xylem vessels (117). Soil warm temperature (28 °C), low soil pH, and ammonium based-fertilizers application favors FOL development and exacerbates VW symptoms (15).

1.2.2 Biology and pathogenicity of *Fusarium oxysporum* f. sp. *lycopersici*.

Fusarium is a cosmopolitan genus of ascomycete fungi characterized by the production of fusoid macroconidia, microconidia, and chlamydospores (118). Members of this genus are important plant pathogens and mycotoxin producers. *Fusarium* species are classified into seven major clades. Clade V contains the *Elegans* and *Liseola* sections, which include the species *F. oxysporum*, belonging to *Elegans* section, and *F. subglutinans*, *F. proliferatum*, and *F. verticillioides*, classified into the *Liseola* section (119).

F. oxysporum is considered a fungal complex composed of several species that can be pathogenic or innocuous towards specific plant hosts. Within this complex *formae speciales* and physiological races are described, according to the host range (*formae speciales*) and cultivar-level (races) specialization (120). More than 140 *formae speciales* are described in the literature, but only two are infective of tomato: *F. oxysporum* f. sp. *lycopersici* (Sacc.) Snyder & Hansen (FOL) and *F. oxysporum* f. sp. *radicis-lycopersici* Jarvis & Shoemaker (FORL) (120).

FOL and FORL are asexually reproducing hemibiotrophic soil-borne pathogens. FOL is the causal agent of tomato VW, while FORL cause crown and root rot in tomato and other plant hosts in the Anacardiaceae; Cruciferae, Cucurbitaceae, Leguminosae, Molluginaceae, Plantaginaceae, Solanaceae, and Umbelliferae families (15).

To date, three physiological races have been described in FOL. Race 1, 2, and 3 were described in the late 19th century, 1945, and 1978, respectively (121). Race 1 and 2 are

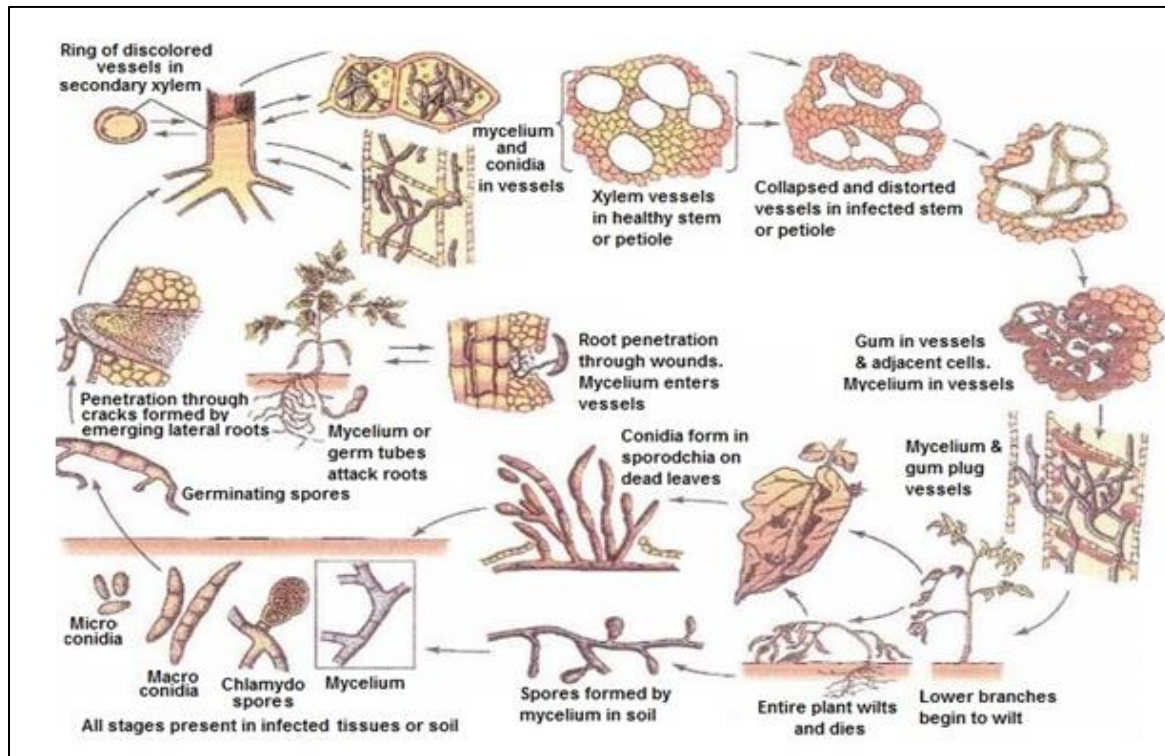
distributed almost worldwide while race 3 distribution has expanded recently on Australia, New Zealand, United Kingdom, Korea, South Africa, USA, Mexico, Brazil, Venezuela, and Chile, among others (122-124). Only FOL race 2 and FORL have been identified and correlated as causal agent of FVW in tomato crops from the Colombian Central Andean Region (115).

Compatible/incompatible interactions between FOL and tomato are controlled by three avirulence genes (*AVR1-3*) in FOL and the corresponding resistance genes (*I-3*) in tomato. In fact, three races of FOL have been described, according to the presence of avirulence genes, being the result of tomato-FOL interaction through a gene-for-gene model (120, 121).

FOL race 1 carried *AVR1*, *AVR2*, and *AVR3* genes, that encodes the small cysteine-rich proteins *SIX4*, *SIX3*, and *SIX1*, respectively. For full virulence, FOL needs the expression of *SIX1* and *SIX3*. These proteins are recognized by the tomato plant resistant *I-3* and *I-2* genes and participate in tomato resistance to race 1. *SIX4* is not required for FOL virulence, although it suppresses *I-2* and *I-3* mediated resistance (125). FOL race 2 carried only *AVR2* and *AVR3* genes. Phylogenetic evidence indicates that race 2 evolved from race 1 by deletion of *AVR1* through homologous recombination. FOL race 3 has *AVR3* and a muted *AVR2*, which caused the loss of its avirulence function (121).

FOL infection can be summarized in four steps: root host recognition, attachment to rhizoplane and external hyphal propagation, invasion of root cortex and vascular and xylem vessels colonization, and mycotoxins and virulence factor production (Figure 1-4) (126, 127). Upon host presence recognition, FOL grows on the root system surface and invades the root cortex asymptotically (10). Subsequently, FOL colonizes xylem vessels by direct hyphal propagation through the xylem pits, interfering with plant water transport (17). Plant immune responses and fungal growth in the xylem conduces to wilting and plant death resulting from vessel clogging (19, 20, 126, 128). During its growth in xylem and after plant death, FOL produces microconidia that spread through the sap stream to upper vessels (117).

Figure 1-4: General vascular wilt disease cycle caused by members of the FOC (129).



During root and xylem vessels colonization, FOL produces several mycotoxins and virulence factors such as fusaric acid, SIX proteins (Secreted in xylem proteins), cell-wall degrading enzymes, such as PG1 (endopolygalacturonase) and PGX6 (exopolygalacturonase), and tomatinases (117, 130-132). These compounds facilitate FOL infection and help it to evade plant immune response.

After xylem vessel colonization, FOL propagates in the parenchymatous tissue and starts sporulating on the plant surfaces, including leaves and stem, which serves as secondary inoculum contributing to the pathogen dissemination and persistence in fields and greenhouses (117, 133). Being a saprophytic fungus, FOL can survive long periods on soil organic matter, mainly as chlamydo spores, remaining as a long-term constraint on crop yield (17, 127, 133). Furthermore, the possible aerial dissemination of FOL (134, 135) and its growth within the vascular tissues contribute to the pathogen dissemination and reduced effectiveness of the chemical and cultural attempts to decrease *Fusarium* VW.

1.2.3 Management strategies for tomato vascular wilt.

Integrated pest and disease management programs are defined as: “A sustainable approach to managing pests that combines available biological, cultural, physical and chemical tactics to minimize the economic, health and environmental risks associated with crop production” (97). These programs aim to reduce the pathogen inoculum viability (population density) and functionality (pathogenicity) (15). McGovern reviewed the main strategies for *F. oxysporum* management in tomato and classified them into five groups: resistance management strategy, chemical control, physical practices, cultural practices, and biological control (15).

Tomato plant breeding has been focused on the introgression of genes from wild relatives (individual *R* genes), generating a high level of resistance (15). To date, plant resistant cultivars use is the most practical, cost-effective, and environmentally safe method for *Fusarium* wilt control in tomato (136). Tomato resistant varieties are produced by intensive breeding programs that started in the 20th century. This process was supported by the high diversity of wild tomato species that drove creation of germplasm collections (137).

Four resistance genes, *I*, *I-2*, *I-3*, and *I-7*, confer resistance to known FOL races in tomato. SP has been used as a genetic source for quality improvement related to resistance against races 1 and 2, being the source of loci *I-1* and *I-2* (138, 139). Similarly, *S. penellii* was used for the introgression of loci *I-3* and *I-7*, which confers resistance to FOL races 1, 2, and 3 (136, 140).

Interestingly, some inorganic compounds such as salicylic acid, calcium chloride (CaCl₂), nanoparticles of cupric oxide (CuO), and chitosan seems to induce resistance in tomato to VW after foliar or root application (141-143). These compounds induce the expression of defense-related genes, and the accumulation of several phenolic compounds like caffeic acid, *p*-coumaric acid, ferulic acid, quercetin, and cinnamic acid involve in plant defense (142-145). Furthermore, plants treated with CuO or CaCl₂ also showed lower VW incidence than infected plants, which allows proposing these compounds as alternatives for FOL management, although studies on field and greenhouse are still needed.

On the other hand, chemical control relies on synthetic compounds that act as fungicides and fumigants (15). Compounds such as sodium hypochlorite (NaClO), hydrogen peroxide (H₂O₂), and ozone (O₃) are used for FOL propagules elimination in seeds, greenhouse surfaces, soil, and tools (15) while fungicides like benomyl or carbendazim are mostly applied to treat the disease on-field and on greenhouse conditions (146).

Other fungicides applied for FOL control in tomato crops are azoxystrobin, caboxin, cymoxanil, difenoconazole, dimetomorph, hexaconazole, hymexazol, metalaxyl, pyrimethanil, thiophanate-methyl, thiram, and prochloraz (15, 93, 111, 146). From them, prochloraz and carbendazim have presented the lowest EC₅₀ against FOL (0.019 and 0.235 µg·mL⁻¹, respectively) (146). Their effect can be preventive or curative, depending on the time of application. However, preliminary results indicate that they are more effective if applied before the pathogen reaches the plant roots (146).

Inadequate application of chemical fungicides is a persistent practice in smallholders. It can cause many side effects including the generation of resistant strains, as has been reported in several *Fusarium* species (147-149). Additionally, this practice could produce phytotoxic effects on tomato seedlings and limit the possibility of fruit exportation (150, 151). Residues of carbendazim, cymoxanil, dimetomorph, hexaconazole, metalaxil, and pyrimethanil have been detected on tomato fruits obtained from Colombian tomato greenhouse and open-field crops. Some of them (carbendazim, cymoxanil, and hexaconazole) above the maximum residue limit established by the EU pesticide residues database (93, 152), making the fruit not suitable for exportation.

On the other hand, Soil disinfestation is a fundamental strategy in managing soil-borne phytopathogens, like FOL (153-155). Initially, soil fumigation used the broad-spectrum fumigant methyl bromide. However, its application is no longer allowed due to severe drawbacks related to its depleting effect on atmospheric ozone; thus, it was substituted with another chemical, physical and biological options (156-158).

Nowadays, soil solarization (physical disinfestation), crop rotation (cultural practices), biofumigation (biological + chemical disinfestation), biosolarization (biological + physical disinfestation) and, anaerobic soil disinfestation (biological + chemical + physical

disinfestation) have been adopted as alternatives to methyl bromide and other chemical soil fumigants use (158-160).

Other than crop rotation, cultural practices that prevent VW on tomato crops are: removing plant residues (with symptoms of any disease), grafting, fallowing, mulching, plant-spacing, irrigation, and weed control (161, 162). These practices reduce the incidence and severity of several diseases, generating minimal risks for the environment and human health.

Similar to cultural practices, biological control agents aim to diminish pathogen's adverse effects, enhancing plant growth in an ecofriendly and sustainable way (163). Biological control can be achieved either by (i) classical approaches (introduction of an antagonist in a new niche to control a target pathogen), (ii) augmentation of an antagonistic or beneficial microbial population, (iii) by manipulation of the plant-microbiome, or (iv) by the use of suppressive soils for crop establishment (163-167).

Biological control agents (BCA) are selected based on *in vitro* and *in vivo* trials that show their efficiency under controlled conditions and are regarded as a safe technology that could improve crop productivity, avoiding undesirable side effects such as food contamination (165, 168). Therefore, biocontrol is a sustainable approach for pest and disease management and has been used for VW control for at least the past twenty years (see numeral 1.3.3).

1.3 Biological control.

Biological control can be broadly defined as the suppression of the phytopathogen population by a living organism (BCA) or the metabolites produced by them (163, 169). This phenomenon can be the result of direct interaction between the antagonist and the phytopathogen (by antibiosis and parasitism), the plant host (by competence or induced systemic resistance, ISR), or both (165).

BCA application can reduce the dose of chemical biocides, dropping the apparition of agrochemicals residuals in food, supporting crops seeking organic certification (170). In the last two decades, the biological control field concentrates on arthropods control (66%),

followed by plant pathogens (15%) and weed management (15%) (171). In the plant pathogen field, phytopathogenic fungi are the most studied organisms, with more than 45% of the research focused on them (171). Likewise, 92% of the studies use the augmentative biocontrol approach, characterized by the application of mass-reared microorganisms to obtain immediate or long-term control over a pest or pathogen. The use of augmentative biocontrol is expected, considering that many of these researches follow traditional isolation to mass production workflow (172).

In such type of workflow, the isolated microorganisms are tested on *in vitro* assays to evaluate their ability to inhibit the target phytopathogen. From these assays, one or more candidates are identified and used for biomass production on artificial media (pilot formulation) (172, 173). Once selected, the inoculant is employed for greenhouse or field trials to determine the microorganism's efficiency under *in vivo* conditions.

During *in vivo* assays, it is possible to evaluate the BCA application method (174, 175), its minimal effective concentration (175, 176), and stability (170, 177). The selected microorganism is then used for upscaling mass-production, full field testing, risk assessment and registration for integration into cropping systems (172).

To date, most of the biocontrol microorganisms come from sources such as soil, rhizospheric environments, or plant tissues. The most used BCAs are bacteria from the Firmicutes (e.g., *Bacillus* spp., *Brevibacillus* spp., *Paenibacillus* spp.) (178-182), Actinobacteria (e.g., *Streptomyces* spp.) (183, 184), and Proteobacteria phylum (e.g., *Pseudomonas* spp.) (185, 186), or fungi such as *Trichoderma* spp., *Beauveria* spp. or *Paecilomyces* spp. (the latter two mainly used for pest management) (187, 188).

Despite its relevance in science, biological inoculants application is lower than agrochemicals. This situation is a consequence of high production costs, problems with reproducibility on field conditions, and the need for knowledge transfer for precise application of the products. Several options have been tested to improve the efficacy of BCA against soil-borne phytopathogens and increase their application. For instance, in tomato, potential antagonists have been evaluated in combination with other BCA or PGPR (189), with chemical pesticides (190-192), after soil solarization (193, 194), and with organic amendments (195-197).

The selection of antagonists with more than one mechanism of biocontrol also improves field efficiency. Currently, antibiosis and ISR are the main mechanisms studied on BCA (198-200). Other mechanisms, such as competitive exclusion and competence for nutrients, are also key traits in BCA since they allow them to reduce phytopathogen growth and survive in the rhizospheric or phyllosphere environments (201, 202). These mechanisms and their application on FOL management will be described in more detail in the next sections.

1.3.1 Mechanisms used by biological control agents.

As previously mentioned, BCA can inhibit direct or indirectly phytopathogens. Direct mechanisms include hyperparasitism and antibiosis, while indirect mechanism involves ISR, microbial communication interference (Quorum quenching) and competence. The effectiveness of each mechanism varies according to the pathogen sensibility, the environmental conditions, and plant physiology (Table 1-2).

Table 1-2: Main modes of action of biological control agents (165).

| Mode of action | Pathogen specificity | Risk of tolerance | Dependence on environmental conditions | Dependence on plant physiology | Use by distributors and end-user |
|---|----------------------|-------------------|--|--------------------------------|----------------------------------|
| Induced resistance | Specific to broad | Low | Low | High | Knowledge transfer needed |
| Competition | Broad | Low | High | Low | Knowledge transfer needed |
| Quorum quenching | Pathogen-specific | Low | Low | Low | Knowledge transfer needed |
| Parasitism | Pathogen-specific | Low | High | Low | Knowledge transfer needed |
| Antimicrobial metabolites <i>in situ</i> | Specific to broad | Low | Moderated | Low | Knowledge transfer needed |
| Antimicrobial metabolites in product | Broad | Moderated | Low | Low | Similar to the use of fungicides |
| Consortia combining different modes of action | Broad | Low | Low | Low | Knowledge transfer needed |

Even though available information may not be sufficient, some studies suggest that biocontrol durability can be higher than chemical control. Since BCA can simultaneously express different action mechanisms, the probability of generating tolerance in the short term is lower (Table 1-2).

However, plant pathogens can and overcome the BCA selection pressure depending on the mechanism used, exhibiting different sensitivity ranges towards a specific BCA (203). Thus, appropriate knowledge of BCA modes of action should be obtained and selected to improve field biocontrol effectiveness. Here, we described the general characteristics of each mechanism and some examples applied in tomato disease control.

a) *Nutrients and space competition*

Many phytopathogens need exogenous nutrients that are not acquired directly from the plant host. Events such as conidial/spores germination, appressorium formation (infection structures), motility (chemotaxis), and multiplication depend on these metabolites, making the phytopathogen vulnerable to **nutrient competition** (165).

Competitive BCA, particularly yeast and bacteria, can obtain and consume nutrients more efficiently than phytopathogens, reducing its population and, therefore, its ability to colonize plant host (165). These microorganisms compete with phytopathogens for the available carbon and nitrogen sources, and ions such as Fe^{+3} . Nutrient competition is commonly used for biocontrol of post-harvest phytopathogens but is also effective against soil-borne fungal pathogens (204-207).

A typical example of nutrient competition is the production of low-molecular weight siderophores. Siderophores production improves the antagonist's ability to obtain Fe^{+3} ions, making them unavailable for the phytopathogen (208). Siderophore producer strains like *P. fluorescens*, *Achromobacter xylosoxydans* and *Streptomyces* SNL2 have been studied for FOL and FORL control in tomato (209, 210). Similarly, several other BCA such as *B. amyloliquefaciens* S1, *B. velezensis* C2, *Burkholderia cenocepacia* TAtl-371 produce siderophores that contribute to their biocontrol ability against tomato phytopathogens such as *Verticillium dahliae* (211), *Ralstonia solanacearum* (212), and *Clavibacter michiganensis* ssp. *Michiganensis* (213).

Competition-mediated biocontrol also can be achieved through **niche exclusion** (space competition). In this case, the antagonist grows on the plant host's surface, reducing the available space for phytopathogen colonization. Bacterial and yeast biofilms formation in plant rhizosphere, phyllosphere, and on fruits surfaces have been related to niche exclusion and are regarded as a significant factor on BCA effectiveness since other biocontrol

processes such as communication interference (Quorum quenching; QQ), antibiotics production, and induction of plant defense (ISR) can take place in BCA biofilms (214-217).

b) Quorum quenching

Quorum sensing (QS) is an intercellular communication system that regulates microbial gene expression according to cellular density (218). Plant pathogens use this mechanism to synchronize gene expression by producing and detecting specific self-produced signal molecules. Quorum sensing signals include N-acyl homoserine lactones (AHLs), γ -butyrolactones, unsaturated fatty acids, and small cyclic peptides (219, 220), among others.

When the bacterial population increases, QS signals are released. When the signal concentration increases to a quorum level, signal molecules are detected by intracellular transcriptional regulators like the LuxR proteins (AHL-QS) or membrane-bound two-component receptor proteins. In this latter case, a typical phosphorylation/dephosphorylation signal transduction cascade derives in specific gene expression (218). For AHL-QS systems, LuxR-AHL complexes promote direct gene expression by recognizing specific sequences in their promoter region (218).

QS regulates virulence factors expression in several tomato phytopathogens like *Pseudomonas corrugata*, *R. solanacearum*, and *Pectobacterium carotovorum* (221). These virulence factors include phytotoxins, type III secretion systems, siderophores, plant cell-wall degrading enzymes, and genes related to epiphytic fitness (222). Additionally, bioluminescence, conjugation, nodulation, swarming, sporulation, antibiotic production and biofilm formation are often regulated by QS (218, 222, 223).

Interference of QS systems or quorum quenching (**QQ**) aims to avoid virulence factors expression on plant pathogens rather than killing the pathogen itself (224). This characteristic decreases the selective pressure on the pathogen, attenuating the development of resistance (218). QQ can be achieved by different BCA through (i) inhibition of the signal biosynthesis, (ii) inhibition of the signal recognition (competitive blocking of the signal receptor) by quorum sensing inhibitors (QSI) or (iii) enzymatic or non-enzymatic degradation of the signal compound (223).

In tomato, the QQ ability of *Pseudomonas segetis* P6 has been used for biocontrol of *Pseudomonas syringae* pv. tomato (PsPto). QQ activity of P6 was associated with the production of acylase enzymes that degrade a broad range of AHLs interfering with QS systems of PsPto, *Dickeya solani*, *Pectobacterium atrosepticum*, and *P. carotovorum* leading to reduced pathogenicity towards tomato, potato, and carrots respectively (219). Similarly, QQ enzymatic activity against other tomato pathogens like *R. solanacearum* and *P. carotovorum* subsp. *carotovorum* have been described in *P. aeruginosa* 2apa (225) and *Ochrobactrum intermedium* D-2 (226).

c) *Induced systemic resistance*

ISR is the enhanced defensive capacity against phytopathogens in a plant host induced by a beneficial microorganism. This response is triggered by MAMPs (microbe-associated molecular pattern) recognition through host PRRs (Pattern Recognition Receptors) after BCA colonization. ISR has broad-spectrum effectiveness and is expressed locally and systemically on the plant host. Unlike SAR (Systemic Acquired Resistance), jasmonic acid (JA) and ethylene (ET) pathways regulate ISR (227). However, some reports indicate that PGPR such as *B. thuringensis*, triggers a salicylic acid-dependent ISR (228).

Several studies indicate that ISR did not induce JA or ET biosynthesis. Instead, ISR seems to enhance plant susceptibility to these hormones leading to a potentiated expression of JA/ET-regulated genes upon pathogen attack. This state, known as *priming*, facilitates a more robust and faster immune response towards phytopathogens, increasing plant resistance (227). In addition to JA/ET-regulated defense genes, ISR also induces cell wall apposition and thickening (e.g. callose deposition), tylose formation on xylem vessels, closure of stomata, and modifications on plant metabolome (227, 229, 230).

Some examples of beneficial microorganisms that trigger ISR are *P. fluorescens*, *P. putida*, *B. subtilis*, *B. amyloliquefaciens*, *B. pumilus*, *Paenibacillus polymyxa*, *Trichoderma* spp. and *Serratia marcescens* (227, 229, 231, 232). Since there is no direct interaction with the pathogen during ISR or competitive exclusion, the probability of resistance generation is low (165). In tomato, ISR was identified as a mechanism of biocontrol triggered by *Pseudomonas* sp. 23S, *P. aeruginosa* PM12 and *B. thuringiensis* B88-82 to control *C. michiganensis* subsp. *michiganensis*, FOL, and *R. solanacearum*, respectively (228, 230, 233).

d) Parasitism

Parasitism refers to the ability of some microorganisms (particularly fungi) to invade and kill mycelium, spores, and cells of fungal and bacterial phytopathogens (165). This mechanism is common in many *Trichoderma* species and involves the recognition, attachment (coiling), penetration, and assimilation of the host's cell wall content (234).

Host recognition is a process mediated by the detection of host-derived signals recognized by receptors located in the mycoparasite cell-wall surface (235). Similarly, attachment in mycoparasites seems to be a host-specific mechanism (236). After attachment, mycoparasites secrete a wide range of cell-wall degrading enzymes (CWDE), including chitinases, proteases, β -glucosidases, β -1,3-glucanases, α -mannosidases, and mutanases (236, 237). The secretion of these enzymes is host-specific and coupled with primary metabolism encoding genes expression that helps in further degradation and metabolization of host cell-wall components (237).

The mycoparasites *T. asperellum*, *T. harzianum*, *T. viride*, and *T. hamatum* have been suggested as BCA for FOL management in tomato (238, 239). Similarly, the mycoparasite *Dicyma pulvinate* has been proposed as a potential foliar BCA by its ability to inhibit the growth of *C. fulvum*, reducing leaf mold symptoms on infected tomato leaves (240).

e) Antibiosis

In a biocontrol context, antibiotics are a large group of low-molecular-weight organic compounds, chemically heterogeneous, produced by microorganisms that inhibit the growth of bacteria, fungi, oomycetes, and others pest or pathogens (241, 242). Antibiotics interfere with DNA, RNA, and protein synthesis, and cell wall biosynthesis and integrity (243). Although broad chemical diversity of antibiotics has been reported, genomics studies of microorganisms lead to finding cryptic gene clusters for which metabolites, regulation, and biosynthetic pathways remain unknown (244).

Most antibiotics are secondary (specialized) metabolites produced as a survival advantage for microbial persistence in different niches (243). At low-concentration, antibiotics work as signaling molecules in microbial interactions, participating in biofilm, sporulation, cryptic antibiotics biosynthesis, and secondary metabolism regulation (244, 245).

Antibiotics production in the rhizosphere is affected by (i) the microbiome composition and interactions, (ii) the plant rhizodeposits (root exudates), (iii) soil physical-chemical characteristics, and (iv) the available nutrients present in the environment (198, 243). These features also influence antibiotics half-lives in soil. Bioactive metabolites can be degraded, inactivated, or absorbed in soil particles. Thus, antibiotic persistence and activity on the rhizosphere should be studied *in situ* to ensure biocontrol effectiveness (198).

BCA produce multiple antibiotics with broad-spectrum activity during their growth on artificial media. Moreover, BCA synthesizes these metabolites as a response to the presence of plants and pathogens. Members of the Actinobacteria, Firmicutes, and Proteobacteria phylum stands out by the number and chemical diversity of antibiotics produced against plant pathogens. From them, *Streptomyces*, *Bacillus*, and *Pseudomonas* genera are the most reported in antibiosis research (241).

The antibiotics produced for these microorganisms are diffusible and volatile compounds including: ribosomal (e.g., bacteriocins) and non-ribosomal peptides (e.g., cyclic and linear lipopeptides), polyketides (e.g., macrolides), phenazines, alcohols, phospholipids, hydrocarbons, aromatics, amines, thiols, terpenes, acids, esters, and ketones, among others (246-250).

These metabolites can generate significant reductions in pathogen populations acting as biocides at high concentrations, while in sub-inhibitory concentrations, induce physiological changes in the pathogen lowering its virulence towards plant host (198, 245, 251). This dose-dependent phenomenon is known as *Hormesis* and constitutes one of the paradigms of microbes-molecules interactions (244).

From all the biocontrol modes of action mentioned above, antibiosis presents a higher risk to generates resistance in plant pathogens (203). Sub-inhibitory doses of antibiotics generate a constant selection pressure in the pathogen population that could lead to resistance development (203). Contrarily to chemical biocides, BCA produces more than one antibiotic simultaneously, which reduces the probability and rate of resistance development. However, other strategies, such as selecting BCA with more than one mode of action, should be considered during the BCA's selection process to increase biocontrol's success rate.

1.3.2 Biological control of *Fusarium* vascular wilt.

Due to the economic relevance of *Fusarium* VW, management programs with BCA have been extensively studied in tomato during the past forty years. Since 1980, more than 8000 research papers related to tomato VW biocontrol, have been published (Data retrieved from Google scholar and Scopus database using the Boolean search "*Fusarium* vascular wilt" AND "biocontrol" AND "tomato"). Almost 550 papers regarding *Fusarium* VW biological control have been published in 2020, including reviews, book chapters, original research, and short communications.

Biological control of *Fusarium* VW started by focusing on rhizospheric-derived microorganism that produces fungicides compounds (21). In the last ten years, the study of non-pathogenic *F. oxysporum* strains, suppressive soils and their microbiomes, endophytic microorganisms, and rhizospheric BCA displaying several modes of action has taken more attention (Table 1-3).

According to Raza *et al.*, BCA's medium biocontrol efficiency in tomato ranged from 30 to 55.4% (21). According to these authors, most studied bacterial BCA for VW control in tomato belong to the *Bacillus*, *Streptomyces*, *Pseudomonas*, and *Serratia* genera. Similarly, VW biocontrol studies based on fungi encompass the genera *Trichoderma*, *Cheatomium*, *Penicillium* and non-pathogenic *Fusarium* (Figure 1-5) (21). Some of these microorganisms, such as *B. amyloliquefaciens* and *Chaetomium globsum*, are even more effective than chemical fungicides like carbendazim and prochloraz (15).

Figure 1-5: Commonly used BCA for *Fusarium* VW control between 2000-2016 (21).

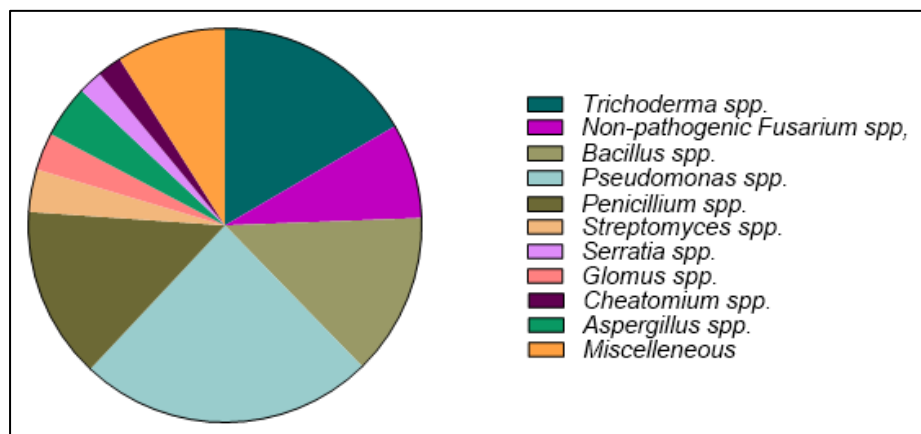


Table 1-3: Examples of BCA used for *Fusarium* VW control in tomato.

| Microorganism (BCA) | Application | Biocontrol suggested mechanism | Ref. |
|---|----------------------|--|------------|
| Fungal BCA | | | |
| <i>F. oxysporum</i> Fo47 | Roots / soil | ISR + nutrient competition | (252-254) |
| <i>F. oxysporum</i> CS-20 | Roots | ISR | (255) |
| <i>Trichoderma asperellum</i> BHU P-1 | Seed | Priming | (256) |
| <i>T. asperellum</i> T34* | Roots | Nutrient competition | (202) |
| <i>T. asperellum</i> TS1-TS44 | <i>In vitro</i> | Mycoparasitism | (239) |
| <i>T. harzianum</i> , <i>T. viride</i> <i>T. hamatum</i> | Soil drenching | Mycoparasitism | (238) |
| Bacterial BCA | | | |
| <i>Achromobacter xylosoxydans</i> MM1 | Roots | Nutrient competition | (209) |
| <i>Bacillus</i> sp. B44 | Soil | Antibiosis (VOCs and diffusible antibiotics) | (257) |
| <i>B. subtilis</i> MSS9 and <i>B. licheniformis</i> MSS14 | Seed | Antibiosis + CWDE + space competition | (258) |
| <i>B. amyloliquefaciens</i> SN16-1 | Soil drenching | Antibiosis + microbiome modulation | (259) |
| <i>B. amyloliquefaciens</i> FZB24* | Seed + soil + foliar | ISR + antibiosis | (260) |
| <i>P. aeruginosa</i> PM12 | Roots | ISR | (230) |
| <i>P. fluorescens</i> PCL1751 | Roots | Nutrients and space competition | (261) |
| <i>P. fluorescens</i> SPs9; SPs20 | Roots | Nutrient competition | (262) |
| <i>Paenibacillus ehimensis</i> KWN38 | Seedling | Antibiosis + CWDE | (263, 264) |
| <i>Paenibacillus elgii</i> HOA73 | <i>in vitro</i> | Antibiosis + CWDE | (265, 266) |
| <i>Paenibacillus polymyxa</i> CF05 | Soil drenching | ISR | (267) |
| <i>Streptomyces griseorubens</i> E44G | Soil | CWDE | (268, 269) |
| <i>S. enissocaesilis</i> IC10; <i>S. rochei</i> Y28 | Soil | ISR | (270) |
| Other | | | |
| Suppressive Compost | Soil amendment | Microbiome modulation | (271) |
| Vermicompost | Soil amendment | Microbiome modulation + SPPI | (272) |
| Crop rotation + suppressive soils | - | Microbiome modulation + SPPI | (273) |

*Registered products in the USA and the EU. SPPI: Soil physicochemical parameters improvement

As shown in Table 1-3, seed, root, and soil applications are the most common methods for antagonist inoculation. A combination of seed and soil inoculation seems to improve BCA effectiveness (260). Similarly, multiple BCA applications and combined treatments of two or more BCA, amendments, and inorganic compounds can improve FOL biological control durability (274-277).

Apart from BCA, plant microbiome modulation is another strategy for *Fusarium* VW control (166, 167, 271). In suppressive soils, natural microbial communities harboring antibiotics BGC and other PGPR related genes contribute to plant health, reducing disease severity. The relative abundance of antibiotic producer microorganisms and gene expression of secondary metabolites biosynthetic gene clusters, like NRPS, in compost and soils, have

allowed understanding the key role of antibiosis, CWDE, and ISR in the establishment of disease-suppressive soils (278-280) and how it can be used for disease management programs.

Although new options are under evaluation, VW biological control still relies on augmentative BCA strategies to develop commercial products (21). From 2000 to 2018, 107 BCA were registered for commercial use in the USA and the European Union (281). Within this group of microorganisms, *T. asperellum* T34 (T34 Biocontrol®; Biocontrol technologies), *B. amyloliquefaciens* FZB24 (Rhizovital®; Agrichembio), *Streptomyces* K61 (Mycostop ®; Verdera), and *S. lydicus* WYEC 108 (Actinovate, Novozymes) are biofungicides with approved use for *Fusarium* VW control in tomato.

In Colombia, six BCA are registered for *Fusarium* VW management. These products correspond to *Trichoderma lignorum* (Mycobac®, Laverlam S.A.), *T. harzianum* (PRQtector®; Biocrop S.A.S and Fungigrasp®; Core biotechnology), *T. koningiopsis* (Tricotec®, Agrosavia), *S. racemochromogenes* (Actybac®, Biocultivos S.A.), and one microbial consortium of four *Bacillus* strains: *B. subtilis*, *B. pumilis*, *B. thuringensis* var. *kurstaki* and *B. amyloliquefaciens* (Promobac®, Bioquirama S.A.S) (282).

Commercial BCA use is limited by reproducibility on field conditions, production cost, need for adequate training for proper application, and lack of information regarding BCA compatibility with other agrochemicals. Specifically for soil-borne diseases, rhizospheric competence and tolerance to soil physicochemical properties are essential for ensuring BCA persistence on soil (22, 283). In this context, there is a need to search for more competent BCA that displays multiple modes of actions, tolerate biotic and abiotic stress, and be easily produced on an artificial medium.

For this reason, new studies focus on isolating novel microorganisms from different ecological niches and sources, including mangroves (284), marine sediments (285), coastal agricultural lands (286), agro-industrial waste-based compost, suppressive soils, and diseased plants (287). It is expected that these efforts result in an increased supply of efficient BCA that can be included into disease management programs.

1.4 Marine-derived bacteria as a source of biological control agents against fungal phytopathogens.

Marine environments are highly diverse ecological niches that sustain an incomparable number of microorganisms whose diversity remains mostly unknown (288, 289). It has been estimated that microbial abundance in marine environments can be as high as 10^6 - 10^9 cells per mL (290, 291). The marine biological diversity is also traduced in metabolic diversity, being the main reason for studying this environment as a source of new bioactive compounds (291, 292).

Marine-derived bacteria are one of the most abundant groups in marine environments. While planktonic bacteria numerically are more abundant, bacteria associated with marine organisms are most interesting for their wide secondary metabolism and biological activities (293). Most eukaryotic marine organisms count with well-established microbiomes that significantly differ in abundance and diversity from the surrounding water columns (291). For example, bacterial populations are 2-4 and 10-100 times higher in macroalgae and sponges than in the surrounding water (294, 295).

Since most of the hosts are soft-tissue and sessile organisms, they rely on chemical defenses against predators and pathogens. In this context, associated bacteria produce metabolites with antipredation and biocide activities to support host health and survival (296, 297). Bacterial antibiotic production and efficient colonization traits (e.g. biofilm formation, tolerance to abiotic stress, and high growth rates) in marine environments are related to competence for nutrients and space, which are very limited in this ecological niche (291, 298).

Annually, more than 150 new metabolites are isolated from marine-derived bacteria. In 2018, 240 new metabolites were reported, including cyclic, linear, depsi- and lipo-peptides, polyketides, angucyclines, naphthoquinones, glycosides, fatty acids, terpenes, and alkaloids (299). Strains of *Streptomyces* and *Bacillus* genera produces most of these metabolites. Marine-derived bacteria metabolites had antimicrobial, antiviral, antiprotozoal, immunomodulatory, antioxidant, anti-inflammatory, antidiabetic, and anticancer activities (298).

Antifungal activity of marine-derived metabolites has been evaluated against different plant and human pathogens (300). Until 2017, 30% of the antifungal metabolites reported from marine organisms were isolated from bacteria (29) and tested under *in vitro* conditions against several phytopathogens (Table 1-4).

Table 1-4: Marine-derived bacteria with antifungal activity against fungal phytopathogens.

An, *Aspergillus niger*; Aa, *A. alternata*; Af, *A. flavus*; As, *A. solani*; Bc, *Botrytis cinerea*; Bf, *B. fabae*; Bs, *Bipolaris sorokiniana*; Ca, *C. acutatum*; Cf, *C. fragariae*; Cfa, *C. falcatum*; Cg, *C. gloeosporioides*; Cl, *C. lamella*; Cm, *C. musae*; Cs, *Cercospora sorghi*; Fg, *F. graminearum*; Fo, *F. oxysporum*; Foc, *F. oxysporum* f. sp. *cucumerinum*; Fp, *F. proliferatum*; Ho, *Helminthosporium oryzae*; Pc, *P. capsici*; Pi, *P. infestans*; Po, *Pyricularia oryzae*; Pu, *Phytium ultimum*; Rs, *R. solani*; Sr, *Sclerotium roysii*; Sp, *Saprolegnia parasitica*; Ss, *Sclerotinia sclerotiorum*. DLA, Detached leaves assay; ND, No described; NI, No identified.

| Microorganism | Source | Screening | Metabolite | Phytopathogen | Ref. |
|---|---|-------------------------------------|---|--------------------------------|-----------|
| <i>Bacillus</i> sp. PPM3 | Marine sediment | <i>In vivo</i> | NI | Fg | (285) |
| <i>B. licheniformis</i> 09IDYM23 | Marine sediment | <i>In vitro</i> | leodoglucomide C, ledoglycolipid | An, Rs, Bc; Ca | (32) |
| <i>B. subtilis</i> RBM01 | ND | <i>In vivo</i> | NI | Pu | (301) |
| <i>B. subtilis</i> 109GGC020 | Marine sediment | <i>In vitro</i> | Gageopeptides A-D | Rs, Pc, Bc, Ca | (302) |
| | | <i>In vitro</i> | Gageomacrolactones | An, Bc, Ca, Rs | (303) |
| | | <i>In vitro</i> | Gageostatine A-C | Rs, Bc | (33) |
| <i>B. marinus</i> | <i>Suaeda salsa</i> | <i>In vitro</i> | Macrolactin T & B | Po, As | (304) |
| <i>Bacillus</i> sp MC3B-22 | Biofilms of <i>Thalassia testudinum</i> | <i>In vitro</i> DLA | NI | Cg, Cf, Fo | (35) |
| <i>B. cereus</i> <i>B. subtilis</i> | Biofilms Tunisian coast | <i>In vitro</i> Potato infection | NI | Rs | (305) |
| <i>B. megaterium</i> | Yellow river | <i>In vitro</i> | NI | Af | (306) |
| <i>Corynebacterium</i> sps-6 | Marine sediment | <i>In vitro</i> | No identified peptide | Aa, Sr, Rs, Cm, Cc, Cl, Pi, An | (307) |
| <i>Haliangium luteum</i> | Macroalgae | <i>In vitro</i> | Haliangicine | Bc, Pu, Sp | (30) |
| <i>Nocardia</i> sp. ALAAA2000 | <i>Laurenica spectabilis</i> | <i>In vitro</i> | Chrysophanol 8-methyl ether, Justicidin B | An, Bf | (308) |
| <i>Streptomyces</i> spp. | Marine sediment | <i>In vitro</i> | NI | Rs, Po, Ho, Cf | (309) |
| <i>S. roseobolascens</i> XAS585 / <i>S. roseofulvus</i> XAS588 | Marine sediment | <i>In vitro</i> | NI | Bc, Foc, Cg, Bs, Ss, Cs | (310) |
| <i>Stenotrophomonas rhizophila</i> | ND | Fruit | VOCs, CWDE | Cg, Fp | (31, 311) |
| <i>P. aeruginosa</i> | Water column | <i>In vitro</i> | Siderophores | Af, An, Fo, Sr | (312) |
| <i>Pseudomonas</i> sp. AMET1140 | Rhizosphere of plants in coastal dunes | <i>In vitro</i> DLA | NI | Rs | (313) |

The results from these studies allow suggesting that marine-derived bacteria can act as sources of new fungicides. For example, the fungicide Kasugamicin, produced by the marine bacteria *Streptomyces rutgersensis* subsp. *gulangyunensis*, is commercially used for the control of *Pyricularia oryzae* and *Fulvia fulva* on rice and tomato crops, respectively (314).

However, a new fungicide's production process requires an adequate identification of the active compound and the achievement of strategies for its commercial production (315). For this purpose, the generation of synthetic or semi-synthetic analogs and heterologous expression are the first strategies aborded (316-318). The chemical complexity of some metabolites and low production yield restricts the synthetic approach (319). On the other hand, heterologous expression requires knowledge about metabolite BGC and its regulation. Since most of the metabolites are new molecules, genetic information is not available, limiting heterologous expression (320).

To overcome the limitations mentioned above, these bacteria have been suggested as candidates for biological control. For example, in the cases of the bacteria *Bacillus* sp. MC3B-22, *B. cereus*, *B. subtilis*, *B. megaterium*, and *Pseudomonas* sp. AMET1140 preliminary analyses have been carried out in plant tissues in which the biocontrol capacity against the evaluated phytopathogen is demonstrated (35, 305, 306, 313). In these assays, the authors emphasize that the evaluated microorganisms are innocuous towards treated plants and remain viable on the inoculated surfaces, suggesting an adaptation process that supports their formulation as BCA.

In an interesting analogy, the authors of the research developed with *Bacillus* sp MC3B-22, propose the use of that bacteria as a BCA because its original niche (surface of the macroalgae *Thalassia testudinum*) and phyllosphere present similar environmental limitations (35). The authors attribute the successful colonization of MC3B-22 on mango leaves to its natural adaptation to similar environmental conditions.

On the other hand, some authors point out that many of the microorganisms evaluated have been previously isolated from terrestrial sources (321). Additionally, some of these bacteria demonstrated the ability to form biofilms and grow in contrasting ranges of temperature (10-40°C), salinity (0.5-6% NaCl), and pH (310, 312). These characteristics could improve

marine bacteria establishment in terrestrial environments, supporting its survival on crop systems.

In vivo evaluation of marine-derived bacteria as BCA is limited. Li-Wei et al., Yandigeri et al., Lara-Capistrans et al., and Radovanović et al. evaluated the ability of marine *Bacillus* sp. PPM3, *Bacillus subtilis* 3512A, *B. subtilis* RBM01, and *Streptomyces vinaceusdrappus* to control *F. graminearum*, *F. oxysporum* f.sp. *cucumerinum*, *Phytophthora ultimum*, and *R. solani* in maize, cucumber, pepper, and tomato crops, respectively, under greenhouse conditions (285, 301, 322, 323). In the latter examples, it was possible to demonstrate that the active bacteria can inhibit the phytopathogen's growth and colonize the rhizospheric soil and rhizoplane of plants treated under greenhouse conditions and promote its growth, making feasible to suggest them as candidates for formulation and scaling up process.

1.5 Study of Colombian marine-derived microorganisms.

Colombia is a transcontinental country bordered by the Caribbean Sea and the Pacific Ocean. It counts with highly diverse marine ecosystems, whose microbial diversity and potential biotechnological applications are poorly studied. The study of marine microbial diversity is led by few research groups and some public institutions like the "Instituto de Investigaciones Marinas y Costeras José Benito Vives de Andrés" INVEMAR.

Within the research done in marine microbiology in Colombia, the immunomodulatory activity (324), antimicrobial activity against human pathogens (325), and the possible production of poly-hydroxyalcanoates (326) by Colombian marine-derived bacteria from the Actinobacteria and Firmicutes phylum have been evaluated. Furthermore, the research group "Estudio y aprovechamiento de productos naturales marinos y frutas de Colombia" has conducted several projects to obtain information about the Colombian marine ecosystems' microbial diversity in the Caribbean region. These projects aimed to evaluate marine-derived bacteria's biotechnological potential for disease management in agronomically relevant crops like rice, yam, carnation, and tree tomato (*S. betaceum*).

During the developed research, 152 bacterial and 42 fungal strains were isolated from the Santa Catalina and Providencia coral reef (27). Given the size of the collection, the research group adopted metabolomic approaches to select microorganisms with biotechnological

potential. This type of evaluation has been used successfully to obtain information about the metabolic diversity of different microorganisms, generating the opportunity to perform the dereplication of unknown compounds *in silico* using metabolomic data through molecular networks (327, 328). This approximation allowed us to increase the rate of identified metabolites that could not be isolated from microbial biological samples either because of their complexity or the low recovery rate.

Some of the bacterial microorganisms evaluated showed antifungal activity against phytopathogens such as *F. oxysporum* f. sp. *dianthi* and *C. gloeosporioides*. This activity was associated with two cyclic tetrapeptides (26) and a linear nonapeptide (329) that inhibit the growth of the pathogens mentioned above. Likewise, they presented antibacterial activity against *Burkholderia glumae*, a rice phytopathogen, through the production of at least two phenethylamides whose role as inhibitors of cellular communication systems (Quorum sensing) was proposed (330).

Despite their potential, it is necessary to determine if these microorganisms can be used for biological control of plant disease or as novel fungicide metabolites sources. In this context, we propose to use the active strains as BCA for *Fusarium* VW control. For this purpose, the present research was divided into three phases. In the first phase, BCA candidates from the bacterial collection were selected based on their antifungal activity against FOL under *in vitro* conditions. Then, molecular and phenotypic approaches were used to identify these microorganisms. The second phase aimed to determine the rhizospheric competence of selected strains, evaluate their effect on treated plant growth and established its *in vivo* antifungal activity under greenhouse conditions. Finally, the third phase aims to characterize the interactions from one BCA candidate, selected from phases one and two, establish with the plant host and the phytopathogen.

2. Selection and characterization of marine-derived bacteria with antifungal activity against FOL.

2.1 Introduction and scope

Soil-borne fungal diseases are one of the main constraints in crop yield. Disease management programs aim to reduce the pathogen presence on soil or reduce its ability to infect the plant host. In phytopathogens like FOL, the production of microconidia, macroconidia, and chlamyospores and the ability of hyphae to remain viable inside dead plant tissues limit the effectiveness of some management strategies like chemical control.

Fungicides application alone is not enough to eliminate FOL from crops in greenhouse and open-field systems. Furthermore, excessive use of chemical fungicides can produce fungal resistance development and have deleterious effects on the environment and beneficial microbial population. The use of BCA as a supporting strategy for FOL control could lead to a decrease in the use of chemical fungicides, improving tomato crops' quality and sustainability.

Some desirable traits should be considered during the BCA candidate's selection process for improving commercial product development. These include BCA identity (related to risk assessment) (281), biocontrol effect against several strains of the pathogen and possible cross-protection against non-target phytopathogens (287, 331), multiple antagonistic mechanisms (332), physiological characteristics (nutritional requirements, growth rates, abiotic stress tolerance) (331), as well as rhizospheric competence (crucial for soil-borne phytopathogen control) (261).

One of the critical criteria evaluated for registration and marketing of BCA's is risk assessment. This evaluation establishes possible deleterious effects of the BCA (or its

active metabolites) on human, animal, and plant health, and the impact that can cause in the environment (281). Therefore, in the early steps of BCA screening selection, the candidates' taxonomical identity of candidates should be considered to discard opportunistic pathogens or strains that produce potentially toxic metabolites (333-335).

Strain identification, done by molecular or phenotypic approaches, is regularly performed with a chosen group of microorganisms retrieved from screening assays. Most of these assays can be phenotypic or marker-based *in vitro* protocols that can give insights about the BCA mechanisms of action (direct or indirect) (287). However, since no universal screening method exists for BCA, all the assays are biased towards specific modes of action (287).

For antibiotic and CWDE producer microorganisms, typical screening by *in vitro* assays such as dual cultured or agar-well diffusion tests, are used (336). These assays can be adapted to evaluate the production of diffusible or volatile antibiotic metabolites and mechanisms such as parasitism or competitive exclusion, although it is difficult to identify these mechanisms relying only based on an *in vitro* assay (287).

On the other hand, phenotypic characterization of potential BCAs is conducted for identification purposes and determines the pre-existence of advantageous traits that improve the microorganism activity and persistence on field conditions. Some of these traits, like biofilm formation and wide-range nutrient metabolization ability, are directly related to rhizospheric competence. Others like endospore formation, and temperature, pH, or salinity tolerance, contribute to the microorganism persistence in soil.

Phenotypic information is particularly useful for microorganisms that were isolated from unusual environments like marine ecosystems. Since not much data about marine-bacteria adaptability to rhizospheric environments are available, it is necessary to evaluate traits that rhizospheric bacteria displays to predict its possible development in soil. Salinity, temperature and pH tolerance, biofilm and endospores formation ability, and persistence in harsh environments are desirable characteristics identified in marine-derived bacteria in their natural environments and rhizospheric environments (337, 338).

The adaptability of marine-derived bacteria to harsh abiotic conditions was one of the reasons that supported their study as potential BCA to control *C. gloeosporioides* and *R. solani* on mango and rice phyllospheres (35, 313). Even more, the ability of these microorganisms to efficiently form biofilms and produce several antibiotics with a wide range of activity makes them good candidates for post-harvest disease management programs of *A. flavus* (306), *C. gloeosporioides* (31, 339), and *F. proliferatum* (311).

Furthermore, many marine-derived bacteria like *Bacillus* sp. CS30, *B. subtilis* BS155 and 109GGC020, and *Streptomyces vinaceusdrappus* S5MW2 have been studied as a source of CWDE and antibiotics for phytopathogenic fungal inhibition like chitinases (323), surfactin (340), fengycin (341), and gageopeptides (342). The chemical diversity of metabolites and enzymes produced by marine bacteria is related to their secondary metabolism and makes them interesting strains for agriculture's biotechnological applications.

Colombia has highly diverse marine ecosystems. The study of microbial populations in these environments started approximately ten years ago. Most of the studies developed so far, have focused on characterizing microbial diversity, searching for specific applications such as PHA production, human pathogen inhibition, and plant-pathogen control. Unfortunately, none of the active microorganisms evaluated have been used for biotechnological processes or derived in a commercial product generation.

In this context, the research group “*Estudio y aprovechamiento de productos naturales marinos y frutas de Colombia*” from Universidad Nacional de Colombia started to evaluate the possible generation of a commercial biological product for biocontrol using the marine microorganisms collection recovered in previous studies (27). For this purpose, a three-phase program was established to find a potential BCA for *Fusarium* VW control in tomato crops.

The first step, presented in this chapter, aims to select and characterize bacteria candidates with antifungal activity against FOL. To achieve this, we used an antifungal activity screening against a panel of ten fungal isolates of *F. oxysporum* recovered from tomato plants with VW symptoms. A pre-selected group of active bacteria was identified, and their phenotypic characteristics were evaluated. The information derived from these analyses prioritize those isolates with the best performance for the *in vivo* assays (Chapter three).

2.2 Materials and methods

2.2.1 Microorganisms used in this study.

a) Bacterial strains.

The marine-derived bacterial collection used in the present has been obtained in previous studies by the research group from the Santa Catalina and Providencia coral reef (27). This collection is composed of 152 bacterial isolates (deposited as IBUN-090-02027 to IBUN-090-02234 in the "*Banco de Cepas y Genes IBUN-Universidad Nacional de Colombia*") that were cryopreserved (-80°C) in Luria Bertani (LB) broth supplemented with glycerol (40%). The evaluation of this collection was granted by "The Ministerio de Ambiente y Desarrollo Sostenible" (Contrato de Acceso a Recurso Genético y Productos Derivados N° 121 otrosí N° 6).

Bacterial reactivation was done by inoculation of 100 µL of each cryopreserved strain in 200 mL of LB broth (tryptose 5g·L⁻¹, yeast extract 5 g·L⁻¹, NaCl 5 g·L⁻¹; pH 7.2). Liquid cultures were incubated at 30°C for five days in constant agitation (120 r.p.m.) and used for the *in vitro* test.

b) Fungal strains.

Nine *F. oxysporum* isolates were obtained from tomato plant roots, leaves, and stems with VW disease's typical symptoms at three different locations in Tolima and Cundinamarca (Colombia). For fungi isolation, plant tissues were surface sterilized by sequential immersion in ethanol (70%) and sodium hypochlorite (2%) for 5 minutes. The sterilized tissue was placed on Potato-Dextrose Agar (PDA) medium supplemented with chloramphenicol (0.3%) and incubated at 25°C for five days (115). Growing *Fusarium*-like colonies were identified by optical microscopy and purified by sub-culturing on PDA. The phenotypic (macro and microscopic) characteristics of these isolates were elucidated from 10-days old PDA cultures.

Molecular characterization of fungal isolates was done by amplifying and sequencing the ITS region, using the universal primers ITS1 (5'- TCCGTAGGTGAACCTGCGG-3') and ITS4 (5'- TCCTCCGCTTATTGATATGC-3'). PCR was carried out with initial denaturation at 94°C for 5 minutes, followed by 30 cycles of denaturation at 94°C for 1 minute, annealing at 55°C for 30 seconds, and extension at 72°C for 30 seconds (343). Amplified PCR products (~550 pb) were sequenced and analyzed for taxonomical identification.

A highly virulent FOL race 2 strain, FOL59, recovered from wilted tomato plants in Caldas (Colombia) (115) was used in the current research for *in vitro* and *in vivo* assays. This strain was kindly provided by "Bancos de Germoplasma de la Nación" from Agrosavia (Colombia).

2.2.2 Primary screening of marine-derived bacterium with antifungal activity against *F. oxysporum*

The 152 isolates from the marine-derived collection of bacteria were tested for antifungal activity against *F. oxysporum* and FOL59 using dual cultured assays as follows: a 6 mm agar plug of each *Fusarium* strain from a 10-day old culture was placed in the middle of a 9 cm petri dish containing Müller Hinton (MH) or PDA agar (Oxoid). Then, a streak of the bacterial suspension was seeded at each extreme of the plate, to allow its growth without immediate contact with the fungal strain. Petri dishes were incubated for eight days at 25°C, and the presence of an inhibition zone between the bacterial strain and the fungi was considered a positive result. Phenotypic changes in the fungal growth were verified by comparison with the negative control. Each bacterial isolate was tested by triplicate in both MH and PDA agar media against the ten fungal strains.

For agar-well diffusion assays, the bacterial strains were grown in triplicate on 200 mL of LB broth, as described previously. After five days of growth, each culture was centrifuged for 10 minutes at 3900 g, and its spent supernatant was filtered using nitrocellulose membranes (0.2 µm). A volume of 100 µL of the filtered solution was added to a 6 mm well aseptically punched on a PDA Petri plate. These plates were previously surface inoculated with 100 µL of a conidial suspension from each fungal strain and incubated for 48 hours at 25°C after bacterial inoculation. The formation of an inhibition halo was a positive result for antimicrobial activity (336). Each bacterium was tested by triplicate, and the complete test was conducted twice.

Inhibition halo diameters were measured and compared for all the evaluated strains by one-way variance analysis (ANOVA) and Tukey's posttest ($p < 0.05$) using the software GraphPad Prism. 100 µL of uninoculated LB media and Benomyl 50WP PhytoCare (50 µg·mL⁻¹) were used as negative and positive control, respectively. Strains that consistently showed activity against two fungal isolates were considered potential antagonistic isolates and selected for further analyses.

2.2.3 Phenotypic and molecular characterization of active strains

a) Biochemical and physiological characteristics

A polyphasic approach was used to identify those strains with proven antifungal activity. First, the strains with antifungal activity were evaluated *in vitro* to determine carbohydrate fermentation, salinity, temperature, pH tolerance, motility, starch hydrolysis capacity, oxidase, and catalase biofilm formation, CWDE production, and gram staining.

Salinity, temperature, and pH tolerance were first determined on LB agar. The LB medium was supplemented with 1, 2 or 3% (w/v) NaCl for salinity tolerance test. For temperature tolerance, all the active isolates were grown in LB agar and incubated at 25, 30, 37, and 40°C. Finally, for the pH tolerance assay, the pH of LB liquid medium was adjusted to 6, 7, and 8. The cultures were incubated at 30°C in constant agitation (120 r.p.m.), and their optical density at 600nm was measured after 48 hours of incubation. Optical density was compared among all conditions, and statistical differences were compared to a growth control (pH 7.0, Temperature 25°C, and NaCl 0.85%).

Cell motility was determined using a sulfide-indole-motility medium, whereas carbohydrate fermentation, starch hydrolysis, oxidase, and catalase assays were assessed using standard methods previously described (344). Biofilm formation was evaluated with the 96 well plate-based protocol described by Pierce et al. (345).

Other traits related to plant growth promotion and biocontrol were determined only for selected strains. Nitrogen fixation, Indol-3-acetic acid (IAA) production, and phosphate solubilization were evaluated through qualitative (Nitrogen fixation and phosphate solubilization) and quantitative (IAA) assays, as described by Goswami et al. (346). Chitinolytic, lipolytic, and proteolytic activities were also evaluated qualitatively on solid medium supplemented with colloidal chitin (5 g·L⁻¹), tween 80 (10 mL·L⁻¹) or skimmed milk (100 g·L⁻¹) respectively, as reported by Budi et al. and Singh, Mehta & Chhatpar (347, 348).

b) Molecular characterization of active strains

Taxonomical identification for antifungal strains was approached by PCR amplification, sequencing, and analysis of the entire 16S rRNA locus. Genomic DNA of each strain was obtained using a modified protocol of CTAB (Cetyltrimethyl Ammonium Bromide) /

Chloroform-isoamyl alcohol extraction described by Clarke (349). For 16S amplification, universal primers 27F (5'-AGAGTTTGATCMTGGCTCAG-3'), 1492R (5'-TACGGYTACCTTGTTACGACTT-3'), 785F (5'-GGATTAGATACCCTGGTA-3') and 907R (5'- CCGTCAATTCMTTTRAGTTT-3') were used (Primer sequences were retrieved from Macrogen, https://dna.macrogen-europe.com/eng/support/ces/guide/universal_primer.jsp).

PCR amplifications were carried out as described by Aw et al. (350). Briefly, the thermal cycling profile of initial denaturation at 95°C for 5 min followed by 30 cycles of denaturation at 95°C for 1 min, annealing at 55°C for 1 min and elongation at 72°C for 1 min were used. Amplimers were sequenced at “*Instituto de Genética-Universidad Nacional de Colombia*”. All 16S rRNA sequences obtained were compared with the corresponding reference sequences retrieved from the databases RDP (Ribosomal Database Project, <http://rdp.cme.msu.edu/>) and EzTaxon (<http://eztaxon-e.ezbiocloud.net/>) (351, 352).

Phylogenetic analysis of the partial 16S gene sequences was conducted using the Maximum Likelihood Method with MEGA7 software (353), after sequence alignment using MUSCLE algorithm. Evolutionary distance matrices were generated by Kimura 2-parameter method. The stability of tree topologies was assessed by bootstrap analysis based on 1000 resampling.

2.2.4 Active strain prioritization.

A principal component analysis was performed to select antifungal strains to be evaluated as promising BCA. This analysis included as variables the qualitative and quantitative antifungal activity of each strain against the ten *F. oxysporum* isolates, their phenotypic characteristics, and their taxonomical identity. The data set consisted of 28 strains, with 13 variables measured for each strain. Before the analysis, the data were mean-centered and scaled by the Pareto scaling method. The strains selected from the score-plot were those with the widest range and the stronger antifungal activity. All the models were constructed using SIMCA-P software (v.15, Umetrics, Umeå, Sweden).

2.3 Results and discussion

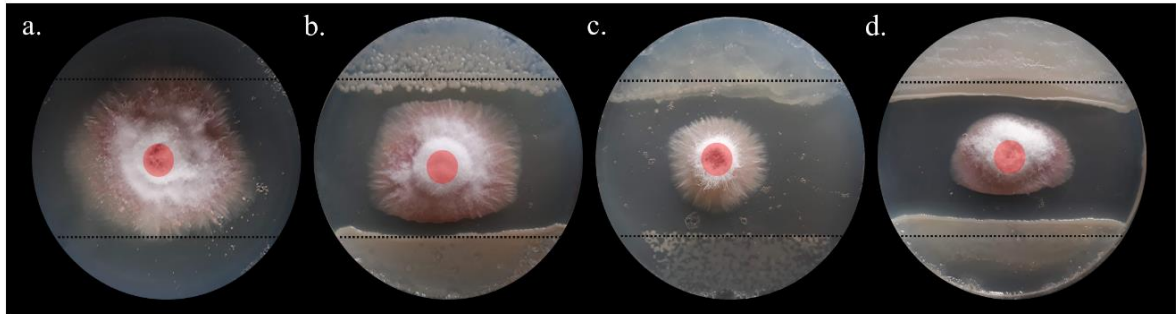
2.3.1 Marine-derived bacteria display antifungal activity against *F. oxysporum*.

Marine-derived bacteria are a heterogeneous group of microorganisms with high biotechnological potential considered as specialized metabolite-factories during the last decades (299, 354-356). Besides their antibacterial and antifungal activity against phytopathogens, there is no clear information that could lead to use them as rhizospheric biocontrol agents. Thus, in this chapter, the selection process of potential BCA against FOL is described.

In the first step, the marine-derived bacterial strains capable of inhibiting the growth of several isolates of *F. oxysporum* (*in-vitro*), including the pathogenic strain FOL59, were identified. Dual-cultured assays and agar well-diffusion tests were conducted during the primary screening. These assays were performed using nine *F. oxysporum* strains, recovered from wilted tomato plants, and one control strain FOL race 2, FOL59 (Appendix B). The dual-cultured assays were non-targeted tests that aimed to identify those bacteria able to inhibit the growth of the *Fusarium* strains, either by competition (space or nutrients) or antibiosis (diffusible or volatile compounds). The second assay allowed identifying isolates able to produce diffusible antifungal compounds under standard liquid culture conditions.

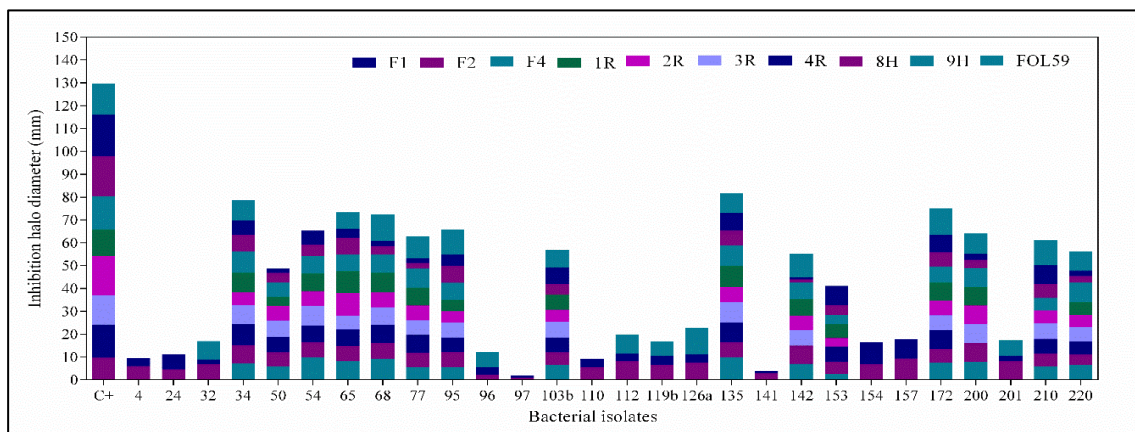
In the dual-cultured test, 42 out of the 152 tested bacterial isolates inhibited the growth of at least one strain of *F. oxysporum*. Some of these bacteria produced evident inhibition zones (Figure 2-1 a, b, d) without generating any phenotypic change in the fungal colony. Interestingly, the interaction between some fungal isolates, like FOL59, and bacterial strains, such as PNM172, generated differences in the fungal growth, including reduced colony diameter and aerial mycelium production, as well as changes in colony pigmentation (Figure 2-1 c). The absence of a clear inhibition halo could be observed in those treatments (Figure 2-1 c), suggesting the possible role of volatile metabolites in the antifungal activity. However, since no specific test for volatile compounds was carried out, this hypothesis should be further confirmed.

Figure 2-1: Dual-cultured assay of Firmicutes-like bacteria against FOL59. The figure shows FOL59 growth control (a) and the results obtained with PNM 34 (b), PNM 172 (c), and PNM 200 (d) on PDA. The red circles indicate the inoculation point of FOL59, whereas the dotted line shows the inoculation zone of each bacteria.



On the other hand, the agar-well diffusion assays with the filtrated supernatant of 63 strains showed antifungal activity against *F. oxysporum*, indicating that these bacteria produce diffusible metabolites responsible for the observed antifungal activity. From the tested bacteria, 28 active strains were pre-selected, considering the consistency in the results obtained from the dual-cultured and the agar well diffusion assays (Figure 2-2). The number of susceptible *F. oxysporum* strains (at least two in both assays) and the inhibition halo diameter generated on the *in vitro* assays (minimum 3mm) were also considered for bacterial strains pre-selection.

Figure 2-2: Antifungal activity of the pre-selected 28 firmicutes-like bacteria on agar well diffusion assay against *F. oxysporum*. C+, Positive control (Benomyl 50W). Only those bacteria with antifungal activity against two (or more) strains of *F. oxysporum* are shown. The bars represent the sum of the inhibition halo (mm) average for three biological replicates per bacteria.



In the agar well diffusion assays, the fungal isolates presented different susceptibility profiles towards the metabolites present in bacterial supernatants. This result may be related to pathogen intraspecies genetic diversity, which leads to the apparition of isolates with higher resistance to the BCA produced antibiotics, resulting in a lower biocontrol effect. This behavior has been observed in studies with *Ralstonia solanacearum* (tomato) and *Rhizoctonia solani* (rice), were potential BCA tested against different strains of the phytopathogens presented biocontrol efficacies between 19-80% (357, 358). In those studies, higher *in vitro* activity was correlated with a higher *in vivo* biocontrol effect.

Fifteen strains, namely PNM34, PNM50, PNM54, PNM65, PNM68, PNM95, PNM103B, PNM135, PNM142, PNM153, PNM172, PNM200, PNM210, and PNM220, showed wide-spectra antifungal activity. These bacterial strains inhibited the growth in at least eight out of the ten fungal strains tested, including the highly virulent FOL59 and the Benomyl-resistant *F. oxysporum* 9H. Those 15 bacterial isolates' antifungal activity can be considered an advantageous trait that will improve the marine-derived BCA performance on different tomato cropping regions. However, as *in vitro* activity does not always correlate with *in vivo* biocontrol effects, other biocontrol traits should be addressed during the BCA selection process.

2.3.2 Potential biocontrol agents against *F. oxysporum* belongs to the order Bacillales.

The 28 pre-selected strains correspond to Gram-positive or Gram variable sporulated rods, with a moderated range of temperature, salinity, and pH tolerance (Appendix A). These strains were oxidase-positive and were able to hydrolyze starch and casein (except for PNM157). Interestingly, the 28 active bacteria were able to form biofilms, and some of them produce CWDE like proteases and cellulases (table 2-1). These traits are common on BCA and contribute to the inhibition of fungal pathogens (CWDE) and persistence in rhizospheric environments (Biofilm formation ability) (165).

According to the 16S rRNA sequences analyses (each >1200 bp in length), all the active strains belong to phylum Firmicutes, order Bacillales (Figure 2-3, Table 2-1). From them, 22 strains are part of the *Paenibacillus* genus, being the most closely related species *P. elgii* for PNM24, PNM154, and PNM210, with similarity percentages of 99.72%, 99.65%,

and 99.77% respectively and, *P. ehimensis* for the remaining 19 strains with percentages of similarity higher than 99%.

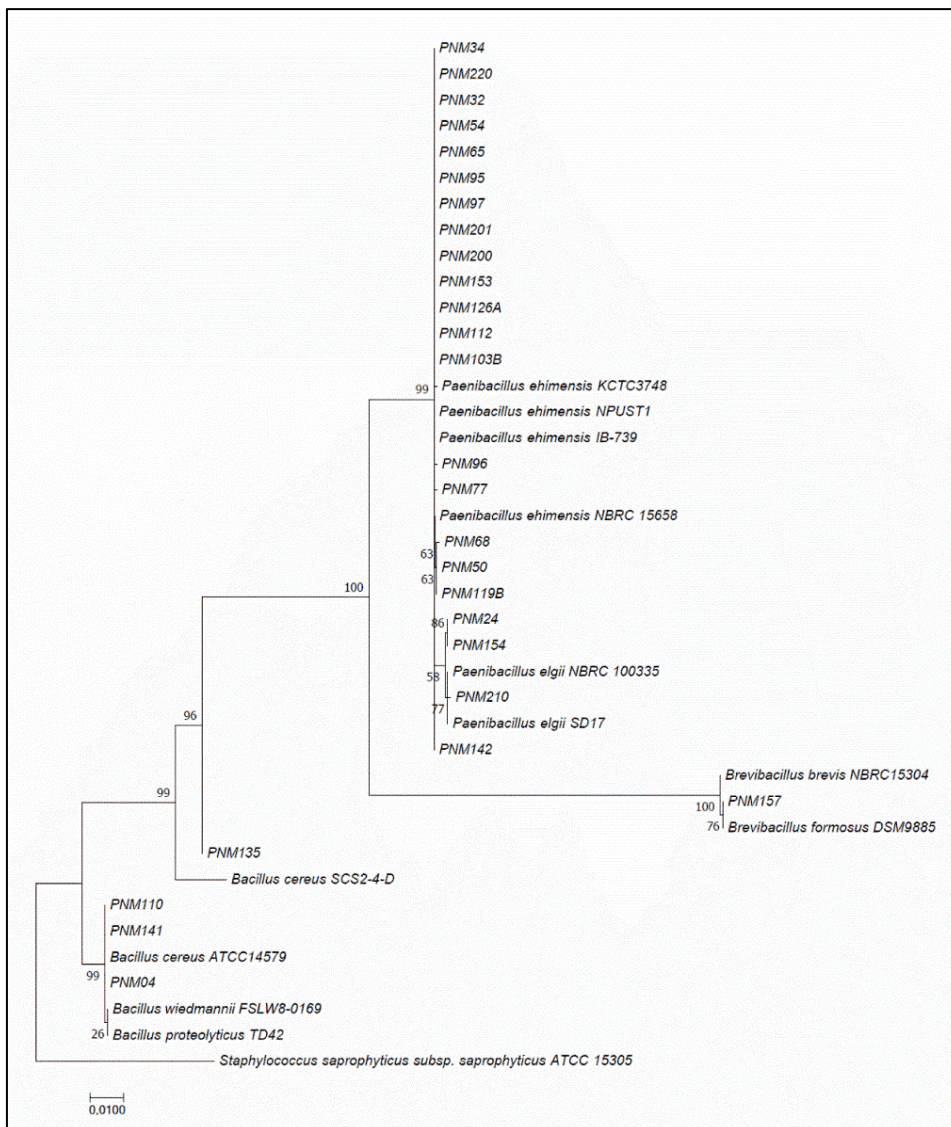
Table 2-1: Active bacterial strains source and CWDE production. In the table, NI, No identified, CH, Chitinase; LP, Lipase; PT, Protease

| Strain ID | Source | Taxonomical identity | CWDE production | | |
|-----------|---|--------------------------|-----------------|----|----|
| | | | CH | LP | PT |
| PNM4 | <i>Niphates digitalis</i> (sponge) | <i>Bacillus</i> sp. | - | + | + |
| PNM24 | Mangrove roots | <i>Paenibacillus</i> sp. | - | + | + |
| PNM32 | Sand sediments (Coral reef) | <i>Paenibacillus</i> sp. | - | + | + |
| PNM34 | <i>Niphates digitalis</i> (Sponge) | <i>Paenibacillus</i> sp. | - | + | + |
| PNM50 | <i>Codium</i> sp. (Algae) | <i>Paenibacillus</i> sp. | - | + | + |
| PNM54 | <i>Codium</i> sp. (Algae) | <i>Paenibacillus</i> sp. | - | + | + |
| PNM65 | <i>Niphates digitalis</i> (Sponge) | <i>Paenibacillus</i> sp. | - | - | + |
| PNM68 | <i>Niphates digitalis</i> (Sponge) | <i>Paenibacillus</i> sp. | - | - | + |
| PNM77 | <i>Amphimedon compressa</i> (Sponge) | <i>Paenibacillus</i> sp. | - | - | + |
| PNM95 | <i>Amphiroa</i> sp. (Algae) | <i>Paenibacillus</i> sp. | - | - | + |
| PNM96 | <i>Erithropodium</i> sp. (soft coral) | <i>Paenibacillus</i> sp. | - | - | + |
| PNM97 | <i>Erithropodium</i> sp. (soft coral) | <i>Paenibacillus</i> sp. | - | + | + |
| PNM103B | <i>Dictyota</i> sp. (Seaweed) | <i>Paenibacillus</i> sp. | - | + | + |
| PNM110 | Mangrove sediments | <i>Bacillus</i> sp. | - | + | + |
| PNM112 | Sand sediments (Coral reef) | <i>Paenibacillus</i> sp. | - | + | + |
| PNM119B | Fish "Pez loro" | <i>Paenibacillus</i> sp. | - | - | + |
| PNM126A | <i>Codium</i> sp. (Algae) | <i>Paenibacillus</i> sp. | - | - | + |
| PNM135 | Mangrove sediments | <i>Paenibacillus</i> sp. | - | - | + |
| PNM141 | <i>Codium</i> sp. (Algae) | <i>Bacillus</i> sp. | - | + | + |
| PNM142 | <i>Niphates digitalis</i> (Sponge) | <i>Paenibacillus</i> sp. | - | + | + |
| PNM153 | <i>Sargassum</i> sp. (Brown macroalgae) | <i>Bacillus</i> sp. | - | + | + |
| PNM154 | <i>Sargassum</i> sp. (Brown macroalgae) | <i>Paenibacillus</i> sp. | - | - | + |
| PNM157 | <i>Erithropodium</i> sp. (soft coral) | <i>Brevibacillus</i> sp. | - | - | + |
| PNM172 | <i>Amphiroa</i> sp. (Algae) | NI | - | + | + |
| PNM200 | Sand sediments (Coral reef) | <i>Paenibacillus</i> sp. | - | + | + |
| PNM201 | Sand sediments (Coral reef) | <i>Paenibacillus</i> sp. | - | + | + |
| PNM210 | <i>Eunicea fusca</i> (Soft coral) | <i>Paenibacillus</i> sp. | - | + | + |
| PNM220 | <i>Dictyota</i> sp. (Seaweed) | <i>Paenibacillus</i> sp. | - | + | + |

Strains PNM04, PNM110, PNM135, and PNM 141 belong to the *Bacillus* genus and were closely related to several species into the *B. cereus* group, including *B. cereus*, *B. toyonensis*, *B. anthracis*, and *B. paranthracis* with percentages of similarity higher than 99%. The PNM135 isolate also belongs to the *Bacillus* genus and is closely related to the species *B. wiedmanni* (97.38% similarity), *B. toyonensis* (97% similarity), and *B.*

proteolyticus (97.31%). Finally, PNM157 belongs to the *Brevibacillus* genera and is closely related to the species *B. brevis* (99.8%), *B. formosus* (99.8%), and *B. agri* (99.7%).

Figure 2-3: Molecular Phylogenetic analysis by Maximum Likelihood method of partial 16S rDNA sequences. The evolutionary history was inferred by using the Maximum Likelihood method based on the Kimura 2-parameter model. The tree with the highest log likelihood (-3210,96) is shown. The percentage of trees in which the associated taxa clustered together is shown next to the branches. A discrete Gamma distribution was used to model evolutionary rate differences among sites (5 categories (+G, parameter = 0,1351)). The tree was drawn to scale, with branch lengths measured in the number of substitutions per site. *Staphylococcus saprophyticus* subsp. *saprophyticus* ATCC 15305 was used as an outgroup.



The biochemical profiling results (phenotypic traits) obtained for the bacteria mentioned above were consistent with the identified genera's information, supporting the proposed classification. Strain PNM172 could not be identified because it was not possible to amplify its 16S rRNA gene after several attempts. Further studies will be conducted to determine the taxonomical identification of PNM172 and to obtain detailed information at the species level for the other selected bacteria.

Most of the bacteria closely related to *P. ehimensis* and *P. elgii* species had a higher inhibition against FOL59 in the agar well-diffusion assays. *Paenibacillus* is a widely distributed bacterial genus. Members of this genus have been used as biocontrol agents and plant growth promoters in tomato(359-361), bentgrass (362), cucumber (363, 364), pepper (263), tobacco, and groundnut (365). Furthermore, *P. ehimensis* and *P. elgii* are acknowledged as biocontrol agents and have been studied by its antifungal activity towards *F. oxysporum*, *F. graminearum*, *F. moniliforme*, *F. solani*, *F. nivale*, *Colletotrichum lini*, *R. solani* (366-368), *C. gloeosporioides* (264, 369) and *Pythium aphanidermatum* (370).

Some phenotypic characteristics of *Paenibacillus* strains such as their fast growth rates, lower nutritional requirements, endospore production, and broad secondary metabolite support the interest in these bacteria as BCA, alongside other firmicutes such as *Bacillus* (246, 363). To date, it has been reported that antibiosis is the main mechanism of action in several *Paenibacillus* strains (182, 246). Antimicrobial compounds such as lipopeptides, non-ribosomal peptides, and polyketides, and CWDE and VOCs, have been isolated from different *Paenibacillus* species (182, 246, 371, 372). These compounds show a wide range of antimicrobial activity and have been used to control tomato pathogens such as *Pseudomonas syringae* pv. *tomato*, FOL, FORL, and *Verticillium* spp. (266, 371, 373).

Interestingly, in this study, most of the active *Paenibacillus* were isolated from sessile soft-tissue organisms like sponges, algae, and soft-corals (Table 2-1). The ecological role of secondary metabolites in marine bacteria associated with a macro-organism is supported by the **hologenome theory** (374, 375). This theory points out that in the holobiont¹, the

¹ **Holobiont**: Ecological unit formed by the association of several species. Considered as the true evolutionary unit in the hologenome theory.

antibiotic-producing microorganisms may play an essential role as the source of chemical defenses that protect their hosts against predators and pathogens, through the production of bioactive metabolites (242, 376-378). This theory could apply to the pre-selected bacteria's antifungal activity and explain the original role of the produced metabolites of these microorganisms in their original ecological niche.

2.3.3 Antifungal activity range leads to bacterial strains prioritization.

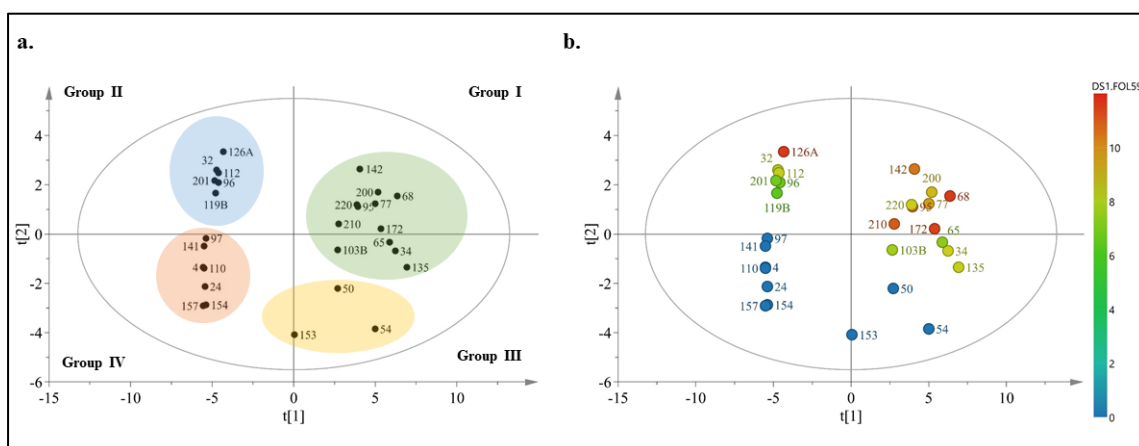
As mentioned above, according to the *in vitro* test, 28 bacteria were selected as promising BCA. However, it was necessary to prioritize which of these strains should be studied *in vivo*. Most non-targeted studies aim to identify BCA select microorganisms through criteria, such as taxonomy (379), *in vitro* or *in vivo* activity, phenotypic characteristics, metabolic profiles, or a combination of these criteria (27). Here, the taxonomical identity, phenotypic characteristics, and biological activity were the criteria for bacterial prioritization.

After taxonomical identification, a PCA was performed to obtain a visual representation of the 28 selected bacteria variances. This process allowed observing four main clusters grouped according to their antifungal activity (Figure 2-4 a). Phenotypic characteristics such as biofilm formation and enzymatic activity did not significantly contribute to group variation.

Group 1 consisted of twelve bacterial isolates with antifungal activity against eight or more *F. oxysporum* isolates and higher antifungal activity against FOL59 (inhibition halo > 6mm). Group 2 consisted of three bacteria with antifungal activity against eight or more *F. oxysporum* isolates, but inactive against FOL59.

Group 3 included six bacteria with antifungal activity against 3, or less *F. oxysporum* isolates but with high inhibition against FOL59 (inhibition halo > 6mm). Finally, group 4 encompassed seven bacteria with antifungal activity against three or less *F. oxysporum* isolates that were inactive against FOL59.

Figure 2-4: Bacterial strains prioritization by PCA. In the left score plot (a) group I, II, III, and IV are highlighted in green, blue, yellow, and red, respectively. The right score plot (b) shows the antifungal activity of the 28 selected bacteria against FOL59 in the agar-well diffusion assay. According to the scale in the right, the color of each point represents the inhibition halo diameter (mm). Scaling model: Pareto, $R^2 = 0.762$; $Q^2 = 0.54$. The first component (t [1]) explains 65% of the variation, the second component (t [2]) explains 11.2% of the variation.



According to this result, bacterial strains of group 1 were selected for colonization analysis on tomato (Milano cv.) roots, under gnotobiotic conditions, and *in vivo* antifungal activity against FOL59, as will be presented in chapter 3.

2.4 Final remarks

Marine-derived microorganisms have been studied for the last decades as a source of bioactive secondary metabolites. To date, several reports indicate the capability of marine-derived bacteria to produce antifungal metabolites that can be used in plant-pathogen management programs. Most of the marine-active strains described so far belong to the Actinobacteria and Firmicutes phylum. In this study, a group of twenty-eight bacteria from the Bacillales order were selected because of their antifungal activity against a panel of ten *F. oxysporum* strains that includes FOL59, a virulent isolate of FOL race 2.

The prioritization process led to the selection of twelve active strains belonging to the *Bacillus* and *Paenibacillus* genera. These isolates had the highest antifungal activity against

the tested phytopathogens and presented traits that made them interesting for mass-production like fast growth rates in simple culture medium like LB (data not showed), production of endospores, and tolerance to different ranges of pH, salinity, and temperature.

The antifungal activity of the selected strains was related to antibiosis since there was evidence of antifungal diffusible metabolites production during liquid fermentation on LB medium. Interestingly, most of these bacteria were recovered from sessile marine organisms such as sponges and algae. It has been reported that sessile marine-organism microbiome participates in host protection against pathogens through secondary metabolites production. This hypothesis could explain the studied bacteria's ability to synthesize antifungal compounds and points out its biotechnological potential for agricultural purposes.

3. Colonization ability and *in vivo* antifungal activity of antagonist bacteria

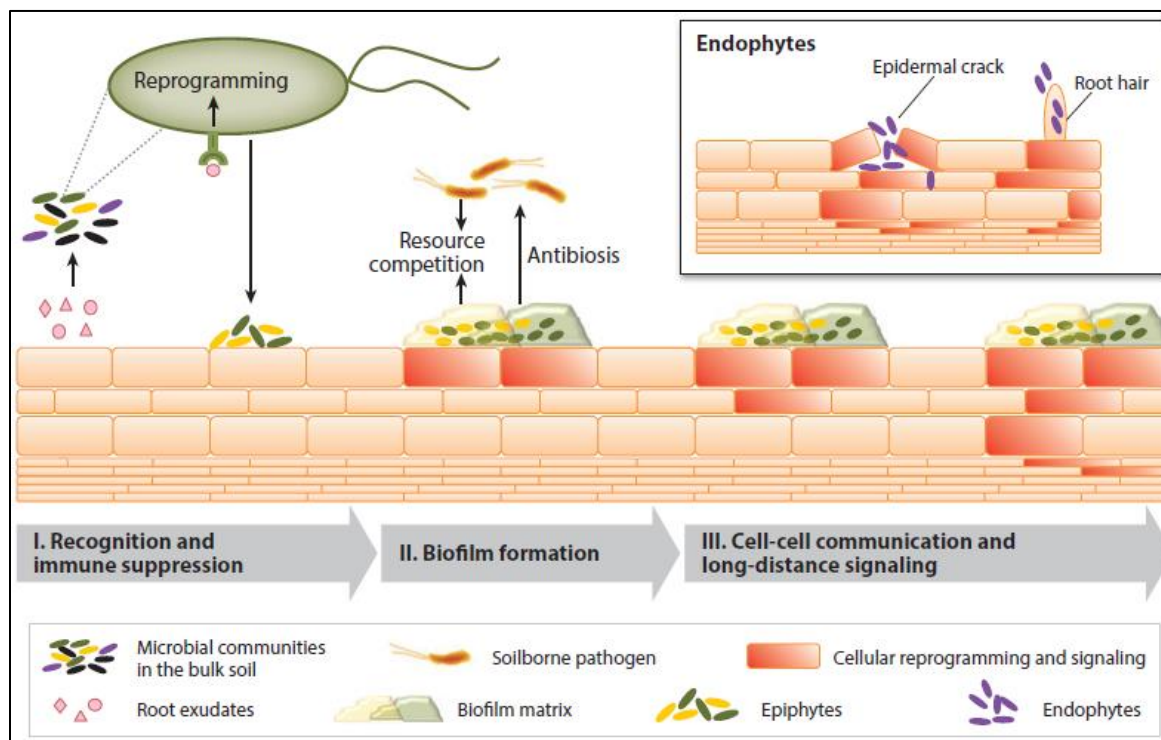
3.1 Introduction and scope

Root colonization has been considered as the first step in the establishment of plant-BCA mutualistic associations. Limited root colonization is related to inconsistent performances of these microorganisms on the field (380). Bacterial rhizosphere colonization and survival on roots systems, broadly known as **rhizospheric competence**, depend on multiple bacterial-related factors including motility, attachment, growth, stress resistance, and secondary metabolites production (381).

Root colonization begins with plant-host recognition, followed by chemotaxis towards the root system, attachment to the root surface, biofilm formation, and propagation into root epidermis or intracellular colonization (only for endophytic microorganisms) (Figure 3-1) (227). Root colonization ensures BCA's successful activity, affecting several antagonist mechanisms like competence, antibiosis, and ISR (283).

Root exudates mediate plant-host recognition in the rhizosphere (382). Primary (e.g. sugar, amino acids, and organic acids) and secondary metabolites (e.g., strigolactones) are released to the rhizosphere as part of the root exudates by diffusion or active transport (383). These compounds play an essential role in recruiting beneficial microorganisms acting as signaling molecules, chemoattractants, phytochemicals, or toxins (384, 385), mediating plant intra-species and inter-species interactions (386).

Figure 3-1: General phases of root colonization by beneficial microorganisms as proposed by Pieterse et al. (227).



For BCAs, root exudates act as carbon and nitrogen sources and as chemoattractant signaling molecules that facilitate the microorganism movement towards plant rhizoplane (387). Different root exudates molecules like sugars, amino acids, and organic acids are detected by histidine-kinase-type transmembrane chemoreceptors (388, 389). Upon signal recognition, the cytoplasmic domain suffers a conformational change that results in transcriptional changes in the microbial cell, affecting the bacterial behavior (388, 389).

Motile bacterial modify their migration patterns and move to the rhizoplane, where the nutrient/signal concentration is higher (chemotaxis) (389). After initial attachment in the rhizoplane, bacteria could settle on the root epidermis in microcolonies. In many rhizospheric competent microorganisms, microcolonies are enclosed in an exopolysaccharide and mucilage matrix, forming multicellular communities known as **biofilms** (227, 283).

Within biofilms and microcolonies, bacteria coordinate the production and release of compounds associated with antibiosis, competence, plant nutrient acquisition (PGPR

traits), and ISR (22, 283, 357). Poor rhizospheric colonization is associated with reduced *in vivo* biocontrol effect (390), whereas highly rhizocompetent microorganisms tend to have a better behavior on field and greenhouse trials (357, 380).

Rhizospheric competence evaluation on gnotobiotic systems is common since it allows determine the BCA's bacterial density on root systems in a specific period. During colonization assessment, the effects of potential BCA on plant growth can be estimated. Remarkably, many BCAs have plant-growth-promoting traits that increase their contribution to plant development (391).

In addition to colonization assays, *in vivo* antifungal activity evaluation is a pre-requisite during the selection process of BCAs. *In vivo* assays are carried out under controlled conditions using sterile or non-sterile substrates like soil (257), humus/peat (392), biochar, or compost amendment soils (393). Usually, *in vivo* tests using one or more highly virulent strains, and root-dip (394) or soil drenching (395) infection methods, aiming to mimic scenarios with highly pathogen pressures. Furthermore, some research selects specific physiological races considering the pathogen distribution on the geographical region of interest (392).

For *in vivo* antifungal activity against FOL, isolates of physiological races 1, 2, and 3 have been used (392, 395). Most of the evaluated phytopathogens are recovered from wilted tomato plants in regions with high VW disease incidence or severity (115, 396). Since each physiological race has a different range of pathogenicity towards specific tomato cultivars, an adequate plant host must be selected. In the present research, strain FOL59 was used for *in vivo* antifungal assays. This fungus was identified by Carmona et al. as a highly virulent strain of FOL race 2, and it was isolated from wilted tomato roots in the Caldas department (Colombia). *In vivo* assays were carried out using the susceptible tomato cultivar Santa Cruz Kada as recommended by Carmona et al. (115).

The colonization process and VW symptoms generated during FOL59 infection on tomato plants were evaluated under greenhouse conditions and compared with the original reports of this strain (Appendix C). This information was used to evaluate, under *in vivo* conditions, the antifungal activity of the nine selected bacteria. Furthermore, data on colonization ability and chemotaxis towards tomato root exudates were obtained to determine if the potential

BCAs could be considered rhizospheric competent microorganisms. Altogether, the results obtained in these experiments led to selecting one BCA candidate that showed the best behavior under *in vivo* conditions. These assays' results constitute the second phase of BCA development for FOL and are present in this chapter.

3.2 Materials and methods

3.2.1 Gnotobiotic root colonization assay on tomato plants.

A gnotobiotic colonization assay was performed to verify the ability of selected antifungal strains for colonizing tomato roots. To this end, a sterile mixture of vermiculite: soil (1:1) was used as substrate. Each bacterium was grown by triplicate in 100 mL of LB broth (120 r.p.m., 30°C, 5 days), and the culture was centrifuged to recover the bacterial pellet (10 minutes 3871 g). Cells were washed three times with a sterile saline solution, and the biomass concentration of each bacterial strain was adjusted to 1×10^6 CFU·mL⁻¹ with saline solution. This solution was used to inoculate the sterile substrate to achieve a final concentration of 1×10^5 CFU·g⁻¹ substrate.

Tomato plant seeds (Milano cv.; Impulsemillas™, Bogotá, Colombia) were surface sterilized using 70% ethanol for 3 min and then washed four times in sterile distilled water. Seeds were sown on water agar for germination. Fifteen-days-old tomato plantlets (with at least two true leaves) were transferred to the inoculated substrate and allowed to grow under sterile conditions, for 30 days at 30°C. Fifteen plants per treatment were taken out of the substrate and used to determine bacterial root concentration on the first four days post-inoculation (dpi) and in 10, 15 and 30 dpi. Bacterial root concentration was determined by viable cell count on mannitol modified solid medium (D-Mannitol 10 g, Beef extract 1 g, tryptose 10 g, NaCl 10g, Phenol red 0.025 g, Agar 15 g per L, pH: 7.2). *Bacillus subtilis* QST713 from Rhapsody biofungicide (BayerCrop®) was used as a positive colonization control.

The entire experiment was repeated three times for all the evaluated bacterial strains. Each isolate was then classified in one of three categories: root-colonizing bacteria (RC) for those bacterial strains that were present in the roots during the whole assay; variable-colonizing bacteria (VC) for those bacterial strains that were present in the roots for at least 15 dpi; or

non-colonizing bacteria (NC) for those bacterial strains that were not recovered from tomato roots.

A second colonization assay using Santa Cruz Kada cultivar (Impulsemillas™, Bogotá, Colombia) was performed following the same methodology previously described. This second assay only included strains from the RC or VC group. In addition to bacterial root counting, scanning electron microscope studies, fresh weight, shoot, and root lengths were also assessed in the treated plants and then compared with those from the non-inoculated control.

For SEM studies, inoculated and non-inoculated roots of each treatment were fixed by immersion on glutaraldehyde (2.5%) for six hours. Subsequently, the samples were dehydrated using a graded ethanol series and critical point dried in CO₂. Root samples were covered with gold and visualized with a COXEM SEM (397). For biometric parameters, significant differences between treatments and control plants were identified by one-way ANOVA followed by Dunnett's multiple comparisons test using GraphPad Prism statistic software (v. 6.0 GraphPad Software, La Jolla California USA, <http://www.graphpad.com>).

3.2.2 Effect of tomato root exudates on the chemotactic response of *Paenibacillus* and *Bacillus* strains (in vitro assays).

The chemotactic response of the selected strains towards tomato root exudates was tested by using a modified version of the qualitative swarming assay described by Park et al. (2008) and Tan et al. (2013) (398, 399). First, the tomato root-exudates were obtained following the protocol reported by Yang et al. (2016), using 20 days-old tomato plants (Santa Cruz Kada cv.) (400). Briefly, fifty plants were carefully removed from a soil: vermiculite sterile substrate and washed with sterile water. The plants were transferred in groups of ten individuals to 100 mL Erlenmeyer flasks containing 10 mL of sterile water and maintained at 25°C for 12 hours. Then, the water was collected, filtered, and stored at -20°C. The process was repeated, and the filtrated samples were pooled and freeze-dried (400). The dried sample was resuspended in 5 mL sterile water (10X) and used for the chemotaxis assay.

For the assay, bacterial cells from a 48-hours liquid culture were centrifuged and washed three times with saline solution and adjusted in phosphate buffer (50 mM) to a final OD_{600nm} of 0.4. A volume of 5µL of this suspension was drop-inoculated at one extreme of 1/10 LB agar medium plates and, 10 µL of concentrated root exudates were added on the opposite side. 5 µL of phosphate buffer was added to one of the wells as a negative control.

After 24 and 48 hours of static incubation at 30°C, each strain's swarming motility towards the root exudates or the organic acids was visually evaluated. These experiments were repeated three times and, the chemotactic responses were considered as positive if there was evident motility towards the tested compounds (colonies with a diameter at least twice compared to the negative control). A weak response was recorded when reduced motility was observed (colonies with a diameter of 1.5 compared to negative control). A negative response was recorded when there was not evident motility (nor growth differences) (398, 399).

3.2.3 *in vivo* biocontrol pot experiments.

Three consecutive *in vivo* experiments were carried out to assess antifungal activity for selected strains under greenhouse conditions, as suggested before (115). For this purpose, FOL59 and tomato plants Santa Cruz Kada were used. In the first experiment, 20 days-old tomato plants were infected by root immersion in a 1×10^6 microconidium·mL⁻¹ suspension of FOL59 for 15 minutes. Forty-five infected plants per treatment (grouped in 3 biological replicates) were transplanted into plastic pots with a soil/humus/vermiculite mixture (1:0.5:0.5), previously inoculated with a 72-hours LB culture suspension of each selected bacteria, adjusted to reach a final concentration of 1×10^5 CFU·g⁻¹ soil. A negative control, treated with sterile water instead of FOL59 suspension, and an infection control without bacterial inoculation to the soil, were used to verify the plant growth and disease development, respectively.

Plants were maintained under greenhouse conditions at 32°C and allowed to grow for 30 days. Once a week, the incidence, severity, and mortality of VW disease were recorded. Amini and Sidovich (2010) and Grattidge and O'Brien (1982) severity scale for VW symptoms were used as follows: 0, 0–24% of leaves yellowed and wilted; 1, 25–49% of leaves yellowed and wilted; 2, 50–74% of leaves yellowed and wilted; 3, 75–99% of leaves

yellowed and wilted; 4, 100% dead plant (150, 401). The severity index was calculated as $[(\sum (F_{IS} \times IS))/n]$ where F_{IS} is the frequency of each severity level, IS is the severity level, and n is the total number of observations. The area under the disease progress curve (AUDPC) was estimated by the trapezoidal integration method, using each treatment's severity values (402).

The marine-derived bacterial strains that reduced vascular wilt incidence or severity in a meaningful way were selected for the second assay. A double inoculation of the biocontrol strain was done in such cases, the first in the soil before transplantation, and the second 15 days post-infection. As in the first experiment, the incidence, severity index, AUDPC, and vascular wilt mortality were recorded once a week for 30 days. The most proficient strain was selected for the last *in vivo* assay to confirm the ability of the complete inoculum and the filtrated supernatant to reduce VW symptoms and compare their efficacy with a commercial BCA and a chemical fungicide.

For this assay, two inoculums of the selected strain were grown in LB broth for 72 hours at 30°C to obtain a filtrated supernatant. The concentration of each inoculum was evaluated by plate counting to exclude significant differences between them. From one culture, the biomass was separated by centrifugation (10752 g, 10 minutes). The obtained supernatant was filtrated through a nitrocellulose membrane (0.2 μm) and used to inoculate the soil mixture, adding the same volume added to the bacterial treatment, prior transplantation, and 15 days post-infection.

As previously mentioned, a formulated BCA, Rhapsody® (Bayer Crop), and a chemical fungicide, Benomyl 50WP® (Phytocare), were evaluated to compare the performance of the potential BCA candidate with commercial products. For Rhapsody inoculation, 4 mL of the BCA suspension (1×10^{10} UFC/mL) were applied by spraying them onto the soil surface. On the other hand, Benomyl® (0.5 g·L⁻¹) was applied by soil-drenching at rates equivalent to 0.5 kg·ha⁻¹ prior plant transplantation.

As previously mentioned, the incidence, severity index, AUDPC, and mortality of vascular wilt were evaluated until 30 days post-infection. The differences between treatments in all the experiments were evaluated through a One-way ANOVA followed by Dunnett's multiple comparisons test ($p \leq 0.05$) using the infection treatment as control group.

3.3 Results and discussion

3.3.1 Biocontrol *Paenibacillus* strains adapt to the tomato rhizosphere and promote plant growth under greenhouse conditions.

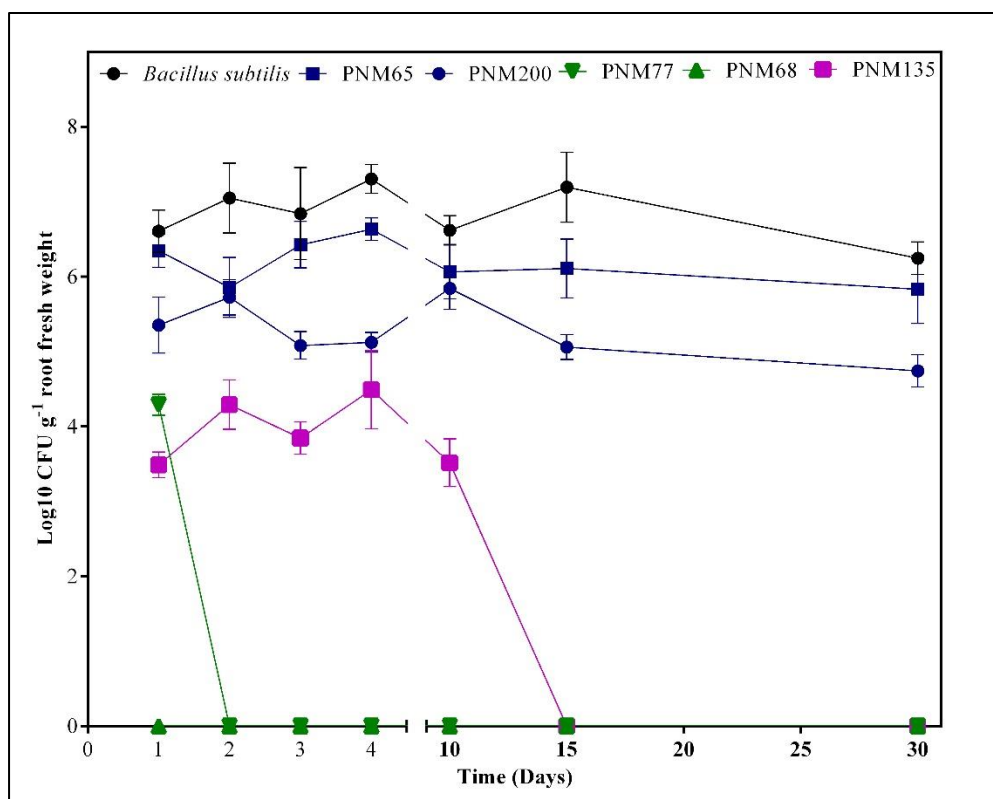
Twelve marine-derived bacteria were selected as BCA candidates for FOL management, based on the process for strain prioritization. These bacteria were classified according to its concentration on tomato roots after a 30-days assay as root-colonizing (RC), variable-colonizing (VC), or non-colonizing strains (NC), (Figure 3-2, Appendix D). The RC group included eight bacteria, PNM34, PNM65, PNM95, PNM103B, PNM172, PNM200, PNM210, and PNM220, that survive and grow in the tomato root system during the whole assay. The colonization profiles of the RC bacteria and the biological control *B. subtilis* (Rhapsody BayerCrop®) follow the same trend, even though the bacterial root concentration was different for each treatment (Figure 3-2).

A fluctuation within the first ten days characterized the growth of RC bacteria and *B. subtilis* on tomato roots, followed by a stabilization in its concentration 15 days post-inoculation. At some points, the RC bacterial population was higher enough to be equal to that of *B. subtilis* in the roots, here included as colonization control ($p < 0.01$, Appendix D). These results suggest that our marine-derived microorganisms could be rhizospheric competent and should be further studied to determine its potential as biocontrol agents.

Bacillus PNM135 was the only bacterial strain classified into VC group since it was possible to recover it from tomato roots during the first ten days of evaluation, but not at the end of the experiment (Figure 3-2). Even so, its colonization profile in the initial measurements followed the same tendency as the RC group suggesting partial rhizospheric competence in the tomato root system (Appendix D).

The three remaining strains, namely PNM68, PNM77, and PNM142, were either not retrieved from the roots since the beginning of the experiment or were only able to colonize the tomato rhizosphere for less than four days after inoculation. These results indicate that they cannot survive in the rhizospheric environment and were classified into the NC bacterial group, and therefore not further studied.

Figure 3-2: Examples of colonization profiles of different Firmicutes strains on tomato roots (Milano cv.). The mean concentration of three biological replicates per bacteria is shown. Error bars indicate the SD of the mean. *Paenibacillus* PNM68 and *Paenibacillus* PNM77 belong to the NC group (green), *Bacillus* PNM135 to the VC group (purple), and *Paenibacillus* PNM65 and *Paenibacillus* PNM200 to the RC group (blue). *B. subtilis* (Rhapsody, BayerCrop®) was used as colonization control in the tomato rhizosphere (Black).

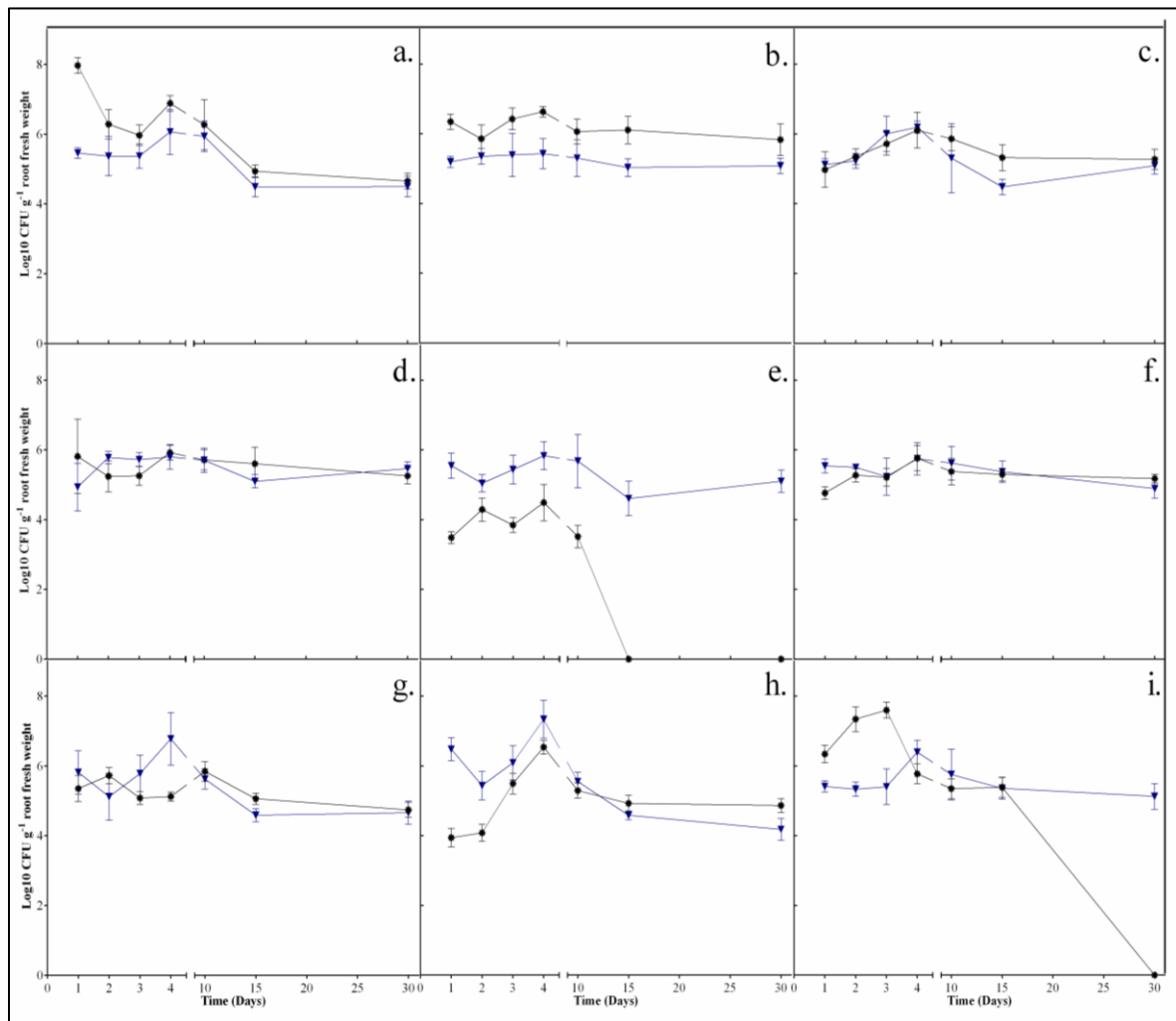


During the second colonization assay, both RC and VC bacteria colonize the tomato root system of Santa Cruz Kada cultivar (Figure 3-3). Even more, *Bacillus* sp. PNM135 was able to survive until the end of the assay in the treated plants' root system compared to the data obtained with Milano cultivar. For most of the isolates, the maximum bacterial recovery rate was observed at 4 dpi in Santa Cruz Kada cultivar.

Strains *Paenibacillus* sp. PNM200, PNM210, and PNM220 had a concentration of 3.41×10^6 , 4.27×10^7 , and 3.18×10^6 CFU·g⁻¹ root fresh weight, respectively. These bacteria reached higher root concentrations when compared to the other treatments (Appendix D). Their cell density was equal to that of *B. subtilis* control, being the higher count of these strains in the entire assay.

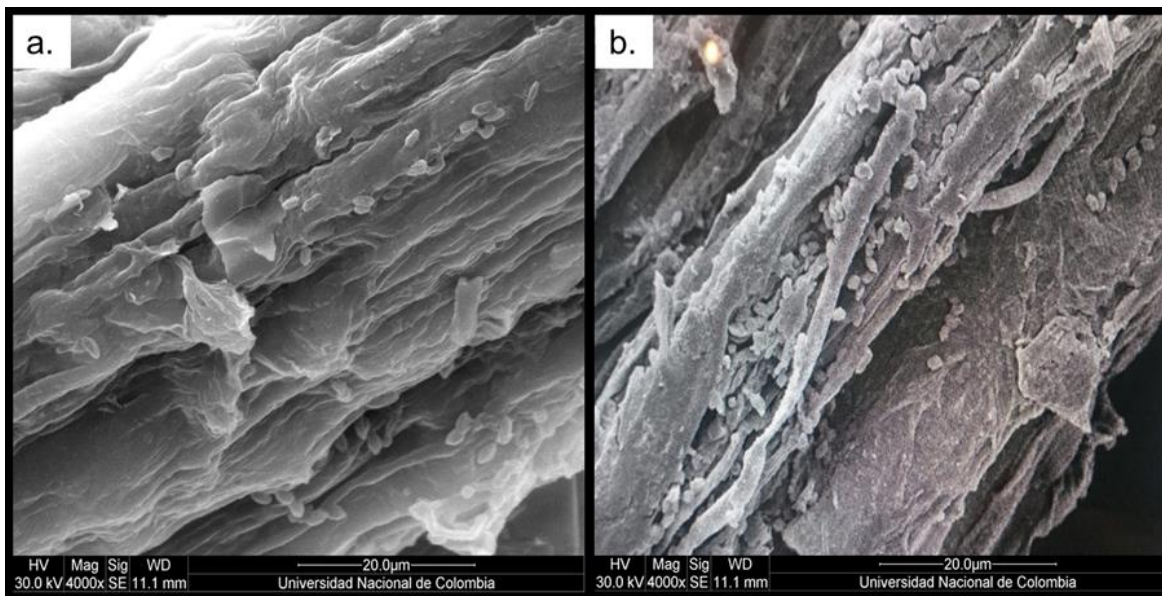
A similar result was obtained for *Paenibacillus* PNM95, which root concentration was the highest recovered in the experiment (1.63×10^6 CFU·g⁻¹ root fresh weight). The obtained data were comparable to the bacterial densities and colonization profiles reported for rhizospheric *Paenibacillus* and *Bacillus* strains like *B. subtilis* PTS-394 in tomato (2×10^6 CFU·g⁻¹) (403), *P. polymyxa* B1 on *Arabidopsis* roots (10^7 CFU·g⁻¹) (397) and *P. alvei* NAS6G6 recovered in wheat (2.03×10^7 CFU·g⁻¹) and tomato (7.73×10^5 CFU·g⁻¹) roots system (404).

Figure 3-3: Colonization profile of the selected bacteria on Milano and Santa Cruz Kada cultivars. The figure presents the colonization profiles of PNM34 (a), PNM65 (b), PNM95 (c), PNM103B (d), PNM135 (e), PNM172 (f), PNM200 (g), PNM210 (h) and PNM220 (i) on Milano (black) and Santa Cruz Kada (blue) cultivars. Error bars represent the standard deviation of the mean from three biological replicates per treatment.



The presence of each isolated in the rhizoplane was evaluated by SEM microscopy at 4 dpi, to confirm if the recovered bacteria were on the root surface. Bacterial colonization was confirmed comparing treated plants against a non-inoculated control (where no significant bacterial growth was observed). These analyses suggested that bacterial rod-shaped bacilli cells were attached to the root surface, particularly on root tips (Figure 3-4). Differences in bacterial density on roots were observed in some treatments such as *Paenibacillus* sp. PNM65 and PNM210. Although no evident biofilm formation was observed, bacterial monolayers could be seen in plants treated with PNM65, PNM95, PNM103B, PNM200, and PNM210. These results were similar to previous observations made by Timmusk and Nevo with *P. polymyxa* B1 (397).

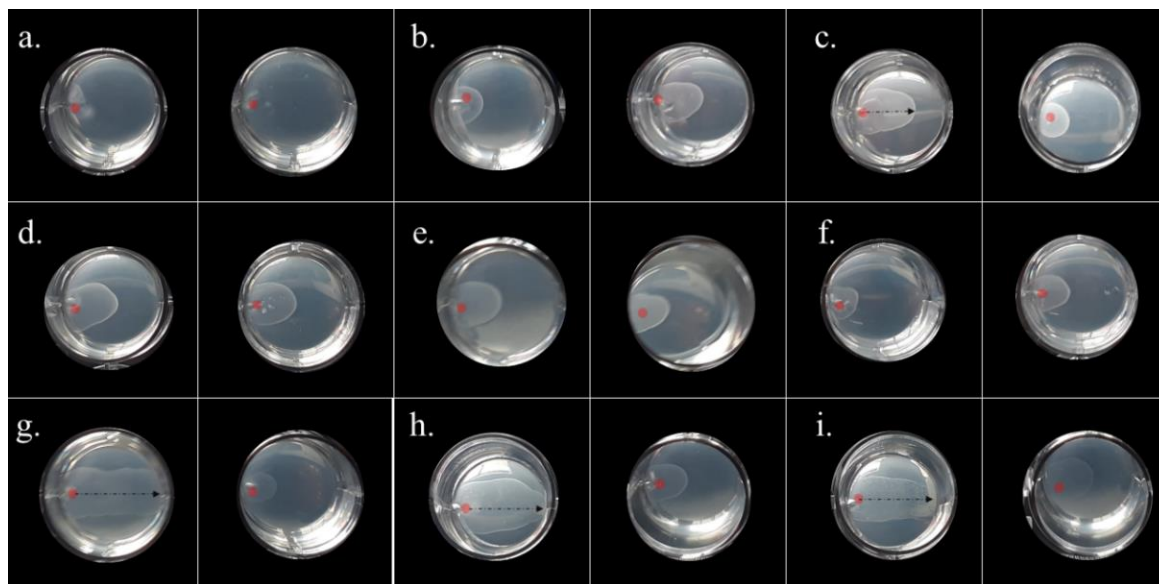
Figure 3-4: SEM depicts root colonization by *Paenibacillus* sp. PNM65 (a) and PNM210 (b) in tomato cv. Santa Cruz Kada roots at 4 dpi.



The obtained results correlated with the chemotactic response of these strains towards 20 days-old tomato root exudates. In other *Paenibacillus*, such as *P. polymyxa* BJSS14 (405) and SQR-21 (361), the chemotactic response towards plant root exudates has been proposed as the basis of the colonization process, and therefore one of the factors that could influence its efficiency as a biocontrol agent. *Paenibacillus* sp. PNM95, PNM200, PNM210, and PNM220 had a positive chemotactic response towards tomato root exudates

(Figure 3-5) while *Paenibacillus* sp. PNM34, PNM65, PNM103B, PNM135, and PNM172 did not show any chemotactic response with the evaluated exudates.

Figure 3-5: Chemotactic response of *Paenibacillus* strains towards tomato root exudates (1X) on the modified soft agar chemotactic assay. The figure shows the chemotactic response of PNM34 (a), PNM65 (b), PNM95 (c), PNM103B (d), PNM135 (e), PNM172 (f), PNM200 (g), PNM210 (h), PNM220 (i) and the assay scheme (j). Each panel presents the bacterial growth in the medium supplemented with tomato root exudates (left) or with phosphate buffer (right). The images were taken 24 hours post-inoculation. The red dot indicates the bacterial inoculation point (a-i).



Interestingly, those plants treated with *Paenibacillus* sp. PNM200 and *Paenibacillus* sp. PNM210 had a significant increase in shoot length and fresh weight compared with a non-inoculated control plants ($p < 0.05$, Figure 3-6). This result allows us to suggest a possible role of these isolates as plant-growth promoters. For this reason, characteristics commonly related to PGPR bacteria such as phosphate solubilization, biological nitrogen fixation, and IAA production, were determined. As presented in table 3-1, PNM200 and PNM210 can solubilize tri-calcium phosphate in Nbrp and SRS medium and produce small amounts of IAA amounts. Neither of them could fix atmospheric nitrogen but had lipolytic activity.

Figure 3-6: Effect of bacterial inoculation on tomato plant growth (Santa Cruz Kada cultivar). NIC: plants without bacterial treatment. Values are mean of three replicates \pm the 95% confidence interval. (*) indicates significant Dunnett's post'hoc differences between treatments and control (NIC) plants ($p < 0.05$). Data were recorded 30 days post-inoculation.

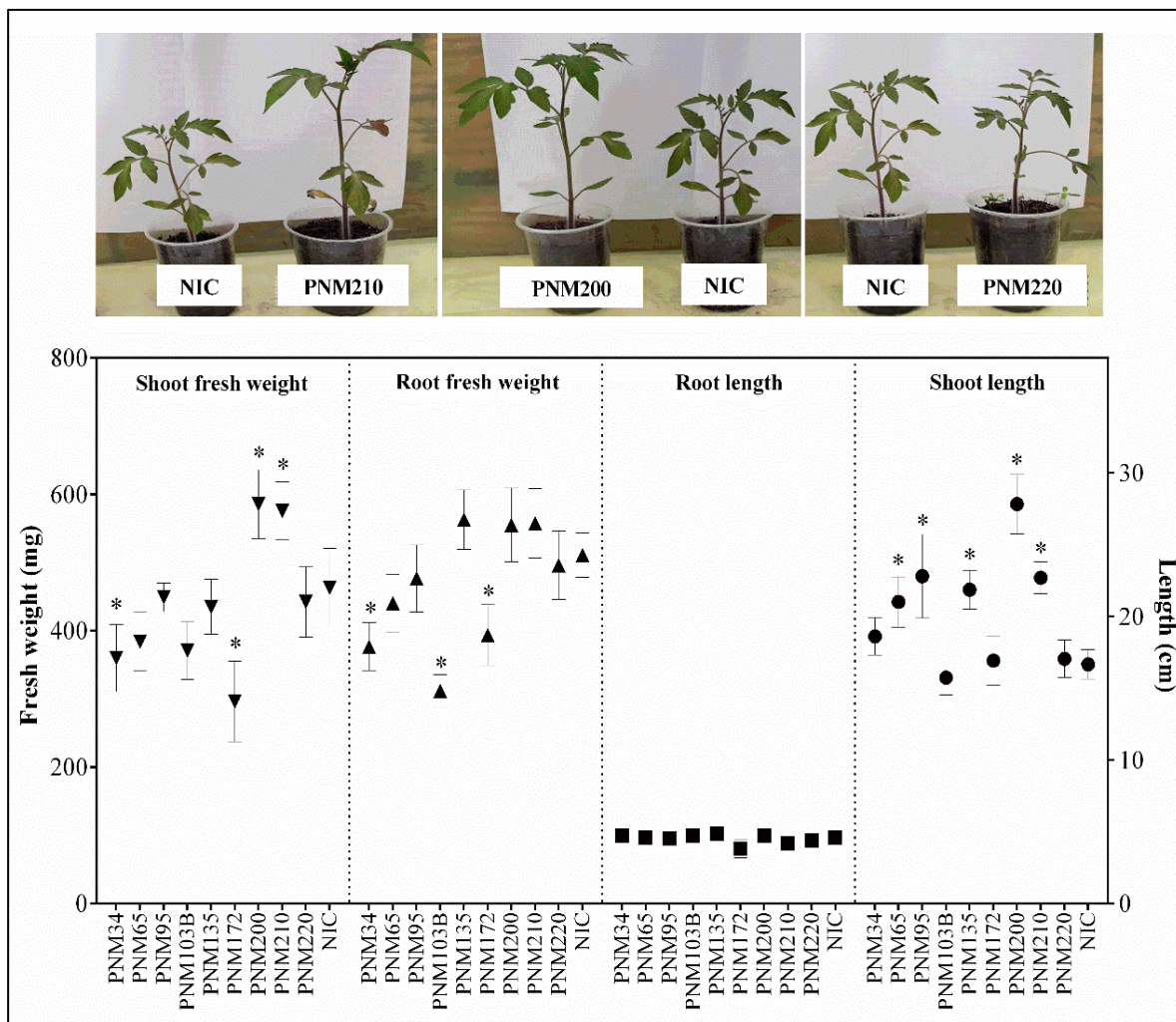


Table 3-1: PGPR related characteristics of the tomato growth-promoting *Paenibacillus* sp. PNM200 and PNM210.

| Strain | Phosphate solubilization (Qualitative assay) | | IAA production (ppm) | NBF |
|---------------------------------|---|--------------|-------------------------|-----|
| | SRS medium | Nbrip medium | | |
| <i>Paenibacillus</i> sp. PNM200 | + | + | 2.14 \pm 0.1 | - |
| <i>Paenibacillus</i> sp. PNM210 | + | + | 3.15 \pm 0.25 | - |

Overall, PNM34, PNM65, PNM95, PNM103B, PNM135, PNM172, PNM200, PNM210 and PNM220 strains showed the ability to be able to move towards root exudates, stay viable in the rhizospheric environment and improve plant growth in the absence of a pathogen (seen in the case of *Paenibacillus* sp. PNM200 and PNM210). Our results depict these bacterial strains' ability to adapt to a new niche, supporting its potential use for agronomical purposes.

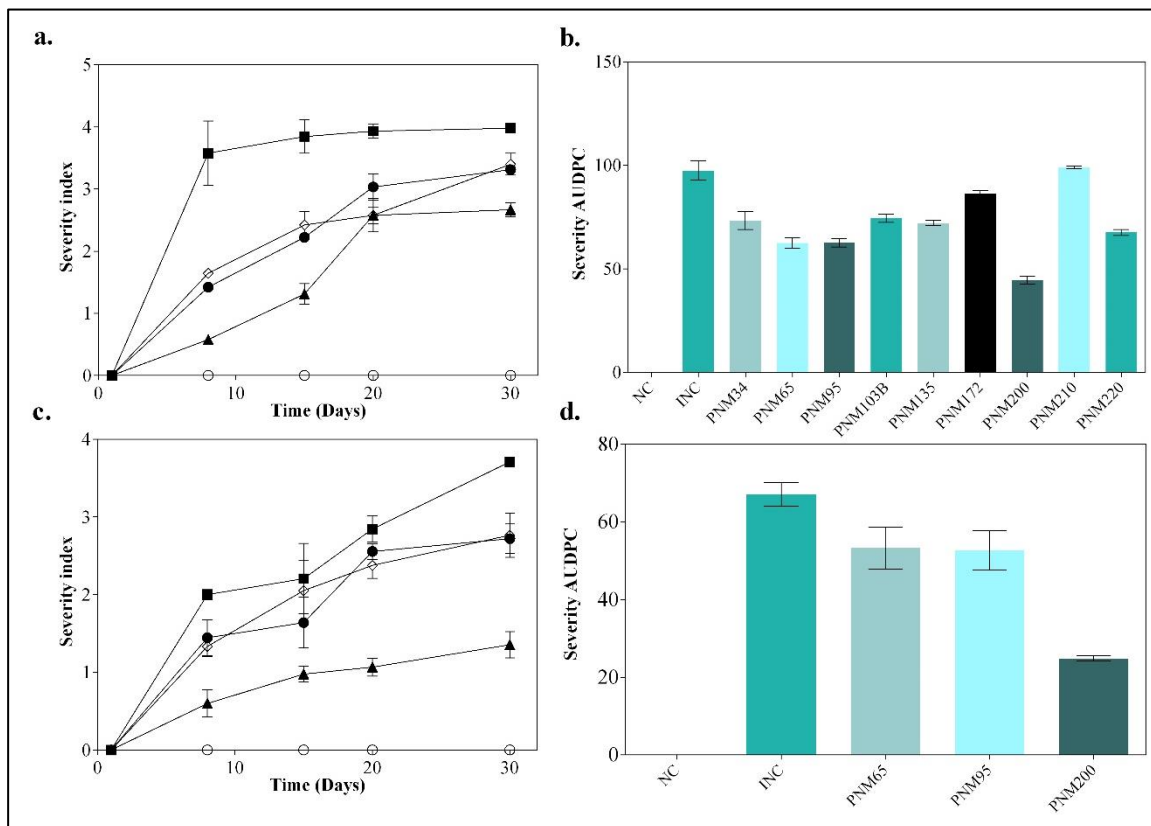
3.3.2 *Paenibacillus* sp. PNM200 reduce tomato vascular wilt severity caused by FOL59.

After colonization assays, the *in vivo* antifungal activity of colonizing selected bacteria was evaluated under greenhouse conditions in three independent assays. In the first assay, the nine selected strains were tested for their antifungal activity by a soil-drenching inoculation method. The treated plants showed a significant reduction on AUDPC compared to the infection control except those treated with PNM210 ($p < 0.05$, Figure 3-7 a,b). *Paenibacillus* sp. PNM65, PNM 95, and PNM200 showed a higher reduction in both AUDPC and severity index at 30-dpi, being the only strains able to maintain the severity index below 2.5 during the first 15-dpi ($p < 0.05$, Figure 3-7).

Remarkably, the beneficial effect of these strains was reduced after 15 dpi. This reduction in effectiveness coincided with the treatment days with a low bacterial population in roots. Reduced colonization (low bacterial concentration) on roots, leaves, or fruits of an antagonist may reduce the suppressive effect on plant pathogens. In several bacteria like *P. chlororaphis* (406), *B. megaterium* (407), and *B. amyloliquefaciens* (408) the colonization is a requirement for biocontrol effects. An increase in bacterial root populations could improve biocontrol, as observed for *P. fluorescens* F113 (409).

During the second experiment, a double inoculation of *Paenibacillus* sp. PNM65, *Paenibacillus* sp. PNM95, and *Paenibacillus* sp. PNM200 was done at 0 and 15 dpi by soil drenching, aiming to improve the first assay's protecting effect. In this case, plants treated with *Paenibacillus* sp. PNM200 showed the lowest severity index (1.356 ± 0.16) and AUDPC (24.85 ± 0.66) (Figure 3-7 c,d). These results represent a reduction of 63.4% in the severity index and 60.54% in the AUDPC compared to the infection control (Severity index 3.71 ± 0.03 , AUDPC 67.13 ± 2.99 at 30 dpi).

Figure 3-7: *in vivo* antifungal activity of *Bacillus* and *Paenibacillus* strains against FOL59. The figures present the severity index profiles (a, c) and the area under the disease progress curve (AUDPC, b, d) of three independent experiments done in Santa Cruz Kada tomato cultivar under greenhouse conditions. ● NC (Negative control), ■ INC (Infection control), ◆ PNM65, ● PNM95, ▲ PNM200. Data present in each graph are the means \pm standard deviation of three biological replicates per treatment.



Moreover, the decrease in the AUDPC suggests that the inoculation of *Paenibacillus* sp. PNM 200 delay the appearance of VW symptoms without affecting plant development. Similar results were obtained for tomato VW control with rhizospheric microorganisms such as *P. putida* 17 (severity reduction 58.6%) (410), *Bacillus* sp. B44 (single application, severity reduction 35.9%) (257), *P. ehimensis* KWN38 (severity reduction 84%) (264), and *P. polymyxa* GBR-508 and *P. lentimorbus* GBR-158 (97.6% and 90.2%, respectively) against the disease complex of FOL and *Meloidogyne incognita* (360).

Plants treated with *Paenibacillus* sp. PNM65 and *Paenibacillus* sp. PNM95 showed a minor improvement, with severity indexes of 2.76 ± 0.28 and 2.72 ± 0.19 , respectively. However,

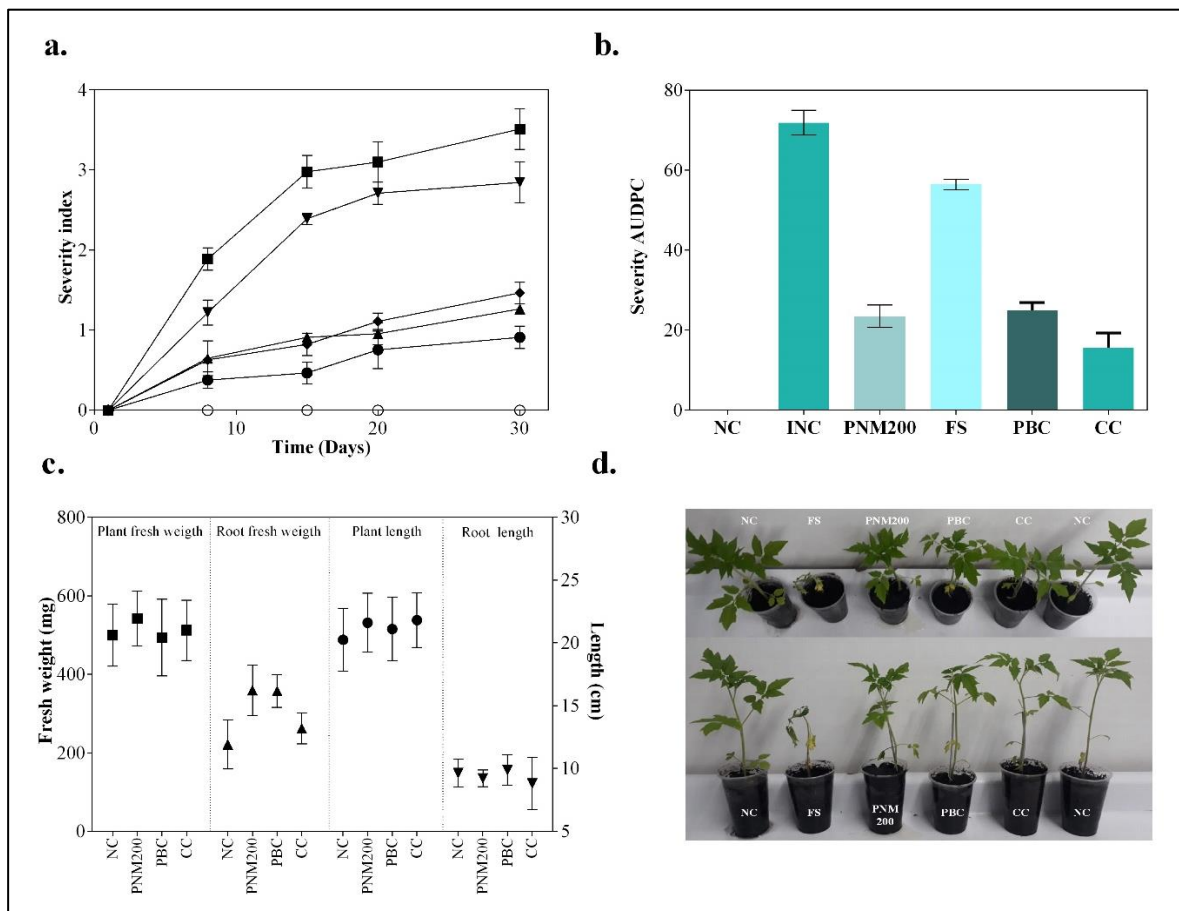
the AUDPC of these treatments did not show the same results. Even when the AUDPC of the treated plants was lower than the disease control, the reduction in the disease progression was less evident than in the first experiment.

Finally, in the third assay, it was evident that *Paenibacillus* sp. PNM200 and Rhapsody® presented similar severity indexes (1.26 ± 0.06 and 1.46 ± 0.13 , respectively) and AUDPC (Figure 3-8 a, b). Although plants of the PNM200 treatment have a higher severity index than plants from the chemical control (0.9 ± 0.13), their biometric parameters were not significantly different from the negative control (Figure 3-8 c, d). These results indicate that an effective *Fusarium* wilt control may be achieved on tomato by using the marine-derived bacteria *Paenibacillus* sp. PNM200, since its performance is comparable to a rhizospheric commercial BCA (*B. subtilis* QST713) and a chemical fungicide.

Paenibacillus sp. PNM200 filtrated supernatant (FS) was used to evaluate its effect on vascular wilt severity. As expected from both treatments, PNM200 and its filtrated supernatant reduced the severity index and AUDPC of vascular wilt disease in infected tomato plants. However, PNM200 treatment showed a significantly higher reduction in both parameters than the ones obtained in the FS treatment (Figure 3-8), indicating that the *in vivo* effect was not a direct result of *Paenibacillus* sp. PNM200 antifungal metabolites produced during fermentation, but a consequence of the bacterial inoculation.

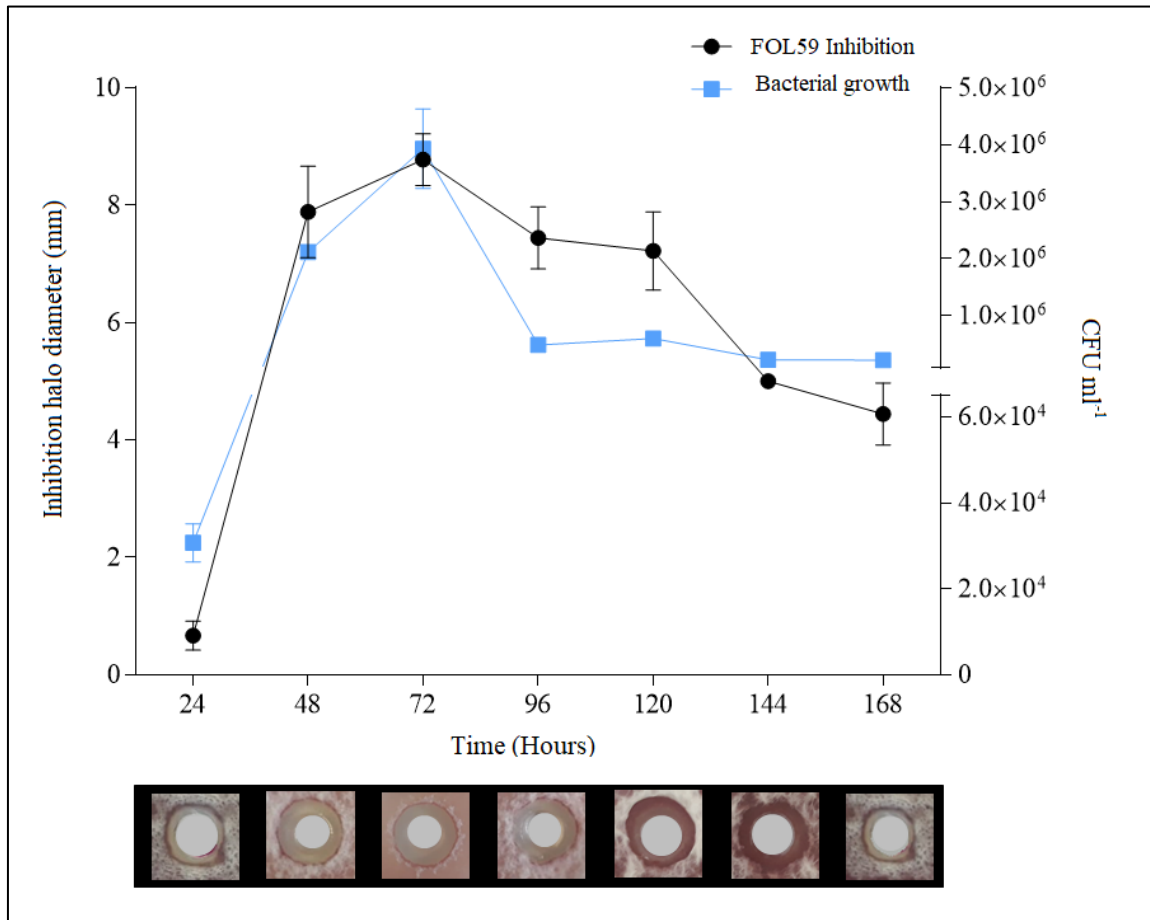
Plants treated with the filtrated supernatant of PNM200 had a lower protection regarding the bacterial strain inoculation results. The antifungal metabolites from *Paenibacillus* sp. PNM200 were recovered in late exponential fermentation when the highest antifungal activity was observed (Figure 3-9). These metabolites (filtrated supernatant) reduced the VW severity during the first days after infection. However, its effect was not enough to control fungal growth, supporting the need to use the entire strain as a biological control agent, and not just as a source of chemical fungicides. These results also indicate that PNM200 presents other no-established antagonism mechanisms that may increase their ability to reduce VW symptoms.

Figure 3-8: *in vivo* antifungal activity of *Paenibacillus* PNM200 against FOL59. The figures present the severity index profiles (a), the area under the disease progress curve (AUDPC, b) and the biometric parameters (c) evaluated in the third *in vivo* assay. In the panel a the symbols represent: ● NC (Negative control), ■ INC (Infection control), ▲ PNM200, ▼ FS (PNM200 filtrated supernatant), ● CC (Chemical control, Benomyl®), ◆ PBC (Positive biological control, Rhapsody®). Data presents in each graph are the means \pm standard deviation of three biological replicates per treatment.



Other than antibiotic production, *Paenibacillus* strains have shown several mechanisms of biocontrol, including ISR, competition with pathogens for space or nutrients, and production of lytic enzymes such as chitinases (182). *Paenibacillus* sp. PNM200 did not produce chitinases but can form biofilms, a common feature of marine bacteria, facilitating its plant-root colonization process, reducing the available space for fungal development.

Figure 3-9: Growth kinetics and antifungal activity of *Paenibacillus* PNM200 under liquid fermentation. Data are the mean \pm SD of three biological replicates.



Furthermore, some studies have shown that *Paenibacillus* and other marine-derived microorganisms produce several antimicrobial metabolites upon interaction with plants or pathogens. These compounds include VOCs (411, 412), amides (365), peptides and polyketides (413), that are not produced by the strain alone and could be related to the biocontrol phenotype of the producer strains. This differential metabolic expression could also be related to the biocontrol observed here and should be further studied in this biological model. Antifungal metabolite production, together with the ability to survive and establish in the tomato rhizosphere, suggests that marine-derived bacteria here studied could be considered as promising biocontrol agents. Moreover, the consistent results obtained from the *in vivo* assays indicate a reproducible effect in the *Paenibacillus* PNM200 inoculation on tomato under greenhouse conditions.

3.4 Final remarks

Rhizospheric competence is one of the most relevant traits in biocontrol agents' development. The low colonization ability of BCA's in the rhizospheric environment has been correlated with poor field performance. Although there is evidence of marine-derived bacteria acting as antagonists of phytopathogens, data regarding their rhizospheric competence and *in vivo* activity is limited. In this study, nine marine-derived bacteria colonized the tomato rhizosphere after thirty days post-inoculation, indicating that they are rhizospheric competent.

Some of the colonizing bacteria displayed colonization profiles similar to that of *B. subtilis*, used as positive colonization control. *Paenibacillus* sp. PNM200 and PNM210 enhance tomato growth. This ability was associated with IAA production and phosphate solubilization. Interestingly, these bacterial strains showed a positive chemotactic response towards tomato root exudates that could contribute to their rhizospheric competence.

The rhizospheric competent *Paenibacillus* sp. PNM200 reduces VW severity under greenhouse conditions. The highest VW severity reduction was achieved using a double inoculation of PNM200 at 0 and 15 dpi. With this inoculation method, the obtained results were comparable to those obtained with a commercial BCA (Rhapsody) and a chemical fungicide (Benomyl). Furthermore, the fact that *Paenibacillus* sp. PNM200 supernatant inoculation on infected plants did not reduce VW severity to the same extent as the whole strain inoculation, suggesting that the observed biocontrol effect results from the plant/bacteria/FOL59 interaction. These data comprise the first evidence for using of marine-derived bacteria as a biocontrol agent for fungal phytopathogens in tomato. Further studies are required to characterize the molecular interaction in this tripartite system, which also could contribute to understanding the biological control ability in *Paenibacillus* species.

4. Metabolic profiling of tomato-*Paenibacillus* PNM200-FOL59 interaction

4.1 Introduction and scope

In the present research, marine-derived bacteria were proposed as potential BCA for FOL control in tomato crops. As a result of phases one and two, one candidate, *Paenibacillus* sp. PNM200 was selected. This bacterium reduces the incidence and severity of *Fusarium* VW symptoms. Furthermore, *Paenibacillus* sp. PNM200 colonized the plant host root system and had a positive chemotaxis response towards tomato root exudates.

Initially, the antifungal activity of *Paenibacillus* sp PNM200 was associated with secondary metabolites production. However, metabolites produced during its liquid fermentation are not the SOLE responsible for VW control, since they did not reduce VW severity during in vivo assays. This observation suggests that *Paenibacillus* sp. PNM200 displays other mechanisms of action like ISR or competence. It is also possible that the interaction between FOL59 and *Paenibacillus* sp. PNM200 in the tomato rhizosphere induce the production of antifungal compounds that are not observed during liquid fermentation.

Several omics approaches can be adopted to identify which of the possibilities above-mentioned explains the plant-pathogen-BCA interaction. Genomics and transcriptomics approaches have led the research on the biotechnological applications of *Paenibacillus* strains. For example, the role of antifungal metabolites, VOCs, and enzyme production on biocontrol properties of *Paenibacillus* strains has been studied using greenhouse and field trials, genome sequencing, transcriptomics, and classical chemical-elucidation workflows (182, 363, 414).

Similarly, proteomics and untargeted metabolomics approaches have been used to evaluate the recruitment of *Paenibacillus* in plant rhizosphere mediated by root exudates

under biotic stress conditions, such as the presence of aphids, as well as the modulation of the proteome or metabolome in healthy or infected plants inoculated with *Paenibacillus* (415-417) (418-420).

Despite the importance of metabolic production to unravel the biocontrol mechanisms of *Paenibacillus* species, these studies began just recently. Since the end of the 1990s, metabolomics has held an important position in systems biology. The metabolome represents the final phenotype produced by the changes in an organism's gene expression under the influence of a physiological stage, a stimulus, and a biotic or abiotic stress condition (44, 421). Its evaluation is a proper approach to support functional gene annotation that allows assessing the cause of biological effects in complex plant-pathogen-antagonist associations (322, 422-424).

Among the diverse analytical platforms, LC-MS, GC-MS, and NMR-based metabolomics have been extensively used to unravel resistant and susceptible plants-responses towards phytopathogens. In tomato plants, these approaches focused on the most prevalent pathogens, including *P. syringae* pv. *tomato* (425, 426), *R. solanacearum* (427, 428), *A. alternata* (429), *A. solani* (430), *Phytophthora infestans* (431), *Verticillium dahliae* (70) and FOL (432, 433). These studies proposed several metabolites derived from the phenylpropanoid and alkaloid biosynthetic pathways as defense mechanisms of tomato against fungal pathogens, allowing to understand their functional roles in plant and how they could be useful in phytopathogens management programs.

Moreover, metabolomics has been applied to the evaluation of tomato metabolic responses towards beneficial bacteria. Some of these studies describe the changes in primary and secondary metabolism of tomato plants in the presence of beneficial microorganisms such as *Bacillus* spp. (432, 434), *Pseudomonas* spp. (434, 435), *Rhizophagus irregularis*, *Funneliformis mosseae* (436), and *Trichoderma harzianum* (434). Interestingly, some of those metabolic changes can be related to ISR signaling pathways in tomato plants against fungal phytopathogens like *R. solani* (437), and *F. oxysporum* (432, 438).

In the case of *Paenibacillus*, some *in vitro* approaches have been used to study this bacteria's capability to produce secondary antifungal metabolites in the presence of tomato root exudates and the phytopathogen FORL (439). Furthermore, the effect of FORL

mycotoxins on *Paenibacillus* secondary metabolism suggested the importance of the bacterial-fungal interaction on biocontrol events (411). Despite the *in vitro* information's relevance, few metabolomic studies followed *in-vivo* tritrophic interactions, leaving a gap in the knowledge of plant-*Paenibacillus* beneficial relationships.

Aiming to understand the molecular interactions between *Paenibacillus*, FOL, and tomato plants, an LC-MS/MS untargeted metabolomics approach was carried out in the third phase of this study. This analysis identified the metabolic variation caused by the co-inoculation of a virulent Colombian FOL strain, FOL59, and the selected BCA *Paenibacillus* sp. PNM200, in the plant root metabolome of susceptible tomato plants. Finally, some metabolites related to FOL infection were proposed to follow VW progress on tomato susceptible cultivars during the early disease stage.

4.2 Materials and methods

4.2.1 *In vivo* interaction assay under controlled conditions.

Commercial seeds of tomato cultivar Santa Cruz Kada, susceptible to FOL races 2 and 3, were sown in a 128 well-plastic tray containing a sterile mixture of soil/humus/vermiculite (2:1:1). The seeds were germinated for two weeks in a germination chamber at 20°C, with a 12 h photoperiod and 60% relative humidity.

For the metabolic profiling analysis of the tomato root, the pathogen, and the microorganism interaction, eight treatments were established as presented in table 4-1. Seedlings belonging to PF and PBF treatments were uprooted, washed in distilled sterile water, and dipped into a FOL59 conidial suspension (1.5×10^6 conidium·mL⁻¹) for 15 minutes. Likewise, seedlings belonging to PB and P treatments were uprooted and dipped in sterile water for 15 minutes.

Both infected and non-infected plants were transplanted into 16 Oz plastic cups filled with sterile soil/humus mixture (2:1 w/w). The soil/humus mixture of B, BF, PB, and PBF treatments was inoculated before the transplant, with a suspension of *Paenibacillus* sp. PNM200, obtaining a final concentration of 1.5×10^5 UFC·g⁻¹ soil. For F and BF treatments, 5 mL of FOL59 conidial suspension were added. Finally, a volume of saline solution

equivalent to the bacterial or fungal inoculum added in PB, PF, and PBF treatments were inoculated in the S control.

Table 4-1: Treatments and control groups established for the metabolic profiling of tomato-FOL59-*Paenibacillus* sp. PNM200 interaction.

| Treatment | Organism present per treatment | | | Sample |
|-----------|--------------------------------|-------|--------|-----------------------------|
| | Plant | FOL59 | PNM200 | |
| P | + | - | - | Roots and Rhizospheric soil |
| PB | + | - | + | Roots and Rhizospheric soil |
| PF | + | + | - | Roots and Rhizospheric soil |
| PBF | + | + | + | Roots and Rhizospheric soil |
| S | - | - | - | Bulk soil |
| B | - | - | + | Bulk soil |
| F | - | + | - | Bulk soil |
| BF | - | + | + | Bulk soil |

The experiment was conducted in a randomized complete block design (RCBD) with three replicates. Each replicate consisted of 60 plants used for metabolite extraction at three different time points (20 plants per time point at 1, 4, and 10 dpi). Plants were grown under greenhouse conditions with photoperiods of 12 hours with 60 % \pm 5 relative humidity and controlled environmental and soil temperature (32 \pm 2 °C and 30 \pm 1.5 °C respectively). Before the metabolite extraction, the vascular wilt disease index was evaluated. For disease index calculation, the disease severity and disease index were determined as previously described (401).

4.2.2 Metabolites extraction and sample preparation.

For studying plant root-microorganism interactions, the secondary metabolites from the roots, the rhizospheric, and the bulk soil of the treated plants were obtained separately at 1, 4, and 10 dpi. Briefly, twenty plants per replicate of each treatment and control were uprooted, and the loosely attached soil particles were carefully separated. The remaining attached soil, considered as rhizospheric soil, was removed by root-dipping in 10 mL of sterile water, and the obtained suspension was then freeze-dried and stored at -20°C until extraction. Similarly, 5 g of bulk soil from S, B, F, and BF treatments were randomly collected and treated as described for the rhizospheric soil. Clean plant roots were excised, pooled, weighed, and immediately extracted as described.

Ultrasound-assisted extraction for plant roots, bulk, and rhizospheric soil was conducted with 500 mg of pooled plant roots (fresh weight) and soil samples. The samples were placed in glass tubes with 5 mL of methanol (90%) and sonicated for 20 minutes at room temperature (50 W, 42 kHz, Cole-Parmer Ultrasonic 8891). The tubes were then centrifugated for 10 minutes at 6.000 r.p.m. The extracts (supernatant) were dried under vacuum using a centrifugal evaporator (CentriVap Vacuum Concentration System, Labconco) and stored at -20°C.

The samples ([1 mg·mL⁻¹]) were reconstituted in 1 mL acetonitrile 50% in water. The samples were filtered through 0.22 µm nylon syringe filters into vials fitted with 500 µL inserts and stored at 4 °C for its analysis. A blank solvent and a pooled sample consisting of aliquots from all the samples were prepared and used as quality control (QC).

4.2.3 Ultrahigh-Performance Liquid Chromatography-MS (UHPLC-MS) analyses.

The extracts from the plant root-microbe interaction samples and bacteria-fungi samples were analyzed with a Thermo Ultimate 3000 UHPLC-DAD coupled to a microTOF-Q IITM LC-Mass spectrometer (Bruker Daltonics, Billerica, MA, USA) using an electrospray ionization source (ESI). UHPLC separation was achieved on a Phenomenex, Kinetex, C18 column (2.1 x 150 mm, 2.6 µm) using a two steps gradient of water (A) and acetonitrile (B) with 0.1% formic acid as mobile phase. The gradient profile started at 10% B to 90% in 30 minutes, from 90% to 98% in 2 min, held in 98% B for 5 min. The flow rate was 0.300 mL/min, and the column temperature was maintained at 40°C. The injection volume was set at 1 µL.

Mass spectrometer parameters were set as follows: Nebulizer gas 2.0 bar, drying gas 10.0 mL/min, Gas temperature 250°C, capillary voltage 3500 V, the mass spectrometer was operated in positive mode and data were collected between 100 and 1650 m/z. The mass spectra were calibrated using the calibration zone between 0.0 and 0.25 minutes, using sodium formate solution as an internal calibrant.

The chromatogram was processed to obtain a matrix for further analysis using Bruker Daltonics Profile Analysis version 2.1. Molecular masses, retention time, and associated

peak intensities were extracted from the raw files using MZmine 2.41.2 (440-442). Data processing parameters used in MZmine are listed in table 4-2. The resulting matrix was further processed to eliminate retention time between 30 to 45 minutes and blank solvent peaks. Matrix exportation allows obtaining a quantification table (.csv) containing features information (retention time, m/z, and peak area) used for data analyses.

Table 4-2: Data processing parameters use in MzMine for data matrix generation of tomato-FOL59-PNM200 interaction.

| Parameter | Value |
|--|-------------------|
| Mass detection (Centroid mass detector) | |
| Noise level MS1 | 5E2 |
| Chromatogram ADAP builder | |
| Min. group size in # of scans | 3 |
| Group intensity threshold | 5.5E2 |
| Min highest intensity | 2E2 |
| m/z tolerance | 0.05 m/z o 10 ppm |
| Chromatogram deconvolution (Baseline cut-off) | |
| Min peak height | 3.0E2 |
| Peak duration range (min) | 0.01-2.0 |
| Baseline level | 1.5E2 |
| Isotopic peaks grouper | |
| m/z tolerance | 0.05 m/z o 20 ppm |
| Retention time tolerance (min) | 0.5 |
| Maximum charge | 3 |
| Alignment (Join aligner) | |
| m/z tolerance | 0.05 m/z o 20 ppm |
| RT tolerance | 0.5 min |
| Weight m/z | 75 |
| Weight for RT | 25 |

4.2.4 Data analyses

The UHPLC-ESI-MS data sets were analyzed with SIMCA-P software (version 15.0.2, Umetrics, Umeå, Sweden). Before PCA and OPLS-DA modeling, the data were mean-centered and Pareto-scaled. R^2 and Q^2 values of each PCA and OPLS-DA analyses were annotated. For OPLS-DA, seven-fold cross-validation analysis were performed by permutation test (1000 replicates), CV-ANOVA, and ROC curve. In the permutation test, Q^2 intercept values on Y ($Q^2 \wedge Y$) below zero and p -value under 0.1 in CV-ANOVA were considered acceptable for model validation (443). Statistically valid models were examined and used in data mining for metabolite annotation. Only statistically significant metabolites

exhibiting variable importance in projection (VIP) score >1 (calculated by the SIMCA software and visualized through S-plot graphics) were further investigated.

4.2.5 Metabolite annotation and semi-quantitative comparison

The chemical and structural identities of significant metabolites were elucidated using their respective fragmentation patterns in the mass spectra, compound's elemental composition, and search in specialized databases. The putative empirical formula and mass information of each statistically significant extracted ion peak was obtained and searched in databases such as ChemSpider (www.chemspider.com), Dictionary of Natural Products (dnp.chemnetbase.com), MetLin, (<http://metlin.scripps.edu>), MotoDB (<http://www.ab.wur.nl/moto/>) (59), and Kasuza Omics Data Market (KomicMarket2) (<http://webs2.kazusa.or.jp/km2/>) (444). The metabolites were tentatively identified/annotated following the recommendations of Ferni et al. 2011 (445). The relative concentration of significant metabolites previously identified, represented as the peak area, were obtained from the original chromatograms. These data were exported to GraphPad PRISM (version 6.0) and used to validated significant differences between treatments by one-way ANOVA.

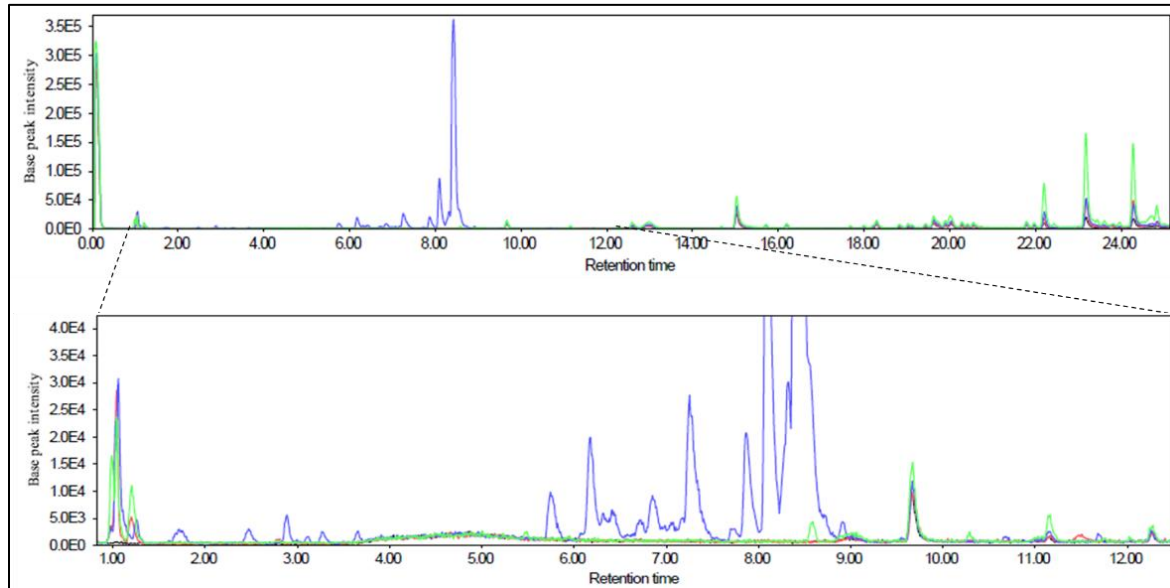
4.3 Results and discussion

4.3.1 Inoculation of *Paenibacillus* sp. PNM200 does not induce significant changes in tomato roots metabolic profile and reduces the effect caused by FOL59.

An LC-MS untargeted-metabolomic profiling strategy was carried out aiming to evaluate the tomato root's metabolic-profile changes during its interaction with *Paenibacillus* sp. PNM200 and FOL59. Samples of root tissue, rhizospheric soil, and bulk soil were obtained from an *in vivo* interaction experiment. The metabolite extraction was carried out in four treatments that included the combinations tomato plants-FOL59, tomato plants-*Paenibacillus* sp. PNM200, *Paenibacillus* sp. PNM200-FOL59, and tomato plants-*Paenibacillus* sp. PNM200-FOL59, with three controls of each organism individually (tomato plants, FOL59, and *Paenibacillus* sp. PNM200) and one control of the matrix used (soil), for a total of 108 samples analyzed.

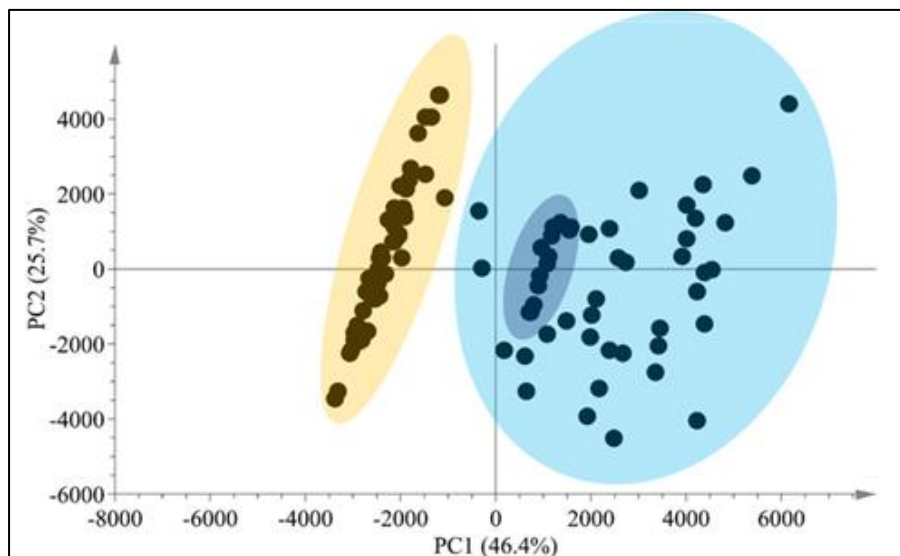
As presented in the overlapped chromatograms in figure 4-1 a significant difference was evidenced between the root extracts and those from the bulk soil and rhizospheric soil was evidenced. Unlike root samples, rhizospheric soil and bulk soil did not show any peak different to those observed on soil control or solvent blanks.

Figure 4-1: Chromatographic profile of tomato roots (blue), soil (red), rhizospheric soil (green) and solvent blank samples.



This observation was further confirmed in the principal component analysis (PCA) of the metabolic profiles, which suggested a clear discrimination among the treatments in two groups was evident. Cluster one encompasses the root samples, and the quality controls (blue ellipse, figure 4-2), while cluster two include the rhizospheric soil and bulk soil samples (yellow ellipse, figure 4.2). Thus, the subsequent analyzes were focused on the root tissue samples

Figure 4-2: Principal components analysis (PCA) score plot indicating the general grouping of the variables in the data sets of root and soil extracts. $R^2 = 0.892$ $Q^2 = 0.602$. The yellow circle highlight data obtained from soil samples and solvent blank. Light blue and dark blue circles indicate data from root samples and QC.



A second PCA without soil samples did not show a clear trend between the treatments (Figure 4-3 a). However, when the treatments (P, PF, PB, and PBF) were analyzed individually, it was evidenced that all the samples tended to cluster according to extraction day. In this way, samples obtained from 10 dpi could be differentiated from those obtained at 1 and 4 dpi (Figure 4-3 b). The PCAs for the four treatments are presented in appendix E.

Similarly, when performing paired analyzes between the control plants and each of the treatments, the PB and PBF treatments' metabolic profiles could not be differentiated from the control plants. This result indicates that there are no significant changes in the plant roots' metabolome induced by the interaction with the bacteria alone or with the bacteria and FOL59 under the conditions tested.

A supervised orthogonal projection analysis of latent structures (OPLS-DA) was carried out to evaluate these hypotheses, using four discrete classes associated with the compared treatment pair (P vs PB, P vs PF, and P vs PBF, respectively) as discriminant variables. As a result, even when the models could differentiate between the PB and PBH treatments

from the control plants (P), these models did not pass the cross-validation tests and were classified as overestimated models (Table 4-3).

Table 4-3: OPLS-DA models cross-validation. In the table, (*) indicates that the model failed the cross-validation test. (^{of}) indicates OPLS-DA overfitted models.

| Treatment | R ² Y | Q ² | Δ R ² Y/Q ² | R ² X [1] | R ² X [o2] | Cross-validation | | |
|---------------------|------------------|----------------|-----------------------------------|----------------------|-----------------------|------------------|-------------------|----------|
| | | | | | | CV-ANOVA | Q ² ^Y | AUROC |
| P/PF ^{of} | 0,597 | 0,2 | 0,397 | 16,60% | 27,70% | 0,540207 | -0,392* | 0,948068 |
| P/PBF ^{of} | 0,940 | 0,558 | 0,382 | 4,85% | 31,30% | 0,305678 | -0,703 | 0,864734 |
| P/PF | 0,957 | 0,682 | 0,275 | 12,30% | 32,70% | 0,05327 | -0,624 | 0,958937 |

During the manual analysis of these treatments' chromatograms, no differences were found in the samples' metabolic profiles indicating that *Paenibacillus* sp. PNM200 did not induce a metabolic change in the roots, that could be related to the activation of plant defenses against infection by FOL59 (Figure 4-4). Thus, the activity of *Paenibacillus* sp. PNM200 may be associated to direct interaction with the fungus in the rhizosphere.

Remarkably, in other plant-fungal and plant-bacteria interaction models like tomato-FORL (71), tomato-*V. dahliae* (70), tomato-*Sclerotinia* sp. (446), or *Arabidopsis*-*Paenibacillus* (419), the plant responses towards a beneficial or pathogenic bacterium were observed at transcriptomic and proteomic level alongside with metabolic reprogramming. Additionally, some studies with tomato and vascular pathogens like *V. dahliae*, or PGPR like *Paenibacillus alvei*, showed major metabolomic changes in stem or foliar tissues (70, 447), pointing out the relevance of further analyzing the induction of systemic metabolomic changes.

Integration of several omics' approaches gives a systematic view of the primary and secondary metabolism reprogramming during plant-microorganisms interaction and how this is regulated. Accordingly, it is necessary to complement the obtained tomato-FOL-PNM200 metabolic profile with transcriptomics or proteomics data to confirm if, once inoculated with *Paenibacillus* sp. PNM200, tomato plants express any significant change that is not represented in metabolome variations.

Figure 4-3: PCA score plot indicating the general grouping of the variables in the data sets of root extracts. (a) PCA score plot of the variables in the data set of all root extracts (depicts by color), $R^2 = 0.819$ $Q^2 = 0.729$. (b) PCA score plot of the variables in the data set of plant-fungi treatment (PF) at 1 (blue dots), 4 (red dots) and 10 (yellow dots) dpi, $R^2 = 0.826$ $Q^2 = 0.498$.

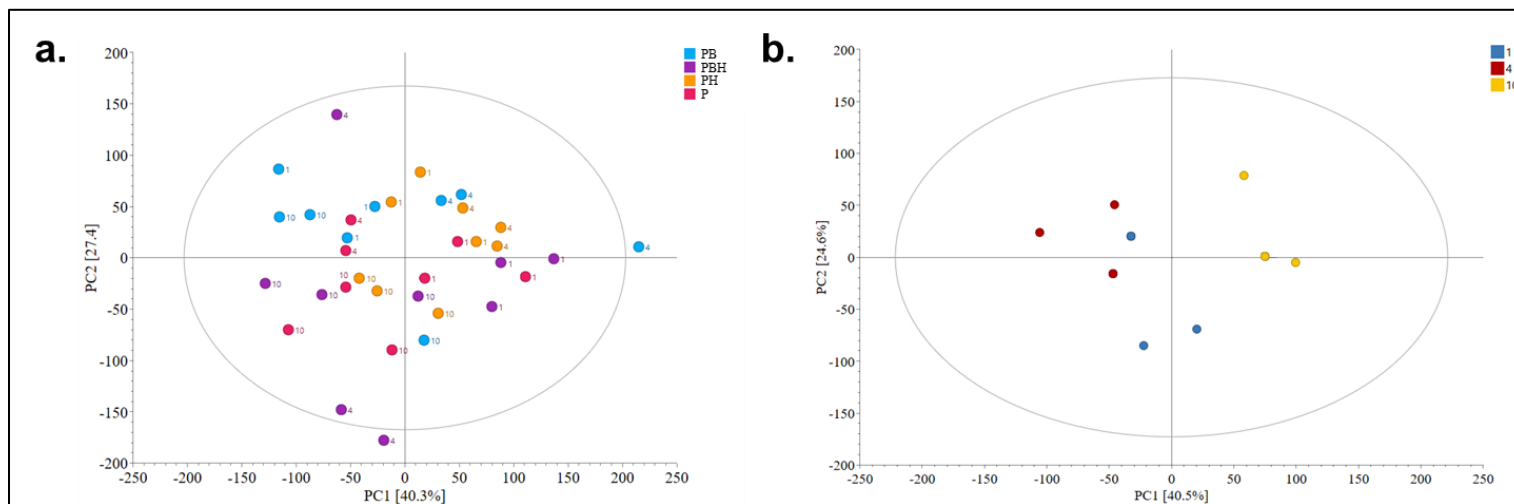
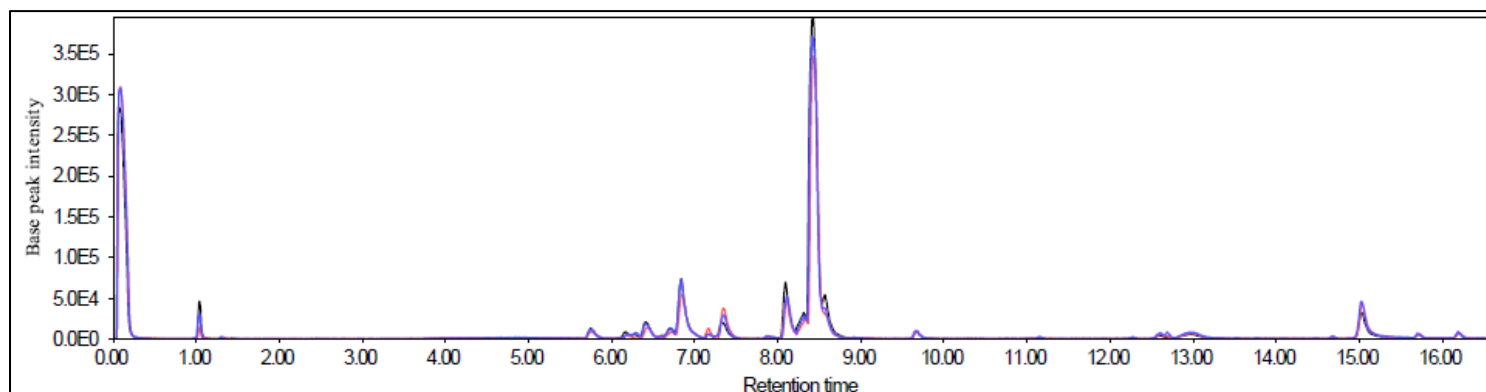


Figure 4-4: Chromatographic profile of P (blue), PB (red) and PBF (black) treatments at 10 dpi.



On the other hand, in the analysis of tomato plant–FOL59 interaction, a validated model obtained from the OPLS-DA analysis (Table 4-2, Figure 4-5) indicate that the plant presents a metabolic variation due to the presence of the fungus at the 10th dpi. These findings will be discussed in the next section.

As mentioned previously, unlike metabolic variations found in root tissue samples, the soil and rhizospheric soil metabolic profiles did not present significant variations in the interaction from the microorganism's perspective. In general, metabolomic studies use less complex matrices such as semi-solid agar or liquid media that aim for a higher recovery of compounds and improve the reproducibility of data and the recovery rate of metabolites (448, 449). However, hydroponic systems and sterile solid matrices generate physiological differences in the development of the plant root system when compared with the growth in soil. These changes induce variations in the metabolites recovered from the rhizosphere (450, 451). Finally, it has been estimated that, in soil and particularly in rhizospheric soil, the metabolites' stability is very short, due to microbial degradation (452), which may have influenced the results obtained here for the interactions occurring in soil. For the reasons mentioned above, we decided to use systems where these interactions are studied under scenarios as close as possible to natural field conditions (detailed in chapter five).

4.3.2 FOL59 infection generates tomatidine and steroidal glycoalkaloid accumulation on tomato roots.

The metabolic variation between the P and PF treatments was correlated with the presence of 22 features that were identified as VIP (Variable influence on projection) in the S-plot generated from the OPLS-DA P / PF model (Figure 4-5 b). Fourteen features (blue dots in figure 4-5 b) were associated to PF treatments variation and correspond to seven metabolites (**2, 3, 5, 6, 7, 10** and **11**). The remaining eight features (red dots in figure 4-5 b) were responsible for plant control variation and were related to four metabolites (**1, 4, 8** and **9**). From these eleven compounds, nine were identified as steroidal glycoalkaloids, including the phytoanticipin α -tomatine (**10**), five isomers of hydroxytomatine (**2-4, 6**, and **7**), two isomers of dehydrotomatine (**8** and **9**), and one compound (**5**) whose MS data coincide with a tomatidine residue with a tetrahexoside chain. Compound **11** correspond to the steroidal alkaloid tomatidine, while compound **1** was an unidentified metabolite with a *m/z* of 381.0683 (Figure 4-6, Table 4-4).

Figure 4-5: OPLS-DA model of P and PF treatments. The figure presents the score plot (a) and the S-plot (b) of the OPLS-DA model. In the S-plot (b), the features related to P or PF treatments are highlighted in red and blue, respectively. $R^2Y = 0.957$ $Q^2 = 0.682$.

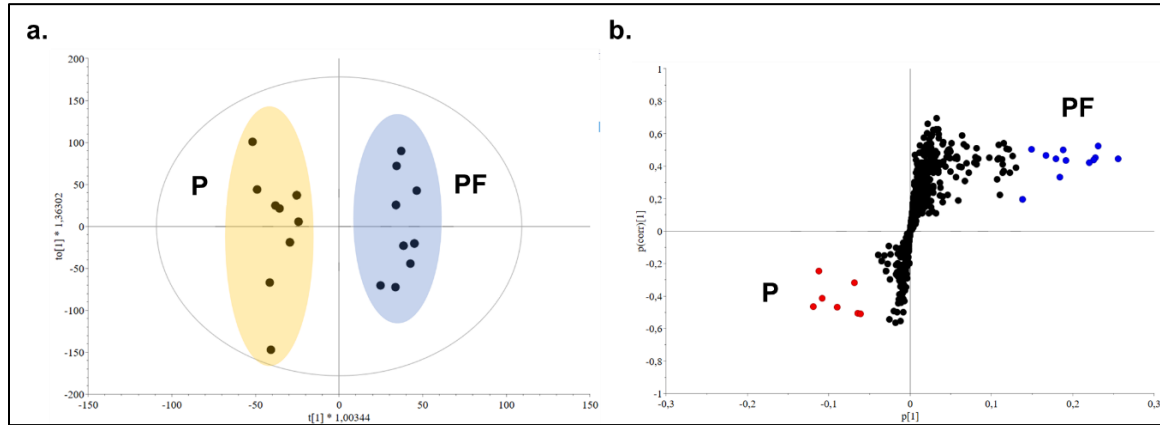
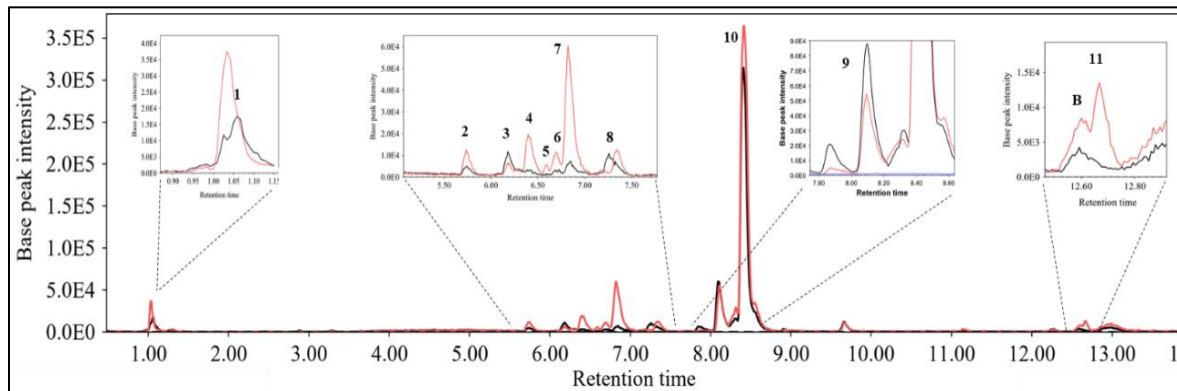


Figure 4-6: Chromatographic profile of uninoculated (P, black) and infected (PF, red) plants at 10 dpi. In the figure, (B) indicates peaks present in the solvent blank control. Peaks numbers correspond to metabolite ID.



Tomatidine (**11**) accumulation in infected plants was six times higher than in control plants, unlike α -tomatine (**10**), whose relative abundance in infected plants was only 1.3 times higher compared to healthy plants despite being the main SGA present in the evaluated samples (Figure 4-6). This same behavior was observed for the hydroxytomatine isomer III (**4**), tomatidine tetrahexoside (**5**), hydroxytomatine isomer IV (**6**), and hydroxytomatine isomer V (**7**), which presented a significant increase on infected plants with relative FC values (Fold change) greater than 5 (Figure 4-7). Similarly, hydroxytomatine isomer I (**2**) had an FC of 1.8, being statistically different from the control plants ($p < 0.05$).

Table 4-4: Annotation of the statistically significant secondary metabolites identified within methanolic extracts of roots from uninoculated (P) and infected (PF) plants treatments. MF, Molecular formula; MM, reported monoisotopic mass; IL, identification level according to Fernie et.al. 2011 (445); SGA, steroidal Glykoalkaloids; SA, steroidal alkaloid.

| Feature (VIP) | ID | m/z [M+H] ⁺ | RT (min) | Putative identification | Class | MF | MM | Δ ppm | Fragments MS1 (+) | IL |
|----------------------------|----|------------------------|----------|----------------------------|-------|--|------------------------------|-------|---|----|
| C825, C842 | 1 | 381.0683 | 1.06 | - | Sugar | - | - | - | 381.07818 [Hex2+K] ⁺ , 365.0994 [Hex2+Na] ⁺ | NI |
| C1140 | 2 | 1050.551 | 5.70 | Hydroxytomatine Isomer I | SGA | C ₅₀ H ₈₃ NO ₂₂ | 1049.540649 | 9.86 | 594.3934, 544.75, 536.7623 | D |
| C1179, C1180, C1186 | 3 | 1050.5406 | 6.15 | Hydroxytomatine Isomer II | SGA | C ₅₀ H ₈₃ NO ₂₂ | 1049.540649 | 0.05 | 1032.5383, 549.3906, 576.3801, 527.7544 | D |
| C1242, C1243 | 4 | 1050.5408 | 6.41 | Hydroxytomatine Isomer III | SGA | C ₅₀ H ₈₃ NO ₂₂ | 1049.540649 | 0.14 | 594.3875, 536.7567 | D |
| C1275, C1278 | 5 | 1064.5458 | 6.60 | Tomatidine tetrahexoside | SGA | C ₅₁ H ₈₅ NO ₂₂ | 1064.5640 [M+H] ⁺ | 17.09 | 608.3696, 544.7549, 594.3892, 536.7567 | D |
| C1301 | 6 | 1050.5446 | 6.71 | Hydroxytomatine Isomer IV | SGA | C ₅₀ H ₈₃ NO ₂₂ | 1049.540649 | 3.76 | 918.5004, 594.3895, 536.7572 | D |
| C1330, C1333 | 7 | 1050.5439 | 6.84 | Hydroxytomatine Isomer V | SGA | C ₅₀ H ₈₃ NO ₂₂ | 1049.540649 | 3.19 | 918.4965, 594.3909, 756.4385, 432.3393 | D |
| C1425, C1432, C1439 | 8 | 1032.5361 | 7.32 | Dehydrotomatine isomer I | SGA | C ₅₀ H ₈₁ NO ₂₁ | 1031.53019 | 5.72 | 576.3832, 528.2561, 527.7574, 414.3281 | D |
| C1558 | 9 | 1032.5273 | 8.10 | Dehydrotomatine isomer II | SGA | C ₅₀ H ₈₁ NO ₂₁ | 1031.53019 | 3.67 | 576.3807, 528.2563, 527.7538 | D |
| C1728, C1731, C1741, C1753 | 10 | 1034.5388 | 8.41 | α-Tomatine | SGA | C ₅₀ H ₈₃ NO ₂₁ | 1033.5457 | 3.13 | 740.4451, 578.3957, 416.34 | D |
| C2114 | 11 | 416.3446 | 12.6 | Tomatidine | SA | C ₂₇ H ₄₅ NO ₂ | 415.3450 | 1.032 | ND | D |

On the other hand, metabolites **1**, the hydroxytomatine isomer II (**3**), and dehydrotomatine isomer I and II (**8** and **9**, respectively), presented a higher relative accumulation in healthy plants when compared with the infected ones. However, the changes observed for compounds **1** and **3** were the most representative among the detected metabolites (Figure 4-7).

SGAs derived from the sterol's biosynthetic pathway (Figure 4-7) and are found in stems, leaves, roots, and fruits of various nightshades, including tomato (453, 454). SGAs participates in plant defense against pests, bacterial, viral and fungal phytopathogens and their abundance in tomato tissues is tissue and time-dependent (455-457). α-tomatine, hydroxytomatine, and dehydrotomatine are structurally diverse SGAs, differentiated by

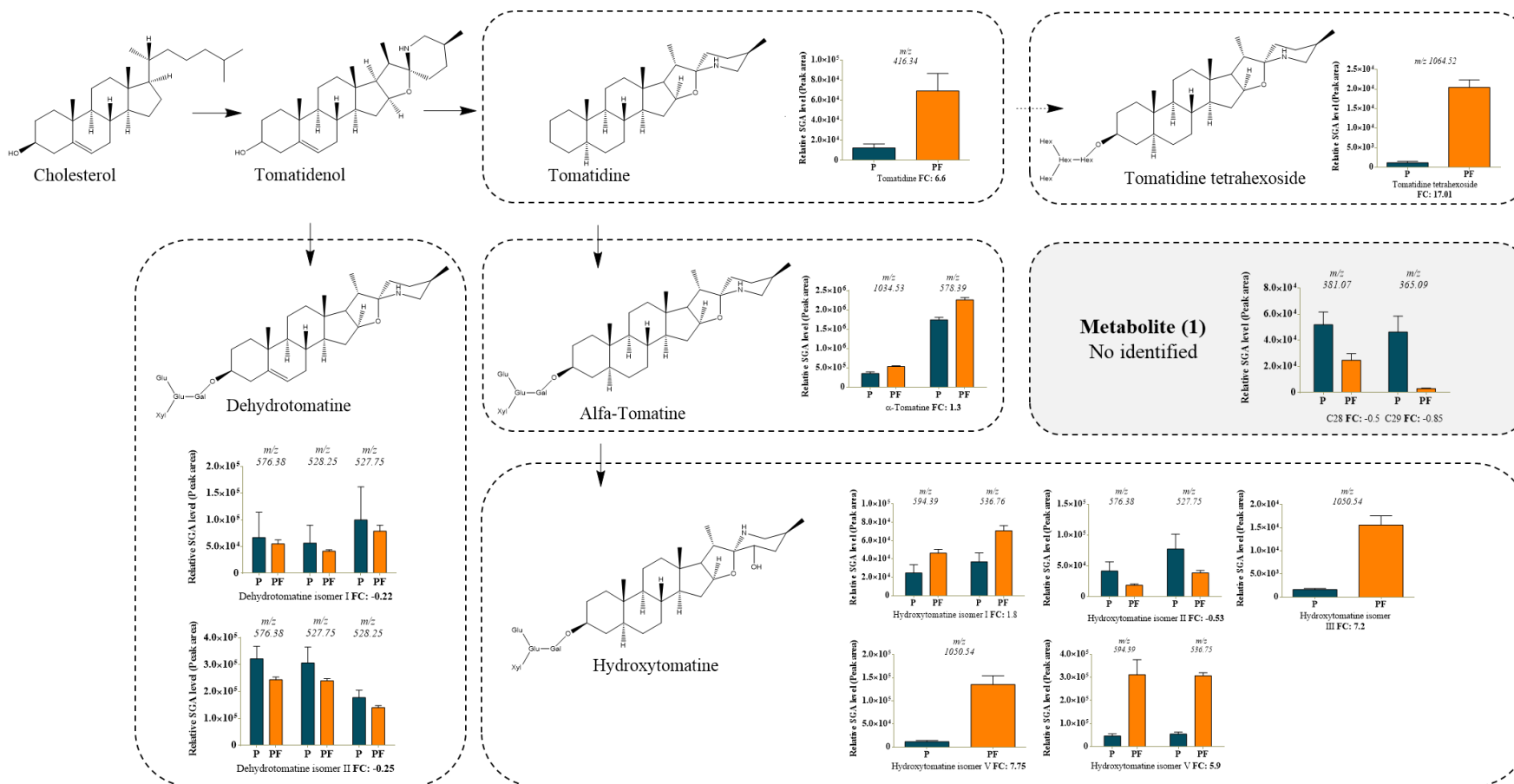
several chemical modifications like glycosylation, acetylation, hydroxylation and isomerization (444, 453, 455, 458).

Different studies have reported the isolation of α -Tomatine, hydroxytomatine, and dehydrotomatine' isomers. The chemical diversity of these metabolites have been related to tomato-pest/pathogen co-evolution process or tomato breeding process (459). However, in the tomato model, SGAs' biological function on plant defense against phytopathogens has been proven for α -Tomatine, alone or in mixture with dehydrotomatine (460). α -Tomatine and dehydrotomatine, are considered as phytoanticipins that participate in plant defense against pest, oomycetes, bacterial and fungal phytopathogens such as *Phytophthora infestans* (431), FOL (461), *Alternaria alternata*, and *Corynespora cassicola* (462). These SGAs are produced along the infection process, being usually detected after 8 dpi (462), even during the infection of low-susceptible phytopathogens such as *P. infestans* (431).

Antifungal activity of α -tomatine has been related to the interaction of a lycotetraose residue with the 3β -hydroxysterols present in fungi membranes (463). Additionally, α -Tomatine can induce a programmed cell death process in *F. oxysporum* associated with the accumulation of reactive oxygen species (ROS) (461). However, it is also known that this compound is degraded by a group of enzymes named tomatinases produced by different phytopathogens, including FOL, FORL, and *Cladosporium fulvum* (131, 464, 465).

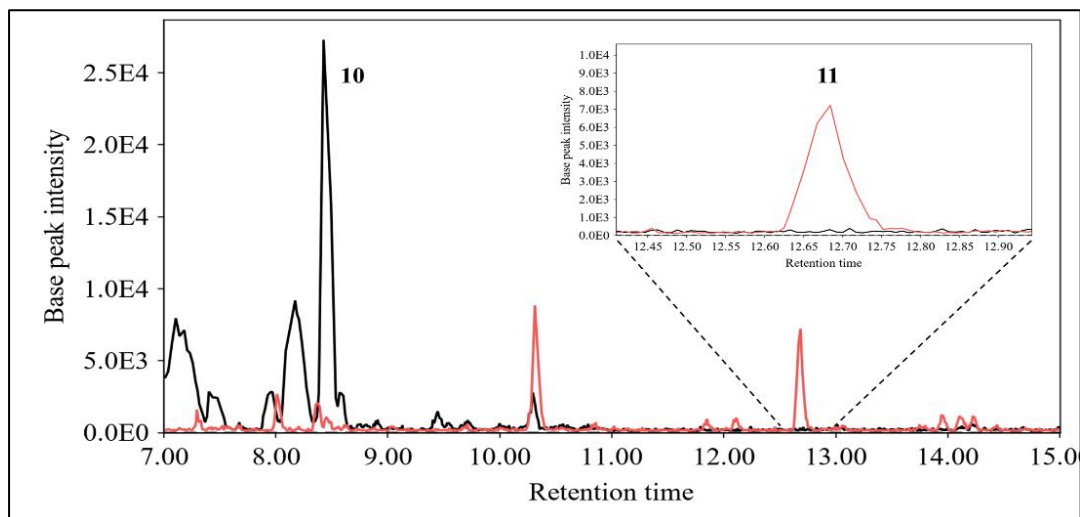
Tomatinases belongs to the glycosyl hydrolases family and degrades α -tomatine by removing the residue of lycotetraose, to form the aglycone tomatidine (465). Accumulation of tomatidine generates inhibition of the plant's immune response and cell damage, through processes associated with the hypersensitivity response mediated by ROS, increasing the damage of plant tissues during infection (131, 464). Detoxification of α -tomatine and accumulation of tomatidine is associated with the beginning of the vascular colonization process by FOL, FORL, and *C. fulvum*, and it has been proposed as one of the early infection markers in these pathosystems (131, 462, 464, 465). The experiments presented here support this hypothesis, as increases in tomatidine and other metabolites were observed in samples from the plant-fungus interaction.

Figure 4-7: Changes in SGA and related molecules levels in tomato roots on uninoculated (P) and infected plants (PF) 10 dpi. Data presents in each graph are the means \pm standard deviation of three biological replicates per treatment. SGA biosynthetic pathway was adapted from Itkin et al., 2011 (453).



Remarkably, the accumulation of tomatidine observed at 10 dpi, without significant increases in α -tomatine, coincided with the moment in which FOL59 begins its intravascular colonization process (Appendix C). Whence, tomatidine accumulation could be a consequence of α -tomatine degradation by FOL59. Furthermore, FOL59 capability to deglycosylate α -tomatine was proved here by HPLC-MS using ethanolic extracts of FOL59 cultures grown in a medium supplemented with tomato vascular tissue. After eight incubation days, α -tomatine peak (RT 8.41 min m/z 1034.53) was not detected in the FOL59 samples, whereas a tomatidine peak (RT 12.6 min m/z 416.34) was clearly observed. This latter peak was not detected in the control media (Figure 4-8).

Figure 4-8: Chromatographic profile of FOL59 culture on tomato supplemented solid medium. Profiles of FOL59 culture (red) and medium control (black) are shown. Peaks 10 and 11 correspond to α -Tomatine (10) and tomatidine (11).



In this study, the relative concentration of dehydrotomatine was lower in infected plants than in healthy plants. Such behavior had already been described in the tomato -*Verticillium dahliae* interaction (70). The concentration of dehydrotomatine in susceptible and resistant varieties was significantly lower compared to healthy controls. This phenomenon was observed after three weeks post-infection and thus considered as a late infection biomarker. However, as the present work only evaluates early infection conditions, it is recommended to follow changes in the concentration of hydroxytomatine and α -tomatine to determine if they are differentially inhibited metabolites in late infection phases.

4.4 Final remarks

The metabolome is one of the final products of gene expression on cells. Untargeted metabolomics is a tool that describes the metabolism changes of a biological system under specific conditions. Metabolic profiles of the tripartite BCA-phytopathogen-plant interaction allow evaluating the metabolites' quantitative and qualitative changes associated with the phenotype observed in the interaction (41, 42). The information derived from these profiles can be used to construct metabolic fingerprints (metabolic signatures) that can identify characteristic biomarkers of the interaction and understand the relationships established in a biocontrol system (420).

Here, an untargeted metabolic profiling approach was used to characterize the interaction between tomato, FOL59, and *Paenibacillus* sp. PNM200. Interestingly, the variation on the metabolic profiles for samples obtained from three treatment (plant, plant inoculated with the bacteria, and the tripartite interaction) was not significant. In this context, we suggest that *Paenibacillus* sp. PNM200 presence on roots reduces the effect of FOL59 on tomato root metabolome observed on infected plants.

The obtained results also indicate that the antifungal activity of *Paenibacillus* sp. PNM200 could be related to its direct interaction with FOL59 in the rhizosphere since it does not seem to be the result of BCA's reprogramming of metabolic expression in tomato plant. However, this affirmation is only valid for the root's metabolome response and it has to be verified by assessing the transcriptome changes in the plant along the process of infection with FOL59, in the presence and absence *Paenibacillus* sp. PNM200

In the plant-FOL59 interaction, FOL59 induced SGA accumulation in tomato roots during early infection stages, including α -tomatine, hydroxytomatine, tomatidine tetrahexoside, and the aglycone tomatidine. SGAs play a crucial role in plant defense against fungal pathogens as phytoanticipins. The increase of tomatidine can be related to α -tomatine biosynthesis induction as a response to fungal vascular growth. However, some previous studies describe tomatidine accumulation due to the enzymatic hydrolysis of α -tomatine by FOL to avoid plant defenses. Experimental results presented here fit with this hypothesis and may explain that the relative abundance of α -tomatine does not significantly change during tomato-FOL59 infection. To confirm which of these two events is responsible for

tomatidine production levels, tomato's metabolic profile should be studied at later infection stages to determine if there is an α -tomatine accumulation or decrease in concordance with FOL complete vascular colonization.

Since the interaction FOL59-*Paenibacillus* sp. PNM200 could be followed neither on rhizospheric soil nor in bulk soil, different experimental approaches should be explored to understand the interaction of these microorganisms in the rhizosphere should be explored. In this context, untargeted metabolic profiling by co-culture is proposed to characterize the bipartite interaction as will be presented in chapter five.

5. Metabolic profiling of *Paenibacillus sp.* PNM200-FOL59 interaction

5.1 Introduction and scope

Chemical mediators determine the outcomes of mutualistic, commensal, or antagonist associations in microbial communities(466). These chemical mediators are secondary metabolites produced under specific conditions on natural niches. Mimicking microbes' interaction in the laboratory could lead to unraveling the ecological function of secondary metabolites on microbial associations since it allows following the expression of biosynthetic gene clusters in a controlled environment. This approach served to describe BCA-pathogen interactions such as *Lysobacter capsica*-*P. infestans*, *B. subtilis*-*A. niger*, and *P. fluorescens*-*Gaeummanomyces graminis* (467-470).

Unfortunately, transcriptional variation occurring during a microbe-microbe interaction cannot always be correlated to the final observed phenotype (471). For this reason, knowledge of the overall response of a BCA to specific pathogens is still needed. In this context, metabolomics and proteomics support and complement the data obtained from genomics and transcriptomics analyses.

Unlike transcriptomics, targeted and untargeted metabolomics do not require prior genome or transcriptome data, a constrain in studies that work with non-model plants or microorganisms (471). For microbial interactions, metabolomics looks forward to obtaining global information about the metabolome variation of a model system involving two microbial partners under specific conditions using mainly co-cultivation (472, 473).

Co-cultivation is a rapid and low-cost technique used for enhancing the chemical diversity of microorganisms when grown *in vitro* (473). Initially, co-cultivation aimed to overcome the high re-discovery isolation rate of known bioactive metabolites obtained from typical

bioprospecting approaches (473). Nowadays, this technique improves the study of BCA-phytopathogens interactions by emulating *in vitro* conditions that may occur in the field (474, 475). These studies allow exploring the overexpression of biologically active metabolites (474, 476), the induction of cryptic genes in a potential BCA (477), and the possible ecological role of the metabolites found during the interaction (478).

Remarkably, co-cultivation of marine-derived microorganisms is a suitable strategy for isolating new bioactive metabolites, including compounds with antifungal activity against phytopathogens (413, 477, 479-481). Despite this approach's success, many metabolites cannot be easily identified due to the complexity of the obtained extracts and the low recovery rate of pure compounds.

Using bioinformatics tools, such as molecular networks (MN), increases metabolites' identification rate in complex samples. Molecular networks are organized visualizations of structurally related molecules grouped according to the similarity between a pair of consensus mass spectra, built for each molecular feature, and their respective MS/MS spectra. In this context, a feature is defined as any peak that had MS, MS/MS, retention time, and a peak area related (482). Clustering between nodes is determined according to a cosine value that indicates the degree of similarity between them. The cosine value ranges from zero to one, depending on if the consensus spectra are identical (one) or not (zero) (482, 483).

This tool can be integrated with Network Annotation Propagation (NAP) and Molecular Network enhancer (MolNetEnhancer) workflows. NAP allows the propagation of the annotation of molecular families in the same network nodes based on the *in silico* analysis of the substructures' fragmentation patterns reported in databases. This analysis considers the topology of the built network, under the principle that neighboring (connected) nodes in a molecular cluster are structurally related and, therefore, can be used to build consensus substructures, improving the structural classification candidates suggested for a particular node (484).

MolNetEnhancer uses each feature's data and integrates it with the information provided by NAP and MS2LDA (complementary unsupervised analysis of substructures), alongside with the ClassyFire automatic chemical classification tool. This analysis generates broader

structural information of the fragmentation spectra, facilitating the analysis of the molecular families present in the analyzed networks (485).

Thanks to their versatility, MNs have been successfully used to study bacteria-bacteria, fungus-bacteria, and fungus-fungus interactions. One of the most relevant examples of MN application for the current research is the interaction between a collection of marine-derived fungi and several phytopathogens that led to the isolation of metabolites with antimicrobial activity against *Xanthomonas campestris*, *P. infestans* (481), *Pseudomonas syringae*, *Ralstonia solanacearum*, *Magnaporthe oryzae* and *Botrytis cinerea* (413).

Molecular Networking-based metabolome studies have increased in the last few years. For instance, MNs supported the study of some microorganisms' metabolome retrieved from the collection evaluated in the present research, including the study of *Purpureocillium lilacinum* PNM67 secondary metabolites production during liquid fermentation (328) and co-culturing with *Paenibacillus* sp. PNM115, *Paenibacillus* sp. PNM123, *Paenibacillus* sp. PNM210, and *Streptomyces* sp. 5.1. Molecular Networks of PNM67 extracts allows identifying different Leucinostatin family members and the variability in their biosynthesis under different growing conditions (327).

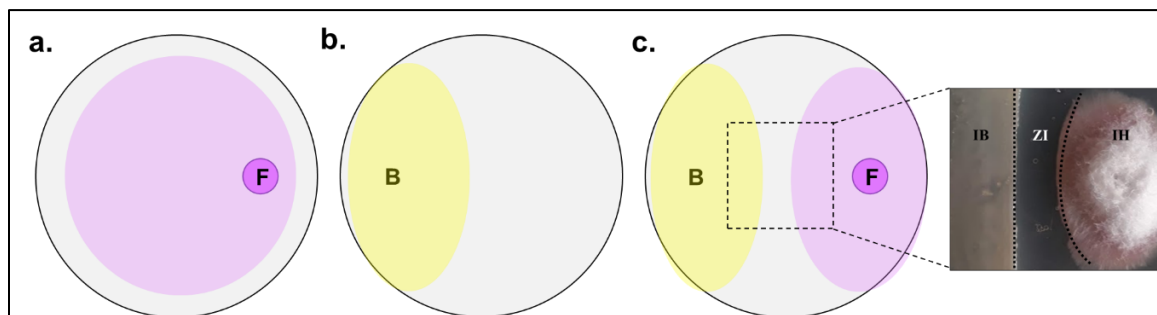
Here, we proposed a co-cultivation workflow, supported by multivariate data analysis and molecular networking as a strategy to give insights about the FOL59-*Paenibacillus* sp. PNM200 chemical communication. Metabolic profiles of the monocultures and co-cultures of both microorganisms in both basal media and tomato-stem supplemented media were analyzed and correlated with the *in vivo* assays' phenotype. Some metabolites produced by FOL59 and *Paenibacillus* sp. PNM200 identified during the *in vitro* interaction were identified and are proposed as biomarkers of the infection process (metabolites produced by FOL59) or the biocontrol phenotype (metabolites produced by *Paenibacillus* sp. PNM200), respectively.

5.2 Materials and methods

5.2.1 Binary co-cultures.

For co-cultivation, 50 μL of *Paenibacillus* sp. PNM200 liquid cultures (obtained as described in numeral 2.2.1) were pipetted on one side of an agar plate (9 cm in diameter) and spread using a sterile inoculation loop. At 5 cm from the bacterial isolate, a 1 cm^2 piece of FOL59 mycelium was placed (Figure 5-1). Agar plates were incubated at 30°C for ten days in the dark. In parallel, mono-cultures of each strain used were prepared and cultivated at the same conditions, for comparison purposes. For each treatment, five biological replicates were used, which were constituted by fifty individual agar plates.

Figure 5-1: Scheme representation of mono and co-cultures of *Paenibacillus* sp. PNM200 and FOL59. The figure shows the monocultures of FOL59 (a), *Paenibacillus* sp. PNM200 (b), and the co-culture of both microorganisms (c). In co-culture scheme (c), ZI indicates the inhibition zone generated during FOL59-PNM200 interaction, B, bacterial growth zone, and F, the fungal growth zone.



Co-cultivation was done in PDA (0.5X) and TPDA (PDA 0.5X supplemented with 10% w/v tomato stem tissue) to evaluate PNM200-FOL59 interaction. The microbial metabolome study on TPDA aimed to determine tomato-tissue metabolites' effect on FOL59 and *Paenibacillus* sp. PNM200 secondary metabolism, and to mimic FOL59-PNM200 chemical interaction in the presence of the plant host.

5.2.2 Metabolite extraction and sample preparation.

For co-culture metabolite extraction, three zones in the dual-culture agar plate were defined: the growing zones of the bacterial (B) and fungal (F) strains and the confrontation

zone (ZI) (Figure 5-1 c). Each zone was excised separately and cut into pieces of 1 cm². The samples were then freeze-dried and sequentially extracted with ethyl acetate and ethanol using 20 mL of each solvent per 200 mg of dry material. For mono-culture samples and medium controls (PDA and TPDA without inoculation), all the agar plates were cut into pieces and extracted alongside the co-culture samples as described below.

For ethyl acetate extracts obtention, the samples immersed in ethyl-acetated were ultrasonicated for 20 minutes at room temperature (50 W, 42 kHz, Cole-Parmer Ultrasonic 8891). The tubes were then centrifugated for 10 minutes at 6.000 r.p.m. The extracts (supernatant) were then dried under vacuum using a centrifugal evaporator (CentriVap Vacuum Concentration System, Labconco) and stored at -20°C until analysis. The remaining material (freeze-dried medium) was then immersed in ethanol, sonicated, centrifuged, dried, and stored as was done with the ethyl acetate solvent.

Dried samples were reconstituted in 1 mL of 50% HPLC-grade acetonitrile MilliQ water solvent at a final concentration of 5 mg·mL⁻¹, filtered through 0.22 µm nylon syringe filters into vials fitted with 500 µL inserts and stored at 4 °C until analyzed. Blank solvent and a pooled sample consisting of aliquots from all the samples were prepared and used as a technical blank and quality control (QC), respectively.

5.2.3 Ultrahigh-Performance Liquid Chromatography-MS/MS (UHPLC-MS7MS) analyses.

Co-culture and mono-culture samples were injected and chromatographically separated on a Thermo Ultimate 3000 UHPLC-DAD coupled to a micrOTOF-Q IITM LC-Mass spectrometer (Bruker Daltonics, Billerica, MA, USA) supplied with an electrospray ionization source (ESI). UHPLC separation was done on a Phenomenex, Kinetex, C18 column (2.1 x 150 mm, 2.6µm) using a two steps gradient of water (A) and acetonitrile (B) with 0.1% formic acid. Gradient program started at 10% B to 90% in 30 minutes, 90% to 98% in 2 min, held in 98% B for 5 min, and return from 98% to 10% B in 2 minutes. The flow rate was set at 0.300 mL/min, and the column temperature was maintained at 40°C. The injection volume was 1 µL per sample.

Mass spectrometer parameters were set as follows: Nebulizer gas 2.0 bar, drying gas 10.0 mL/min, Gas temperature 250°C, capillary voltage 4500 V, the mass spectrometer was operated in positive mode, and data were collected between 100 and 1650 m/z. For MS/MS fragmentation, the ten most intense ions were selected. The collision energy was set as reported by Garg et al. (2015) (486).

The obtained data were processed to produce a matrix for further analysis using Bruker Daltonics Profile Analysis (version 2.1). The chromatograms were calibrated using the calibration zone between 0.0 and 0.25 minutes, employing sodium formate solution as an internal calibrant. Molecular masses, retention time, and associated peak intensities were extracted from the raw files using MZmine 2.53 (440-442). Data processing parameters used in MZmine are listed in table 5-1. The resulting matrix was further processed to eliminate data from retention time between 30 to 45 minutes and blank solvent peaks.

Table 5-1: Data processing parameters use in MZmine for data matrix generation of ethyl acetate and ethanol extracts of co-culture samples.

| Parameter | Value (Ethyl acetate extracts) | Value (ethanolic extracts) |
|--|--------------------------------------|-------------------------------|
| Mass detection (Centroid mass detector) | | |
| Noise level MS1 | 8E2 | 2E2 |
| Noise level MS2 | 8E1 | 2E1 |
| Chromatogram ADAP builder | | |
| Min. group size in # of scans | 5 | 5 |
| Group intensity threshold | 8E2 | 6E2 |
| Min highest intensity | 1E3 | 5E2 |
| m/z tolerance | 0.05 m/z o 10 ppm | 0.05 m/z o 10 ppm |
| Chromatogram deconvolution (Baseline cut-off) | | |
| Min peak height | 5E2 | 2.5E2 |
| Peak duration range (min) | 0.01-2 | 0.01-2.1 |
| Baseline level | 2E2 | 2E2 |
| m/z range for MS2 scan pairing (Da) | 0.05 | 0.05 |
| RT range for MS2 scan pairing (min) | 0.5 | 0.5 |
| Isotopic peaks grouper | | |
| m/z tolerance | 0.05 m/z o 10 ppm | 0.05 m/z o 10 ppm |
| Retention time tolerance (min) | 0.5 | 0.5 |
| Maximum charge | 3 | 3 |
| Alignment (Join aligner) | | |
| m/z tolerance | 0.05 m/z o 10 ppm | 0.05 m/z o 10 ppm |
| RT tolerance | 0.5 | 0.5 |
| Weight m/z | 75 | 75 |
| Weight for RT | 25 | 50 |

5.2.4 Data analyses

The UHPLC-ESI-MS data sets were analyzed with SIMCA-P software (version 15.0.2, Umetrics, Umeå, Sweden). Before PCA and OPLS-DA modeling, the data were mean-centered and Pareto-scaled. R^2 and Q^2 values of each PCA and OPLS-DA analyses were annotated. For OPLS-DA, seven-fold cross-validation analyses were performed by permutation test (1000 replicates), CV-ANOVA, and ROC curve. In the permutation test, Q^2 intercept values on Y ($Q^2 \wedge Y$) below zero and p -value under 0.1 in CV-ANOVA were considered acceptable for model validation (443). Statistically valid models were examined and used in data mining for metabolite annotation. Only statistically significant metabolites exhibiting variable importance in projection (VIP) score >1 (calculated by the SIMCA software and visualized through S-plot graphics) were further investigated.

5.2.5 Metabolite annotation

The chemical and structural identities of the significant metabolites were elucidated using their respective mass spectral patterns. MS spectral-based metabolite identification was performed based on tandem mass fragment information, compound's elemental composition, and database searches for metabolite annotation. The putative empirical formula and mass information of each statistically significant extracted ion peak was obtained and searched in databases such as ChemSpider (www.chemspider.com), Dictionary of Natural Products (dnp.chemnetbase.com), MetLin, (<http://metlin.scripps.edu>), and the Natural Products Atlas (<https://www.npatlas.org/joomla/>) (487).

5.2.6 Biological activity.

Antifungal activity of ethyl acetate and ethanolic extracts of *Paenibacillus* sp. PNM200 co-culture and monocultures was evaluated by assessing growth of *F. oxysporum f. sp. lycopersici* CBS 164.85 (Westerdijk Fungal Biodiversity Institute, The Netherlands) upon addition of each extract. Briefly, 10 μ L of a conidial suspension of FOL strain CBS 164.85 (1×10^5 conidium \cdot mL $^{-1}$) was added to 200 μ L of MM 2X (10 mL Asp+N 2 , 10 mL glucose

² **Asp+N**: dilute 297.5 g NaNO $_3$, 26.1 g KCl, 74.8 g KH $_2$ PO $_4$ in 600 mL distilled water. Adjust to pH 5.5 with KOH 5 M. Composition per liter.

50% w/v, 1 mL MgSO₄ 1M, 0.5 mL VN 1000X³, 0.5 mL yeast extract 0.3%) in a 96 well-plate.

Prior to fungus addition, MM 2X medium was supplemented with each extract to reach concentrations of 2, 1.5, 1, 0.7, 0.5, 0.25, and 0.125 mg·mL⁻¹. After fungus inoculation, plates were sealed and incubated without agitation for 36 hours at 27°C. Optical density (600nm) of FOL strain CBS 164.85 was evaluated by spectrophotometrically after incubation. Fungal growth of treatments, solvent control and blank medium were compared. The half-maximal inhibitory concentration (IC₅₀) was calculated from the obtained data by non-linear regression in GraphPad PRISM (version 6.0).

5.2.7 GNPS Feature-based molecular networking workflow

All datasets were uploaded to the Global Natural Products Social (GNPS) MN webserver and analyzed using the Feature-based MN workflow published by Nothias et al. (2019) (488). FBMN workflow used the following parameters: Precursor ion mass tolerance 0.05 Da, Fragment ion mass tolerance 0.05 Da, Minimum cosine score 0.70, Maximum number of neighbor nodes for one single node 10, Minimum matched fragment ions 6, Maximum size of nodes allowed in a single connected network 100, Maximum shift between precursors 500 Da, Library search min matched peaks 6, Score threshold 0.7. Further edges between two nodes were kept in the network only if each node appeared in each other's respective top 10 most similar nodes. The spectra in the network were then searched against GNPS spectral libraries. The library spectra were filtered in the same manner as the input data. All matches kept between network spectra and library spectra were required to have a score above 0.7 and at least six matched peaks (413, 488).

The MNs are publicly available, and can be consulted in the links: <https://gnps.ucsd.edu/ProteoSAFe/status.jsp?task=060cdcd6cb9e462482cddb62c879a2d> (ethyl acetate extracts), and <https://gnps.ucsd.edu/ProteoSAFe/status.jsp?task=2bc2597131ba4c73997802bf2a58bbd0>

³ **VN 1000X**: dilute 10 g EDTA, 4.4 g ZnSO₄·7H₂O, 1.01 g MnCl₂·4H₂O, 0.32 g CoCl₂·6H₂O, 0.315 g CuSO₄·5H₂O, 0.22 g (NH₄)₆Mo₇O₂₄·4H₂O, 1.11 g CaCl₂ y 1.0 g FeSO₄·7H₂O in 600 mL distilled water. Adjust to pH 4.0 with NaOH 1 M and HCl 1 M. composition per liter.

(ethanolic extracts). MN were visualized using Cytoscape version 3.6.14 (489). The ions that presented hits with previously reported compounds were manually annotated and verified with the data obtained to corroborate the identification.

5.2.8 Compound isolation

Interesting metabolites present in ethanolic extracts of *Paenibacillus* sp. PNM200 co-culture on TPDA medium were isolated. To this end, 672 mg of a pooled sample obtained from the five replicates from the co-culture of *Paenibacillus* sp. PNM200 was subjected to a solid phase fractionation using a RP-18 cartridge. MeOH/H₂O mixtures 1:9, 3:7, 1:1, 7:3 and 1:0 were used to obtain 5 fractions (CC1.1 to CC1-5). Later, an antifungal activity test against FOL CBS 164.85 was carried out by paper disk diffusion assay for these five fractions (336).

The active fractions (CC1.4 and CC1.5) were initially examined by analytical HPLC-DAD using a Phenomenex Luna® C18 (2) column (150 X 4.6 mm, 5 µm). The samples were dissolved in acetonitrile (10%) at a concentration of 1 mg·mL⁻¹. The chromatographic separation was carried out using Water with 0.1% formic acid (A) and acetonitrile with 0.1% formic acid (B) as elution solvents. The gradient program started with 10% of phase B, and increased linearly to 100% in 20 minutes, maintaining this proportion for 5 minutes. The flow was set at 0.5 mL·min⁻¹ with an injection volume of 2 µL.

Given the complexity of the active fractions' chromatographic profile, an optimization process for the separation program was carried out. This program was scaled for use in the semi-preparative column Phenomenex Luna® C18 (2) column (250 X 10 mm, 5 µm). For semi-preparative chromatography, the samples were dissolved in acetonitrile (10%) at a concentration of 5 and 10 mg·mL⁻¹ for CC1.4 and CC1.5, respectively. Elution solvents A and B were acidified with trifluoroacetic acid (TFA 0.1%) instead of formic acid. The chromatographic program consisted of a four-step gradient starting at 10% of B, which increased linearly to 32% in 15 minutes, then to 39% in 13 minutes, to 45% in 32 minutes, and finally to 100% in 5 minutes, maintaining this proportion for additional 10 minutes. Column flow and temperature were set at 3.5 mL/min and 24 °C, respectively.

Twenty-three fractions from CC1.4 and twenty-two from CC1.5 were obtained. These fractions were further analyzed by HPLC-MS/MS using the conditions described in section 5.2.3 (samples concentration 1 mg·mL⁻¹). Fractions C4-3 (0.34 mg), C4-5 (0.76 mg) and C5-3 (0.64 mg), were used for NMR analysis in deuterated methanol (CD₃OD). One-dimensional (¹H-NMR), and two-dimensional (TOCSY, HSQC, HMBC, COSY, NOESY) experiments were measured using a cryoprobe at 25 °C in an AV-600 MHz NMR spectrometer (Bruker, Karlsruhe, Germany).

5.3 Results and discussion

Metabolic profiling of the *Paenibacillus* sp. PNM200-FOL59 co-culturing was performed to evaluate significant variations in the metabolic profiles of both microorganisms caused by their interaction. Additionally, the evaluation of this interaction on PDA and TPDA aimed to establish if the variations on the metabolic profile could be related to tomato tissue present in the supplemented TPDA medium.

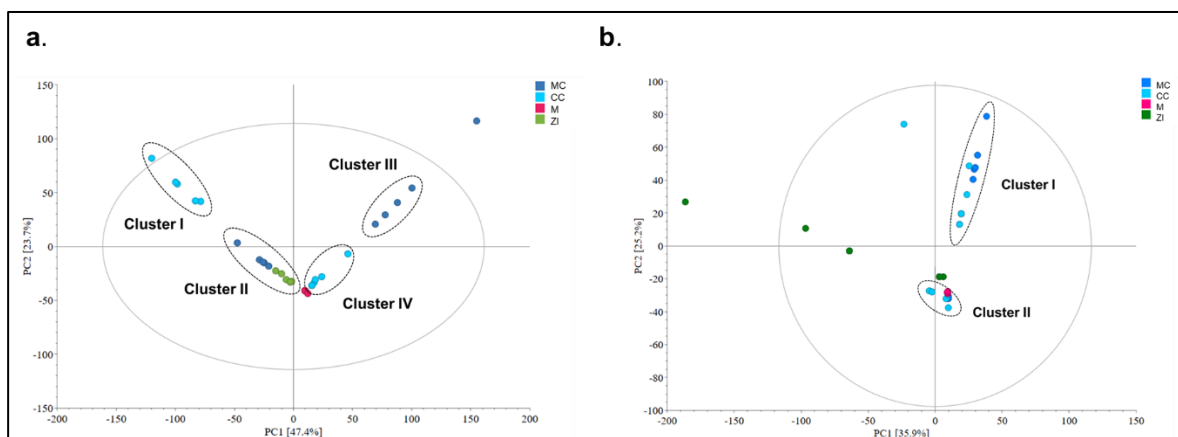
The performed principal component analysis (PCA) of the ethyl acetate and ethanolic extracts allowed discriminating FOL59 and *Paenibacillus* sp. PNM200 samples, clustering them in two different groups. Significant variations of FOL59 and *Paenibacillus* sp. PNM200 metabolic profiles were observed in ethyl acetate and ethanolic extracts, respectively. Growth on TPDA and Co-cultivation generated a significant effect on the microorganism's secondary metabolism by eliciting or reducing several compounds' biosynthesis. These results, as well as the dereplication process and MNs for the metabolites of interest are presented below.

5.3.1 FOL59 metabolome changes in presence of tomato tissue and *Paenibacillus* sp. PNM200.

Differences in the metabolic profiles of FOL59 monocultures and co-cultures were evidenced in ethyl acetate samples (Appendix F). PCA performed for this dataset showed two clusters related to FOL59, Cluster III and IV (Figure 5-2a). Cluster III include samples corresponding to FOL59 monoculture, whereas cluster IV encompasses FOL59 co-culture extracts. Individual clustering of mono and co-culture treatments indicates that the metabolic profile of the fungus change in the presence or absence of *Paenibacillus* sp. PNM200.

Samples from monoculture and coculture grown in PDA medium were not statistically different, and they clustered in one single group (Cluster I, Figure 5-2 b). In contrast, substantial differences were observed when microorganisms were cultured on tomato supplemented media (TPDA) (Clusters III and IV, figure 5-2 a). Thus, the higher variation observed on TPDA may also correspond to a medium effect on FOL59 metabolome.

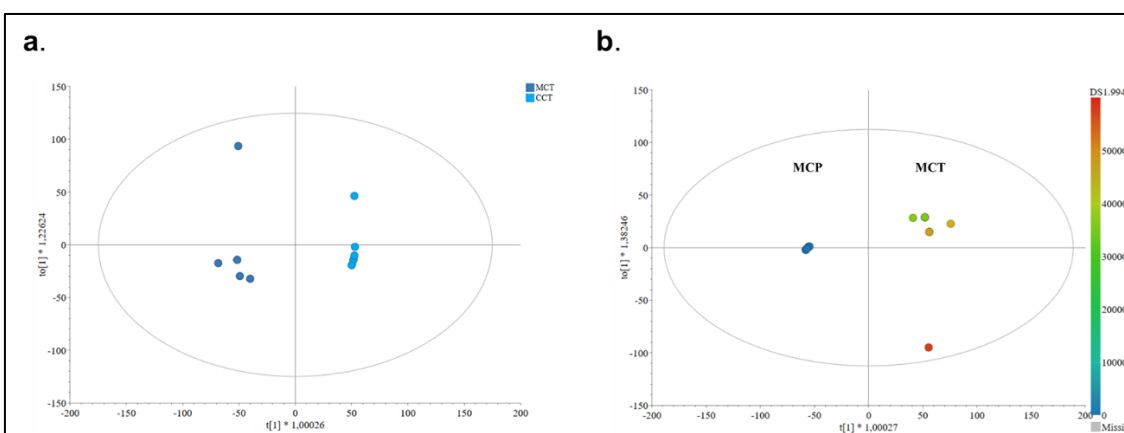
Figure 5-2: Principal components analysis (PCA) score plot indicating the general grouping of the variables in the ethyl acetate extracts datasets. In the figure, *in vitro* FOL59- *Paenibacillus* sp. PNM200 interactions on TPDA (a), and PDA (b) medium are shown. (a) $R^2 = 0.711$ $Q^2 = 0.588$; (b) $R^2 = 0.703$ $Q^2 = 0.438$. MC, Monoculture; CC, Co-culture; ZIT, Inhibition zone; M, medium control.



Bacterial-fungal Interaction and medium effects on FOL59 metabolome were further analyzed by OPLS-DA. In those analyses, the type of culture and medium were used as discriminant variables (Table 5-1). Paired analysis of ethyl acetate extracts from FOL59 monocultures on both PDA and TPDA (MCP/MCT) indicated that FOL59 metabolic profiles were statistically different in both culture media. Similarly, paired analysis between monoculture and co-culture TPDA extracts (MCT/CCT) confirmed the clustering observed on PCA score plots (Figure 5-3).

Table 5-2: OPLS-DA models cross-validation. In the table (^{of}) indicates OPLS-DA overfitted models.

| | Treatment | OPLS-DA | | | | | | | |
|-------|-----------------------|------------------|----------------|---|----------------------|----------------------|------------------|--------------------|----------|
| | | R ² Y | Q ² | Δ R ² Y/Q ² | R ² X [1] | R ² X[o2] | Cross-validation | | |
| | | | | | | | CV-ANOVA | Q ² ^AY | AUROC |
| FOL59 | MCP/CCP | 0,961 | 0,869 | 0,092 | 41,80% | 32,2% | 0,0198 | -0,501 | 0,914286 |
| | MCT/CCT | 0,984 | 0,948 | 0,036 | 52,60% | 26,8% | 0,0113 | -0,461 | 0,736364 |
| | CCP/CCT ^{of} | 0,961 | 0,859 | 0,102 | 34,70% | 37% | 0,0754 | -0,456 | 0,961039 |
| | MCP/MCT | 0,98 | 0,955 | 0,025 | 66,60% | 23,6% | 0,0147 | -0,489 | 0,862338 |

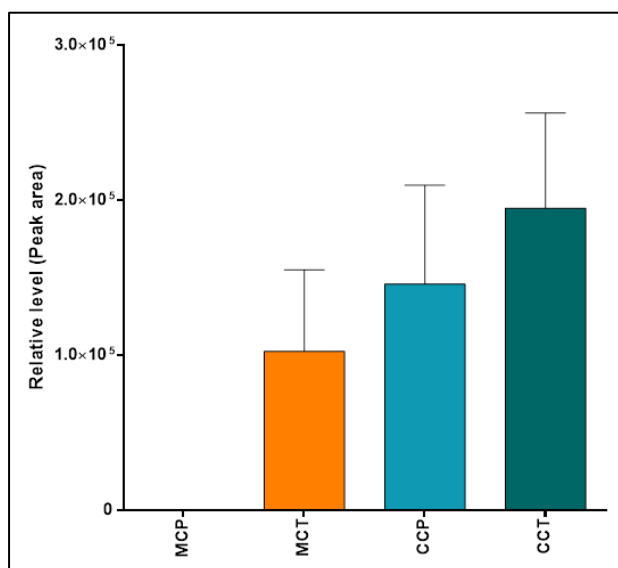
Figure 5-3: OPLS-DA model score plot (a,b) of ethyl acetate extracts of FOL59. The figure presents the score plot of the MCT/CCT (a) and MCP/MCT (b) OPLS-DA models. In the MCT/MCP score plot (b), each replicate is colored by the relative concentration (peak area) of feature 994. (a) R²Y =0.984 Q² =0.948 (b) R²Y =0.980 Q² =0.955.

Discrimination between PDA and TPDA monocultures was associated to six features corresponding to compounds **12**, **13** and **14** (Table 5-3). Compound **12**, putatively annotated as fusaric acid, was detected on TPDA mono and co-culture, and in PDA FOL59 co-culture but not in the corresponding monoculture. This result indicates that fusaric acid biosynthesis is basal in presence of tomato tissue and it could be elicited in response to *Paenibacillus* sp. PNM200 presence. The relative level of this compound in TPDA was significantly higher in FOL59 co-culture than in monoculture, supporting the previous affirmation ($p < 0.05$, Figure 5-4).

Table 5-3: Statistically significant secondary metabolites identified within FOL59 ethyl acetate extracts. RT, Retention time; MM, reported monoisotopic mass; IL, identification level according to Fernie et al. 2011 (445). (*) indicates the features that were observed exclusively in TPDA.

| Feature ID | ID | RT (min) | m/z | Adduct | Putative identification (IL) | Molecular formula | MM | Δ ppm |
|------------|----|----------|----------|-----------------------------------|------------------------------|---|----------|--------------|
| 948 | 12 | 4,3317 | 180,0934 | [M+H] ⁺ | Fusaric acid (D) | C ₁₀ H ₁₃ NO ₂ | 179.0946 | 6.68 |
| 1141 | | 4,2960 | 202,0724 | [M+Na] ⁺ | | | | |
| 992* | 13 | 10,2791 | 496,3070 | [M+H] ²⁺ | | | | |
| 994* | | 10,2791 | 518,2889 | [M+Na] ²⁺ | | | | |
| | | 10,2791 | 991.6108 | [M+H] ⁺ | NI | | - | - |
| 995* | 14 | 21,1113 | 317,2048 | [M+H] ⁺ | | | | |
| 999* | | 20,5976 | 335,2154 | [M+H ₂ O] ⁺ | NI | | - | - |
| 1247 | 15 | 3,1056 | 178,0773 | - | NI | | - | - |
| 1475 | 16 | 16,0604 | 787,1336 | - | NI | | - | - |
| 1529 | 17 | 21,1250 | 706,4039 | - | NI | | - | - |
| 1573 | 18 | 20,7614 | 317,2064 | - | NI | | - | - |

Figure 5-4: Relative amounts of fusaric acid produced by FOL59 in PDA and TPDA mediums. Data present in each graph are the means \pm standard deviation of five biological replicates per treatment. MCP, Monoculture on PDA; MCT, Monoculture on TPDA; CCP, co-culture on PDA; CCT, Co-culture on TPDA.

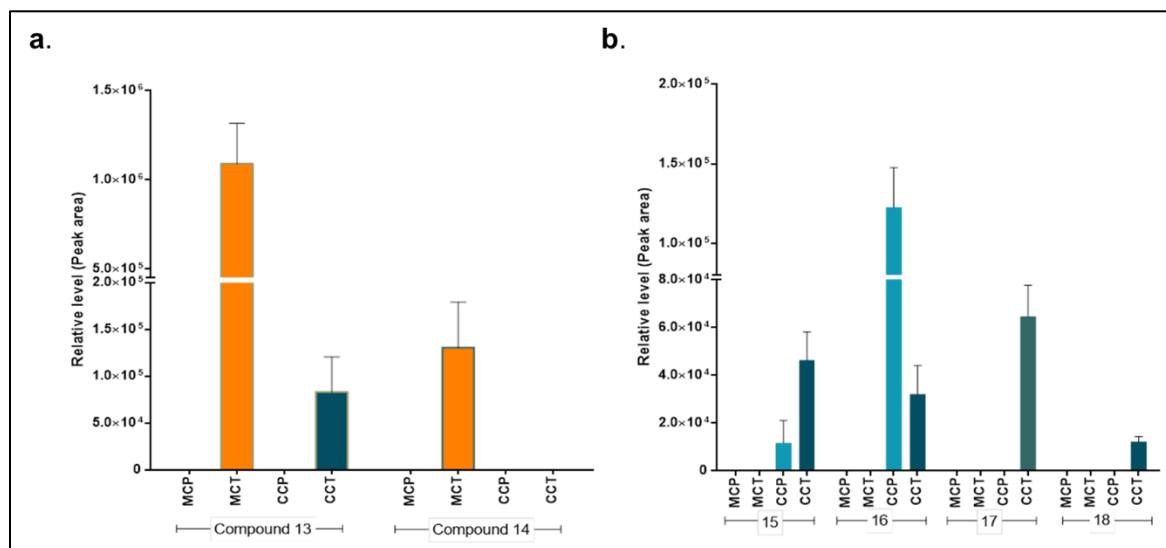


Fusaric acid is a broad-spectrum phytotoxin that contributes to FOL virulence inducing plant cell death by accumulating of reactive oxygen species (ROS) (116). This compound is synthesized during early tomato infection stages (490) and had antibacterial activity against several Gram-positive and Gram-negative microorganisms (491, 492). Fusaric acid production is strain-dependent in several *Fusarium* species and its elicited by fungal-fungal

co-culturing (493). Considering its biological function as phytotoxin and antimicrobial activity, it is likely to suggest that FOL59 secretes fusaric acid either as a mechanism of pathogenicity towards tomato cells or to inhibit the growth of a second microorganism (antagonism against *Paenibacillus* sp. PNM200).

On the other hand, compounds **13** and **14** were produced exclusively on TPDA medium. However, its relative amount was significantly reduced on co-culture samples (Figure 5-5 a, $p < 0.05$). This result suggests that compounds **13** and **14** are elicited by tomato tissue but their biosynthesis is inhibited during FOL59 interaction with *Paenibacillus* sp. PNM200. Neither compound 13 nor 14 were identified. However, the MS profile of **13** is similar to those reported for peptides.

Figure 5-5: Relative amounts of metabolites 13 to 18 produced by FOL59 in PDA and TPDA mediums. Data present in each graph are the means \pm standard deviation of five biological replicates per treatment. MCP, Monoculture on PDA; MCT, Monoculture on TPDA; CCP, co-culture on PDA; CCT, Co-culture on TPDA.



Regarding FOL59 co-culture metabolic variation, OPLS-DA models allow selecting four VIP features, corresponding to metabolites **15** to **18**, that explained the discrimination between TPDA and PDA co-culture from their corresponding monocultures. These four metabolites were produced only on co-culture treatments (Figure 5-5 b). Out of those, metabolites **17** and **18** were only induced on TPDA medium, while metabolites **15** and **16** were produced

in both co-cultures. Remarkably, metabolite **16** had a higher abundance in PDA than in TPDA co-culture. These results suggest that *Paenibacillus* sp. PNM200 induces the biosynthesis of metabolites 15 to 18 by FOL59. As suggested for metabolite 13, metabolite 17 is likely a peptide-like molecule since its MS and fragmentation profile present doubly and triply charged ions, which are characteristic of peptides.

Since no further information could be retrieved from the chemical nature of the VIP metabolites, an FBMN approximation was used to gain more in-depth information regarding secondary metabolites produced by FOL59, as it will be presented below.

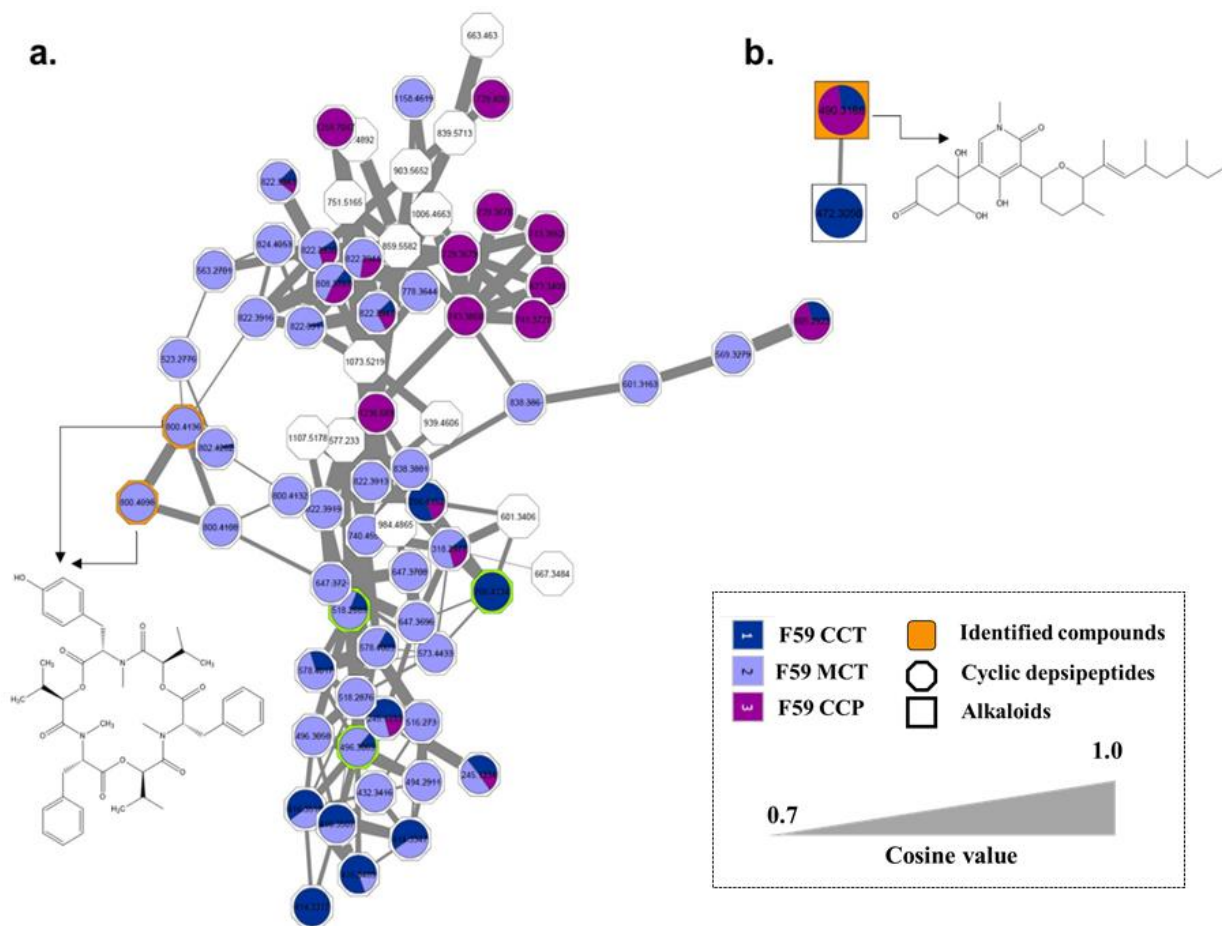
5.3.2 Metabolites produced by FOL59 on TPDA are related to Beauvericin phytotoxins family

For analyzing the chemical variation of mono- and co-cultures comparatively, a global molecular network based on HPLC-MS/MS data was generated using the GNPS platform. The composite molecular network (MN) of all the mono- and co-culture ethyl acetate extracts consisted of 946 nodes, grouped in 11 clusters (with at least two nodes per cluster) and 754 self-loops (Appendix F). Some nodes represented adducts; thus, not all network nodes correspond to a single molecule.

Cluster 1, composed by 70 nodes, mostly expressed in FOL59 on TPDA monoculture, include some of the significant features identified in the OPLS-DA model like 992 (m/z 496.307), 994 (m/z 518.2889) from compound **13**, and 1529 (m/z 706.4039) from compound **17** (Figure 5-4). These metabolites were annotated within the cyclic depsipeptide molecular family according to the results of NAP and MolNetEnhancer analysis.

One of the nodes in cluster 1 corresponds to feature 1194, that was identified as Beauvericin J (molecular formula: $C_{45}H_{57}N_3O_{10}$, monoisotopic mass: 799.4043; Δ ppm 0.7). Beauvericins are a family of hexadepsipeptides produced by several phytopathogenic fungi, including *F. oxysporum* (494). These metabolites are mycotoxins with phytotoxic activity on tomato protoplast induced by oxidative burst, interference with ROS detoxification and damage in plasmatic membrane permeability (495, 496). Beauvericin inoculation on tomato plants causes oxidative stress, induce APX and CAT enzymatic activity and plant cell lignification (496).

Figure 5-6: Ethyl acetate extracts molecular networks 1 (a) and 14 (b) created from FOL59 dataset. Pie charts represent relative summed precursor ion intensities per MS² spectrum detected within each metadata group (bottom box). Green nodes indicate VIP features from compound 13 and 17. Orange nodes indicate metabolites annotated using the GNPS platform public databases. Octagonal and square nodes were classified as cyclic depsipeptides and terpene glycosides, respectively, by the NAP and MolNetEnhancer analysis tools. Chemical structures correspond to Beauvericin J (a) and oxysporidinone (b).



Furthermore, Beauvericin depsipeptides have strong antibacterial activity against Gram-positive and Gram-negative bacteria including some *Bacillus* and *Paenibacillus* species (497). Beauvericin biosynthesis is up-regulated during *F. oxysporum* co-culture with microorganisms such as the endophyte fungi *Paraconiothyrium variable* (498). Interestingly, *P. variable* is also capable of biotransform beauvericin reducing its toxicity towards plant cells and to itself.

Since metabolites **13** and **17** belong to the same cluster as Beauvericin J, they are likely chemically similar, whose synthesis seems to be induced either by tomato vascular tissue on the growth media (**13**) or via the co-culturing with *Paenibacillus* sp. PNM200 (**17**). They may increase FOL59 pathogenicity towards tomato or act as a defense mechanism against the biocontrol strain. Isolation of both metabolites is required to assess their toxicity *in vivo* against tomato plants and *Paenibacillus* sp. PNM200. This approach could determine the capability of the later one to either biotransform metabolite **17** or down-regulate its biosynthesis.

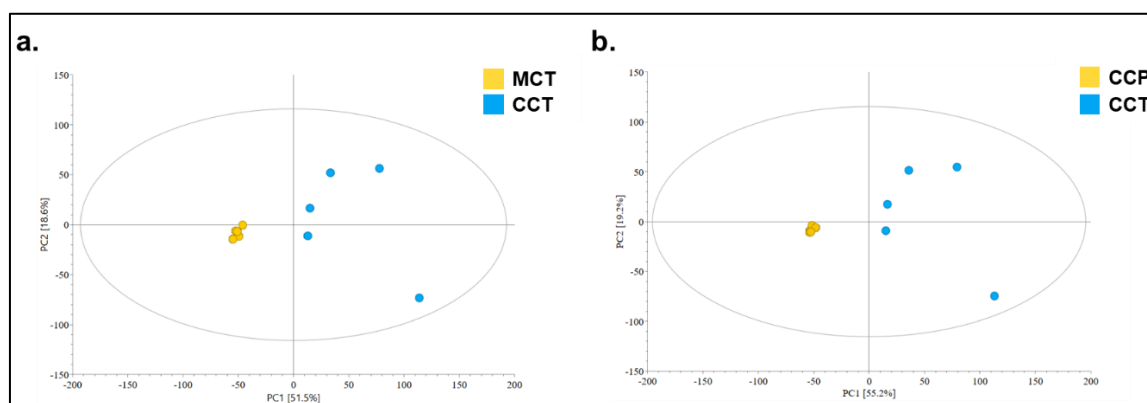
On the other hand, the molecular network generated in this study identified the alkaloid oxysporidinone within the metabolites produced by FOL59 (cluster 14, Figure 5-4 b). within the metabolites produced by FOL59. This metabolite corresponds to feature 1476 (Molecular formula: $C_{28}H_{43}NO_6$, monoisotopic mass: 489.3090, Δ ppm 0.4) and has one structurally related metabolite (feature 1483).

Oxysporidinone, is an active antifungal alkaloid initially isolated from an endophytic *F. oxysporum* (499). Its activity has been proved against *A. niger*, *Botrytis cinerea*, *A. alternata* and *Venturia inequalis*, however it does not display antibacterial activity (500). Interestingly, the features related to oxysporidinone were produced on co-culture treatments in PDA and TPDA media but not in FOL59 monoculture. This result suggests that oxysporidinone synthesis is induced as a response to *Paenibacillus* sp. PNM200 presence. Nevertheless, this alkaloid's exact role on FOL59-PNM200 interaction is not clear and should be further studied.

5.3.3 *Paenibacillus* sp. PNM200 produces peptides with antifungal activity during co-culture with FOL59 on TPDA medium.

Co-cultivation of *Paenibacillus* sp. PNM200 with FOL59 enhanced chemical diversity of secondary metabolites produced by strain PNM200. The PCA analysis of the dataset corresponding to ethanolic extracts dataset showed that bacterial zone growth on TPDA co-culture (CCT) presented the highest variance (Figure 5-7) among all evaluated treatments.

Figure 5-7: Principal components analysis (PCA) score plot indicating the general grouping of the variables in ethanolic extracts from monoculture and co-culture of *Paenibacillus* sp. PNM200 growth zone. In the figure, PCA score plot of the monoculture and co-culture datasets on TPDA (a), and the PCA score plot of the co-culture dataset on PDA and TPDA (b) are presented.



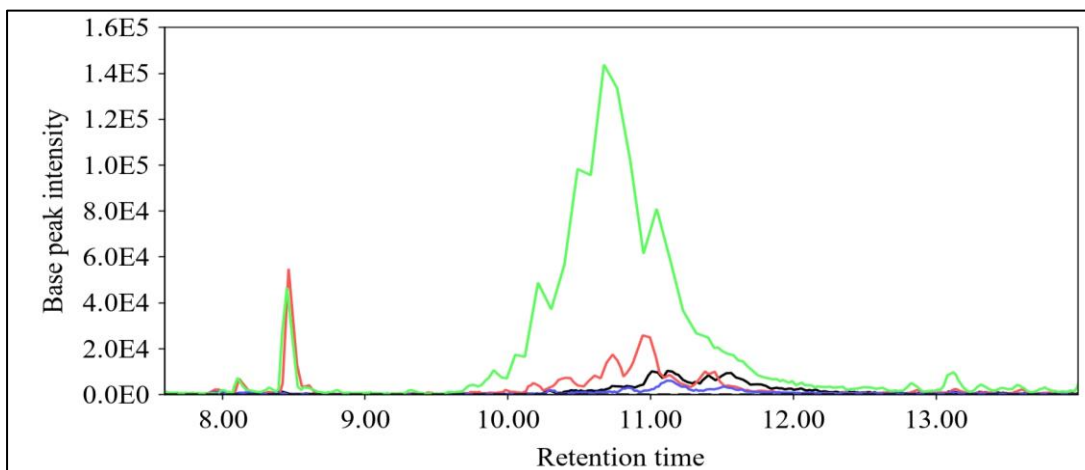
Discrimination of treatments observed on PCA was further confirmed in the OPLS-DA models. The paired analysis showed that the variance between co-culture extracts on TPDA versus the corresponding monoculture samples, and co-culture extracts on TPDA versus the co-culture extracts from PDA was significantly different (Table 5-4). From the OPLS-DA model, 20 features identified as discriminative were selected for further analyses. These features were related to nine metabolites with similar chromatographic properties (retention time 10-12 minutes, Figure 5-8), m/z between 1000 to 1600, and fragmentation profiles characteristic of peptides-like molecules (Table 5-5).

Table 5-4: PCA and OPLS-DA models cross-validation of ethanolic extracts from *Paenibacillus* sp. PNM200 monoculture and co-culture.

| Treatment | PCA | | | | OPLS-DA | | | |
|-----------|----------------|----------------|--------|--------|----------------|----------------|-----------|-------------------|
| | R ² | Q ² | PC1 | PC2 | R ² | Q ² | CV-ANOVA | Q ² ^Y |
| MCT/CCT | 0,702 | 0,465 | 51,50% | 18,60% | 0,99 | 0,892 | 0,0249153 | -0,251 |
| CCP/CCT | 0,744 | 0,407 | 55,20% | 19,20% | 0,995 | 0,94 | 0,1124030 | -0,369 |

Discriminant features related to molecular ions m/z 1411.79, 1587.86, and 1101.70 (metabolites **19**, **21**, and **26**, respectively) were exclusively produced on mono and co-culture treatments on TPDA. Remarkably, metabolite **19** had an 11.2-fold increase in TPDA co-culture regarding to their respective monoculture. Similarly, a 2.53 and 3.87-fold increases were observed for metabolites **16** and **21** in *Paenibacillus* sp. PNM200 co-culture. Ions m/z 1263.68 (**23**), 1601.88 (**24**), and 1439.82 (**25**) were produced on both TPDA and PDA. However, their abundance was higher in TPDA co-culture with 10.4, 9.2, and 56.4-fold increases compared to *Paenibacillus* sp. PNM200 monoculture (on the same medium).

Figure 5-8: Chromatographic profile of ethanolic extracts from monoculture and co-culture of *Paenibacillus* sp. PNM200 on PDA and TPDA medium. In the figure, chromatographic profiles of MCP, CCP, MCT, and CCT are presented in blue, black, red, and green, respectively.



Considering these results, it is possible to suggest that the synthesis of the metabolites describe above is induced by tomato tissue present in the growth media. This production, as well as the synthesis of m/z 1250.74 (**20**), 1425.81 (**22**), and 1277.77 (**27**), is stimulated during the interaction of *Paenibacillus* sp. PNM200 with FOL59.

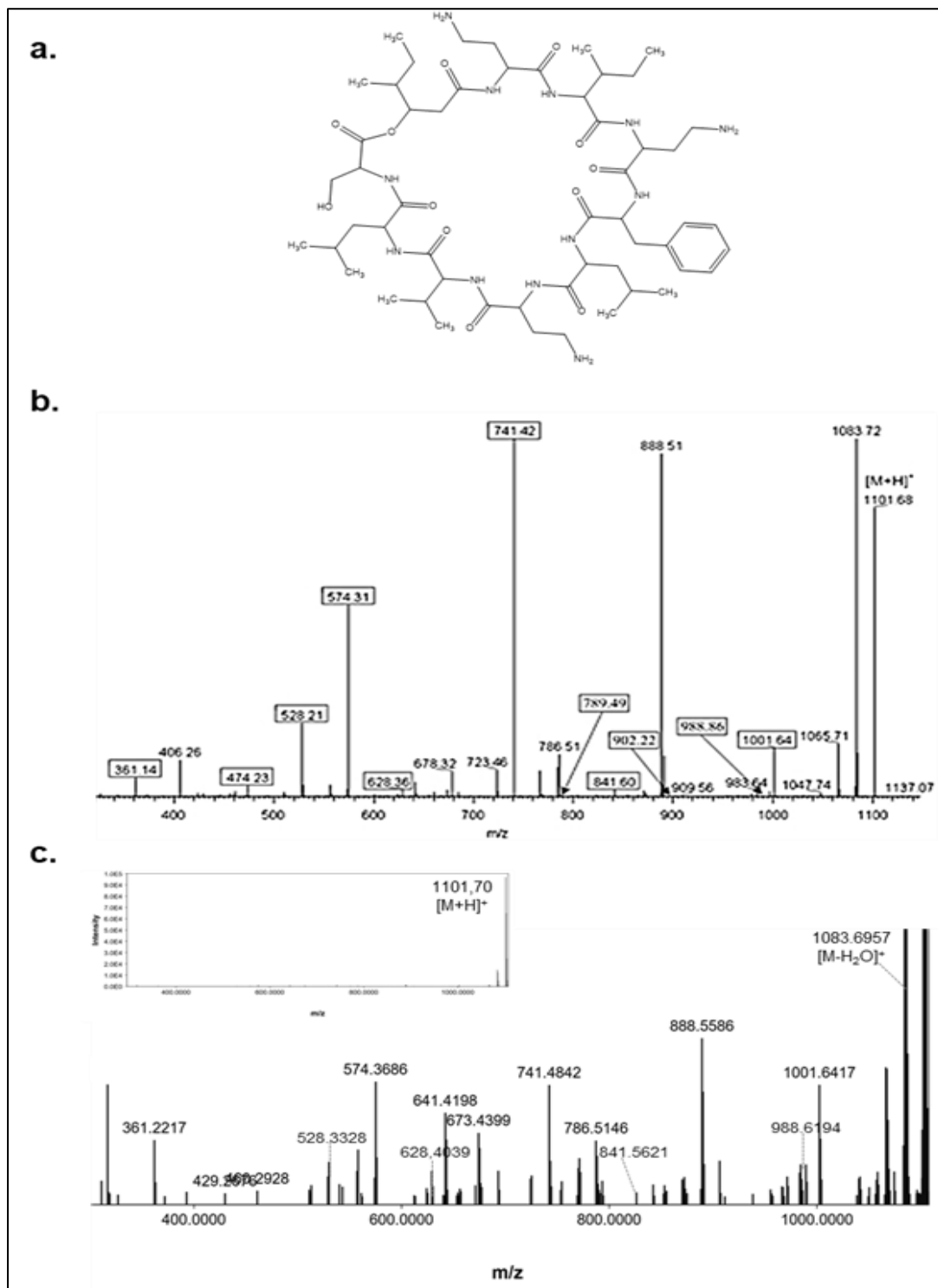
Table 5-5: Statistically significant secondary metabolites identified within ethanolic extracts from *Paenibacillus* sp. PNM200 monoculture and co-culture on TPDA. RT, Retention time; CC, Co-culture; *Fold change (FC) was calculated as the rate between CCT versus MCT using the VIP feature peak area. ND, No determined.

| Feature | ID | m/z | Adducts | RT (min) | Precursor ion [M+H] ⁺ | Exclusively Induced on CC | FC CCT/MCT* | Feature present on LB |
|---------|----|-----------|------------------------|----------|----------------------------------|---------------------------|-------------|-----------------------|
| 2812 | 19 | 706.3986 | [M+2H] ²⁺ | 10.01 | 1411.7887 | No | 11.2 | No |
| 7612 | 20 | 625.3717 | [M + 2H] ²⁺ | 10.12 | 1250.7434 | Yes | N.D. | Yes |
| 7629 | | 1271.7250 | [M+Na] ⁺ | | | | | |
| 3993 | 21 | 529.9586 | [M + 3H] ³⁺ | 10.15 | 1587.8601 | No | 3.9 | No |
| 2796 | | 794.4335 | [M+2H] ²⁺ | | | | | |
| 7607 | 22 | 1425.8075 | [M+H] ⁺ | 10.43 | 1425.8142 | Yes | N.D. | Yes |
| 4130 | | 475.9409 | [M+2H] ²⁺ | | | | | |
| 7605 | 23 | 1263.7555 | [M+H] ⁺ | 10.53 | 1263.6840 | No | 10.4 | Yes |
| 2854 | | 1285.7383 | [M+Na] ⁺ | | | | | |
| 2043 | | 632.3783 | [M+2H] ²⁺ | | | | | |
| 7596 | 24 | 801.9419 | [M+2H] ²⁺ | 10.71 | 1601.8811 | No | 9.3 | No |
| 2324 | | 534.6292 | [M + 3H] ³⁺ | | | | | |
| 7603 | 25 | 1461.8025 | [M+Na] ⁺ | 10.75 | 1439.8258 | No | 56.5 | No |
| 2819 | | 1439.8200 | [M+H] ⁺ | | | | | |
| 2441 | | 480.6110 | [M + 3H] ³⁺ | | | | | |
| 381 | | 551.3530 | [M + 2H] ²⁺ | | | | | |
| 7611 | 26 | 1123.6840 | [M+Na] ⁺ | 10.76 | 1101.7014 | No | 2.5 | Yes |
| 7598 | | 1277.7704 | [M+H] ⁺ | | | | | |
| 362 | 27 | 1299.7512 | [M+Na] ⁺ | 10.86 | 1277.7706 | Yes | N.D. | No |

Compound **26** MS data coincided with the [M+H]⁺ reported for the nonribosomal cyclic lipopeptide permetin A, also known as pelgipeptin B (C₅₄H₉₂N₁₂O₁₂, monoisotopic mass: 1100.6958; Δ 5.1 ppm) (Figure 5-9 a). Moreover, MSMS fragmentation profiles of **26** and pelgipeptin B (PGP-B) were the same (Figure 5-9), which lead us to annotate compound 26 as PGP-B.

To date, five pelgipeptins have been described (PGP A-E). PGPs have a chemical structure composed by a cyclic nonapeptide backbone with a short β-hydroxy fatty acid (501). These metabolites have been isolated from *B. circulans* (502), *Paenibacillus* sp. OSY-N (503), *P. ehimensis* IB-x-B (366), and *P. elgii* B69 (504) and present a broad-spectrum antimicrobial activity against human and plant pathogens including *Fusarium* species such as *F. oxysporum*, *F. graminearum*, and *F. moniliforme*, and have been used for *R. solani* control in rice plants (367).

Figure 5-9: Structural elucidation of cyclic lipopeptide Permetin A/PGP-B and compound 26 by tandem MS analysis. (a) Permetin A/PGP-B chemical structure and (b) MSMS fragmentation reported by Chang Wu et al. (367). (c) compound 26 MSMS fragmentation obtained in this study.



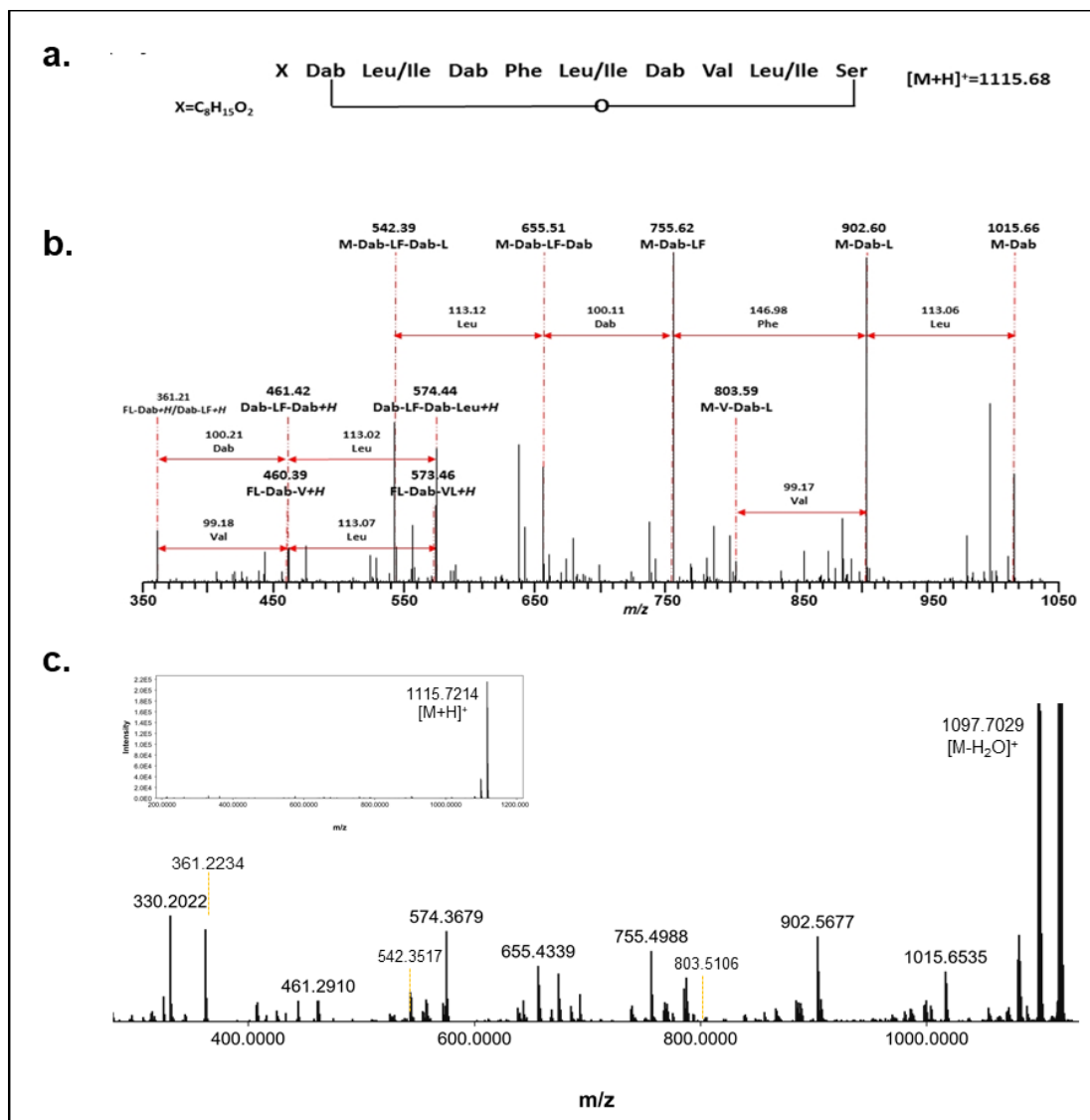
Apart from this compound, no other coincidences were found in databases or literature for the VIP features, which suggest that the metabolites produced by *Paenibacillus* sp. PNM200 have not been reported previously.

Interestingly, some of the discriminant co-culture induced metabolites were also detected on the *Paenibacillus* sp. PNM200' supernatant used for *in vivo* assays (metabolites **20**, **22**, **23**, and **26**), although their abundance was significantly higher in the LB supernatant than in solid medium. Within the metabolites produced during *Paenibacillus* sp. PNM200 liquid fermentation, an ion with m/z 1115.7214 was identified as the major compound (**28**). This ion was detected on PNM200 mono and co-cultures in both media, but its variance was not significant.

This metabolite was putative annotated as **Paenipeptin C** (Figure 5-9 b) since it had a molecular ion that matched with that of **28** (m/z 1115.68 [M+H]⁺) and had the same MSMS fragmentation profiles (Figure 5-10). Paenipeptin C is a cyclic lipopeptide isolated from *Paenibacillus* sp. OSY-N and has a strong antibacterial activity against Gram positive and Gram negative bacteria (503). The synthetic linear analog of paenipeptin C, paenipeptin C', has been used for the synthesis of a set of linear lipopeptides analogs that act as bactericides against carbapenem-resistant and polymyxin-resistant human pathogens (501, 505-507).

As far as we know, Paenipeptin C has not been previously isolated from a marine-derived bacterium and does not has antifungal activity. However, Paenipeptin C is an analogue of Permetin A, and thus probably of compound **26**. The mass difference between both metabolites could be explained by the loss of a methylene group and is supported by their chromatographic properties and mass fragmentation profiles similarities (503).

Figure 5-10: Structural elucidation of cyclic lipopeptide Paenipeptin C and compound 28 by tandem MS analysis. (a) Paenipeptin C chemical structure and (b) MSMS fragmentation reported by Huang et al. (503) (c) compound 28 MSMS fragmentation obtained in this study..



Considering that PGP-B has antifungal activity, it was proposed that other metabolites identified from the OPLS-DA models could be also active against FOL. This hypothesis was confirmed by a microdilution test using the biosensor FOL CBS 164.85. In those assays, the antifungal activity of the ethanolic and ethyl acetate extracts from *Paenibacillus* sp. PNM200 mono- and co-cultures were confirmed (Table 5-6). Only ethanolic extracts

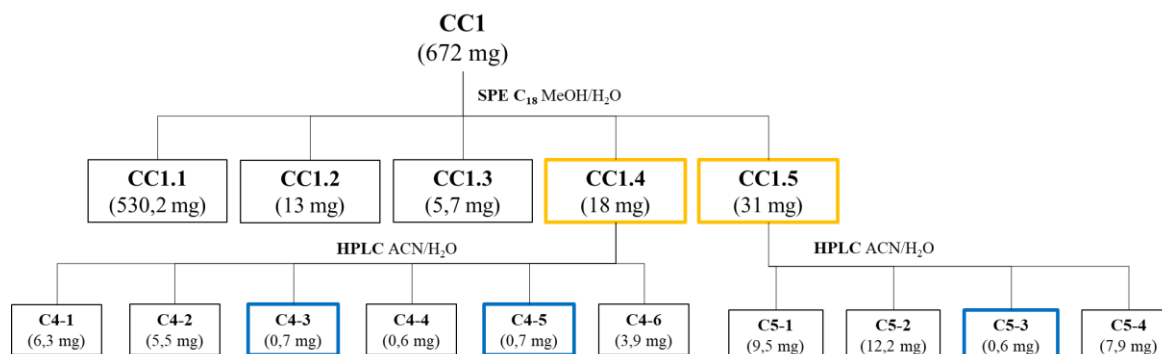
showed antifungal activity against CBS 164.85. As expected, according to the IC₅₀ values, TPDA co-culture samples had higher antifungal activity which was correlated to the presence of the peptide-like molecules studied so far.

Table 5-6: Antifungal activity of ethyl acetate and ethanolic extracts of *Paenibacillus* sp. PNM200 against FOL CBS 164.85. The data are the mean of five replicates per treatment ± SD.

| Extract | Treatment | IC ₅₀ (µg·mL ⁻¹) | Extract | Treatment | IC ₅₀ (µg·mL ⁻¹) |
|-----------|------------|---|---------------|-----------|---|
| Ethanolic | MCP | 1235.4 ± 94.4 | Ethyl acetate | MCP | NA |
| | CCP | 1770 ± 251.9 | | CCP | NA |
| | ZIP | NA | | ZIP | NA |
| | MCT | 1408 ± 207.1 | | MCT | NA |
| | CCT | 124.59 ± 37.5 | | CCT | NA |
| | ZIT | NA | | ZIT | NA |

In this context, it was necessary to isolate those peptides-like molecules. For this purpose, the pooled sample of co-cultured *Paenibacillus* sp. PNM200 ethanolic extracts were used for a bio-guided separation workflow as presented in Figure 5-11. From the active fractions CC1.4 and CC 1.5 obtained by SPE, 23 and 22 fractions were obtained, respectively. These fractions were pooled into six fractions for CC1.4 (C4.1-C4.6) and four fractions for CC1.5 (C5.1-C5.4).

Figure 5-11: Peptide bio-guided isolation workflow. In the figure, the yellow box highlights the active fractions against FOL CBS164.85. Blue boxes highlight fractions evaluated by NMR.



These fractions were evaluated by HPLC-MS/MS to verify their purity. It should be noted that given their structural similarity, the peptides of interest, present in CC1.4 and CC 1.5, coeluted at the same retention times, and although the program was optimized to improve the separation of metabolites, no pure compounds were obtained.

Fractions C4-3, C4-5, and C5-3 correspond to compounds **25**, **27**, and **28**, respectively. These fractions had a purity higher than 80%, and therefore were selected for analysis by NMR. The spectroscopic information obtained from the ¹H-NMR experiments for fraction C5-1 was similar to that reported by Hee Moon et al.(501), supporting the annotation of **28** as paenipeptin C (Appendix H).

Unfortunately, the remaining fractions presented a purity below 50% and could not be further purified. For this reason, it is necessary to implement other approaches that allow to identify the induced peptides and complete FOL59-PNM200 interaction's characterization.

5.3.4 Antifungal peptides produced by *Paenibacillus* sp. PNM200 are lipopeptides related to Pelgipeptin B and Paenipeptin C.

For analyzing the chemical variation of mono- and co-cultures of ethanolic extracts, a global molecular network based on UHPLC-MS/MS data was generated using the GNPS platform. The composite MN of all the mono- and co-culture ethanolic extracts consisted of 1254 nodes, grouped in 37 cluster (with at least two nodes per cluster) and 735 self-loops (Appendix I). As with the MN of ethyl acetate extracts, some nodes represented adducts; thus, not all network nodes correspond to a single molecule.

The discriminant features identified in the OPLS-DA model were grouped into three clusters. Cluster 1 include the metabolites with m/z 1587.86, 1411.79 and 1250.74 (Detected Features 794.43, 706.39, and 625.37 corresponding to $[M+2H]^{2+}$). In cluster 2, the nodes corresponding to the ions m/z 1425.81, 1123.68 (Adduct $[M+Na]^+$ of 1101.70, **26**), 1285.7478 (Adduct $[M+Na]^+$ of 1263.6840), 1439.82 and 1277.77 were observed. Finally, in cluster 6, a node associated with the ion m/z 1601.88 (m/z 801.9438 $[M+2H]^{2+}$) was observed. Unlike the results obtained with the ethyl acetate extracts, no hits were acquired during the data's dereplication from these extracts with the GNPS platform

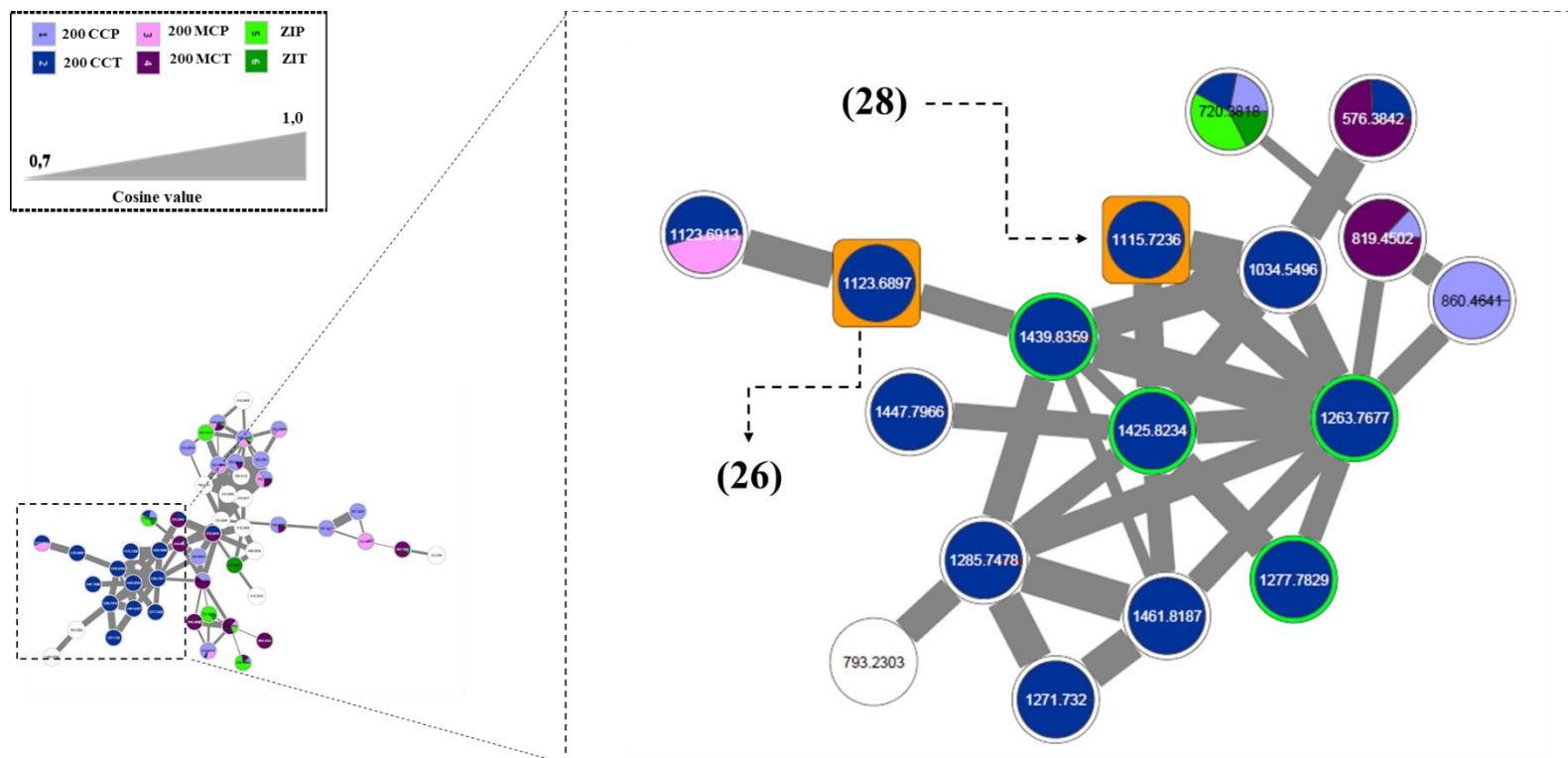
databases. This result support the hypothesis that the discriminant peptides have not been detected before.

According to the NAP and MolNetEnhancer analyses, most of the nodes in cluster 2 (Figure 5-11) can be classified as lipopeptides. In this network the molecular ion of paenipeptin C (m/z 1115.7246) was also present, being associated with the features of interest with cosine values higher than 0.85, which suggests that these metabolites are part of the same family of peptides (Figure 5-9).

The relative abundance of each metabolite presented in the pie diagrams of the molecular networks allowed to confirm that ion 706.3971 ($[M+2H]^{2+}$ of 1411.79) was found in the monocultures of *Paenibacillus* sp. PNM200 in PDA and TPDA, and in the co-culture in TPDA. Interestingly, the highest relative abundance of this metabolite was observed in TDPA coculture. Likewise, $[M+Na]^+$ of 1101.70 (m/z 1123.68), the ions m/z 1439.85, 1285.74 ($[M+Na]^+$ of m/z 1263.76) presented the highest relative abundance in the co-culture in TPDA, being scarcely found in the other treatments. While the ions 1277.78, 1425.82 and 1271.73 ($[M+Na]^+$ 1250.74) were only found in the co-culture of TPDA.

GNPS-FBMN based dereplication of ethanolic extracts did not allow identifying any additional metabolite. However, given the chemical similarity observed within each cluster, we suggest that the unknown compounds may be new analogs of either PGP-B or paenipeptin C, which would increase the secondary metabolic diversity reported for *Paenibacillus* species. However, it is necessary to isolate and purify these compounds to confirm the previous affirmation and give a proper identification for these peptides.

Figure 5-12: Cluster 2 from the molecular network obtained from the ethanolic extracts from *Paenibacillus* sp. PNM200 dataset. Pie charts represent relative summed precursor ion intensities per MS² spectrum detected within each metadata group (upper box). Square orange nodes indicate metabolites annotated using public databases. Circular green nodes indicate significant metabolites retrieved from OPLS-DA models. Numbers correspond to Pelgipeptin B (**26**) and Paenipeptin C (**28**).



5.4 Final remarks

Overall, the co-culture technique allowed identifying that FOL secondary metabolism diversity is enhanced once the pathogen grows in tomato supplement media. The coculture *in vitro* approach could give insights about the metabolic reprogramming of FOL during the infection process. The results obtained in the present research allowed to determine that FOL increases the production of several metabolites related to plant cell damage, including fusaric acid and beauvericin-related molecules.

Interestingly, this metabolic variation was reduced once the phytopathogen grew in co-culture with *Paenibacillus* sp. PNM200. Although the mechanism is not clear, the result indicates that PNM200 is able to decrease the production of depsipeptide-like molecules by FOL59, which could indirectly contribute to the biocontrol of the pathogen.

On the other hand, *Paenibacillus* sp. PNM200 recognizes the presence of FOL59, which triggers the production of new compounds and enhances the expression of antifungal peptides detected in *Paenibacillus* sp. PNM200 monoculture. The above-mentioned metabolites correspond to a peptide family composed of at least nine metabolites structurally related to PGP-B or paenipeptin C. Besides compounds **26** and **28**, none of the mentioned peptides could be annotated to any known compound, suggesting that they are new metabolites and therefore, should be purified in future works.

Some of these metabolites are produced during *Paenibacillus* sp. PNM200 growth on liquid media. However, they seem to play a minor role *in vivo*, since they did not reduce the severity of VW symptoms.

The metabolites produced only during the co-culture of *Paenibacillus* sp. PNM200 and FOL59 in the presence of tomato vascular tissue, such as 1277.7, could have a more critical role in *Paenibacillus* sp. PNM200 biocontrol effect. It is necessary to follow the identified peptides' production using an *in vivo* interaction assay by targeted metabolomics analysis or using transcriptomic approaches.

6. Conclusions and recommendations

6.1 Conclusions.

The study of a marine-derived bacterial collection obtained from the Santa Catalina and Providencia coral reef (Colombian Caribbean) allowed the identification of 28 microorganisms with antifungal activity against the tomato phytopathogen FOL. Of these isolates, nine bacteria, belonging to the phylum Firmicutes, order Bacillales, were selected for their activity against a panel of *F. oxysporum* genus, and their ability to colonize the rhizospheres of two tomato cultivars (Milano and Santa Cruz Kada). These features evidenced these bacteria's ability to adapt and survive in different ecological niches and highlight the biotechnological potential of microorganisms derived from marine environments.

Paenibacillus sp. PNM200 was selected out of those nine bacterial isolates, as a promising candidate for a biological control based on its ability to reduce the severity of *Fusarium* vascular wilt symptoms in tomato plants, under greenhouse conditions. This bacterium was proposed as a rhizospheric competent microorganism, taking into consideration that; (i) it can remain viable in tomato rhizosphere for at least thirty days and (ii) it can form biofilms and presents a positive chemotactic response towards tomato root exudates, which contributes in the bacterial survival on the rhizospheric environment.

Furthermore, *Paenibacillus* sp. PNM200 has potential as PGPR, taking into account that its inoculation in tomato plants generated a positive impact on tomato growth, which was associated with this bacterium's ability to produce IAA and solubilize phosphates.

Metabolomic studies indicated that after 10 dpi, tomato plants infected with FOL59 presented a significant accumulation of different steroidal glycoalkaloids and the aglycone

Tomatidine. Other experimental results from this thesis also indicated that tomatidine and hydroxytomatine may be proposed as early FOL59 infection markers in tomato plants.

Metabolic profiling studies of the tomato-*Paenibacillus* sp. PNM200 interactions indicate that the inoculation of *Paenibacillus* sp. PNM200 does not generate any significant metabolic change in the plant root metabolome. Notably, when the tripartite tomato-*Paenibacillus* sp. PNM200-FOL59 was analyzed, the effects induced by FOL59 infection in the tomato-root metabolome were reduced. Therefore, it is suggested that the activity of *Paenibacillus* sp. PNM200 is the result of direct interaction with the fungal phytopathogen in the tomato rhizosphere. Further transcriptomic and proteomic studies may be required to confirm this hypothesis.

The study of the *Paenibacillus* sp. PNM200-FOL59 interaction in co-culture allowed to verify that the metabolome of both microorganisms varies depending on the interaction and the presence of vascular tissue in the culture medium. In the case of FOL59, tomato stem tissue induced the production of at least five depsipeptides, structurally related to the mycotoxin Beauvericin J and two alkaloids associated with the antifungal compound Oxysporidinone.

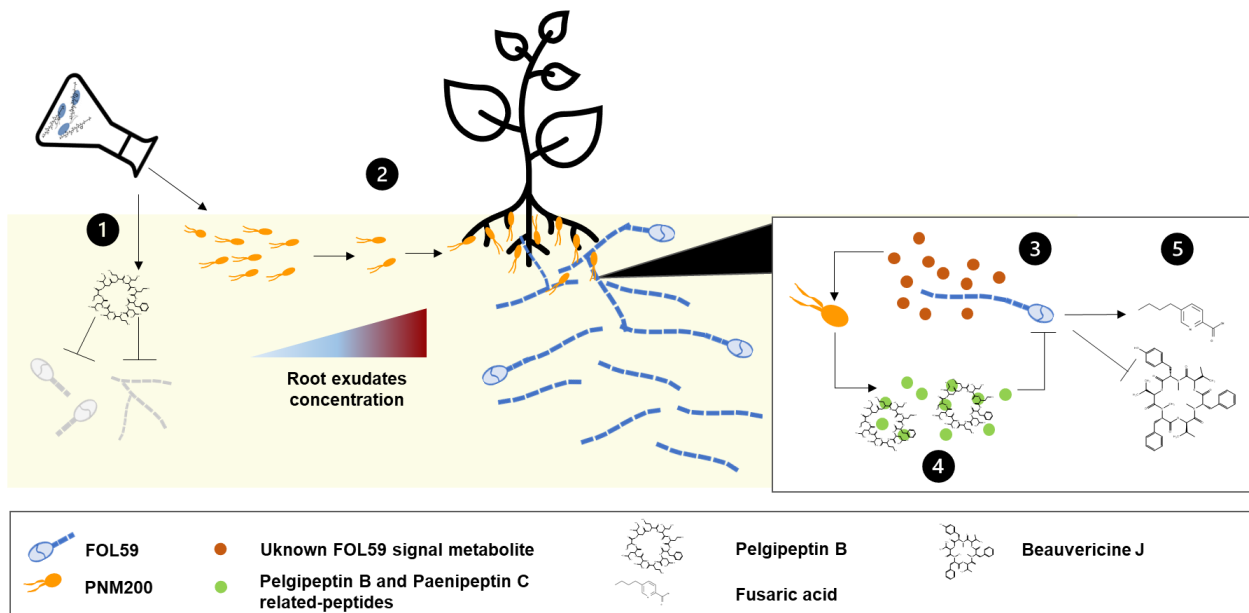
The interaction with FOL59 in TPDA medium induced the production of a group of 9 peptides that combined, show antifungal activity against FOL. Most of the metabolites induced during co-cultivation were grouped in the same molecular network of the lipopeptides PGP-B and paenipeptin C, which allows us to suggest that they are structurally related compounds.

Considering that in the liquid culture of *Paenibacillus* sp. PNM200, five of the peptides described in the co-culture were detected (including paenipeptin C), and that the supernatant of this culture does not display antifungal activity *in vivo*, it is proposed that the biocontrol activity of *Paenibacillus* sp. PNM200 is associated with the production of new peptides which, appear to be synthesized only during interaction with FOL59.

Finally, the interaction model presented in **Figure 6-1** is proposed to describe the biocontrol phenotype observed in the tritrophic tomato-FOL59-*Paenibacillus* PNM200 interaction as follows:

- (1) During liquid fermentation, *Paenibacillus* sp. PNM 200 produce several peptides with antifungal activity against FOL59, including paenipeptin C. After inoculation by soil drenching, active peptides partially inhibit FOL59 conidial germination and mycelium growth.
- (2) Once in soil, *Paenibacillus* sp. PNM200, detects root exudates and moves towards tomato rhizosphere, where it colonize root surface without causing any deleterious effect on plant growth.
- (3) FOL59 produce an unknown signal molecule that is recognized by *Paenibacillus* sp. PNM200.
- (4) Signal recognition triggers the expression of new lipopeptides on *Paenibacillus* sp. PNM200, which inhibit FOL59 growth in the rhizosphere.
- (5) As a side effect of FOL59-*Paenibacillus* sp. PNM200 interaction, the production of fusaric acid, beauvericin J and other related depsipeptides is modified, limiting FOL59 pathogenicity towards tomato plant.

Figure 6-1: Proposed model of tomato-*Paenibacillus* sp. PNM 200-FOL59 interaction.



6.2 Future perspectives

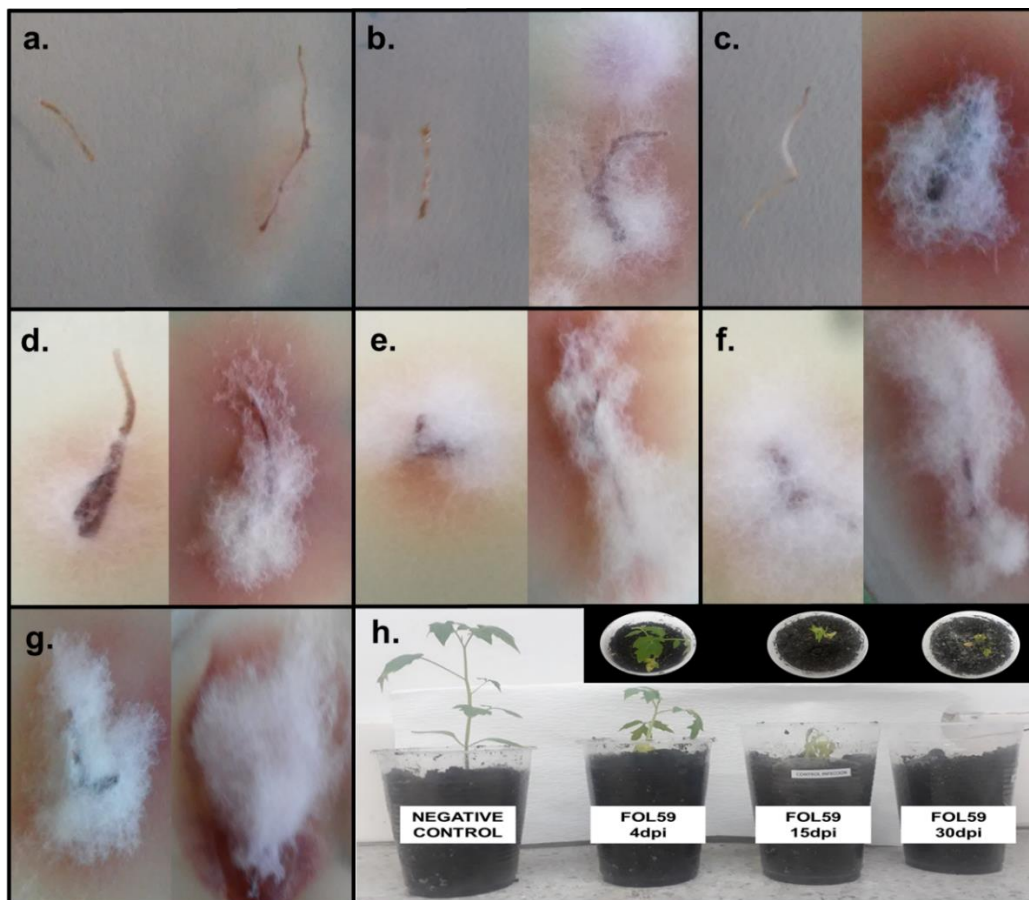
1. Aiming to develop a commercial product based on *Paenibacillus* sp. PNM200 it is necessary to complement the obtained data with field trials that confirm the antifungal activity of this bacterium under real conditions. Furthermore, it is necessary to start the scaling-up process for PNM200 production under batch fermentation conditions.
2. It is suggested to evaluate the tomato metabolome with the same treatments described in this work, using stem/xylem samples upon 15 or 30 dpi. These studies could contribute to determining the changes that may occur at the systemic level in the plant and, to identify if there are other modifications induced by both organisms during the late infection stages.
3. New targeted metabolomic analysis using a controlled matrix (liquid medium) must verify that peptides induced in the *Paenibacillus* sp. PNM200-FOL59 co-culture are also produced during *in vivo* interaction with the plant. These assays could be supported by other omics approaches, including transcriptomic or proteomic studies of the tripartite interaction, addressed to obtain insights about the molecular regulation process controlling plant-BCA-pathogen interaction.
4. We suggest that the volatile compounds produced by PNM200 and FOL59 should be studied to identify (1) if PNM200 produces antifungal volatile metabolites that contribute to FOL59 control and (2) if FOL59 produces volatile compounds that could be acting as signals that triggers PNM200 antifungal diffusible compounds biosynthesis.
5. Finally, further research is required to isolate and purify the new family of peptides produced by *Paenibacillus* sp. PNM200 during its interaction with FOL59. Besides, it is necessary to evaluate the specific biological activity of these peptides, aiming to unravel the specific mechanisms involve on FOL59 growth inhibition.

Appendix B: Fungal phytopathogen used in this study²

| Strain | Taxonomical classification | Related species | GenBank accession number | Source |
|------------------------------------|----------------------------|--|--------------------------|---|
| <i>Fusarium oxysporum</i> isolates | | | | |
| FOL59 | <i>F. oxysporum</i> | <i>F. oxysporum</i> f. sp. <i>lycopersici</i> physiological race 2 | - | Reference strain provided by Agrosavia, Colombia. (508) |
| F1 | <i>F. oxysporum</i> | <i>F. oxysporum</i> F11 (100%) <i>F. oxysporum</i> f sp. <i>lycopersici</i> KY587331 (98.1%) | MT579550 | Tomato plant root (Cundinamarca, Colombia) |
| F2 | <i>F. oxysporum</i> | <i>F. oxysporum</i> M81A (99,81%) <i>F. oxysporum</i> f sp. <i>lycopersici</i> FWT-8 (99.81%) | MT579551 | Tomato plant root (Cundinamarca, Colombia) |
| F4 | <i>F. oxysporum</i> | <i>F. oxysporum</i> DY9 (100%) <i>F. oxysporum</i> f sp <i>lentis</i> FLS75 (100%) | MT579552 | Tomato plant root (Tolima, Colombia) |
| 1R | <i>F. oxysporum</i> | <i>F. oxysporum</i> LEMM_111009 (100%) <i>F. oxysporum</i> f sp. <i>lycopersici</i> KY587331 (99,81%) | MT579553 | Tomato plant root (Tolima, Colombia) |
| 2R | <i>F. oxysporum</i> | <i>F. oxysporum</i> M81A (100%) <i>F. oxysporum</i> FoSt01 (100%) | MT579554 | Tomato plant root (Tolima, Colombia) |
| 3R | <i>F. oxysporum</i> | <i>F. oxysporum</i> F11 (100%) <i>F. oxysporum</i> UFA0019 (100%) | MT579555 | Tomato plant root (Tolima, Colombia) |
| 4R | <i>F. oxysporum</i> | <i>F. oxysporum</i> DY9 (99,81%) <i>F. oxysporum</i> f sp <i>lentis</i> FLS75 (99,81%) | MT579556 | Tomato plant root (Tolima, Colombia) |
| 8H | <i>F. oxysporum</i> | <i>F. oxysporum</i> f. sp. <i>radicis-lycopersici</i> F1 (100%) <i>F. oxysporum</i> UFA0019 (100%) | MT579557 | Tomato plant wilting leaves (Tolima, Colombia) |
| 9H | <i>F. oxysporum</i> | <i>Fusarium oxysporum</i> SCUf2021 (100%) <i>Fusarium</i> sp. S3-2 (100%) | MT579558 | Tomato plant wilting leaves (Tolima, Colombia) |

²The related species were retrieved from GenBank nucleotide sequence database using the ITS partial sequences (>500 pb in length) obtained for each isolate.

Appendix C. Isolation of FOL59 on tomato cv. Santa Cruz Kada root system, and symptoms of VW observed at 4, 15 and 30 dpi⁴.



⁴ The figure presents the growth of FOL59 on tomato root with (left) and without surface sterilization (right) at 1(a), 2 (b), 3 (c), 4 (d), 10 (e), 15 (f) and 30 (g) dpi. VW symptoms on infected plants at 4, 15 and 30 dpi (h).

Appendix D. Concentration of BCA candidates on tomato roots.

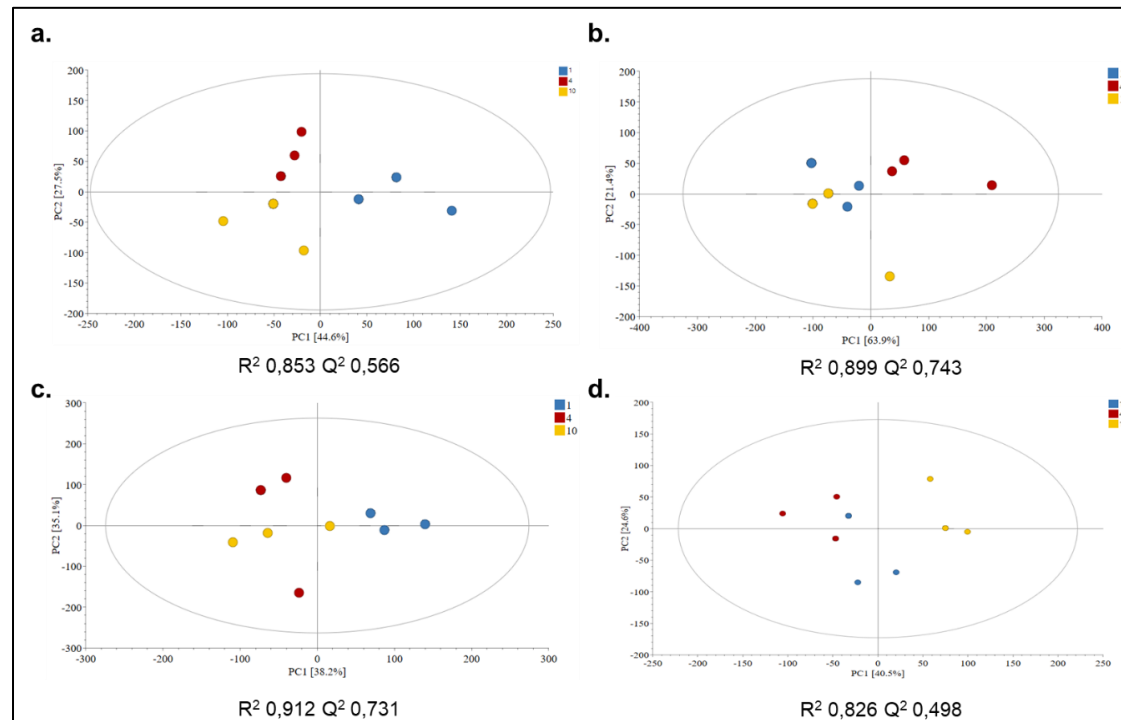
Table D-1. Concentration of BCA candidates on Milano cv. Bacterial concentrations are shown as Log₁₀ CFU·g⁻¹ root fresh weight. Data are the mean of three biological replicates ± SD per treatment. Data marked with an asterisk (*) in the same column are not statistically different to *B. subtilis* concentration (Dunnett's pos'hoc test p<0.01).

| Isolate | Time (Days) | | | | | | |
|--------------------|-------------|------------|------------|-----------|------------|-----------|------------|
| | 1 | 2 | 3 | 4 | 10 | 15 | 30 |
| <i>B. subtilis</i> | 6,61±0.28 | 7,05±0.47 | 6,84±0.6 | 7,31±0.19 | 6,62±0.19 | 7,19±0.47 | 6,25±0.22 |
| PNM34 | 7.97±0.23 | 6.28±0.41 | 5.96±0.3 | 6.88±0.22 | 6.27±0.71* | 4.93±0.18 | 4.5±0.23 |
| PNM65 | 6.35±0.22* | 5.85±0.4 | 6.42±0.31* | 6.63±0.15 | 6.06±0.36 | 6.11±0.4 | 5.83±0.45* |
| PNM68 | 0 | 0 | 0 | 0 | 0 | 0 | 0 |
| PNM77 | 4.29±0.14 | 0 | 0 | 0 | 0 | 0 | 0 |
| PNM95 | 4.97±0.5 | 5.34±0.22 | 5.71±0.32 | 6.10±0.51 | 5.86±0.34 | 5.32±0.37 | 5.27±0.28 |
| PNM103B | 5.81±1.06 | 5.23±0.44 | 5.25±0.27 | 5.92±0.21 | 5.71±0.29 | 5.6±0.47 | 5.25±0.23 |
| PNM135 | 3.48±0.17 | 4.29±0.32 | 3.84±0.21 | 4.48±0.52 | 3.51±0.31 | 0 | 0 |
| PNM142 | 4.28±0.16 | 4.74±0.16 | 4.20±0.23 | 0 | 0 | 0 | 0 |
| PNM172 | 4,77±0.18 | 5,28±0.19 | 5,21±0.26 | 5,76±0.36 | 5,38±0.38 | 5,30±0.18 | 5,18±0.12 |
| PNM200 | 5,35±0.37 | 5,72±0.24 | 5,08±0.18 | 5,12±0.13 | 5,84±0.28 | 5,06±0.16 | 4,74±0.22 |
| PNM210 | 3,94±0.26 | 4,08±0.24 | 5,49±0.29 | 6,53±0.2 | 5,29±0.22 | 4,92±0.24 | 4,86±0.2 |
| PNM220 | 6.33±0.25* | 7.33±0.35* | 7.59±0.23 | 5.77±0.28 | 5.34±0.28 | 5.38±0.29 | 0 |

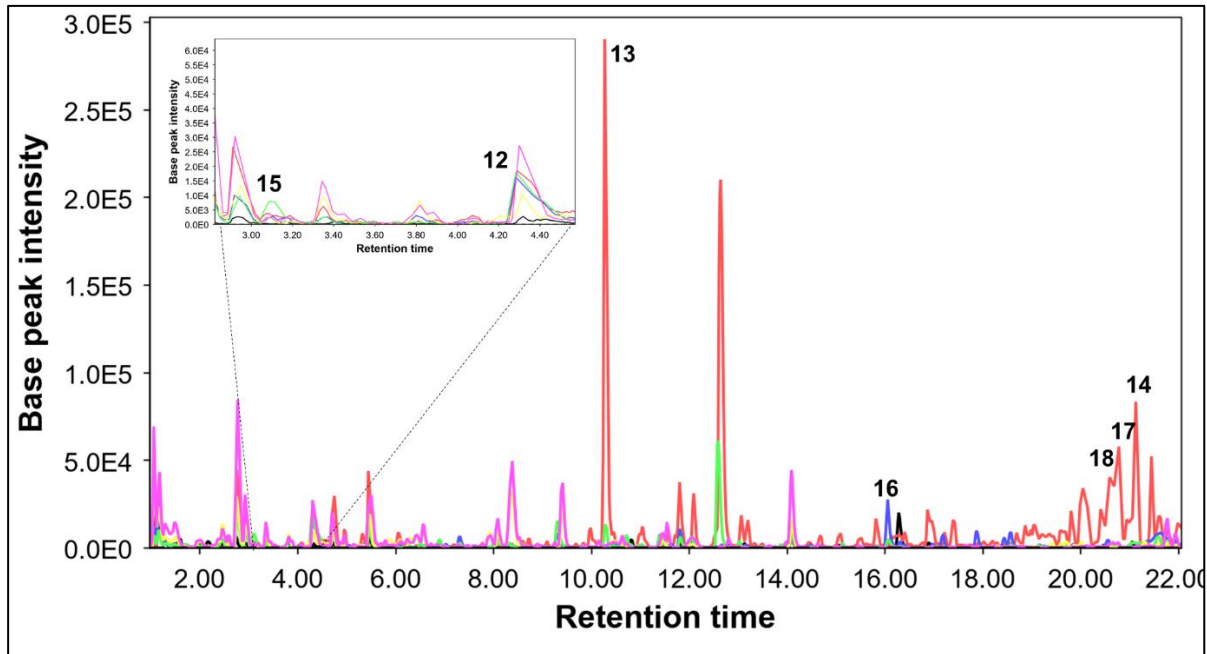
Table D-2. Concentration of BCA candidates on Santa Cruz Kada cv. Bacterial concentrations are shown as Log₁₀ CFU·g⁻¹ root fresh weight. Data are the mean of three biological replicates ± SD per treatment. Data marked with an asterisk (*) in the same column are not statistically different to *B. subtilis* concentration (Dunnett's pos'hoc test p<0.01).

| Isolate | Time (Days) | | | | | | |
|--------------------|-------------|-----------|-----------|------------|------------|-----------|-----------|
| | 1 | 2 | 3 | 4 | 10 | 15 | 30 |
| <i>B. subtilis</i> | 6.75±0.27 | 7.26±0.31 | 7.01±0.41 | 7.27±0.18 | 6.80±0.18 | 7.37±0.32 | 6.39±0.33 |
| PNM34 | 5,46±0.14 | 5,37±0.56 | 5,37±0.34 | 6,07±0.64 | 5,94±0.44* | 4,49±0.28 | 4,50±0.30 |
| PNM65 | 5,20±0.16 | 5,35±0.22 | 5,39±0.61 | 5,43±0.43 | 5,30±0.53 | 5,03±0.26 | 5,08±0.22 |
| PNM95 | 5,12±0.16 | 5,23±0.21 | 6,00±0.5 | 6,19±0.16 | 5,31±0.99 | 4,48±0.21 | 5,09±0.24 |
| PNM103B | 4,93±0.68 | 5,78±0.17 | 5,72±0.2 | 5,80±0.35 | 5,70±0.34 | 5,10±0.19 | 5,47±0.2 |
| PNM135 | 5,55±0.36 | 5,04±0.25 | 5,44±0.41 | 5,83±0.39 | 5,68±0.76 | 4,61±0.5 | 5,10±0.32 |
| PNM172 | 5,54±0.2 | 5,50±0.07 | 5,23±0.52 | 5,75±0.46 | 5,62±0.48 | 5,37±0.3 | 4,89±0.27 |
| PNM200 | 5,82±0.62 | 5,12±0.67 | 5,78±0.52 | 6,77±0.75* | 5,63±0.29 | 4,59±0.18 | 4,66±0.33 |
| PNM210 | 6,48±0.33* | 5,44±0.4 | 6,09±0.5 | 7,33±0.54* | 5,55±0.26 | 4,58±0.12 | 4,18±0.31 |
| PNM220 | 5,41±0.16 | 5,33±0.2 | 5,40±0.5 | 6,39±0.34* | 5,75±0.72* | 5,36±0.31 | 5,13±0.36 |

Appendix E. Principal Component Analyses (PCA) score-plot of P (a), PB (b), PF (c) and PBF (d) treatments.

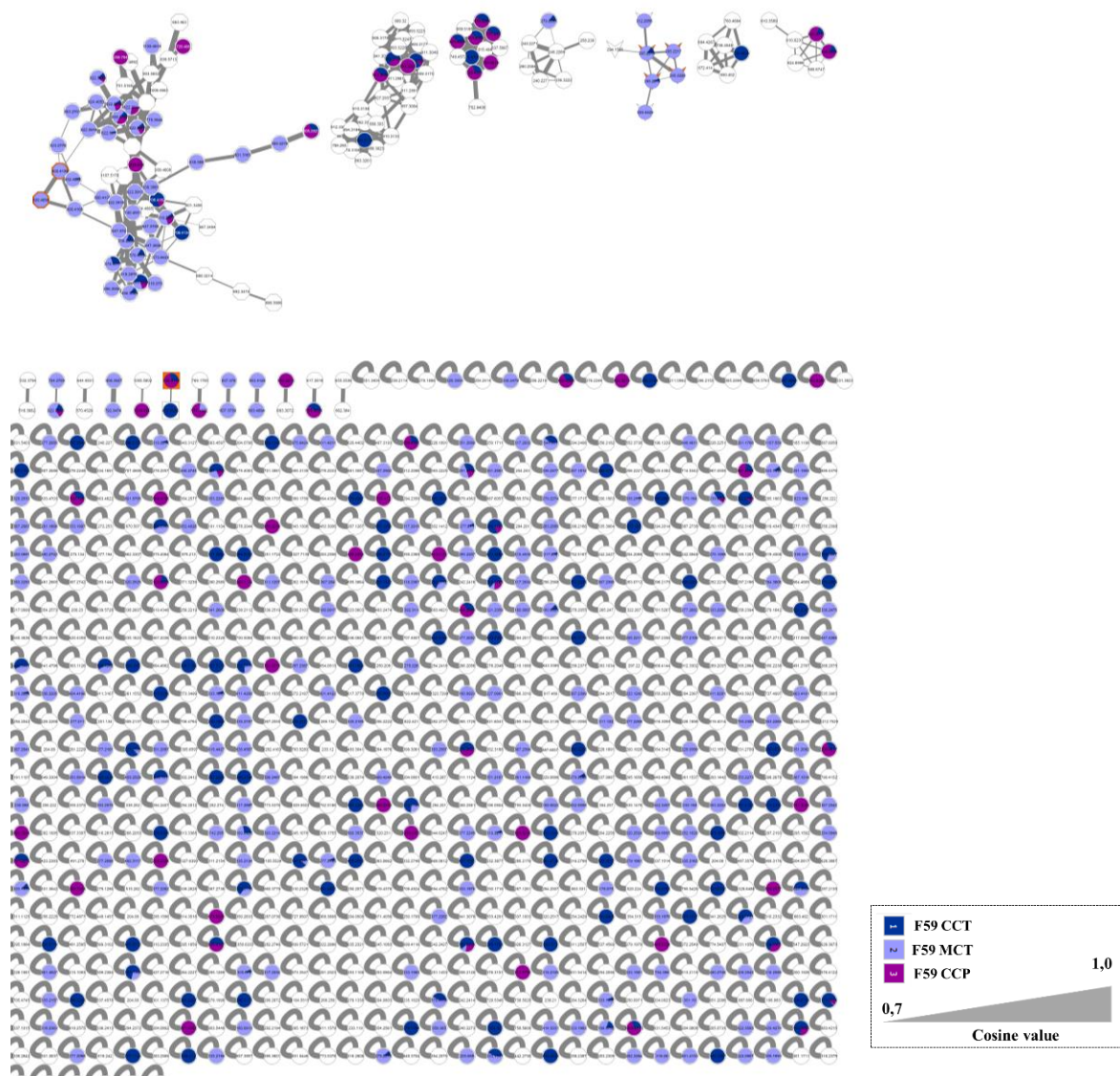


Appendix F. Metabolic profile of FOL59 ethyl acetate extracts⁵.

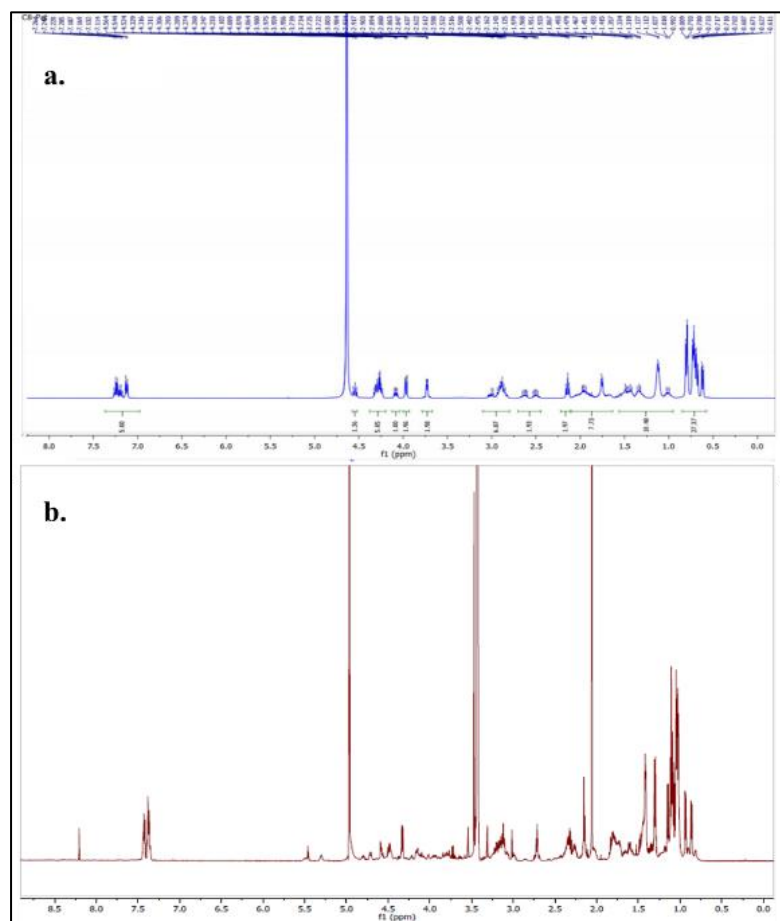


⁵ In the figure the metabolic profile of FOL59 monoculture in TPDA and PDA are presented in red and black, respectively, FOL59 co-culture samples in TPDA and PDA are presented in green and blue, and TPDA and PDA blank medium are presented in pink and yellow. Numbers correspond to metabolite ID.

Appendix G. Global molecular network of ethyl acetate extracts of *Paenibacillus* sp. PNM200-FOL59 interaction.

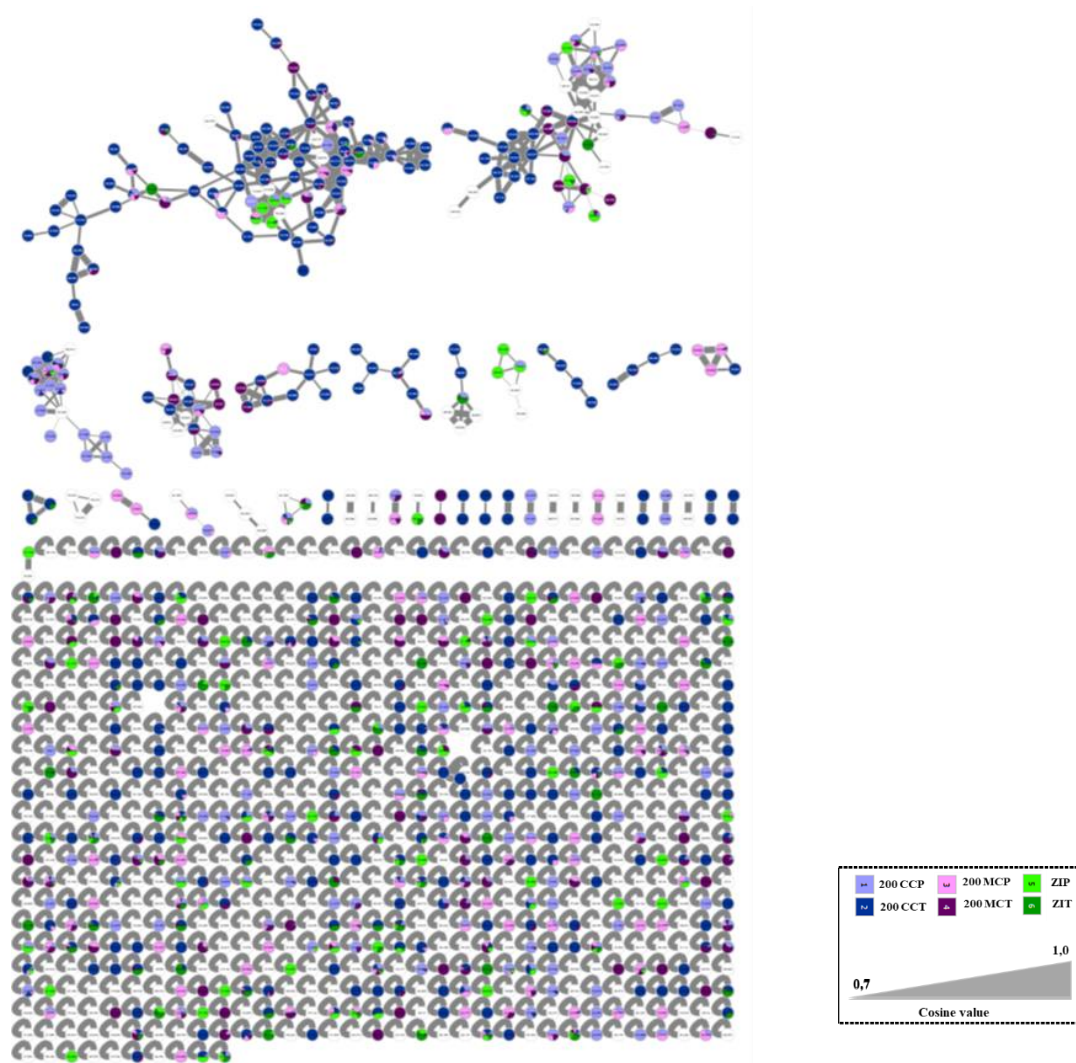


Appendix H. Representative ^1H - NMR spectra of paenipeptin C (a) and compound 28 (b) ⁶



⁶ Paenipeptin C ^1H NMR spectra was retrieved from the study of Hee Moon et al. 2017 (501)

Appendix I. Global molecular network of ethanolic extracts of *Paenibacillus* sp. PNM200-FOL59 interaction.



References.

1. Kimura S, Sinha N. Tomato (*Solanum lycopersicum*): a model fruit-bearing crop. . Cold Spring Harb Prot. 2008;3(11).
2. Costa JM, Heuvelink E. The global tomato industry. In: Heuvelink E, editor. Tomatoes, 2nd Edition. Oxfordshire, UK: CABI; 2018. p. 388.
3. Value of Agricultural Production [Internet]. 2019 [cited 05 September 2019]. Available from: <http://www.fao.org/faostat/en/#data/QC/visualize>.
4. Research&Markets. Tomato - Market Analysis, Forecast, Size, Trends and Insights. Research & Markets; 2019.
5. Alseekh S, Tohge T, Wendenberg R, Scossa F, Omranian N, Li J, et al. Identification and mode of inheritance of quantitative trait loci for secondary metabolite abundance in tomato. Plant Cell. 2015;27(3):485-512.
6. Koenig D, Jimenez-Gomez JM, Kimura S, Fulop D, Chitwood DH, Headland LR, et al. Comparative transcriptomics reveals patterns of selection in domesticated and wild tomato. Proc Natl Acad Sci U S A. 2013;110(28):E2655-62.
7. Li H, Qi M, Sun M, Liu Y, Liu Y, Xu T, et al. Tomato Transcription Factor SIWUS Plays an Important Role in Tomato Flower and Locule Development. Front Plant Sci. 2017;8:457.
8. Tomato Genome C. The tomato genome sequence provides insights into fleshy fruit evolution. Nature. 2012;485(7400):635-41.
9. Arie T, Takahashi H, Kodama M, Teraoka T. Tomato as a model plant for plant-pathogen interactions. Plant Biotechnology. 2007;24(1):135-47.
10. Husaini AM, Sakina A, Cambay SR. Host-Pathogen Interaction in *Fusarium oxysporum* Infections: Where Do We Stand? Mol Plant Microbe Interact. 2018;31(9):889-98.
11. Jashni MK, Mehrabi R, Collemare J, Mesarich CH, de Wit PJGM. The battle in the apoplast: further insights into the roles of proteases and their inhibitors in plant–pathogen interactions. 2015;6(584).
12. Takken F, Rep M. The arms race between tomato and *Fusarium oxysporum*. Mol Plant Pathol. 2010;11(2):309-14.
13. Ma LJ, Geiser DM, Proctor RH, Rooney AP, O'Donnell K, Trail F, et al. Fusarium pathogenomics. Annu Rev Microbiol. 2013;67:399-416.
14. Rampersad SN. Pathogenomics and Management of *Fusarium* Diseases in Plants. Pathogens. 2020;9(5).
15. McGovern RJ. Management of tomato diseases caused by *Fusarium oxysporum*. Crop Prot. 2015;73:78-92.

16. Nirmaladevi D, Venkataramana M, Srivastava RK, Uppalapati SR, Gupta VK, Yli-Mattila T, et al. Molecular phylogeny, pathogenicity and toxicogenicity of *Fusarium oxysporum* f. sp. *lycopersici*. *Sci Rep*. 2016;6:21367.
17. Akhter A, Hage-Ahmed K, Soja G, Steinkellner S. Potential of *Fusarium* wilt-inducing chlamydospores, in vitro behaviour in root exudates and physiology of tomato in biochar and compost amended soil. *Plant Soil*. 2016;406(1):425-40.
18. Di X, Takken FL, Tintor N. How Phytohormones Shape Interactions between Plants and the Soil-Borne Fungus *Fusarium oxysporum*. *Frontiers in plant science*. 2016;7.
19. Turra D, El Ghalid M, Rossi F, Di Pietro A. Fungal pathogen uses sex pheromone receptor for chemotropic sensing of host plant signals. *Nature*. 2015;527(7579):521-4.
20. vanderDoes HC, Constantin ME, Houterman PM, Takken FLW, Cornelissen BJC, Haring MA, et al. *Fusarium oxysporum* colonizes the stem of resistant tomato plants, the extent varying with the R-gene present. *European Journal of Plant Pathology*. 2019;154(1):55-65.
21. Raza W, Ling N, Zhang R, Huang Q, Xu Y, Shen Q. Success evaluation of the biological control of *Fusarium* wilts of cucumber, banana, and tomato since 2000 and future research strategies. *Crit Rev Biotechnol*. 2017;37(2):202-12.
22. Schreiter S, Sandmann M, Smalla K, Grosch R. Soil Type Dependent Rhizosphere Competence and Biocontrol of Two Bacterial Inoculant Strains and Their Effects on the Rhizosphere Microbial Community of Field-Grown Lettuce. *PLOS ONE*. 2014;9(8):e103726.
23. Gómez Expósito R, de Bruijn I, Postma J, Raaijmakers JM. Current insights into the role of rhizosphere bacteria in disease suppressive soils. *J Frontiers in Microbiology*. 2017;8:2529.
24. Rodríguez MA, Rothen C, Lo TE, Cabrera GM, Godeas AM. Suppressive soil against *Sclerotinia sclerotiorum* as a source of potential biocontrol agents: selection and evaluation of *Clonostachys rosea* BAFC1646. *J Biocontrol science technology*. 2015;25(12):1388-409.
25. De Carvalho CC, Fernandes P. Production of metabolites as bacterial responses to the marine environment. *J Marine drugs*. 2010;8(3):705-27.
26. Betancur LA, Forero AM, Romero-Otero A, Sepulveda LY, Moreno-Sarmiento NC, Castellanos L, et al. Cyclic tetrapeptides from the marine strain *Streptomyces* sp. PNM-161a with activity against rice and yam phytopathogens. *J Antibiot (Tokyo)*. 2019;72(10):744-51.
27. Betancur LA, Naranjo-Gaybor SJ, Vinchira-Villarraga DM, Moreno-Sarmiento NC, Maldonado LA, Suarez-Moreno ZR, et al. Marine Actinobacteria as a source of compounds for phytopathogen control: An integrative metabolic-profiling / bioactivity and taxonomical approach. *PLOS ONE*. 2017;12(2):e0170148.
28. Blunt JW, Carroll AR, Copp BR, Davis RA, Keyzers RA, Prinsep MR. Marine natural products. *Nat Prod Rep*. 2018;35(1):8-53.
29. El-Hossary EM, Cheng C, Hamed MM, El-Sayed Hamed AN, Ohlsen K, Hentschel U, et al. Antifungal potential of marine natural products. *Eur J Med Chem*. 2017;126:631-51.
30. Fudou R, Iizuka T, Sato S, Ando T, Shimba N, Yamanaka S. Haliangicin, a novel antifungal metabolite produced by a marine myxobacterium. 2. Isolation and structural elucidation. *J Antibiot (Tokyo)*. 2001;54(2):153-6.

31. Reyes-Perez JJ, Hernandez-Montiel LG, Vero S, Noa-Carrazana JC, Quiñones-Aguilar EE, Rincón-Enríquez G. Postharvest biocontrol of *Colletotrichum gloeosporioides* on mango using the marine bacterium *Stenotrophomonas rhizophila* and its possible mechanisms of action. *Journal of Food Science and Technology*. 2019;56(11):4992-9.
32. Tareq FS, Lee HS, Lee YJ, Lee JS, Shin HJ. leodoglucomide C and leodoglycolipid, New Glycolipids from a Marine-Derived Bacterium *Bacillus licheniformis* 09IDYM23. *Lipids*. 2015;50(5):513-9.
33. Tareq FS, Lee MA, Lee HS, Lee YJ, Lee JS, Hasan CM, et al. Non-cytotoxic antifungal agents: isolation and structures of gageopeptides A-D from a *Bacillus* strain 109GGC020. *J Agric Food Chem*. 2014;62(24):5565-72.
34. Hernandez Montiel LG, Zulueta Rodriguez R, Angulo C, Rueda Puente EO, Quiñonez Aguilar EE, Galicia R. Marine yeasts and bacteria as biological control agents against anthracnose on mango. *J Journal of Phytopathology*. 2017;165(11-12):833-40.
35. Ortega-Morales BO, Ortega-Morales FN, Lara-Reyna J, De la Rosa-Garcia SC, Martinez-Hernandez A, Montero MJ. Antagonism of *Bacillus* spp. isolated from marine biofilms against terrestrial phytopathogenic fungi. *Mar Biotechnol (NY)*. 2009;11(3):375-83.
36. Escudero N, Marhuenda-Egea FC, Ibanco-Cañete R, Zavala-Gonzalez EA, Lopez-Llorca LV. A metabolomic approach to study the rhizodeposition in the tritrophic interaction: tomato, *Pochonia chlamydosporia* and *Meloidogyne javanica*. *Metabolomics*. 2014;10(5):788-804.
37. Matilla MA, Ramos JL, Bakker PAHM, Doornbos R, Badri DV, Vivanco JM, et al. *Pseudomonas putida* KT2440 causes induced systemic resistance and changes in *Arabidopsis* root exudation. *Environmental Microbiology Reports*. 2010;2(3):381-8.
38. Scherling C, Ulrich K, Ewald D, Weckwerth W. A metabolic signature of the beneficial interaction of the endophyte *Paenibacillus* sp. Isolate and in vitro-grown poplar plants revealed by metabolomics. *Mol Plant Microbe In*. 2009;22(8):1032-7.
39. van de Mortel JE, de Vos RC, Dekkers E, Pineda A, Guillod L, Bouwmeester K, et al. Metabolic and transcriptomic changes induced in *Arabidopsis* by the rhizobacterium *Pseudomonas fluorescens* SS101. *Plant physiology*. 2012;pp. 112.207324.
40. Walker V, Bertrand C, Bellvert F, Moëne-Loccoz Y, Bally R, Comte G. Host plant secondary metabolite profiling shows a complex, strain-dependent response of maize to plant growth-promoting rhizobacteria of the genus *Azospirillum*. *New Phytologist*. 2011;189(2):494-506.
41. Kiely PD, Haynes JM, Higgins CH, Franks A, Mark GL, Morrissey JP, et al. Exploiting new systems-based strategies to elucidate plant-bacterial interactions in the rhizosphere. *Microbial ecology*. 2006;51(3):257-66.
42. van Dam NM, Bouwmeester HJ. Metabolomics in the Rhizosphere: Tapping into Belowground Chemical Communication. *Trends Plant Sci*. 2016;21(3):256-65.
43. Aliferis KA, Jabaji S. Deciphering plant-pathogen interactions applying metabolomics: principles and applications. *Can J Plant Pathol*. 2012;34(1):29-33.
44. Wolfender JL, Rudaz S, Choi YH, Kim HK. Plant metabolomics: from holistic data to relevant biomarkers. *Curr Med Chem*. 2013;20(8):1056-90.
45. Särkinen T, Bohs L, Olmstead RG, Knapp S. A phylogenetic framework for evolutionary study of the nightshades (*Solanaceae*): a dated 1000-tip tree. *BMC Evolutionary Biology*. 2013;13(1):214.
46. Weese TL, Bohs L. A three-gene phylogeny of the genus *Solanum* (*Solanaceae*). *Systematic Botany*. 2007;32(2):445-63.

47. Spooner DM, Anderson GJ, Jansen RK. Chloroplast DNA evidence for the interrelationships of tomatoes, potatoes, and pepinos (*Solanaceae*). *American Journal of Botany*. 1993;80(6):676-88.
48. Peralta IE, Spooner DM, Knapp S. Taxonomy of wild tomatoes and their relatives (*Solanum* sect. *Lycopersicoides*, sect. *Juglandifolia*, sect. *Lycopersicon*; *Solanaceae*). *Systematic botany monographs*. 2008;84.
49. Blanca J, Canizares J, Cordero L, Pascual L, Diez MJ, Nuez F. Variation revealed by SNP genotyping and morphology provides insight into the origin of the tomato. *PLoS One*. 2012;7(10):e48198.
50. Lin T, Zhu G, Zhang J, Xu X, Yu Q, Zheng Z, et al. Genomic analyses provide insights into the history of tomato breeding. *Nat Genet*. 2014;46(11):1220-6.
51. Razifard H, Ramos A, Della Valle AL, Bodary C, Goetz E, Manser EJ, et al. Genomic Evidence for Complex Domestication History of the Cultivated Tomato in Latin America. *Mol Biol Evol*. 2020;37(4):1118-32.
52. Peralta IE, Spooner DM. History, origin and early cultivation of tomato (*Solanaceae*). In: Razdan MK, Mattoo AK, editors. *Genetic improvement of solanaceous crops*. 2. New Hampshire, USA: Science Publishers; 2006. p. 1-27.
53. Rothan C, Diouf I, Causse M. Trait discovery and editing in tomato. *The Plant Journal*. 2019;97(1):73-90.
54. Salehi B, Sharifi-Rad R, Sharopov F, Namiesnik J, Roointan A, Kamle M, et al. Beneficial effects and potential risks of tomato consumption for human health: An overview. *Nutrition*. 2019;62:201-8.
55. Khachik F, Carvalho L, Bernstein PS, Muir GJ, Zhao D-Y, Katz NB. Chemistry, distribution, and metabolism of tomato carotenoids and their impact on human health. *J Experimental biology medicine*. 2002;227(10):845-51.
56. Friedman M. Anticarcinogenic, Cardioprotective, and Other Health Benefits of Tomato Compounds Lycopene, α -Tomatine, and Tomatidine in Pure Form and in Fresh and Processed Tomatoes. *Journal of Agricultural and Food Chemistry*. 2013;61(40):9534-50.
57. Kubatka P, Liskova A, Kello M, Mojzis J, Solar P, Solarova Z, et al. Plant-derived functional foods with chemopreventive and therapeutic potential against breast cancer: A review of the preclinical and clinical data. In: Kabir Y, editor. *Functional Foods in Cancer Prevention and Therapy*: Academic Press; 2020. p. 283-314.
58. Sant'Ana, Parrine DV, Lefsrud M. Tomato proteomics: Tomato as a model for crop proteomics. *Scientia Horticulturae*. 2018;239:224-33.
59. Moco S, Bino RJ, Vorst O, Verhoeven HA, de Groot J, van Beek TA, et al. A liquid chromatography-mass spectrometry-based metabolome database for tomato. *Plant Physiol*. 2006;141(4):1205-18.
60. Pentimone I, Colagiero M, Rosso LC, Ciancio A. Omics applications: towards a sustainable protection of tomato. *Appl Microbiol Biotechnol*. 2020;104(10):4185-95.
61. Sant'Ana DVP, Lefsrud M. Tomato proteomics: Tomato as a model for crop proteomics. *Scientia Horticulturae*. 2018;239:224-33.
62. Barone A, Chiusano ML, Ercolano MR, Giuliano G, Grandillo S, Frusciante L. Structural and functional genomics of tomato. *Int J Plant Genomics*. 2008;2008:820274.
63. Gao L, Gonda I, Sun H, Ma Q, Bao K, Tieman DM, et al. The tomato pan-genome uncovers new genes and a rare allele regulating fruit flavor. *Nat Genet*. 2019;51(6):1044-51.

64. Pesaresi P, Mizzotti C, Colombo M, Masiero S. Genetic regulation and structural changes during tomato fruit development and ripening. *Front Plant Sci.* 2014;5:124.
65. Ballester AR, Tikunov Y, Molthoff J, Grandillo S, Viquez-Zamora M, de Vos R, et al. Identification of Loci Affecting Accumulation of Secondary Metabolites in Tomato Fruit of a *Solanum lycopersicum* x *Solanum chmielewskii* Introgression Line Population. *Front Plant Sci.* 2016;7:1428.
66. Panthee DR, Chen F. Genomics of fungal disease resistance in tomato. *Curr Genomics.* 2010;11(1):30-9.
67. Hanson P, Lu S-F, Wang J-F, Chen W, Kenyon L, Tan C-W, et al. Conventional and molecular marker-assisted selection and pyramiding of genes for multiple disease resistance in tomato. *Scientia Horticulturae.* 2016;201:346-54.
68. de Toledo Thomazella DP, Brail Q, Dahlbeck D, Staskawicz B. CRISPR-Cas9 mediated mutagenesis of a DMR6 ortholog in tomato confers broad-spectrum disease resistance. *BioRxiv.* 2016:064824.
69. Prihatna C, Barbetti MJ, Barker SJ. A Novel Tomato *Fusarium* Wilt Tolerance Gene. *Front Microbiol.* 2018;9:1226.
70. Hu X, Puri KD, Gurung S, Klosterman SJ, Wallis CM, Britton M, et al. Proteome and metabolome analyses reveal differential responses in tomato -*Verticillium dahliae*-interactions. *J Proteomics.* 2019;207:103449.
71. Manzo D, Ferriello F, Puopolo G, Zoina A, D'Esposito D, Tardella L, et al. *Fusarium oxysporum* f. sp. *radicis-lycopersici* induces distinct transcriptome reprogramming in resistant and susceptible isogenic tomato lines. *BMC Plant Biology.* 2016;16(1):53.
72. Petrasch S, Silva CJ, Mesquida-Pesci SD, Gallegos K, van den Abeele C, Papin V, et al. Infection Strategies Deployed by *Botrytis cinerea*, *Fusarium acuminatum*, and *Rhizopus stolonifer* as a Function of Tomato Fruit Ripening Stage. *Front Plant Sci.* 2019;10:223.
73. Chen F, Ma R, Chen X-L. Advances of metabolomics in fungal pathogen–plant interactions. *Metabolites.* 2019;9(8):169.
74. Friedman M, Levin CE, Lee SU, Kim HJ, Lee IS, Byun JO, et al. Tomatine-containing green tomato extracts inhibit growth of human breast, colon, liver, and stomach cancer cells. *J Agric Food Chem.* 2009;57(13):5727-33.
75. Liu J, Kanetake S, Wu YH, Tam C, Cheng LW, Land KM, et al. Antiprotozoal Effects of the Tomato Tetrasaccharide Glycoalkaloid Tomatine and the Aglycone Tomatidine on Mucosal Trichomonads. *J Agric Food Chem.* 2016;64(46):8806-10.
76. Shamshiri R, Jones J, Thorp K, Ahmad D, Che Man H, Taheri S. Review of optimum temperature, humidity, and vapour pressure deficit for microclimate evaluation and control in greenhouse cultivation of tomato: A review. *International Agrophysics.* 2018;32:287-302.
77. Jones J. Instructions for growing tomatoes in the garden and green-house. SC, USA: GroSystems, Anderson; 2013.
78. Heuvelink E, Okello CO. Developmental processes. In: Heuvelink E, editor. *Tomatoes*, 2nd Edition. Oxfordshire, UK: CABI; 2018. p. 388.
79. Santos BM, Torres-Quezada EA. Irrigation and fertilization In: Heuvelink E, editor. *Tomatoes*, 2nd Edition. Oxfordshire, UK: CABI; 2018. p. 388.
80. Heuvelink E, Li T, Dorais M. Crop growth and yield. In: Heuvelink E, editor. *Tomatoes*, 2nd Edition. Oxfordshire, UK: CABI; 2018. p. 388.
81. Baudoin W, Nersisyan A, Shamilov A, Hodder A, Gutierrez D, Nicola S, et al. Good Agricultural Practices for greenhouse vegetable production in the South East European countries-Principles for sustainable intensification of smallholder farms. Duffy R, editor.

Rome, Italy: FOOD AND AGRICULTURE ORGANIZATION OF THE UNITED NATIONS; 2017.

82. Wang X, Xing Y. Evaluation of the effects of irrigation and fertilization on tomato fruit yield and quality: a principal component analysis. *Scientific Reports*. 2017;7(1):350.

83. Chen J, Kang S, Du T, Qiu R, Guo P, Chen R. Quantitative response of greenhouse tomato yield and quality to water deficit at different growth stages. *Agricultural Water Management*. 2013;129:152-62.

84. Park Y, Na MH, Cho W. Determination on environmental factors and growth factors affecting tomato yield using pattern recognition techniques. *Multimedia Tools and Applications*. 2019;78(20):28815-34.

85. Silva RS, Kumar L, Shabani F, PicanÇO MC. Assessing the impact of global warming on worldwide open field tomato cultivation through CSIRO-Mk3-0 global climate model. *The Journal of Agricultural Science*. 2017;155(3):407-20.

86. Barrientos-Fuentes JC, Torrico-Albino JC. Socio-economic perspectives of family farming in South America: cases of Bolivia, Colombia and Peru. *Agronomía Colombiana*. 2014;32(2):266-75.

87. Schneider S. Family farming in Latin America and the Caribbean: looking for new paths of rural development and food security. Brasília, Brazil: FAO; IPC-IG; 2016.

88. Ulrichs C, Fischer G, Büttner C, Mewis I. Comparison of lycopene, β -carotene and phenolic contents of tomato using conventional and ecological horticultural practices, and arbuscular mycorrhizal fungi (AMF). *Agronomía Colombiana*. 2008;26(1):40-6.

89. DANE. Encuesta Nacional Agropecuaria (ENA) 2019. In: DANE, editor. <https://www.dane.gov.co/index.php/estadisticas-por-tema/agropecuario/encuesta-nacional-agropecuaria-ena2019>. p. 31.

90. FIRA. Panorama agroalimentario. Tomate rojo 2019. In: sectorial Ddiyeey, editor. México: FIRA; 2019. p. 26.

91. Agronet. Colombian Ministry of Agriculture and Rural Development Statistics for the Agricultural Sector: AGRONET; 2010 [Available from: <http://www.agronet.gov.co>

92. Miranda D, Fischer G, Carranza C, Rodríguez M, Lanchero O, Barrientos J. Characterization of productive systems of tomato (*Solanum lycopersicum* L.) in producing zones of Colombia. *Acta Hort*. 2009;821:35-46.

93. Bojacá CR, Arias LA, Ahumada DA, Casilimas HA, Schrevens E. Evaluation of pesticide residues in open field and greenhouse tomatoes from Colombia. *Food Control*. 2013;30(2):400-3.

94. Gil R, Bojacá CR, Schrevens E. Understanding the heterogeneity of smallholder production systems in the Andean tropics – The case of Colombian tomato growers. *NJAS - Wageningen Journal of Life Sciences*. 2019;88:1-9.

95. Gil R, Bojacá C, Schrevens E. A tailor-made crop growth model for the tomato production systems in Colombia. *Agronomía Colombiana*. 2018;35:301-13.

96. Singh VK, Singh AK, Kumar A. Disease management of tomato through PGPB: current trends and future perspective. *3 Biotech*. 2017;7(4):255.

97. Gary E. Vallad, Messelink G, Smith HA. Crop protection. Pest and disease management. In: Heuvelink E, editor. *Tomatoes*, 2nd Edition. Oxfordshire, UK: CABI; 2018. p. 388.

98. Desneux N, Wajnberg E, Wyckhuys KAG, Burgio G, Arpaia S, Narváez-Vasquez CA, et al. Biological invasion of European tomato crops by *Tuta absoluta*: ecology, geographic expansion and prospects for biological control. *Journal of Pest Science*. 2010;83(3):197-215.

99. Desneux N, Luna MG, Guillemaud T, Urbaneja A. The invasive South American tomato pinworm, *Tuta absoluta*, continues to spread in Afro-Eurasia and beyond: the new threat to tomato world production. *Journal of Pest Science*. 2011;84(4):403-8.
100. Chailleux A, Desneux N, Seguret J, Do Thi Khanh H, Maignet P, Tabone E. Assessing European Egg Parasitoids as a Mean of Controlling the Invasive South American Tomato Pinworm *Tuta absoluta*. *PLOS ONE*. 2012;7(10):e48068.
101. Giorgini M, Guerrieri E, Cascone P, Gontijo L. Current strategies and future outlook for managing the Neotropical tomato pest *Tuta absoluta* (Meyrick) in the Mediterranean Basin. *Neotropical entomology*. 2019;48(1):1-17.
102. Hanssen IM, Lapidot M, Thomma BP. Emerging viral diseases of tomato crops. *Mol Plant Microbe In*. 2010;23(5):539-48.
103. Kil E-J, Kim S, Lee Y-J, Byun H-S, Park J, Seo H, et al. Tomato yellow leaf curl virus (TYLCV-IL): a seed-transmissible geminivirus in tomatoes. *Scientific Reports*. 2016;6(1):19013.
104. Shattock RC. *Phytophthora infestans*: populations, pathogenicity and phenylamides. *Pest Manag Sci*. 2002;58(9):944-50.
105. Foolad MR, Merk HL, Ashrafi H. Genetics, Genomics and Breeding of Late Blight and Early Blight Resistance in Tomato. *Critical Reviews in Plant Sciences*. 2008;27(2):75-107.
106. Nowicki M, Foolad MR, Nowakowska M, Kozik EU. Potato and Tomato Late Blight Caused by *Phytophthora infestans*: An Overview of Pathology and Resistance Breeding. *Plant Dis*. 2012;96(1):4-17.
107. Hausbeck MK, Lamour KH. *Phytophthora capsici* on vegetable crops: research progress and management challenges. *Plant disease*. 2004;88(12):1292-303.
108. Naveed ZA, Ali GS. Comparative Transcriptome Analysis between a Resistant and a Susceptible Wild Tomato Accession in Response to *Phytophthora parasitica*. *International Journal of Molecular Sciences*. 2018;19(12).
109. Jupe J, Stam R, Howden AJM, Morris JA, Zhang R, Hedley PE, et al. *Phytophthora capsici*-tomato interaction features dramatic shifts in gene expression associated with a hemi-biotrophic lifestyle. *Genome Biology*. 2013;14(6):R63.
110. CamaradecomerciodeBogotá. Manual de tomate. agroindustrial Pdaay, editor. Bogotá, Colombia: Camara de comercio de Bogotá; 2015. 56 p.
111. Montenegro I, Madrid A, Cuellar M, Seeger M, Alfaro JF, Besoain X, et al. Biopesticide Activity from Drimanic Compounds to Control Tomato Pathogens. *Molecules*. 2018;23(8).
112. Bawa I. Management strategies of *Fusarium* wilt disease of tomato incited by *Fusarium oxysporum* f. sp. *lycopersici*(Sacc.) A Review. *Int J Adv Acad Res*. 2016;2(5).
113. Apodaca-Sánchez MA, Zavaleta ME, Osada KS, García ER. Hospedantes asintomáticos de *Fusarium oxysporum* Schlechtend. f. sp. *radicis-lycopersici* WR Jarvis y Shoemaker en Sinaloa, México. . *Rev Mex Fitopatol*. 2004;22(1):7-13.
114. Enespa, Dwivedi SK. Effectiveness of some antagonistic fungi and botanicals against *Fusarium solani* and *Fusarium oxysporum* f. sp. *lycopersici* infecting brinjal and tomato plants. *Asian J Plant Pathol*. 2014;8(1):18-25.
115. Carmona SL, Burbano-David D, Gómez MR, Lopez W, Ceballos N, Castaño-Zapata J, et al. Characterization of Pathogenic and Nonpathogenic *Fusarium oxysporum* Isolates Associated with Commercial Tomato Crops in the Andean Region of Colombia. *Pathogens*. 2020;9(1).

116. Singh VK, Singh HB, Upadhyay RS. Role of fusaric acid in the development of 'Fusarium wilt' symptoms in tomato: Physiological, biochemical and proteomic perspectives. *Plant Physiology and Biochemistry*. 2017;118:320-32.
117. Srinivas C, Nirmala Devi D, Narasimha Murthy K, Mohan CD, Lakshmeesha TR, Singh B, et al. *Fusarium oxysporum* f. sp. *lycopersici* causal agent of vascular wilt disease of tomato: Biology to diversity– A review. *Saudi Journal of Biological Sciences*. 2019;26(7):1315-24.
118. Suga H, Hyakumachi M. Genomics of Phytopathogenic *Fusarium*. *Applied Mycology and Biotechnology*. 2004;4:161-89.
119. Watanabe M, Yonezawa T, Lee K-i, Kumagai S, Sugita-Konishi Y, Goto K, et al. Molecular phylogeny of the higher and lower taxonomy of the *Fusarium* genus and differences in the evolutionary histories of multiple genes. *BMC evolutionary biology*. 2011;11:322-.
120. Edel-Hermann V, Lecomte C. Current Status of *Fusarium oxysporum* Formae Speciales and Races. *Phytopathology*. 2019;109(4):512-30.
121. Biju VC, Fokkens L, Houterman PM, Rep M, Cornelissen BJC. Multiple Evolutionary Trajectories Have Led to the Emergence of Races in *Fusarium oxysporum* f. sp. *lycopersici*. *Appl Environ Microbiol*. 2017;83(4).
122. Gonçalves A, Costa H, Fonseca M, Boiteux L, Lopes C, Reis A, editors. Variability and geographical distribution of *Fusarium oxysporum* f. sp. *lycopersici* physiological races and field performance of resistant sources in Brazil. V International Symposium on Tomato Diseases: Perspectives and Future Directions in Tomato Protection 1207; 2016.
123. Sepúlveda-Chavera G, Huanca W, Salvatierra-Martínez R, Latorre BA. First Report of *Fusarium oxysporum* f. sp. *lycopersici* Race 3 and *F. oxysporum* f. sp. *radicis-lycopersici* in Tomatoes in the Azapa Valley of Chile. *Plant Disease*. 2014;98(10):1432-.
124. Reis A, Costa H, Boiteux LS, Lopes CA. First report of *Fusarium oxysporum* f. sp. *lycopersici* race 3 on tomato in Brazil. *Fitopatologia Brasileira*. 2005;30(4):426-8.
125. de Sain M, Rep M. The Role of Pathogen-Secreted Proteins in Fungal Vascular Wilt Diseases. *Int J Mol Sci*. 2015;16(10):23970-93.
126. Di XT, Takken FLW, Tintor N. How Phytohormones Shape Interactions between Plants and the Soil-Borne Fungus *Fusarium oxysporum*. *Frontiers in Plant Science*. 2016;7.
127. Gordon TR. *Fusarium oxysporum* and the *Fusarium* Wilt Syndrome. *Annu Rev Phytopathol*. 2017;55:23-39.
128. Pietro AD, Madrid MP, Caracuel Z, Delgado-Jarana J, Roncero MI. *Fusarium oxysporum*: exploring the molecular arsenal of a vascular wilt fungus. *Mol Plant Pathol*. 2003;4(5):315-25.
129. Agrios GN. chapter eleven - PLANT DISEASES CAUSED BY FUNGI. In: Agrios GN, editor. *Plant Pathology (Fifth Edition)*. San Diego: Academic Press; 2005. p. 385-614.
130. Bravo Ruiz G, Di Pietro A, Roncero MI. Combined action of the major secreted exo- and endopolygalacturonases is required for full virulence of *Fusarium oxysporum*. *Mol Plant Pathol*. 2016;17(3):339-53.
131. Ito S, Eto T, Tanaka S, Yamauchi N, Takahara H, Ikeda T. Tomatidine and lycotetraose, hydrolysis products of alpha-tomatine by *Fusarium oxysporum* tomatinase, suppress induced defense responses in tomato cells. *FEBS Lett*. 2004;571(1-3):31-4.
132. Ito S, Kawaguchi T, Nagata A, Tamura H, Matsushita H, Takahara H, et al. Distribution of the FoTomI gene encoding tomatinase in formae speciales of *Fusarium oxysporum* and identification of a novel tomatinase from *F. oxysporum* f. sp. *radicis-*

- lycopersici*, the causal agent of *Fusarium* crown and root rot of tomato. Journal of General Plant Pathology. 2004;70(4):195-201.
133. Kang S, Demers J, Jimenez-Gasco MdM, Rep M. *Fusarium oxysporum*. In: Dean RA, Kole C, Lichens-Park A, editors. Genomics of Plant-Associated Fungi and Oomycetes: Dicot Pathogens. Berlin Heidelberg: Springer-Verlag; 2014. p. 244.
134. Katan T, Shlevin E, Katan J. Sporulation of *Fusarium oxysporum* f. sp. *lycopersici* on Stem Surfaces of Tomato Plants and Aerial Dissemination of Inoculum. Phytopathology. 1997;87(7):712-9.
135. Gale LR, Katan T, Kistler HC. The Probable Center of Origin of *Fusarium oxysporum* f. sp. *lycopersici* VCG 0033. Plant Dis. 2003;87(12):1433-8.
136. Gonzalez-Cendales Y, Catanzariti AM, Baker B, McGrath DJ, Jones DA. Identification of I-7 expands the repertoire of genes for resistance to *Fusarium* wilt in tomato to three resistance gene classes. Mol Plant Pathol. 2016;17(3):448-63.
137. Mata-Nicolás E, Montero-Pau J, Gimeno-Paez E, Garcia-Carpintero V, Ziarsolo P, Menda N, et al. Exploiting the diversity of tomato: the development of a phenotypically and genetically detailed germplasm collection. Horticulture Research. 2020;7(1):66.
138. El Mohtar CA, Atamian HS, Dagher RB, Abou-Jawdah Y, Salus MS, Maxwell DP. Marker-Assisted Selection of Tomato Genotypes with the I-2 Gene for Resistance to *Fusarium oxysporum* f. sp. *lycopersici* Race 2. Plant Dis. 2007;91(6):758-62.
139. Segal G, Sarfatti M, Schaffer MA, Ori N, Zamir D, Fluhr R. Correlation of genetic and physical structure in the region surrounding the I2 *Fusarium oxysporum* resistance locus in tomato. Molecular and General Genetics MGG. 1992;231(2):179-85.
140. Bournival BL, Vallejos CE, Scott JW. Genetic analysis of resistances to races 1 and 2 of *Fusarium oxysporum* f. sp. *lycopersici* from the wild tomato *Lycopersicon pennellii*. Theoretical and Applied Genetics. 1990;79(5):641-5.
141. Mandal S, Mallick N, Mitra A. Salicylic acid-induced resistance to *Fusarium oxysporum* f. sp. *lycopersici* in tomato. Plant Physiol Biochem. 2009;47(7):642-9.
142. Benhamou N, Lafontaine P, Nicole M. Induction of systemic resistance to *Fusarium* crown and root rot in tomato plants by seed treatment with chitosan. Phytopathology. 1994;84(12):1432-44.
143. Elmer WH, White JC. The use of metallic oxide nanoparticles to enhance growth of tomatoes and eggplants in disease infested soil or soilless medium. Environmental Science: Nano. 2016;3(5):1072-9.
144. Kumar A, Biswas S. Biochemical evidences of induced resistance in tomato plant against *Fusarium* with through inorganic chemicals. Journal of Mycopathological Research. 2010;48(2):213-9.
145. Chakraborty N, Chandra S, Acharya K. Biochemical basis of improvement of defense in tomato plant against *Fusarium* wilt by CaCl₂. Physiology and Molecular Biology of Plants. 2017;23(3):581-96.
146. Song W, Zhou L, Yang C, Cao X, Zhang L, Liu X. Tomato *Fusarium* wilt and its chemical control strategies in a hydroponic system. Crop Prot. 2004;23(3):243-7.
147. Chen C, Wang J, Luo Q, Yuan S, Zhou M. Characterization and fitness of carbendazim-resistant strains of *Fusarium graminearum* (wheat scab). Pest Manag Sci. 2007;63(12):1201-7.
148. Liu S, Fu L, Wang S, Chen J, Jiang J, Che Z, et al. Carbendazim Resistance of *Fusarium graminearum* From Henan Wheat. Plant Dis. 2019:PDIS02190391RE.
149. Yin Y, Liu X, Li B, Ma Z. Characterization of sterol demethylation inhibitor-resistant isolates of *Fusarium asiaticum* and *F. graminearum* collected from wheat in China. Phytopathology. 2009;99(5):487-97.

150. Amini J, Sidovich D. The effects of fungicides on *Fusarium oxysporum* f. sp. *lycopersici* associated with Fusarium wilt of tomato. J Plant Prot Res. 2010;50(2):172-8.
151. Shoaib A, Dliferoze A, Khan A, Khurshid S, Akhtar S. Effect of Fungicides on the Morphology, Physiology and Biochemistry of Tomato Seedlings Infected with *Fusarium oxysporum* f. sp. *lycopersici*. Philipp Agric Sci. 2014;97(4):416-21.
152. Arias LA, Bojacá CR, Ahumada DA, Schrevens E. Monitoring of pesticide residues in tomato marketed in Bogota, Colombia. Food Control. 2014;35(1):213-7.
153. Bonanomi G, Antignani V, Pane C, Scala F. Suppression of soilborne fungal diseases with organic amendments. Journal of Plant Pathology. 2007;89(3):311-24.
154. Stevens C, Khan VA, Rodriguez-Kabana R, Ploper LD, Backman PA, Collins DJ, et al. Integration of soil solarization with chemical, biological and cultural control for the management of soilborne diseases of vegetables. Plant Soil. 2003;253(2):493-506.
155. Barakat RM, Al-Masri MI. Enhanced Soil Solarization against *Fusarium oxysporum* f. sp. *lycopersici* in the Uplands. International Journal of Agronomy. 2012;2012:368654.
156. Yücel S, Ozarlandan A, Colak A, Ay T. Methyl bromide alternatives for controlling *Fusarium* wilt and root knot nematodes in tomatoes in Turkey. Acta Horticulturae. 2009;808:381-6.
157. Xie H, Yan D, Mao L, Wang Q, Li Y, Ouyang C, et al. Evaluation of methyl bromide alternatives efficacy against soil-borne pathogens, nematodes and soil microbial community. PloS one. 2015;10(2):e0117980-e.
158. Roskopf EN, Chellemi DO, Kokalis-Burelle N, Church GT. Alternatives to methyl bromide: A Florida perspective. Plant Health Progress. 2005;6(1):19.
159. Ioannou N. Soil solarization as a substitute for methyl bromide fumigation in greenhouse tomato production in Cyprus. Phytoparasitica. 2000;28(3):248-56.
160. Paudel BR, Di Gioia F, Zhao X, Ozores-Hampton M, Hong JC, Kokalis-Burelle N, et al. Evaluating anaerobic soil disinfestation and other biological soil management strategies for open-field tomato production in Florida. Renewable Agriculture and Food Systems. 2020;35(3):274-85.
161. Ajilogba C, Babalola O. Integrated Management Strategies for Tomato Fusarium Wilt. Biocontrol science. 2013;18:117-27.
162. Cary LR, Frank JL. Grafting to Manage Soilborne Diseases in Heirloom Tomato Production. HortScience horts. 2008;43(7):2104-11.
163. Syed Ab Rahman SF, Singh E, Pieterse CMJ, Schenk PM. Emerging microbial biocontrol strategies for plant pathogens. Plant Sci. 2018;267:102-11.
164. Cha J-Y, Han S, Hong H-J, Cho H, Kim D, Kwon Y, et al. Microbial and biochemical basis of a *Fusarium* wilt-suppressive soil. The ISME Journal. 2016;10(1):119-29.
165. Köhl J, Kolnaar R, Ravensberg WJ. Mode of Action of Microbial Biological Control Agents Against Plant Diseases: Relevance Beyond Efficacy. 2019;10(845).
166. Orozco-Mosqueda MdC, Rocha-Granados MdC, Glick BR, Santoyo G. Microbiome engineering to improve biocontrol and plant growth-promoting mechanisms. Microbiological Research. 2018;208:25-31.
167. Wallenstein MD. Managing and manipulating the rhizosphere microbiome for plant health: A systems approach. Rhizosphere. 2017;3:230-2.
168. Koch E, Ole Becker J, Berg G, Hauschild R, Jehle J, Köhl J, et al. Biocontrol of plant diseases is not an unsafe technology! Journal of Plant Diseases and Protection. 2018;125(2):121-5.
169. Heimpel GE, Mills NJ. Biological control: Cambridge University Press; 2017.

170. Fravel D. Commercialization and implementation of biocontrol. *Annu Rev Phytopathol.* 2005;43:337-59.
171. Brodeur J, Abram PK, Heimpel GE, Messing RH. Trends in biological control: public interest, international networking and research direction. *BioControl.* 2018;63(1):11-26.
172. Köhl J, Postma J, Nicot P, Ruocco M, Blum B. Stepwise screening of microorganisms for commercial use in biological control of plant-pathogenic fungi and bacteria. *Biol Control.* 2011;57(1):1-12.
173. Gardener BBM, Fravel DRJPHP. Biological control of plant pathogens: research, commercialization, and application in the USA. 2002;3(1):17.
174. El-Mohamedy RSR. Efficiency of different application methods of biocontrol agents and biocides in control of *Fusarium* root rot on some citrus rootstocks. *Archives of Phytopathology Plant Protection.* 2009;42(9):819-28.
175. Hinarejos E, Castellano M, Rodrigo I, Bellés JM, Conejero V, López-Gresa MP, et al. *Bacillus subtilis* IAB/BS03 as a potential biological control agent. *European Journal of Plant Pathology.* 2016;146(3):597-608.
176. Jang Y, Kim SG, Kim YH. Biocontrol efficacies of *Bacillus* species against *Cylindrocarpum destructans* causing ginseng root rot. *Plant Pathol J.* 2011;27(333):e41.
177. Wei Z, Huang J, Yang T, Jousset A, Xu Y, Shen Q, et al. Seasonal variation in the biocontrol efficiency of bacterial wilt is driven by temperature-mediated changes in bacterial competitive interactions. *J Appl Ecol.* 2017;54(5):1440-8.
178. Jacobsen BJ, Zidack NK, Larson BJ. The Role of *Bacillus*-Based Biological Control Agents in Integrated Pest Management Systems: Plant Diseases. *Phytopathology®.* 2004;94(11):1272-5.
179. Schisler DA, Slininger PJ, Behle RW, Jackson MA. Formulation of *Bacillus* spp. for Biological Control of Plant Diseases. *Phytopathology®.* 2004;94(11):1267-71.
180. Fira D, Dimkić I, Berić T, Lozo J, Stanković S. Biological control of plant pathogens by *Bacillus* species. *Journal of Biotechnology.* 2018;285:44-55.
181. Rybakova D, Cernava T, Köberl M, Liebminger S, Etemadi M, Berg G. Endophytes-assisted biocontrol: novel insights in ecology and the mode of action of *Paenibacillus*. *Plant Soil.* 2016;405(1):125-40.
182. Grady EN, MacDonald J, Liu L, Richman A, Yuan ZC. Current knowledge and perspectives of *Paenibacillus*: a review. *Microb Cell Fact.* 2016;15(1):203.
183. Law JW-F, Ser H-L, Khan TM, Chuah L-H, Pusparajah P, Chan K-G, et al. The Potential of *Streptomyces* as Biocontrol Agents against the Rice Blast Fungus, *Magnaporthe oryzae* (*Pyricularia oryzae*). 2017;8(3).
184. Schrey SD, Tarkka MT. Friends and foes: *Streptomyces* as modulators of plant disease and symbiosis. *Antonie van Leeuwenhoek.* 2008;94(1):11-9.
185. Panpatte DG, Jhala YK, Shelat HN, Vyas RV. *Pseudomonas fluorescens*: a promising biocontrol agent and PGPR for sustainable agriculture. *Microbial inoculants in sustainable agricultural productivity*: Springer; 2016. p. 257-70.
186. Mark GL, Morrissey JP, Higgins P, O'Gara F. Molecular-based strategies to exploit *Pseudomonas* biocontrol strains for environmental biotechnology applications. *FEMS Microbiology Ecology.* 2006;56(2):167-77.
187. Verma M, Brar SK, Tyagi RD, Surampalli RY, Valéro JR. Antagonistic fungi, *Trichoderma* spp.: Panoply of biological control. *Biochemical Engineering Journal.* 2007;37(1):1-20.
188. Sharma A. Fungi as Biological Control Agents. In: Giri B, Prasad R, Wu Q, Varma A, editors. *Biofertilizers for Sustainable Agriculture and Environment*: Springer; 2019. p. 395-411.

189. Datnoff LE, Nemeš S, Pernezny K. Biological Control of *Fusarium* Crown and Root Rot of Tomato in Florida Using *Trichoderma harzianum* and *Glomus intraradices*. *Biol Control*. 1995;5(3):427-31.
190. Omar I, O'Neill TM, Rossall S. Biological control of *Fusarium* crown and root rot of tomato with antagonistic bacteria and integrated control when combined with the fungicide carbendazim. *Plant Pathol*. 2006;55(1):92-9.
191. Fravel DR, Deahl KL, Stommel JR. Compatibility of the biocontrol fungus *Fusarium oxysporum* strain CS-20 with selected fungicides. *Biol Control*. 2005;34(2):165-9.
192. Someya N, Tsuchiya K, Yoshida T, Noguchi MT, Sawada H. Combined use of the biocontrol bacterium *Pseudomonas fluorescens* strain LRB3W1 with reduced fungicide application for the control of tomato *Fusarium* wilt. *Biocontrol science*. 2006;11(2):75-80.
193. Minuto A, Spadaro D, Garibaldi A, Gullino ML. Control of soilborne pathogens of tomato using a commercial formulation of *Streptomyces griseoviridis* and solarization. *Crop Prot*. 2006;25(5):468-75.
194. Jayaraj J, Radhakrishnan NV. Enhanced activity of introduced biocontrol agents in solarized soils and its implications on the integrated control of tomato damping-off caused by *Pythium* spp. *Plant Soil*. 2008;304(1):189-97.
195. Spadaro D, Gullino ML. Improving the efficacy of biocontrol agents against soilborne pathogens. *Crop Prot*. 2005;24(7):601-13.
196. Dukare AS, Prasanna R, Chandra Dubey S, Nain L, Chaudhary V, Singh R, et al. Evaluating novel microbe amended composts as biocontrol agents in tomato. *Crop Prot*. 2011;30(4):436-42.
197. Ji P, Wilson M. Enhancement of Population Size of a Biological Control Agent and Efficacy in Control of Bacterial Speck of Tomato through Salicylate and Ammonium Sulfate Amendments. *Applied and Environmental Microbiology*. 2003;69(2):1290.
198. Arseneault T, Filion M. Biocontrol through antibiosis: exploring the role played by subinhibitory concentrations of antibiotics in soil and their impact on plant pathogens. *Canadian Journal of Plant Pathology*. 2017;39(3):267-74.
199. Nguvo KJ, Gao X. Weapons hidden underneath: bio-control agents and their potentials to activate plant induced systemic resistance in controlling crop *Fusarium* diseases. *Journal of Plant Diseases and Protection*. 2019;126(3):177-90.
200. Bakker PAHM, Ran LX, Pieterse CMJ, van Loon LC. Understanding the involvement of rhizobacteria-mediated induction of systemic resistance in biocontrol of plant diseases. *Canadian Journal of Plant Pathology*. 2003;25(1):5-9.
201. Bais HP, Fall R, Vivanco JM. Biocontrol of *Bacillus subtilis* against Infection of Arabidopsis Roots by *Pseudomonas syringae* is Facilitated by Biofilm Formation and Surfactin Production. *Plant Physiology*. 2004;134(1):307.
202. Segarra G, Casanova E, Avilés M, Trillas I. *Trichoderma asperellum* strain T34 controls *Fusarium* wilt disease in tomato plants in soilless culture through competition for iron. *Microbial ecology*. 2010;59(1):141-9.
203. Bardin M, Ajouz S, Comby M, Lopez-Ferber M, Graillet B, Siegwart M, et al. Is the efficacy of biological control against plant diseases likely to be more durable than that of chemical pesticides? *Front Plant Sci*. 2015;6(566).
204. Liu P, Luo L, Long C-a. Characterization of competition for nutrients in the biocontrol of *Penicillium italicum* by *Kloeckera apiculata*. *Biol Control*. 2013;67(2):157-62.
205. Elad Y, Chet I. Possible role of competition for nutrients in biocontrol of *Pythium* damping-off by bacteria. *Phytopathology*. 1987;77(2):190-5.

206. Vero S, Mondino P, Burgueño J, Soubes M, Wisniewski M. Characterization of biocontrol activity of two yeast strains from Uruguay against blue mold of apple. *Postharvest Biology and Technology*. 2002;26(1):91-8.
207. Bencheqroun SK, Bajji M, Massart S, Labhilili M, Jaafari SE, Jijakli MH. In vitro and in situ study of postharvest apple blue mold biocontrol by *Aureobasidium pullulans*: Evidence for the involvement of competition for nutrients. *Postharvest Biology and Technology*. 2007;46(2):128-35.
208. Sayyed R, Chincholkar S, Reddy M, Gangurde N, Patel P. Siderophore producing PGPR for crop nutrition and phytopathogen suppression. In: D. M, editor. *Bacteria in Agrobiology: Disease Management*. Berlin, Heidelberg: Springer; 2013. p. 449-71.
209. Moretti M, Gilardi G, Gullino ML, Garibaldi A. Biological control potential of *Achromobacter xylosoxydans* for suppressing *Fusarium* wilt of tomato. *J Int J Bot*. 2008;4(4):369-75.
210. Goudjal Y, Zamoum M, Sabaou N, Mathieu F, Zitouni A. Potential of endophytic *Streptomyces* spp. for biocontrol of *Fusarium* root rot disease and growth promotion of tomato seedlings. *Biocontrol Science and Technology*. 2016;26(12):1691-705.
211. Dhoub H, Zouari I, Ben Abdallah D, Belbahri L, Taktak W, Triki MA, et al. Potential of a novel endophytic *Bacillus velezensis* in tomato growth promotion and protection against *Verticillium* wilt disease. *Biol Control*. 2019;139:104092.
212. Rojas-Rojas FU, Salazar-Gómez A, Vargas-Díaz ME, Vásquez-Murrieta MS, Hirsch AM, De Mot R, et al. Broad-spectrum antimicrobial activity by *Burkholderia cenocepacia* TAtl-371, a strain isolated from the tomato rhizosphere. 2018;164(9):1072-86.
213. Gautam S, Chauhan A, Sharma R, Sehgal R, Shirkot CK. Potential of *Bacillus amyloliquefaciens* for biocontrol of bacterial canker of tomato incited by *Clavibacter michiganensis* ssp. *michiganensis*. *Microbial Pathogenesis*. 2019;130:196-203.
214. Pandin C, Le Coq D, Canette A, Aymerich S, Briandet R. Should the biofilm mode of life be taken into consideration for microbial biocontrol agents? *Microbial Biotechnology*. 2017;10(4):719-34.
215. Haggag WM, Timmusk S. Colonization of peanut roots by biofilm-forming *Paenibacillus polymyxa* initiates biocontrol against crown rot disease. *J Appl Microbiol*. 2008;104(4):961-9.
216. Di Francesco A, Ugolini L, D'Aquino S, Pagnotta E, Mari M. Biocontrol of *Monilinia laxa* by *Aureobasidium pullulans* strains: Insights on competition for nutrients and space. *International Journal of Food Microbiology*. 2017;248:32-8.
217. Tan S, Gu Y, Yang C, Dong Y, Mei X, Shen Q, et al. *Bacillus amyloliquefaciens* T-5 may prevent *Ralstonia solanacearum* infection through competitive exclusion. *Biology Fertility of Soils*. 2016;52(3):341-51.
218. Defoirdt T, Boon N, Bossier P. Can Bacteria Evolve Resistance to Quorum Sensing Disruption? *PLOS Pathogens*. 2010;6(7):e1000989.
219. Rodríguez M, Torres M, Blanco L, Béjar V, Sampedro I, Llamas I. Plant growth-promoting activity and quorum quenching-mediated biocontrol of bacterial phytopathogens by *Pseudomonas segetis* strain P6. *Scientific Reports*. 2020;10(1):4121.
220. Fetzner S. Quorum quenching enzymes. *Journal of biotechnology*. 2015;201:2-14.
221. Gutiérrez-Pacheco MM, Bernal-Mercado AT, Vázquez-Armenta FJ, Martínez-Tellez MA, González-Aguilar GA, Lizardi-Mendoza J, et al. Quorum sensing interruption as a tool to control virulence of plant pathogenic bacteria. *Physiological and Molecular Plant Pathology*. 2019;106:281-91.
222. von Bodman SB, Bauer WD, Coplin DL. Quorum sensing in plant-pathogenic bacteria. *Annual review of phytopathology*. 2003;41(1):455-82.

223. Helman Y, Chernin L. Silencing the mob: disrupting quorum sensing as a means to fight plant disease. *Mol Plant Pathol*. 2015;16(3):316-29.
224. Katoch S, Kumari N, Salwan R, Sharma V, Sharma PN. Recent developments in social network disruption approaches to manage bacterial plant diseases. *Biol Control*. 2020;150:104376.
225. Kumar Jayanna S, Umesha S. Quorum quenching activity of rhizosphere bacteria against *Ralstonia solanacearum*. *Rhizosphere*. 2017;4:22-4.
226. Fan X, Ye T, Li Q, Bhatt P, Zhang L, Chen S. Potential of a Quorum Quenching Bacteria Isolate *Ochrobactrum intermedium* D-2 Against Soft Rot Pathogen *Pectobacterium carotovorum* subsp. *carotovorum*. *Front Microbiol*. 2020;11(898).
227. Pieterse CMJ, Zamioudis C, Berendsen RL, Weller DM, Van Wees SCM, Bakker PAHM. Induced Systemic Resistance by Beneficial Microbes. *Annual Review of Phytopathology*. 2014;52(1):347-75.
228. Takahashi H, Nakaho K, Ishihara T, Ando S, Wada T, Kanayama Y, et al. Transcriptional profile of tomato roots exhibiting *Bacillus thuringiensis*-induced resistance to *Ralstonia solanacearum*. *Plant Cell Reports*. 2014;33(1):99-110.
229. Nawrocka J, Małolepsza U. Diversity in plant systemic resistance induced by *Trichoderma*. *Biol Control*. 2013;67(2):149-56.
230. Fatima S, Anjum T. Identification of a Potential ISR Determinant from *Pseudomonas aeruginosa* PM12 against *Fusarium* Wilt in Tomato. *Front Plant Sci*. 2017;8(848).
231. Choudhary DK, Johri BN. Interactions of *Bacillus* spp. and plants – With special reference to induced systemic resistance (ISR). *Microbiological Research*. 2009;164(5):493-513.
232. Couillerot O, Prigent-Combaret C, Caballero-Mellado J, Moëgne-Loccoz Y. *Pseudomonas fluorescens* and closely-related fluorescent pseudomonads as biocontrol agents of soil-borne phytopathogens. *Letters in Applied Microbiology*. 2009;48(5):505-12.
233. Takishita Y, Charron J-B, Smith DLJFim. Biocontrol rhizobacterium *Pseudomonas* sp. 23S induces systemic resistance in tomato (*Solanum lycopersicum* L.) against bacterial canker *Clavibacter michiganensis* subsp. *michiganensis*. 2018;9:2119.
234. Benítez T, Rincón AM, Limón MC, Codon AC. Biocontrol mechanisms of *Trichoderma* strains. *International microbiology*. 2004;7(4):249-60.
235. Omann M, Zeilinger S. How a Mycoparasite Employs G-Protein Signaling: Using the Example of *Trichoderma*. *Journal of Signal Transduction*. 2010;2010:123126.
236. Monteiro VN, do Nascimento Silva R, Steindorff AS, Costa FT, Noronha EF, Ricart CAO, et al. New insights in *Trichoderma harzianum* antagonism of fungal plant pathogens by secreted protein analysis. *Current microbiology*. 2010;61(4):298-305.
237. Steindorff AS, Ramada MHS, Coelho ASG, Miller RNG, Pappas GJ, Jr., Ulhoa CJ, et al. Identification of mycoparasitism-related genes against the phytopathogen *Sclerotinia sclerotiorum* through transcriptome and expression profile analysis in *Trichoderma harzianum*. *BMC Genomics*. 2014;15:204-.
238. Ojha S, Chatterjee NC. Mycoparasitism of *Trichoderma* spp. in biocontrol of fusarial wilt of tomato. *Archives of Phytopathology and Plant Protection*. 2011;44(8):771-82.
239. El Komy MH, Saleh AA, Eranthodi A, Molan YY. Characterization of Novel *Trichoderma asperellum* Isolates to Select Effective Biocontrol Agents Against Tomato *Fusarium* Wilt. *Plant Pathol J*. 2015;31(1):50-60.
240. Iida Y, Ikeda K, Sakai H, Nakagawa H, Nishi O, Higashi Y. Evaluation of the potential biocontrol activity of *Dicyma pulvinata* against *Cladosporium fulvum*, the causal agent of tomato leaf mould. *Plant Pathol*. 2018;67(9):1883-90.

241. Raaijmakers JM, Vlami M, de Souza JT. Antibiotic production by bacterial biocontrol agents. *Antonie van Leeuwenhoek*. 2002;81(1):537.
242. Thomashow L, Bonsall R, Weller D. Antibiotic production by soil and rhizosphere microbes in situ. In: Hurst C, Knudsen G, McInerney M, Stetzenbach L, Walter M, editors. *Manual of Environmental Microbiology*. Washington, DC: ASM Press; 1997. p. 493–99.
243. Raaijmakers JM, Mazzola M. Diversity and natural functions of antibiotics produced by beneficial and plant pathogenic bacteria. *Annu Rev Phytopathol*. 2012;50:403-24.
244. Okada BK, Seyedsayamdost MR. Antibiotic dialogues: induction of silent biosynthetic gene clusters by exogenous small molecules. *FEMS Microbiol Rev*. 2017;41(1):19-33.
245. Pishchany G, Kolter R. On the possible ecological roles of antimicrobials. *Molecular Microbiology*. 2020;113(3):580-7.
246. Cochrane SA, Vederas JC. Lipopeptides from *Bacillus* and *Paenibacillus* spp.: A Gold Mine of Antibiotic Candidates. *Medicinal Research Reviews*. 2016;36(1):4-31.
247. Mavrodi DV, Blankenfeldt W, Thomashow LS. Phenazine compounds in fluorescent *Pseudomonas* spp. biosynthesis and regulation. *Annu Rev Phytopathol*. 2006;44:417-45.
248. Fickers P. Antibiotic compounds from *Bacillus*: why are they so amazing. *American Journal of Biochemistry Biotechnology*. 2012(8):38-43.
249. Chater KF. *Streptomyces* inside-out: a new perspective on the bacteria that provide us with antibiotics. *Philos Trans R Soc Lond B Biol Sci*. 2006;361(1469):761-8.
250. Danaei M, Baghizadeh A, Pourseyedi S, Amini J, Yaghoobi MM. Biological control of plant fungal diseases using volatile substances of *Streptomyces griseus*. *Eur J Exp Biol*. 2014;4(1):334-9.
251. Deryabin DG, Inchagova KS. Inhibitory effect of aminoglycosides and tetracyclines on quorum sensing in *Chromobacterium violaceum*. *Microbiology*. 2018;87(1):1-8.
252. Olivain C, Humbert C, Nahalkova J, Fatehi J, L'Haridon F, Alabouvette C. Colonization of tomato root by pathogenic and nonpathogenic *Fusarium oxysporum* strains inoculated together and separately into the soil. *Appl Environ Microbiol*. 2006;72(2):1523-31.
253. Aimé S, Alabouvette C, Steinberg C, Olivain C. The Endophytic Strain *Fusarium oxysporum* Fo47: A Good Candidate for Priming the Defense Responses in Tomato Roots. *Molecular Plant-Microbe Interactions*. 2013;26(8):918-26.
254. Constantin ME, de Lamo FJ, Vlieger BV, Rep M, Takken FLW. Endophyte-Mediated Resistance in Tomato to *Fusarium oxysporum* Is Independent of ET, JA, and SA. 2019;10(979).
255. Shcherbakova LA, Odintsova TI, Stakheev AA, Fravel DR, Zavriev SK. Identification of a Novel Small Cysteine-Rich Protein in the Fraction from the Biocontrol *Fusarium oxysporum* Strain CS-20 that Mitigates *Fusarium* Wilt Symptoms and Triggers Defense Responses in Tomato. *Front Plant Sci*. 2016;6(1207).
256. Singh P, Singh J, Ray S, Rajput RS, Vaishnav A, Singh RK, et al. Seed biopriming with antagonistic microbes and ascorbic acid induce resistance in tomato against *Fusarium* wilt. *Microbiological Research*. 2020;237:126482.
257. Jangir M, Pathak R, Sharma S, Sharma S. Biocontrol mechanisms of *Bacillus* sp., isolated from tomato rhizosphere, against *Fusarium oxysporum* f. sp. *lycopersici*. *Biol Control*. 2018;123:60-70.
258. Patel S, Saraf M. Interaction of root colonizing biocontrol agents demonstrates the antagonistic effect against *Fusarium oxysporum* f. sp. *lycopersici* on tomato. *European Journal of Plant Pathology*. 2017;149(2):425-33.

259. Wan T, Zhao H, Wang W. Effects of the biocontrol agent *Bacillus amyloliquefaciens* SN16-1 on the rhizosphere bacterial community and growth of tomato. *Journal of Phytopathology*. 2018;166(5):324-32.
260. Elanchezhiyan K, Keerthana U, Nagendran K, Prabhukarthikeyan SR, Prabakar K, Raguchander T, et al. Multifaceted benefits of *Bacillus amyloliquefaciens* strain FBZ24 in the management of wilt disease in tomato caused by *Fusarium oxysporum* f. sp. *lycopersici*. *Physiological and Molecular Plant Pathology*. 2018;103:92-101.
261. Kamilova F, Validov S, Azarova T, Mulders I, Lugtenberg B. Enrichment for enhanced competitive plant root tip colonizers selects for a new class of biocontrol bacteria. *Environ Microbiol*. 2005;7(11):1809-17.
262. Arya N, Rana A, Rajwar A, Sahgal M, Sharma AK. Biocontrol Efficacy of Siderophore Producing Indigenous *Pseudomonas* Strains Against Fusarium Wilt in Tomato. *National Academy Science Letters*. 2018;41(3):133-6.
263. Naing KW, Anees M, Kim SJ, Nam Y, Kim YC, Kim KY. Characterization of antifungal activity of *Paenibacillus ehimensis* KWN38 against soilborne phytopathogenic fungi belonging to various taxonomic groups. *Annals of Microbiology*. 2014;64(1):55-63.
264. Naing KW, Nguyen XH, Anees M, Lee YS, Kim YC, Kim SJ, et al. Biocontrol of *Fusarium* wilt disease in tomato by *Paenibacillus ehimensis* KWN38. *World J Microbiol Biotechnol*. 2015;31(1):165-74.
265. Kim YH, Park SK, Hur JY, Kim YC. Purification and Characterization of a Major Extracellular Chitinase from a Biocontrol Bacterium, *Paenibacillus elgii* HOA73. *Plant Pathol J*. 2017;33(3):318-28.
266. Lee YS, Nguyen XH, Cho JY, Moon JH, Kim KY. Isolation and antifungal activity of methyl 2,3-dihydroxybenzoate from *Paenibacillus elgii* HOA73. *Microb Pathog*. 2017;106:139-45.
267. Mei L, Liang Y, Zhang L, Wang Y, Guo Y. Induced systemic resistance and growth promotion in tomato by an indole-3-acetic acid-producing strain of *Paenibacillus polymyxa*. *Annals of Applied Biology*. 2014;165(2):270-9.
268. Al-Askar AA, Baka ZA, Rashad YM, Ghoneem KM, Abdulkhair WM, Hafez EE, et al. Evaluation of *Streptomyces griseorubens* E44G for the biocontrol of *Fusarium oxysporum* f. sp. *lycopersici*: ultrastructural and cytochemical investigations. *Annals of Microbiology*. 2015;65(4):1815-24.
269. Rashad YM, Al-Askar AA, Ghoneem KM, Saber WIA, Hafez EE. Chitinolytic *Streptomyces griseorubens* E44G enhances the biocontrol efficacy against Fusarium wilt disease of tomato. *Phytoparasitica*. 2017;45(2):227-37.
270. Abbasi S, Safaie N, Sadeghi A, Shamsbakhsh M. *Streptomyces* Strains Induce Resistance to *Fusarium oxysporum* f. sp. *lycopersici* Race 3 in Tomato Through Different Molecular Mechanisms. 2019;10(1505).
271. Antoniou A, Tsolakidou M-D, Stringlis IA, Pantelides IS. Rhizosphere Microbiome Recruited from a Suppressive Compost Improves Plant Fitness and Increases Protection against Vascular Wilt Pathogens of Tomato. *Front Plant Sci*. 2017;8(2022).
272. Zhao F, Zhang Y, Dong W, Zhang Y, Zhang G, Sun Z, et al. Vermicompost can suppress *Fusarium oxysporum* f. sp. *lycopersici* via generation of beneficial bacteria in a long-term tomato monoculture soil. *Plant Soil*. 2019;440(1):491-505.
273. De Corato U, Patruno L, Avella N, Salimbeni R, Lacolla G, Cucci G, et al. Soil management under tomato-wheat rotation increases the suppressive response against *Fusarium* wilt and tomato shoot growth by changing the microbial composition and chemical parameters. *Applied Soil Ecology*. 2020;154:103601.

274. De Cal A, Melgarejo P. Repeated applications of *Penicillium oxalicum* prolongs biocontrol of fusarium wilt of tomato plants. *European journal of plant pathology*. 2001;107(8):805-11.
275. Dubey SC, Tripathi A, Tak R, Devi SI. Evaluation of bio-formulations of fungal and bacterial biological control agents in combination with fungicide in different mode of application for integrated management of tomato wilt. *Indian Phytopathology*. 2020.
276. Zhang J, Chen J, Jia R, Ma Q, Zong Z, Wang Y. Suppression of plant wilt diseases by nonpathogenic *Fusarium oxysporum* Fo47 combined with actinomycete strains. *Biocontrol Science and Technology*. 2018;28(6):562-73.
277. Mwangi MW, Muiro WM, Narla RD, Kimenju JW, Kariuki GM. Management of *Fusarium oxysporum* f. sp. *lycopersici* and root-knot nematode disease complex in tomato by use of antagonistic fungi, plant resistance and neem. *Biocontrol Science and Technology*. 2019;29(3):229-38.
278. Mazurier S, Corberand T, Lemanceau P, Raaijmakers JM. Phenazine antibiotics produced by fluorescent pseudomonads contribute to natural soil suppressiveness to Fusarium wilt. *The ISME Journal*. 2009;3(8):977-91.
279. Kinkel LL, Schlatter DC, Bakker MG, Arenz BE. *Streptomyces* competition and co-evolution in relation to plant disease suppression. *Research in microbiology*. 2012;163(8):490-9.
280. Zhao M, Yuan J, Zhang R, Dong M, Deng X, Zhu C, et al. Microflora that harbor the NRPS gene are responsible for *Fusarium* wilt disease-suppressive soil. *Applied Soil Ecology*. 2018;132:83-90.
281. Frederiks C, Wesseler JHH. A comparison of the EU and US regulatory frameworks for the active substance registration of microbial biological control agents. *Pest Management Science*. 2019;75(1):87-103.
282. ICA. Productos y bioinsumos registrados. Diciembre 2019. In: Agricultura Md, editor. Bogotá, Colombia: Intituto Colombiano Agropecuario; 2019.
283. Weert Sd, Bloemberg GV. Rhizosphere competence and the role of root colonization in biocontrol. . In: Gnanamanickam SS, editor. *Plant-Associated Bacteria* Dordrecht: Springer; 2007.
284. Hu HQ, Li XS, He H. Characterization of an antimicrobial material from a newly isolated *Bacillus amyloliquefaciens* from mangrove for biocontrol of Capsicum bacterial wilt. *Biol Control*. 2010;54(3):359-65.
285. Radovanović N, Milutinović M, Mihajlovski K, Jović J, Nastasijević B, Rajilić-Stojanović M, et al. Biocontrol and plant stimulating potential of novel strain *Bacillus* sp. PPM3 isolated from marine sediment. *Microbial Pathogenesis*. 2018;120:71-8.
286. Patel KB, Thakker JN. Growth promotion and biocontrol activity of *Nocardioopsis dassonvillei* strain YM12: an isolate from coastal agricultural land of Khambhat. *Vegetos*. 2019;32(4):571-82.
287. Raymaekers K, Ponet L, Holtappels D, Berckmans B, Cammue BPA. Screening for novel biocontrol agents applicable in plant disease management – A review. *Biol Control*. 2020;144:104240.
288. DeLong EF, Preston CM, Mincer T, Rich V, Hallam SJ, Frigaard N-U, et al. Community genomics among stratified microbial assemblages in the ocean's interior. *Science*. 2006;311(5760):496-503.
289. Simon C, Daniel R. Metagenomic analyses: past and future trends. *Applied and environmental microbiology*. 2011;77(4):1153-61.
290. Fenical W, Jensen PR. Developing a new resource for drug discovery: marine actinomycete bacteria. *Nature chemical biology*. 2006;2(12):666-73.

291. Penesyan A, Kjelleberg S, Egan S. Development of novel drugs from marine surface associated microorganisms. *Marine drugs*. 2010;8(3):438-59.
292. Egan S, Thomas T, Kjelleberg S. Unlocking the diversity and biotechnological potential of marine surface associated microbial communities. *Current opinion in microbiology*. 2008;11(3):219-25.
293. Smith DC, Simon M, Alldredge AL, Azam F. Intense hydrolytic enzyme activity on marine aggregates and implications for rapid particle dissolution. *Nature*. 1992;359(6391):139-42.
294. Peixoto RS, Rosado PM, de Assis Leite DC, Rosado AS, Bourne DG. Beneficial Microorganisms for Corals (BMC): proposed mechanisms for coral health and resilience. *Frontiers in Microbiology*. 2017;8.
295. Rosenberg E, Koren O, Reshef L, Efrony R, Zilber-Rosenberg I. The role of microorganisms in coral health, disease and evolution. *Nature Reviews Microbiology*. 2007;5(5):355-62.
296. Harder T. Marine epibiosis: concepts, ecological consequences and host defence. 2008.
297. Sharp KH, Eam B, Faulkner DJ, Haygood MG. Vertical transmission of diverse microbes in the tropical sponge *Corticium* sp. *Applied and Environmental Microbiology*. 2007;73(2):622-9.
298. Ortega-Morales BO, Chan-Bacab MJ, De la Rosa SdC, Camacho-Chab JC. Valuable processes and products from marine intertidal microbial communities. *Current opinion in biotechnology*. 2010;21(3):346-52.
299. Carroll AR, Copp BR, Davis RA, Keyzers RA, Prinsep MR. Marine natural products. *Natural Product Reports*. 2020;37(2):175-223.
300. El-Hossary EM, Cheng C, Hamed MM, Hamed ANE-S, Ohlsen K, Hentschel U, et al. Antifungal potential of marine natural products. *European Journal of Medicinal Chemistry*. 2016.
301. Lara-Capistran L, Zulueta-Rodriguez R, Castellanos-Cervantes T, Reyes-Perez JJ, Preciado-Rangel P, Hernandez-Montiel LG. Efficiency of Marine Bacteria and Yeasts on the Biocontrol Activity of *Pythium ultimum* in Ancho-Type Pepper Seedlings. *Agronomy*. 2020;10(3):408.
302. Tareq FS, Hasan CM, Lee H-S, Lee Y-J, Lee JS, Surovy MZ, et al. Gageopeptins A and B, new inhibitors of zoospore motility of the phytopathogen *Phytophthora capsici* from a marine-derived bacterium *Bacillus* sp. 109GGC020. *Bioorganic & medicinal chemistry letters*. 2015;25(16):3325-9.
303. Tareq FS, Kim JH, Lee MA, Lee H-S, Lee J-S, Lee Y-J, et al. Antimicrobial gageomacrolactins characterized from the fermentation of the marine-derived bacterium *Bacillus subtilis* under optimum growth conditions. *Journal of agricultural and food chemistry*. 2013;61(14):3428-34.
304. Xue C, Tian L, Xu M, Deng Z, Lin W. A New 24-membered Lactone and a New Polyene [delta]-Lactone from the Marine Bacterium *Bacillus marinus*. *Journal of antibiotics*. 2008;61(11):668.
305. Elkahoui S, Djéballi N, Tabbene O, Hadjbrahim A, Mnasri B, Mhamdi R, et al. Evaluation of antifungal activity from *Bacillus* strains against *Rhizoctonia solani*. *African Journal of Biotechnology*. 2012;11(18):4196-201.
306. Kong Q, Shan S, Liu Q, Wang X, Yu F. Biocontrol of *Aspergillus flavus* on peanut kernels by use of a strain of marine *Bacillus megaterium*. *International journal of food microbiology*. 2010;139(1):31-5.

307. Dhinakaran A, Rajasekaran R, Jayalakshmi S. Antiphytopathogenic activity of bacterial protein of a marine *Corynebacterium* sp. isolated from Mandapam, Gulf of Mannar. *Journal of Biopesticides*. 2012;5(17):2012.
308. El-Gendy MM, Hawas UW, Jaspars M. Novel bioactive metabolites from a marine derived bacterium *Nocardia* sp. ALAA 2000. *Journal of Antibiotics*. 2008;61(6):379.
309. Kathiresan K, Balagurunathan R, Selvam MM. Fungicidal activity of marine actinomycetes against phytopathogenic fungi. *Indian journal of Biotechnology*. 2005;4(2):271-6.
310. Jianyou L, Jianrong X, Yongheng C. Isolation and identification of two marine-derived *Streptomyces* from marine mud of coast and offshore Zhuhai, and bioactive potential for plant pathogenic fungi. *African Journal of Biotechnology*. 2011;10(56):11855-60.
311. Rivas-Garcia T, Murillo-Amador B, Nieto-Garibay A, Rincon-Enriquez G, Chiquito-Contreras RG, Hernandez-Montiel LG. Enhanced biocontrol of fruit rot on muskmelon by combination treatment with marine *Debaryomyces hansenii* and *Stenotrophomonas rhizophila* and their potential modes of action. *Postharvest Biology and Technology*. 2019;151:61-7.
312. Manwar A, Khandelwal S, Chaudhari B, Meyer J, Chincholkar S. Siderophore production by a marine *Pseudomonas aeruginosa* and its antagonistic action against phytopathogenic fungi. *Applied biochemistry and biotechnology*. 2004;118(1-3):243-51.
313. Jayaprakashvel M, Sharmika N, Vinothini S, Muthezhilan MVR, Hussain AJ. Biological Control of Sheath Blight of Rice using Marine Associated Fluorescent pseudomonads. 2014.
314. Huang C-Y, Ho C-H, Lin C-J, Lo C-C. Exposure effect of fungicide kasugamycin on bacterial community in natural river sediment. *Journal of Environmental Science and Health, Part B*. 2010;45(5):485-91.
315. Leal MC, Sheridan C, Osinga R, Dionísio G, Rocha RJM, Silva B, et al. Marine microorganism-invertebrate assemblages: perspectives to solve the “supply problem” in the initial steps of drug discovery. *Marine drugs*. 2014;12(7):3929-52.
316. Piel J. Bacterial symbionts: prospects for the sustainable production of invertebrate-derived pharmaceuticals. *Current medicinal chemistry*. 2006;13(1):39-50.
317. Piel J. Approaches to capturing and designing biologically active small molecules produced by uncultured microbes. *Annual review of microbiology*. 2011;65:431-53.
318. Radjasa OK, Vaske YM, Navarro G, Vervoort HC, Tenney K, Linington RG, et al. Highlights of marine invertebrate-derived biosynthetic products: Their biomedical potential and possible production by microbial associates. *Bioorganic & medicinal chemistry*. 2011;19(22):6658-74.
319. Mayer AM, Glaser KB, Cuevas C, Jacobs RS, Kem W, Little RD, et al. The odyssey of marine pharmaceuticals: a current pipeline perspective. *Trends in pharmacological sciences*. 2010;31(6):255-65.
320. Wilkinson B, Micklefield J. Mining and engineering natural-product biosynthetic pathways. *Nature chemical biology*. 2007;3(7):379-86.
321. Devi N, Balakrishnan K, Gopal R, Padmavathy S. *Bacillus clausii* MB9 from the east coast regions of India: Isolation, biochemical characterization and antimicrobial potentials. *Current Science (00113891)*. 2008;95(5).
322. Allwood JW, Ellis DI, Goodacre R. Metabolomic technologies and their application to the study of plants and plant-host interactions. *Physiol Plant*. 2008;132(2):117-35.
323. Yandigeri MS, Malviya N, Solanki MK, Shrivastava P, Sivakumar G. Chitinolytic *Streptomyces vinaceusdrappus* S5MW2 isolated from Chilika lake, India enhances plant

- growth and biocontrol efficacy through chitin supplementation against *Rhizoctonia solani*. World J Microbiol Biotechnol. 2015;31(8):1217-25.
324. Tabares P, Pimentel-Elardo SM, Schirmeister T, Hunig T, Hentschel U. Anti-protease and immunomodulatory activities of bacteria associated with Caribbean sponges. Mar Biotechnol (NY). 2011;13(5):883-92.
325. Quintero M, Velásquez A, Jutinico LM, Jiménez-Vergara E, Blandón LM, Martínez K, et al. Bioprospecting from marine coastal sediments of Colombian Caribbean: screening and study of antimicrobial activity. Journal of Applied Microbiology. 2018;125(3):753-65.
326. Blandón L, Alvarado-Campo KL, Patiño AD, Jiménez-Vergara E, Quintero M, Montoya-Giraldo M, et al. Polyhydroxyalkanoate Production from Two Species of Marine Bacteria: A Comparative Study. Journal of Polymers and the Environment. 2020;28(9):2324-34.
327. Martínez-Buitrago PA, Ramos FA, Castellanos L. Binary co-culture selection from marine-derived microorganisms for differential production of specialized metabolites. J Química Nova. 2019;42(7):713-9.
328. Romero-Otero A. Búsqueda de compuestos con actividad antimicrobiana a partir de hongos aislados de ambientes marinos. Fase I. Bogotá, Colombia: Universidad Nacional de Colombia 2016.
329. Cárdenas-Martínez JD. Evaluación de la producción metabólica de un aislamiento bacteriano obtenido de ambientes marinos para el control de fitopatógenos. Bogotá D.C, Colombia: Universidad Nacional de Colombia; 2019.
330. Betancur LA, Forero AM, Vinchira-Villarraga DM, Cárdenas-Martínez JD, Romero-Otero A, Chagas FO, et al. NMR-based metabolic profiling to follow the production of anti-phytopathogenic compounds in the culture of the marine strain *Streptomyces* sp. PNM-9. Microbiological research. 2020;239:126507.
331. Deketelaere S, Tyvaert L, Franca SC, Hofte M. Desirable Traits of a Good Biocontrol Agent against *Verticillium* Wilt. Front Microbiol. 2017;8:1186.
332. Karthika S, Varghese S, Jisha MS. Exploring the efficacy of antagonistic rhizobacteria as native biocontrol agents against tomato plant diseases. 3 Biotech. 2020;10(7):320.
333. Mahenthiralingam E, Baldwin A, Dowson CG. *Burkholderia cepacia* complex bacteria: opportunistic pathogens with important natural biology. Journal of Applied Microbiology. 2008;104(6):1539-51.
334. Handelsman J. Future trends in biocontrol. In: Gnanamanickam SS, editor. Biological control of crop diseases. New York: Marcel Dekker; 2002. p. 443-8.
335. Deising HB, Gase I, Kubo Y. The unpredictable risk imposed by microbial secondary metabolites: how safe is biological control of plant diseases? Journal of Plant Diseases and Protection. 2017;124(5):413-9.
336. Balouiri M, Sadiki M, Ibsouda SK. Methods for in vitro evaluating antimicrobial activity: A review. J Pharm Anal. 2016;6(2):71-9.
337. Das P, Chatterjee S, Behera BK, Dangar TK, Das BK, Mohapatra T. Isolation and characterization of marine bacteria from East Coast of India: functional screening for salt stress tolerance. Heliyon. 2019;5(6):e01869.
338. Röthig T, Ochsenkühn MA, Roik A, van der Merwe R, Voolstra CR. Long-term salinity tolerance is accompanied by major restructuring of the coral bacterial microbiome. Molecular Ecology. 2016;25(6):1308-23.
339. Chiquito-Contreras RG, Murillo-Amador B, Carmona-Hernandez S, Chiquito-Contreras CJ, Hernandez-Montiel LG. Effect of Marine Bacteria and Ulvan on the Activity

- of Antioxidant Defense Enzymes and the Bio-Protection of Papaya Fruit against *Colletotrichum gloeosporioides*. *Antioxidants* (Basel). 2019;8(12).
340. Wu S, Liu G, Zhou S, Sha Z, Sun C. Characterization of Antifungal Lipopeptide Biosurfactants Produced by Marine Bacterium *Bacillus* sp. CS30. *Mar Drugs*. 2019;17(4).
341. Zhang L, Sun C. Fengycins, Cyclic Lipopeptides from Marine *Bacillus subtilis* Strains, Kill the Plant-Pathogenic Fungus *Magnaporthe grisea* by Inducing Reactive Oxygen Species Production and Chromatin Condensation. *Applied and Environmental Microbiology*. 2018;84(18):e00445-18.
342. Chakraborty M, Mahmud NU, Gupta DR, Tareq FS, Shin HJ, Islam T. Inhibitory Effects of Linear Lipopeptides From a Marine *Bacillus subtilis* on the Wheat Blast Fungus *Magnaporthe oryzae* *Triticum*. *Front Microbiol*. 2020;11(665).
343. Gurjar G, Barve M, Giri A, Gupta V. Identification of Indian pathogenic races of *Fusarium oxysporum* f. sp. *ciceris* with gene specific, ITS and random markers. *Mycologia*. 2009;101(4):484-95.
344. Cowan ST, Steel KJ. *Cowan and Steel's Manual for the Identification of Medical Bacteria*. 3 ed. Cambridge: Cambridge University Press; 1993.
345. Pierce CG, Uppuluri P, Tristan AR, Wormley FL, Jr., Mowat E, Ramage G, et al. A simple and reproducible 96-well plate-based method for the formation of fungal biofilms and its application to antifungal susceptibility testing. *Nat Protoc*. 2008;3(9):1494-500.
346. Goswami D, Parmar S, Vaghela H, Dhandhukia P, Thakker JN. Describing *Paenibacillus mucilaginosus* strain N3 as an efficient plant growth promoting rhizobacteria (PGPR). *J Cogent Food Agriculture*. 2015;1(1):1000714.
347. Budi S, Van Tuinen D, Arnould C, Dumas-Gaudot E, Gianinazzi-Pearson V, Gianinazzi S. Hydrolytic enzyme activity of *Paenibacillus* sp. strain B2 and effects of the antagonistic bacterium on cell integrity of two soil-borne pathogenic fungi. *J Applied Soil Ecology*. 2000;15(2):191-9.
348. Singh A, Mehta G, Chhatpar H. Optimization of medium constituents for improved chitinase production by *Paenibacillus* sp. D1 using statistical approach. *Letters in applied microbiology*. 2009;49(6):708-14.
349. Clarke JD. Cetyltrimethyl ammonium bromide (CTAB) DNA miniprep for plant DNA isolation. *Cold Spring Harb Protoc*. 2009;2009(3):pdb prot5177.
350. Aw YK, Ong KS, Lee LH, Cheow YL, Yule CM, Lee SM. Newly Isolated *Paenibacillus tyrfis* sp. nov., from Malaysian Tropical Peat Swamp Soil with Broad Spectrum Antimicrobial Activity. *Front Microbiol*. 2016;7:219.
351. Cole JR, Wang Q, Fish JA, Chai B, McGarrell DM, Sun Y, et al. Ribosomal Database Project: data and tools for high throughput rRNA analysis. *Nucleic Acids Res*. 2014;42(Database issue):D633-42.
352. Kim OS, Cho YJ, Lee K, Yoon SH, Kim M, Na H, et al. Introducing EzTaxon-e: a prokaryotic 16S rRNA gene sequence database with phylotypes that represent uncultured species. *Int J Syst Evol Microbiol*. 2012;62(Pt 3):716-21.
353. Kumar S, Stecher G, Tamura K. MEGA7: Molecular Evolutionary Genetics Analysis Version 7.0 for Bigger Datasets. *Mol Biol Evol*. 2016;33(7):1870-4.
354. Buijs Y, Bech PK, Vazquez-Albacete D, Bentzon-Tilia M, Sonnenschein EC, Gram L, et al. Marine Proteobacteria as a source of natural products: advances in molecular tools and strategies. *Nat Prod Rep*. 2019;36(9):1333-50.
355. Carroll AR, Copp BR, Davis RA, Keyzers RA, Prinsep MR. Marine natural products. *Nat Prod Rep*. 2019;36(1):122-73.
356. Petersen L-E, Kellermann MY, Schupp PJ. Secondary Metabolites of Marine Microbes: From Natural Products Chemistry to Chemical Ecology. In: Jungblut S, Liebich

- V, Bode-Dalby M, editors. YOUMARES 9 - The Oceans: Our Research, Our Future: Proceedings of the 2018 conference for YOUng MARine RESearcher in Oldenburg, Germany. Cham: Springer International Publishing; 2020. p. 159-80.
357. Xue Q-Y, Ding G-C, Li S-M, Yang Y, Lan C-Z, Guo J-H, et al. Rhizocompetence and antagonistic activity towards genetically diverse *Ralstonia solanacearum* strains – an improved strategy for selecting biocontrol agents. *Applied Microbiology and Biotechnology*. 2013;97(3):1361-71.
358. Yu Y-Y, Jiang C-H, Wang C, Chen L-J, Li H-Y, Xu Q, et al. An improved strategy for stable biocontrol agents selecting to control rice sheath blight caused by *Rhizoctonia solani*. *Microbiological Research*. 2017;203:1-9.
359. Algam SAE, Xie G, Li B, Yu S, Su T, Larsen J. Effects of *Paenibacillus* strains and chitosan on plant growth promotion and control of *Ralstonia* wilt in tomato. *Journal of Plant Pathology*. 2010;92(3):593-600.
360. Son SH, Khan Z, Kim SG, Kim YH. Plant growth-promoting rhizobacteria, *Paenibacillus polymyxa* and *Paenibacillus lentimorbis* suppress disease complex caused by root-knot nematode and fusarium wilt fungus. *J Appl Microbiol*. 2009;107(2):524-32.
361. Xu SJ, Kim BS. Biocontrol of fusarium crown and root rot and promotion of growth of tomato by *Paenibacillus* strains isolated from soil. *Mycobiology*. 2014;42(2):158-66.
362. Jeon SW, Naing KW, Lee YS, Nguyen XH, Kim SJ, Kim KY. Promotion of growth and biocontrol of brown patch disease by inoculation of *Paenibacillus ehimensis* KWN38 in bentgrass. *Horticulture, Environment, and Biotechnology*. 2015;56(2):263-71.
363. Jeong H, Choi SK, Ryu CM, Park SH. Chronicle of a Soil Bacterium: *Paenibacillus polymyxa* E681 as a Tiny Guardian of Plant and Human Health. *Front Microbiol*. 2019;10:467.
364. Shi L, Du N, Shu S, Sun J, Li S, Guo S. *Paenibacillus polymyxa* NSY50 suppresses *Fusarium* wilt in cucumbers by regulating the rhizospheric microbial community. *Sci Rep*. 2017;7:41234.
365. Das SN, Dutta S, Kondreddy A, Chilukoti N, Pullabhotla SVSRN, Vadlamudi S, et al. Plant Growth-Promoting Chitinolytic *Paenibacillus elgii* Responds Positively to Tobacco Root Exudates. *Journal of Plant Growth Regulation*. 2010;29(4):409-18.
366. Aktuganov G, Jokela J, Kivela H, Khalikova E, Melentjev A, Galimzianova N, et al. Isolation and identification of cyclic lipopeptides from *Paenibacillus ehimensis*, strain IB-X-b. *J Chromatogr B Analyt Technol Biomed Life Sci*. 2014;973C:9-16.
367. Wu XC, Shen XB, Ding R, Qian CD, Fang HH, Li O. Isolation and partial characterization of antibiotics produced by *Paenibacillus elgii* B69. *FEMS Microbiol Lett*. 2010;310(1):32-8.
368. Aktuganov G, Melentjev A, Galimzianova N, Khalikova E, Korpela T, Susi P. Wide-range antifungal antagonism of *Paenibacillus ehimensis* IB-X-b and its dependence on chitinase and beta-1,3-glucanase production. *Can J Microbiol*. 2008;54(7):577-87.
369. Seo DJ, Lee YS, Kim KY, Jung WJ. Antifungal activity of chitinase obtained from *Paenibacillus ehimensis* MA2012 against conidial of *Collectotrichum gloeosporioides* *in vitro*. *Microb Pathog*. 2016;96:10-4.
370. Kim D-S, Rae C-Y, Chun S-J, Kim D-H, Choi S-W, Choi K-H. *Paenibacillus elgii* SD17 as a biocontrol agent against soil-borne turf diseases. *J The Plant Pathology Journal*. 2005;21(4):328-33.
371. Kim J, Le KD, Yu NH, Kim JI, Kim JC, Lee CW. Structure and antifungal activity of pelgipeptins from *Paenibacillus elgii* against phytopathogenic fungi. *Pestic Biochem Physiol*. 2020;163:154-63.

372. Vater J, Herfort S, Doellinger J, Weydmann M, Dietel K, Faetke S, et al. Fusaricidins from *Paenibacillus polymyxa* M-1, a family of lipohexapeptides of unusual complexity—a mass spectrometric study. *J Mass Spectrom.* 2017;52:7-15.
373. Hollensteiner J, Wemheuer F, Harting R, Kolarzyk AM, Diaz Valerio SM, Poehlein A, et al. *Bacillus thuringiensis* and *Bacillus weihenstephanensis* Inhibit the Growth of Phytopathogenic *Verticillium* Species. *Front Microbiol.* 2016;7:2171.
374. Morris JJ. What is the hologenome concept of evolution? *F1000Res.* 2018;7:F1000 Faculty Rev-664.
375. Carrier TJ, Reitzel AM. The Hologenome Across Environments and the Implications of a Host-Associated Microbial Repertoire. *Front Microbiol.* 2017;8:802.
376. Offret C, Desriac F, Le Chevalier P, Mounier J, Jegou C, Fleury Y. Spotlight on Antimicrobial Metabolites from the Marine Bacteria *Pseudoalteromonas*: Chemodiversity and Ecological Significance. *Mar Drugs.* 2016;14(7).
377. Engel S, Jensen PR, Fenical W. Chemical ecology of marine microbial defense. *J Chem Ecol.* 2002;28(10):1971-85.
378. Tianero MD, Balaich JN, Donia MS. Localized production of defence chemicals by intracellular symbionts of *Haliclona* sponges. *Nat Microbiol.* 2019;4(7):1149-59.
379. Rojas EC, Jensen B, Jørgensen HJL, Latz MAC, Esteban P, Ding Y, et al. Selection of fungal endophytes with biocontrol potential against *Fusarium* head blight in wheat. *Biol Control.* 2020;144:104222.
380. Weng J, Wang Y, Li J, Shen Q, Zhang R. Enhanced root colonization and biocontrol activity of *Bacillus amyloliquefaciens* SQR9 by *abrB* gene disruption. *Appl Microbiol Biotechnol.* 2013;97(19):8823-30.
381. Barret M, Morrissey JP, O'Gara F. Functional genomics analysis of plant growth-promoting rhizobacterial traits involved in rhizosphere competence. *Biology and Fertility of Soils.* 2011;47(7):729.
382. Kravchenko LV, Azarova TS, Leonova-Erko EI, Shaposhnikov AI, Makarova NM, Tikhonovich IA. Root Exudates of Tomato Plants and Their Effect on the Growth and Antifungal Activity of *Pseudomonas* Strains. *Microbiology.* 2003;72(1):37-41.
383. Canarini A, Kaiser C, Merchant A, Richter A, Wanek W. Root Exudation of Primary Metabolites: Mechanisms and Their Roles in Plant Responses to Environmental Stimuli. *Front Plant Sci.* 2019;10:157.
384. Venturi V, Keel C. Signaling in the Rhizosphere. *Trends Plant Sci.* 2016;21(3):187-98.
385. Raguso RA, Agrawal AA, Douglas AE, Jander G, Kessler A, Poveda K, et al. The raison d'etre of chemical ecology. *Ecology.* 2015;96(3):617-30.
386. Rudrappa T, Czymmek KJ, Pare PW, Bais HP. Root-secreted malic acid recruits beneficial soil bacteria. *Plant Physiol.* 2008;148(3):1547-56.
387. Tan S, Yang C, Mei X, Shen S, Raza W, Shen Q, et al. The effect of organic acids from tomato root exudates on rhizosphere colonization of *Bacillus amyloliquefaciens* T-5. *Applied Soil Ecology.* 2013;64:15-22.
388. Bi S, Sourjik V. Stimulus sensing and signal processing in bacterial chemotaxis. *Current opinion in microbiology.* 2018;45:22-9.
389. Scharf BE, Hynes MF, Alexandre GM. Chemotaxis signaling systems in model beneficial plant-bacteria associations. *Plant Mol Biol.* 2016;90(6):549-59.
390. Chen Y, Yan F, Chai Y, Liu H, Kolter R, Losick R, et al. Biocontrol of tomato wilt disease by *Bacillus subtilis* isolates from natural environments depends on conserved genes mediating biofilm formation. *Environ Microbiol.* 2013;15(3):848-64.

391. Aydi Ben Abdallah R, Mokni-Tlili S, Nefzi A, Jabnoun-Khiareddine H, Daami-Remadi M. Biocontrol of *Fusarium* wilt and growth promotion of tomato plants using endophytic bacteria isolated from *Nicotiana glauca* organs. *Biol Control*. 2016;97:80-8.
392. Debbi A, Boureghda H, Monte E, Hermosa R. Distribution and Genetic Variability of *Fusarium oxysporum* Associated with Tomato Diseases in Algeria and a Biocontrol Strategy with Indigenous *Trichoderma* spp. *Front Microbiol*. 2018;9(282).
393. Akhter A, Hage-Ahmed K, Soja G, Steinkellner S. Potential of *Fusarium* wilt-inducing chlamydospores, in vitro behaviour in root exudates and physiology of tomato in biochar and compost amended soil. *Plant Soil*. 2016;406(1):425-40.
394. Jelinski NA, Broz K, Jonkers W, Ma L-J, Kistler HC. Effector Gene Suites in Some Soil Isolates of *Fusarium oxysporum* Are Not Sufficient Predictors of Vascular Wilt in Tomato. *Phytopathology*®. 2017;107(7):842-51.
395. Rocha FYO, Oliveira CMD, da Silva PRA, Melo LHVd, Carmo MGFd, Baldani JI. Taxonomical and functional characterization of *Bacillus* strains isolated from tomato plants and their biocontrol activity against races 1, 2 and 3 of *Fusarium oxysporum* f. sp. *lycopersici*. *Applied Soil Ecology*. 2017;120:8-19.
396. Manikandan R, Harish S, Karthikeyan G, Raguchander T. Comparative Proteomic Analysis of Different Isolates of *Fusarium oxysporum* f.sp. *lycopersici* to Exploit the Differentially Expressed Proteins Responsible for Virulence on Tomato Plants. *Front Microbiol*. 2018;9(420).
397. Timmusk S, Grantcharova N, Wagner EG. *Paenibacillus polymyxa* invades plant roots and forms biofilms. *Appl Environ Microbiol*. 2005;71(11):7292-300.
398. Park SY, Kim R, Ryu CM, Choi SK, Lee CH, Kim JG, et al. Citrinin, a mycotoxin from *Penicillium citrinum*, plays a role in inducing motility of *Paenibacillus polymyxa*. *FEMS Microbiol Ecol*. 2008;65(2):229-37.
399. Tan S, Yang C, Mei X, Shen S, Raza W, Shen Q, et al. The effect of organic acids from tomato root exudates on rhizosphere colonization of *Bacillus amyloliquefaciens* T-5. *J Applied Soil Ecology*. 2013;64:15-22.
400. Yang G, Zhou B, Zhang X, Zhang Z, Wu Y, Zhang Y, et al. Effects of Tomato Root Exudates on *Meloidogyne incognita*. *PLoS One*. 2016;11(4):e0154675.
401. Grattidge R, O'Brien R. Occurrence of a third race of *Fusarium* wilt of tomatoes in Queensland. *J Plant Disease*. 1982;66(2):165-6.
402. Madden LV, A Hughes G, A van den Bosch F. *The Study of Plant Disease Epidemics*. Minnesota, USA: The American Phytopathological Society; 2007.
403. Qiao J, Yu X, Liang X, Liu Y, Borriss R, Liu Y. Addition of plant-growth-promoting *Bacillus subtilis* PTS-394 on tomato rhizosphere has no durable impact on composition of root microbiome. *BMC Microbiol*. 2017;17(1):131.
404. Hassen A, Labuschagne N. Root colonization and growth enhancement in wheat and tomato by rhizobacteria isolated from the rhizoplane of grasses. *World Journal of Microbiology and Biotechnology*. 2010;26:1837-46.
405. Li P, Ma L, Feng YL, Mo MH, Yang FX, Dai HF, et al. Diversity and chemotaxis of soil bacteria with antifungal activity against *Fusarium* wilt of banana. *J Ind Microbiol Biotechnol*. 2012;39(10):1495-505.
406. Chin AWTF, Bloemberg GV, Mulders IH, Dekkers LC, Lugtenberg BJ. Root colonization by phenazine-1-carboxamide-producing bacterium *Pseudomonas chlororaphis* PCL1391 is essential for biocontrol of tomato foot and root rot. *Mol Plant Microbe Interact*. 2000;13(12):1340-5.

407. Zheng XY, Sinclair JB. The effects of traits of *Bacillus megaterium* on seed and root colonization and their correlation with the suppression of *Rhizoctonia* root rot of soybean. *BioControl*. 2000;45(2):223-43.
408. Salvatierra-Martinez R, Arancibia W, Araya M, Aguilera S, Olalde V, Bravo J, et al. Colonization ability as an indicator of enhanced biocontrol capacity—An example using two *Bacillus amyloliquefaciens* strains and *Botrytis cinerea* infection of tomatoes. *J Journal of Phytopathology*. 2018;166(9):601-12.
409. Barahona E, Navazo A, Martinez-Granero F, Zea-Bonilla T, Perez-Jimenez RM, Martin M, et al. *Pseudomonas fluorescens* F113 mutant with enhanced competitive colonization ability and improved biocontrol activity against fungal root pathogens. *Appl Environ Microbiol*. 2011;77(15):5412-9.
410. Akköprü A, Demir S. Biological control of *Fusarium* wilt in tomato caused by *Fusarium oxysporum* f. sp. *lycopersici* by AMF *Glomus intraradices* and some rhizobacteria. *J Journal of Phytopathology*. 2005;153(9):544-50.
411. Raza W, Yuan J, Wu YC, Rajer FU, Huang Q, Qirong S. Biocontrol traits of two *Paenibacillus polymyxa* strains SQR-21 and WR-2 in response to fusaric acid, a phytotoxin produced by *Fusarium* species. *Plant Pathol*. 2015;64(5):1041-52.
412. Rybakova D, Rack-Wetzlinger U, Cernava T, Schaefer A, Schmuck M, Berg G. Aerial Warfare: A Volatile Dialogue between the Plant Pathogen *Verticillium longisporum* and Its Antagonist *Paenibacillus polymyxa*. 2017;8(1294).
413. Oppong-Danquah E, Parrot D, Blumel M, Labes A, Tasdemir D. Molecular Networking-Based Metabolome and Bioactivity Analyses of Marine-Adapted Fungi Co-cultivated With Phytopathogens. *Front Microbiol*. 2018;9:2072.
414. Rybakova D, Cernava T, Koberl M, Liebminger S, Etemadi M, Berg G. Endophytes-assisted biocontrol: novel insights in ecology and the mode of action of *Paenibacillus*. *Plant Soil*. 2016;405(1-2):125-40.
415. Kim B, Song GC, Ryu CM. Root Exudation by Aphid Leaf Infestation Recruits Root-Associated *Paenibacillus* spp. to Lead Plant Insect Susceptibility. *J Microbiol Biotechnol*. 2016;26(3):549-57.
416. Ling N, Huang QW, Guo SW, Shen QR. *Paenibacillus polymyxa* SQR-21 systemically affects root exudates of watermelon to decrease the conidial germination of *Fusarium oxysporum* f.sp. *niveum*. *Plant Soil*. 2011;341(1-2):485-93.
417. Ling N, Raza W, Ma JH, Huang QW, Shen QR. Identification and role of organic acids in watermelon root exudates for recruiting *Paenibacillus polymyxa* SQR-21 in the rhizosphere. *Eur J Soil Biol*. 2011;47(6):374-9.
418. Du N, Shi L, Yuan Y, Li B, Shu S, Sun J, et al. Proteomic Analysis Reveals the Positive Roles of the Plant-Growth-Promoting Rhizobacterium NSY50 in the Response of Cucumber Roots to *Fusarium oxysporum* f. sp. *cucumerinum* Inoculation. *Front Plant Sci*. 2016;7:1859.
419. Kwon YS, Lee DY, Rakwal R, Baek SB, Lee JH, Kwak YS, et al. Proteomic analyses of the interaction between the plant-growth promoting rhizobacterium *Paenibacillus polymyxa* E681 and *Arabidopsis thaliana*. *Proteomics*. 2016;16(1):122-35.
420. Scherling C, Ulrich K, Ewald D, Weckwerth W. A Metabolic Signature of the Beneficial Interaction of the Endophyte *Paenibacillus* sp Isolate and In Vitro-Grown Poplar Plants Revealed by Metabolomics. *Mol Plant Microbe In*. 2009;22(8):1032-7.
421. Kim HK, Choi YH, Verpoorte R. NMR-based plant metabolomics: where do we stand, where do we go? *Trends Biotechnol*. 2011;29(6):267-75.
422. Fiehn O. Metabolomics - the link between genotypes and phenotypes. *Plant Mol Biol*. 2002;48(1-2):155-71.

423. Kumar R, Bohra A, Pandey AK, Pandey MK, Kumar A. Metabolomics for Plant Improvement: Status and Prospects. *Front Plant Sci.* 2017;8:1302.
424. Tohge T, Fernie AR. Combining genetic diversity, informatics and metabolomics to facilitate annotation of plant gene function. *Nat Protoc.* 2010;5(6):1210-27.
425. Camanes G, Scalschi L, Vicedo B, Gonzalez-Bosch C, Garcia-Agustin P. An untargeted global metabolomic analysis reveals the biochemical changes underlying basal resistance and priming in *Solanum lycopersicum*, and identifies 1-methyltryptophan as a metabolite involved in plant responses to *Botrytis cinerea* and *Pseudomonas syringae*. *Plant J.* 2015;84(1):125-39.
426. Lopez-Gresa MP, Maltese F, Belles JM, Conejero V, Kim HK, Choi YH, et al. Metabolic response of tomato leaves upon different plant-pathogen interactions. *Phytochem Anal.* 2010;21(1):89-94.
427. Zeiss DR, Mhlongo MI, Tugizimana F, Steenkamp PA, Dubery IA. Comparative Metabolic Phenotyping of Tomato (*Solanum lycopersicum*) for the Identification of Metabolic Signatures in Cultivars Differing in Resistance to *Ralstonia solanacearum*. *Int J Mol Sci.* 2018;19(9).
428. Zeiss DR, Mhlongo MI, Tugizimana F, Steenkamp PA, Dubery IA. Metabolomic Profiling of the Host Response of Tomato (*Solanum lycopersicum*) Following Infection by *Ralstonia solanacearum*. *Int J Mol Sci.* 2019;20(16).
429. Wojciechowska E, Weinert CH, Egert B, Trierweiler B, Schmidt-Heydt M, Horneburg B, et al. Chlorogenic acid, a metabolite identified by untargeted metabolome analysis in resistant tomatoes, inhibits the colonization by *Alternaria alternata* by inhibiting alternariol biosynthesis. *European Journal of Plant Pathology.* 2014;139(4):735-47.
430. Shinde BA, Dholakia BB, Hussain K, Panda S, Meir S, Rogachev I, et al. Dynamic metabolic reprogramming of steroidal glycol-alkaloid and phenylpropanoid biosynthesis may impart early blight resistance in wild tomato (*Solanum arcanum* Peralta). *Plant Mol Biol.* 2017;95(4-5):411-23.
431. Galeano Garcia P, Neves Dos Santos F, Zanotta S, Eberlin MN, Carazzone C. Metabolomics of *Solanum lycopersicum* Infected with *Phytophthora infestans* Leads to Early Detection of Late Blight in Asymptomatic Plants. *Molecules.* 2018;23(12).
432. Akram W, Anjum T, Ali B. Phenylacetic Acid Is ISR Determinant Produced by *Bacillus fortis* IAGS162, Which Involves Extensive Re-modulation in Metabolomics of Tomato to Protect against Fusarium Wilt. *Front Plant Sci.* 2016;7:498.
433. Anjum T, Akram W, Shafique S, Shafique S, Ahmad A. Metabolomic Analysis Identifies Synergistic Role of Hormones Biosynthesis and Phenylpropanoid Pathways during *Fusarium* Wilt Resistance in Tomato Plants. *Int J Agric Biol.* 2017;19(5):1073-8.
434. Nebbioso A, De Martino A, Eltlbany N, Smalla K, Piccolo A. Phytochemical profiling of tomato roots following treatments with different microbial inoculants as revealed by IT-TOF mass spectrometry. *Chem Biol Technol Ag.* 2016;3.
435. Kamilova F, Kravchenko LV, Shaposhnikov AI, Makarova N, Lugtenberg B. Effects of the tomato pathogen *Fusarium oxysporum* f. sp. *radicis-lycopersici* and of the biocontrol bacterium *Pseudomonas fluorescens* WCS365 on the composition of organic acids and sugars in tomato root exudate. *Mol Plant Microbe Interact.* 2006;19(10):1121-6.
436. Rivero J, Gamir J, Aroca R, Pozo MJ, Flors V. Metabolic transition in mycorrhizal tomato roots. *Frontiers in Microbiology.* 2015;6.
437. Manganiello G, Sacco A, Ercolano MR, Vinale F, Lanzuise S, Pascale A, et al. Modulation of Tomato Response to *Rhizoctonia solani* by *Trichoderma harzianum* and Its Secondary Metabolite Harzianic Acid. *Front Microbiol.* 2018;9(1966).

438. Fatima S, Anjum T. Identification of a Potential ISR Determinant from *Pseudomonas aeruginosa* PM12 against *Fusarium* Wilt in Tomato. *Front Plant Sci.* 2017;8:848.
439. Debois D, Ongena M, Cawoy H, De Pauw E. MALDI-FTICR MS Imaging as a Powerful Tool to Identify *Paenibacillus* Antibiotics Involved in the Inhibition of Plant Pathogens. *J Am Soc Mass Spectr.* 2013;24(8):1202-13.
440. Du X, Smirnov A, Pluskal T, Jia W, Sumner S. Metabolomics Data Preprocessing Using ADAP and MZmine 2. *Methods Mol Biol.* 2020;2104:25-48.
441. Olivon F, Grelier G, Roussi F, Litaudon M, Touboul D. MZmine 2 Data-Preprocessing To Enhance Molecular Networking Reliability. *Anal Chem.* 2017;89(15):7836-40.
442. Pluskal T, Castillo S, Villar-Briones A, Oresic M. MZmine 2: modular framework for processing, visualizing, and analyzing mass spectrometry-based molecular profile data. *BMC Bioinformatics.* 2010;11:395.
443. Worley B, Powers R. PCA as a practical indicator of OPLS-DA model reliability. *Current Metabolomics.* 2016;4(2):97-103.
444. Iijima Y, Watanabe B, Sasaki R, Takenaka M, Ono H, Sakurai N, et al. Steroidal glycoalkaloid profiling and structures of glycoalkaloids in wild tomato fruit. *Phytochemistry.* 2013;95:145-57.
445. Fernie AR, Aharoni A, Willmitzer L, Stitt M, Tohge T, Kopka J, et al. Recommendations for reporting metabolite data. *Plant Cell.* 2011;23(7):2477-82.
446. Ghosh S, Narula K, Sinha A, Ghosh R, Jawa P, Chakraborty N, et al. Proteometabolomic analysis of transgenic tomato overexpressing oxalate decarboxylase uncovers novel proteins potentially involved in defense mechanism against *Sclerotinia*. *J Proteomics.* 2016;143:242-53.
447. Mhlongo MI, Piater LA, Steenkamp PA, Labuschagne N, Dubery IA. Metabolic Profiling of PGPR-Treated Tomato Plants Reveal Priming-Related Adaptations of Secondary Metabolites and Aromatic Amino Acids. *Metabolites.* 2020;10(5).
448. Oburger E, Jones DL. Sampling root exudates – Mission impossible? *Rhizosphere.* 2018;6:116-33.
449. Petriacq P, Williams A, Cotton A, McFarlane AE, Rolfe SA, Ton J. Metabolite profiling of non-sterile rhizosphere soil. *Plant J.* 2017;92(1):147-62.
450. Mimmo T, Hann S, Jaitz L, Cesco S, Gessa CE, Puschenreiter M. Time and substrate dependent exudation of carboxylates by *Lupinus albus* L. and *Brassica napus* L. *Plant Physiology and Biochemistry.* 2011;49(11):1272-8.
451. Tavakkoli E, Rengasamy P, McDonald GK. The response of barley to salinity stress differs between hydroponic and soil systems. *J Functional Plant Biology.* 2010;37(7):621-33.
452. Fischer H, Ingwersen J, Kuzyakov Y. Microbial uptake of low-molecular-weight organic substances out-competes sorption in soil. *J European Journal of Soil Science.* 2010;61(4):504-13.
453. Itkin M, Rogachev I, Alkan N, Rosenberg T, Malitsky S, Masini L, et al. GLYCOALKALOID METABOLISM1 is required for steroidal alkaloid glycosylation and prevention of phytotoxicity in tomato. *Plant Cell.* 2011;23(12):4507-25.
454. Schwahn K, de Souza LP, Fernie AR, Tohge T. Metabolomics-assisted refinement of the pathways of steroidal glycoalkaloid biosynthesis in the tomato clade. *J Integr Plant Biol.* 2014;56(9):864-75.
455. Milner SE, Brunton NP, Jones PW, O'Brien NM, Collins SG, Maguire AR. Bioactivities of glycoalkaloids and their aglycones from *Solanum* species. *J Agric Food Chem.* 2011;59(8):3454-84.

456. Friedman M. Tomato glycoalkaloids: role in the plant and in the diet. *J Agric Food Chem.* 2002;50(21):5751-80.
457. Cardenas PD, Sonawane PD, Heinig U, Jozwiak A, Panda S, Abebie B, et al. Pathways to defense metabolites and evading fruit bitterness in genus *Solanum* evolved through 2-oxoglutarate-dependent dioxygenases. *Nat Commun.* 2019;10(1):5169.
458. Dzakovich MP, Hartman JL, Cooperstone JL. A High-Throughput Extraction and Analysis Method for Steroidal Glycoalkaloids in Tomato. *J bioRxiv.* 2019.
459. Zhu G, Wang S, Huang Z, Zhang S, Liao Q, Zhang C, et al. Rewiring of the Fruit Metabolome in Tomato Breeding. *Cell.* 2018;172(1):249-61.e12.
460. Sandrock RW, Vanetten HD. Fungal Sensitivity to and Enzymatic Degradation of the Phytoanticipin α -Tomatine. *Phytopathology.* 1998;88(2):137-43.
461. Ito S, Ihara T, Tamura H, Tanaka S, Ikeda T, Kajihara H, et al. α -Tomatine, the major saponin in tomato, induces programmed cell death mediated by reactive oxygen species in the fungal pathogen *Fusarium oxysporum*. *FEBS Lett.* 2007;581(17):3217-22.
462. Oka K, Okubo A, Kodama M, Otani H. Detoxification of α -tomatine by tomato pathogens *Alternaria alternata* tomato pathotype and *Corynespora cassiicola* and its role in infection. *J Journal of general plant pathology.* 2006;72(3):152-8.
463. Osbourn A. Saponins and plant defence; a soap story. *Trends in Plant Science.* 1996;1(1):4-9.
464. Ökmen B, Etalo DW, Joosten MHAJ, Bouwmeester HJ, de Vos RCH, Collemare J, et al. Detoxification of α -tomatine by *Cladosporium fulvum* is required for full virulence on tomato. *New Phytologist.* 2013;198(4):1203-14.
465. Pareja-Jaime Y, Roncero MIG, Ruiz-Roldán MC. Tomatinase from *Fusarium oxysporum* f. sp. *lycopersici* is required for full virulence on tomato plants. *J Molecular plant-microbe interactions.* 2008;21(6):728-36.
466. Majumdar S, Pal S. Information transmission in microbial and fungal communication: from classical to quantum. *J Cell Commun Signal.* 2018;12(2):491-502.
467. Hennessy RC, Glaring MA, Olsson S, Stougaard P. Transcriptomic profiling of microbe–microbe interactions reveals the specific response of the biocontrol strain *P. fluorescens* In5 to the phytopathogen *Rhizoctonia solani*. *BMC Research Notes.* 2017;10(1):376.
468. Tomada S, Sonogo P, Moretto M, Engelen K, Pertot I, Perazzolli M, et al. Dual RNA-Seq of *Lysobacter capsici* AZ78 – *Phytophthora infestans* interaction shows the implementation of attack strategies by the bacterium and unsuccessful oomycete defense responses. *Environ Microbiol.* 2017;19(10):4113-25.
469. Barret M, Frey-Klett P, Boutin M, Guillermin-Erckelboudt AY, Martin F, Guillot L, et al. The plant pathogenic fungus *Gaeumannomyces graminis* var. *tritici* improves bacterial growth and triggers early gene regulations in the biocontrol strain *Pseudomonas fluorescens* Pf29Arp. *New Phytol.* 2009;181(2):435-47.
470. Benoit I, van den Esker MH, Patyshakuliyeva A, Mattern DJ, Blei F, Zhou M, et al. *Bacillus subtilis* attachment to *Aspergillus niger* hyphae results in mutually altered metabolism. *Environ Microbiol.* 2015;17(6):2099-113.
471. Feussner I, Polle A. What the transcriptome does not tell—Proteomics and metabolomics are closer to the plants' patho-phenotype. *Current Opinion in Plant Biology.* 2015;26.
472. Arora D, Gupta P, Jaglan S, Roullier C, Grovel O, Bertrand S. Expanding the chemical diversity through microorganisms co-culture: Current status and outlook. *Biotechnology Advances.* 2020;40:107521.

473. Marmann A, Aly AH, Lin W, Wang B, Proksch P. Co-cultivation--a powerful emerging tool for enhancing the chemical diversity of microorganisms. *Mar Drugs*. 2014;12(2):1043-65.
474. Wu Q, Ni M, Dou K, Tang J, Ren J, Yu C, et al. Co-culture of *Bacillus amyloliquefaciens* ACCC11060 and *Trichoderma asperellum* GDFS1009 enhanced pathogen-inhibition and amino acid yield. *Microbial Cell Factories*. 2018;17(1):155.
475. Kombrink A, Tayyrov A, Essig A, Stöckli M, Micheller S, Hintze J, et al. Induction of antibacterial proteins and peptides in the coprophilous mushroom *Coprinopsis cinerea* in response to bacteria. *The ISME Journal*. 2019;13(3):588-602.
476. Vinale F, Nicoletti R, Borrelli F, Mangoni A, Parisi OA, Marra R, et al. Co-Culture of Plant Beneficial Microbes as Source of Bioactive Metabolites. *Scientific Reports*. 2017;7(1):14330.
477. Wakefield J, Hassan HM, Jaspars M, Ebel R, Rateb ME. Dual Induction of New Microbial Secondary Metabolites by Fungal Bacterial Co-cultivation. *Front Microbiol*. 2017;8(1284).
478. Shank EA. Using coculture to detect chemically mediated interspecies interactions. *J Vis Exp*. 2013(80):e50863-e.
479. Shin D, Byun WS, Moon K, Kwon Y, Bae M, Um S, et al. Coculture of Marine *Streptomyces* sp. With *Bacillus* sp. Produces a New Piperazic Acid-Bearing Cyclic Peptide. *Front Chemistry*. 2018;6(498).
480. Huang S, Ding W, Li C, Cox DG. Two new cyclopeptides from the co-culture broth of two marine mangrove fungi and their antifungal activity. *Pharmacogn Mag*. 2014;10(40):410-4.
481. Oppong-Danquah E, Budnicka P, Blumel M, Tasdemir D. Design of Fungal Co-Cultivation Based on Comparative Metabolomics and Bioactivity for Discovery of Marine Fungal Agrochemicals. *Mar Drugs*. 2020;18(2).
482. Wang M, Carver JJ, Phelan VV, Sanchez LM, Garg N, Peng Y, et al. Sharing and community curation of mass spectrometry data with Global Natural Products Social Molecular Networking. *Nat Biotechnol*. 2016;34(8):828-37.
483. Guthals A, Watrous JD, Dorrestein PC, Bandeira N. The spectral networks paradigm in high throughput mass spectrometry. *Mol Biosyst*. 2012;8(10):2535-44.
484. Da Silva RR, Wang M, Nothias L-F, van der Hooft JJ, Caraballo-Rodríguez AM, Fox E, et al. Propagating annotations of molecular networks using in silico fragmentation. *J PLoS computational biology*. 2018;14(4):e1006089.
485. Ernst M, Kang KB, Caraballo-Rodríguez AM, Nothias LF, Wandy J, Chen C, et al. MolNetEnhancer: Enhanced Molecular Networks by Integrating Metabolome Mining and Annotation Tools. *Metabolites*. 2019;9(7).
486. Garg N, Kaponi CA, Lim YW, Koyama N, Vermeij MJ, Conrad D, et al. Mass spectral similarity for untargeted metabolomics data analysis of complex mixtures. *J International Journal of Mass Spectrometry*. 2015;377:719-27.
487. van Santen JA, Jacob G, Singh AL, Aniebok V, Balunas MJ, Bunsko D, et al. The Natural Products Atlas: An Open Access Knowledge Base for Microbial Natural Products Discovery. *ACS Cent Sci*. 2019;5(11):1824-33.
488. Nothias LF, Petras D, Schmid R, Dührkop K, Rainer J, Sarvepalli A, et al. Feature-based Molecular Networking in the GNPS Analysis Environment. *bioRxiv*. 2019:812404.
489. Shannon P, Markiel A, Ozier O, Baliga NS, Wang JT, Ramage D, et al. Cytoscape: a software environment for integrated models of biomolecular interaction networks. *Genome Res*. 2003;13(11):2498-504.

490. Yun Y, Zhou X, Yang S, Wen Y, You H, Zheng Y, et al. *Fusarium oxysporum* f. sp. *lycopersici* C2H2 transcription factor FolCzf1 is required for conidiation, fusaric acid production, and early host infection. *Current Genetics*. 2019;65(3):773-83.
491. Sondergaard TE, Fredborg M, Oppenhagen Christensen A-M, Damsgaard SK, Kramer NF, Giese H, et al. Fast Screening of Antibacterial Compounds from Fusaria. *Toxins*. 2016;8(12).
492. Son SW, Kim HY, Choi GJ, Lim HK, Jang KS, Lee SO, et al. Bikaverin and fusaric acid from *Fusarium oxysporum* show antioomycete activity against *Phytophthora infestans*. *Journal of Applied Microbiology*. 2008;104(3):692-8.
493. Bohni N, Hofstetter V, Gindro K, Buyck B, Schumpp O, Bertrand S, et al. Production of Fusaric Acid by *Fusarium* spp. in Pure Culture and in Solid Medium Co-Cultures. *Molecules*. 2016;21(3):370.
494. Wang X, Gong X, Li P, Lai D, Zhou L. Structural Diversity and Biological Activities of Cyclic Depsipeptides from Fungi. *Molecules*. 2018;23(1).
495. Paciolla C, Dipierro N, Mule G, Logrieco A, Dipierro S. The mycotoxins beauvericin and T-2 induce cell death and alteration to the ascorbate metabolism in tomato protoplasts. *J Physiological Molecular Plant Pathology*. 2004;65(1):49-56.
496. Paciolla C, Ippolito MP, Logrieco A, Dipierro N, Mule G, Dipierro SJP, et al. A different trend of antioxidant defence responses makes tomato plants less susceptible to beauvericin than to T-2 mycotoxin phytotoxicity. 2008;72(1-3):3-9.
497. Wang Q, Xu L. Beauvericin, a bioactive compound produced by fungi: a short review. *Molecules*. 2012;17(3):2367-77.
498. Barenstrauch M, Mann S, Jacquemin C, Bibi S, Sylla OK, Baudouin E, et al. Molecular crosstalk between the endophyte *Paraconiothyrium variabile* and the phytopathogen *Fusarium oxysporum* - Modulation of lipoxygenase activity and beauvericin production during the interaction. *Fungal Genet Biol*. 2020;139:103383.
499. Wang Q-X, Li S-F, Zhao F, Dai H-Q, Bao L, Ding R, et al. Chemical constituents from endophytic fungus *Fusarium oxysporum*. *J Fitoterapia*. 2011;82(5):777-81.
500. Breinhold J, Ludvigsen S, Rassing BR, Rosendahl CN, Nielsen SE, Olsen CE. Oxysporidinone: a novel, antifungal N-methyl-4-hydroxy-2-pyridone from *Fusarium oxysporum*. *J Nat Prod*. 1997;60(1):33-5.
501. Moon SH, Zhang X, Zheng G, Meeker DG, Smeltzer MS, Huang E. Novel Linear Lipopeptide Paenipeptins with Potential for Eradicating Biofilms and Sensitizing Gram-Negative Bacteria to Rifampicin and Clarithromycin. *Journal of Medicinal Chemistry*. 2017;60(23):9630-40.
502. Takeuchi Y, Murai A, Takahara Y, Kainosho M. The structure of permetin A, a new polypeptin type antibiotic produced by *Bacillus circulans*. *J Antibiot (Tokyo)*. 1979;32(2):121-9.
503. Huang E, Yang X, Zhang L, Moon SH, Yousef AE. New *Paenibacillus* strain produces a family of linear and cyclic antimicrobial lipopeptides: cyclization is not essential for their antimicrobial activity. *FEMS Microbiol Lett*. 2017;364(8).
504. Ding R, Wu XC, Qian CD, Teng Y, Li O, Zhan ZJ, et al. Isolation and identification of lipopeptide antibiotics from *Paenibacillus elgii* B69 with inhibitory activity against methicillin-resistant *Staphylococcus aureus*. *J Microbiol*. 2011;49(6):942-9.
505. Moon SH, Huang E. Lipopeptide Paenipeptin Analogues Potentiate Clarithromycin and Rifampin against Carbapenem-Resistant Pathogens. *Antimicrob Agents Chemother*. 2018;62(8).

506. Moon SH, Huang E. Novel linear lipopeptide paenipeptin C' binds to lipopolysaccharides and lipoteichoic acid and exerts bactericidal activity by the disruption of cytoplasmic membrane. *BMC Microbiol.* 2019;19(1):6.
507. Moon SH, Kaufmann Y, Huang E. Paenipeptin Analogues Potentiate Clarithromycin and Rifampin against mcr-1-Mediated Polymyxin-Resistant *Escherichia coli* In Vivo. *Antimicrob Agents Chemother.* 2020;64(4).
508. Carmona SL, Burbano-David D, Gomez MR, Lopez W, Ceballos N, Castano-Zapata J, et al. Characterization of Pathogenic and Nonpathogenic *Fusarium oxysporum* Isolates Associated with Commercial Tomato Crops in the Andean Region of Colombia. *Pathogens.* 2020;9(1).